

Study of the Time-dependent Rheological Behaviour of Lead-free Solder Pastes and Flux Mediums used for Flip-Chip Assembly Applications

Sabuj Mallik

Electronics Manufacturing Engineering Research Group
School of Engineering
University of Greenwich at Medway
Kent, UK

A thesis submitted in partial fulfilment of the requirements of
the University of Greenwich for the Degree of Doctor of
Philosophy

FOR USE IN THE
LIBRARY ONLY

January 2009



ACKNOWLEDGEMENTS

I would like to thank my supervisor Prof. N. N. Ekere who has given me the opportunity to pursue this PhD study. His support, valuable guidance and suggestions have greatly helped me through my studies.

I would like to express my deep gratitude to my parents and my elder brother for their encouragement and support over the period of the project. My special thanks go to my beloved wife who has inspired me throughout my PhD thesis writing period.

I would like to thank Dr. Rajkumar Durairaj for his hands-on support, expertise and helpful guidance during the PhD period.

I am also grateful to my colleagues in EMERG team: Anton Seman, Antony Marks, Christopher Hughes, Peter Bernesko, Nicola Cox and Petra Navarro-Clark for their support, helpful suggestions and advices during the period of my PhD study.

ABSTRACT

The two most important trends in electronic industry are “miniaturisation” and “increased functionality”. Over the last fifteen years, the electronic manufacturing industries have experienced tremendous pressure to meet the requirements for miniaturised products, particularly, hand-held consumer products. Functionality of these products has also evolved at the same pace through packing in more and more features. As these trends are set to continue, there is an increasing demand for better understanding of soldering technology, particularly in the area of solder pastes used in the reflow soldering of surface mount devices. Successful assembly of electronic devices for ultra-fine pitch and flip-chip applications requires the deposition of small and consistent paste deposits from pad to pad, and from board to board. The paste printing process at this chip-scale geometry depends on conditions such as good paste roll, complete aperture filling and paste release from the apertures onto the substrate pads. This means that the paste flow and deformation behaviour is very important in defining the printing performance of any solder paste.

In order to understand rheological phenomena associated with the flow of solder pastes, it is necessary to understand time dependent rheological behaviour. Such behaviour is common to many industrial fluids and consequently has been of interest to rheologists for many years. The time dependent behaviour observed in solder pastes is largely due to the breakdown of the flocculated structure formed during storage or idle period. In general, the breakdown of the structure with shear results in a decrease in apparent viscosity. Recovery after shear is generally a very slow process and depends on the intensity of the breakdown and previous shear history.

The work reported in this thesis on the characterisation and modelling of time-dependent rheological behaviour of solder paste and flux mediums used in surface mount applications is made up of four main parts. The first part concerns the characterisation of the time-dependent behaviour of solder pastes and flux mediums. Two types of tests were performed at this stage: hysteresis-loop test and step-shear-rate test. In the second part of

the study the time-dependent rheology of solder pastes and flux mediums has been modelled to evaluate the mechanisms for the break-down of the internal structure of the paste materials. A novel technique has been developed which combines the experimental rheological data with a modified structural kinetic model (SKM) to investigate the rate and extent of structural change of solder paste and flux medium. The third part of the study deals with the experimental and modelling studies of the short term build-up of solder paste and flux medium structure using the stretched exponential model. In the final part of the study the printing trials of four different solder paste samples were carried out to investigate the effect of post-print rest period on slumping behaviour of solder paste.

From the experimental characterisation it was evident that both the solder paste and flux samples are strongly thixotropic and shear-thinning in nature. The thixotropic breakdown behaviour of solder paste and fluxes has been satisfactorily modelled using a second-order structural kinetic model. The results from this study can be of great help for the solder paste manufacturers and formulators in quantifying and predicting the effect of long term shearing on the solder paste samples. The technique developed can also be utilized for similar materials such as solar pastes and conductive adhesives. The short-term build-up of solder pastes and fluxes has been successfully modelled using the stretched exponential model. The paste manufacturers and formulators can use the technique developed to predict and quantify the slumping behaviour of solder paste. The end-users, for example the electronics assemblers may use the technique to optimize their assembly process by minimising/preventing slumping of solder paste.

TABLE OF CONTENTS

List of Figures	ix
List of Tables.....	xiv

Chapter 1: Introduction

1.1 Electronics Packaging – The Challenges.....	2
1.2 Challenges in Flip Chip Technology.....	4
1.3 Driving Forces for Lead-Free Solders.....	5
1.4 Lead-free Soldering Issues.....	7
1.5 The Processing of Paste Materials	9
1.6 Stencil Printing Process	10
1.7 Problem statement and Research Objectives	13
1.8 Overview of the Thesis.....	14

Chapter 2: Literature Review

2.1 Introduction	17
2.2 Previous studies on solder paste and stencil printing process.....	19
2.3 Previous studies on rheological characterisation and modelling of solder pastes	24
2.4 Previous studies on thixotropic behaviour of suspensions.....	31
2.5 Summary	38

Chapter 3: Fundamentals of Rheology

3.1 Introduction	40
3.2 Elastic, viscous and Viscoelastic materials.....	41
3.3 Non-Newtonian Behaviour of Fluids	44
3.3.1 Non-Newtonian Fluids without a yield stress.....	46
3.3.2 Non-Newtonian Fluids with a yield stress	47
3.4 Rheology of Suspensions	49
3.4.1 Particle-Particle Interactions – Interparticle Forces	50

3.4.2 Factors Influencing Suspension Rheology	53
3.5 Time-dependent Behaviour of Suspensions	58
3.6 Summary	61
 Chapter 4: Materials and Methods	
4.1 Introduction	62
4.2 Solder Paste Characteristics	63
4.2.1 Solder Alloy Powder	64
4.2.2 Flux/vehicle System	71
4.2.3 Materials Used in the Experimental Studies.....	83
4.3 Rheometry	85
4.3.1 Anomalous Effects in Rheometry	94
4.3.2 The Rheometer and the Peripherals	97
4.3.3 Geometries used for rheological measurements	100
4.3.4 Rheological test methods used in this study	101
4.4 Summary	109
 Chapter 5: Investigation of The Time-Dependent Behaviour of Solder Pastes and Flux Mediums	
5.1 Introduction	110
5.2 Experimental Test Method	110
5.3 Experimental Results and Analysis	114
5.3.1 Hysteresis loop test results.....	114
5.3.2 Step-shear-rate test results	122
5.4 Summary	128
 Chapter 6: Modelling of The Break-down of the Paste Structure Using the Structural Kinetic Model	
6.1 Introduction	129
6.2 Theory - Structural Kinetic Model	130
6.3 Experimental design.....	133
6.3.1 Materials and preparation.....	133

6.3.2 Rheological measurements	133
6.4 Results and discussion	134
6.4.1 Results and Discussion for Solder Paste Samples.....	134
6.4.2 Results and Discussion for Flux samples.....	140
6.5 Summary	144

Chapter 7: Modelling of the Build-up of the Paste Structure Using the Stretched Exponential Model

7.1 Introduction	145
7.2 Modelling the build-up of thixotropic fluids	146
7.3 Experimental Design	147
7.3.1 Materials.....	147
7.3.2 Rheological measurements	147
7.4 Results and Discussion	149
7.4.1 Preliminary investigation of build-up phenomenon.....	149
7.4.2 Results from the investigation of short-term build-up behaviour	151
7.4.2.1 Solder Paste Samples.....	151
7.4.2.2 Flux Samples	158
7.4.3 Study of the structural build-up using oscillatory time sweep data	163
7.5 Summary	166

Chapter 8: Evaluation of Slump and Spread Behaviour of Solder Pastes and Their correlation to The Rheological Properties

8.1 Introduction	167
8.2 Experimental Equipment and Materials.....	168
8.2.1 Printing Parameters	168
8.2.2 Printer.....	169
8.2.3 Squeegee System	170
8.2.4 Test Board	171
8.2.5 Stencil	172
8.2.6 Inspection	173
8.2.7 Batch Reflow Oven.....	174

8.2.8 Areas of Observation/interest.....	175
8.3 Experimental Procedure.....	179
8.4 Discussion of the printing test results.....	180
8.4.1 Slump Test Results.....	180
8.3.2 Spread test Results.....	189
8.4 Correlation of Paste Flow Behaviour to the Printing Results.....	194
8.5 Summary.....	197

Chapter 9: Summary, Conclusions and Recommendations for Future Work

9.1 Introduction.....	199
9.2 Summary.....	200
9.2.1 Investigation of the time-dependent behaviour of solder pastes and flux mediums.....	200
9.2.2 Modelling of the break-down of the paste structure using the structural kinetic model.....	201
9.2.3 Modelling of the Build-Up of the Paste Structure Using the Stretched Exponential Model.....	202
9.2.4 Printing test results.....	203
9.2 Conclusions.....	205
9.4 Recommendations for Future Work.....	207
Publications.....	209
References.....	212

LIST OF FIGURES

Figure 1.1: Interconnect levels for flip chip and wire bond packages	3
Figure 1.2: The stencil printing process	11
Figure 1.3: Aperture emptying process	12
Figure 2.1: Viscosity changes during screen printing.....	25
Figure 3.1: Schematic illustration of typical Newtonian fluids flow.	42
Figure 3.2: Spring and dashpot representation of Maxwell model (left) and Kelvin model (right).....	43
Figure 3.3: Flow curve of a Newtonian fluid	44
Figure 3.4: Flow curves of fluids without a yield stress and with a yield stress.....	45
Figure 3.5: Viscosity Vs shear stress for a polystyrene ethylacrylate latex at different volume fractions.....	50
Figure 3.6: The effect of particle size on viscosity	54
Figure 3.7: Relative viscosity versus volume fraction of particles for sterically stabilized suspensions of silica spheres (radius = 110 nm) in cyclohexane, for low and high shear rates.....	55
Figure 3.8: Viscosity as a function of shear rate for different volume fractions, for a latex/pressure-sensitive adhesive system	56
Figure 3.9: Viscosity as a function of polydispersity.....	57
Figure 3.10: The flow curve of a thixotropic fluid with a hysteresis loop.....	60
Figure 4.1: SEM micrograph of gas atomized solder powder (Hwang, 1989)	68
Figure 4.2: SEM micrographs of spherical solder powders	68
Figure 4.3: Particle Size Distribution for pastes P1 to P4.....	84
Figure 4.4: Classification of rheological measuring instruments.....	85
Figure 4.5: Poiseuille flow in a cylindrical tube	87
Figure 4.6: Ostwald and Canon-Fenske glass capillary viscometer.....	87
Figure 4.7: High-pressure Capillary Viscometer	88
Figure 4.8: Gas driven Pipe viscometer	88
Figure 4.9: Schematic of a concentric cylinder system where the inner cylinder is rotating at a speed of ω rad/sec	89

Figure 4.10: Cone-and-plate arrangement.....	91
Figure 4.11: Typical parallel plate geometry	93
Figure 4.12: Bohlin Gemini-150 Controlled-stress/strain rheometer.....	99
Figure 4.13: The Rhometer Measuring System	99
Figure 4.14: Serrated Upper Plate (left) and Lower Plate (right) geometries.	101
Figure 4.15: Hysteresis loop test.....	102
Figure 4.16: Typical hysteresis loop test result.....	102
Figure 4.17: Typical step-shear experiment.....	103
Figure 4.18: Typical response of a constant shear rate test, in apparent viscosity vs time plot.....	104
Figure 4.19: High Shear-Low Shear (HSLs) test design	105
Figure 4.20: Typical result of a high shear – low shear test.....	105
Figure 4.21: Applied oscillatory stress and resulting strain for a typical visco-elastic material.....	107
Figure 4.22: Complex modulus and its components.....	108
Figure 5.1: Hysteresis loop test.....	111
Figure 5.2: Typical hysteresis loop test result.....	112
Figure 5.3: Typical step-shear experiment.....	113
Figure 5.4: Shear rate values used in the step-shear-rate test.....	114
Figure 5.5: Single-Hysteresis-Loop test results for the solder paste samples (P1 to P4)	116
Figure 5.6: Multiple-hysteresis-loop test result for paste P1	117
Figure 5.7: Multiple-hysteresis-loop test result for paste P2	118
Figure 5.8: Multiple-hysteresis-loop test result for paste P3	118
Figure 5.9: Multiple-hysteresis-loop test result for paste P4	119
Figure 5.10: Shear stress response to single-hysteresis-loop test for F1 and F2 flux mediums	120
Figure 5.11: Multiple-hysteresis-loop test (3 cycles) results for F1 flux medium.....	121
Figure 5.12: Multiple-hysteresis-loop test results for F2 flux medium.....	122
Figure 5.13: Shear stress response for a step-wise application of shear rates on paste P1.....	125

Figure 5.14: Shear stress response for a step-wise application of shear rates on paste P2.....	125
Figure 5.15: Shear stress response for a step-wise application of shear rates on paste P3.....	126
Figure 5.16: Shear stress response for a step-wise application of shear rates on paste P4.....	126
Figure 5.17: Shear stress response for a step-wise application of shear rates on paste P1.....	127
Figure 5.18: Shear stress response for a step-wise application of shear rates on paste P1.....	127
Figure 6.1: Effect of shear rate on apparent viscosity for paste P1 at 25 ⁰ C.....	135
Figure 6.2: Effect of shear rate on apparent viscosity for paste P2 at 25 ⁰ C.....	136
Figure 6.3: Effect of shear rate on apparent viscosity for paste P3 at 25 ⁰ C.....	136
Figure 6.4: Effect of shear rate on apparent viscosity for paste P4 at 25 ⁰ C.....	136
Figure 6.5: Testing of the structural kinetic model with different solder paste samples at 25 ⁰ C.	139
Figure 6.6: Apparent viscosity data at constant shear rates for flux medium F1 at 25 ⁰ C. Effect of shear rate.	142
Figure 6.7: Apparent viscosity data at constant shear rates flux medium F2 at 25 ⁰ C. Effect of shear rate.	142
Figure 6.8: Testing of the structural kinetic model with different flux samples at 25 ⁰ C.	143
Figure 7.1: Apparent viscosity data of solder pastes as a function of time at a shear rate of 0.0005 s ⁻¹	150
Figure 7.2: Apparent viscosity of solder paste P1 as a function of time at low shear rates.	152
Figure 7.3: Apparent viscosity of solder paste P2 as a function of time at low shear rates.	152
Figure 7.4: Apparent viscosity of solder paste P3 as a function of time at low shear rates.	153

Figure 7.5: Apparent viscosity of solder paste P4 as a function of time at low shear rates.	153
Figure 7.6: Equilibrium viscosity from the stretched exponential model for the solder paste samples.	156
Figure 7.7: Characteristic time of the stretched exponential model for the solder paste samples.	156
Figure 7.8: Apparent viscosity of flux F1 as a function of time at low shear rates. ..	160
Figure 7.9: Apparent viscosity of flux F2 as a function of time at low shear rates. ..	160
Figure 7.10: Initial viscosity of the stretched exponential model for flux samples. ..	161
Figure 7.11: Equilibrium viscosity of the stretched exponential model for flux samples.	162
Figure 7.12: Characteristic time of the stretched exponential model for flux samples.	163
Figure 7.13: Changes in storage modulus (G') during ageing at 25 ⁰ C for 8 hours....	164
Figure 7.14: Phase angle (δ) as a function of time, measured at 25 ⁰ C for different solder paste samples.	165
Figure 8.1: DEK 260 Stencil Printing Machine.....	169
Figure 8.2: Metal Squeegees.....	170
Figure 8.3: Heraeus Bechmarker II test board	171
Figure 8.4: Benchmarker II laser-cut stencil.....	172
Figure 8.5: Close up view of openings on the stencil	173
Figure 8.6: Lica S6D zoom stereomicroscope with the camera kit.....	174
Figure 8.7: Reddish forced convection reflow oven	175
Figure 8.8: The three areas of interest on the Benchmarker II stencil.	176
Figure 8.9: Slump Location-1	177
Figure 8.10: Slump location-2.....	178
Figure 8.11: Spread test location on the Benchmarker II stencil	178
Figure 8.12: Cold slump results for horizontal 2.03 × 0.33 mm pads for different resting time.	183
Figure 8.13: Cold slump results for vertical 2.03 × 0.33 mm pads for different resting time.	183

Figure 8.14: Cold slump results for horizontal 2.03×0.20 mm pads.....	184
Figure 8.15: Cold slump results for vertical 2.03×0.20 mm pads.....	184
Figure 8.16: Hot slump behaviour of P2 solder paste after 5 minutes (left) and 10 minutes (right) of resting time.....	186
Figure 8.17: Hot slump results for horizontal 2.03×0.33 mm pads for different resting period.....	186
Figure 8.18: Hot slump results for vertical 2.03×0.33 mm pads for different resting period.....	187
Figure 8.19: Hot slump results for horizontal 2.03×0.20 mm pads for different resting period.....	187
Figure 8.20: Hot slump results for vertical 2.03×0.20 mm pads for different resting period.....	187
Figure 8.21: Spread Test location	191
Figure 8.22: Spread test results at room temperature with different resting periods.	192
Figure 8.23: Spread test results after temperature conditioning (150° C, 10 minutes) at different resting periods.....	192
Figure 8.24: High temperature spread test behaviour of P3 solder paste after 5 minutes (left) and 10 minutes (right) of resting time.	193
Figure 8.25: Flow curves for the solder paste samples	194

LIST OF TABLES

Table 4.1: Summary of major research carried out world-wide for lead-free solder selection.....	66
Table 4.2a: Solder powder particle size distribution for solder paste: type 1 to 3 (J-STD-005).....	70
Table 4.2b: Solder powder particle size distribution for solder paste: type 4 to 6 (J-STD-005).....	70
Table 4.3: Solder powder particle size distribution for solder paste (DIN 32 513).....	70
Table 4.4: Classification of fluxes to J-STD-004.....	75
Table 4.5: Commonly used solvents in fluxes of solder paste	81
Table 4.6: Some commonly used rheological additives.....	82
Table 4.7: Test materials	83
Table 4.8: Particle size distribution for the solder paste samples.....	83
Table 4.9: Details of the measuring geometry used	101
Table 5.1: Hysteresis loop area (A_t) and thixotropy coefficient (K_t) for solder paste samples	117
Table 5.2: Hysteresis loop area (A_t) and thixotropy coefficient (K_t) for flux mediums	120
Table 6.1: The parameters from the second-order kinetic model for solder paste samples evaluated at different shear rates.	138
Table 6.2: The parameters from the second-order kinetic model for flux samples evaluated at different shear rates.	143
Table 7.1: Estimated values of stretched exponential model parameters for the build-up of solder paste samples.....	155
Table 7.2: Estimated values of parameters for the equilibrium viscosity model fit for solder paste samples	157
Table 7.3: Estimated values of parameters for the characteristic time model fit for solder paste samples	157
Table 7.4: Parameters of the stretched exponential model for the flux samples	161

Table 7.5: Estimated values of parameters for the initial viscosity model fit for flux samples.	162
Table 7.6: Estimated values of parameters for the equilibrium viscosity model fit for flux samples.....	162
Table 7.7: Estimated values of parameters for the characteristic time model fit for flux samples.	163
Table 8.1: Printing parameters	168
Table 8.2: Cold slump results, minimum spacing (in mm) where bridging was observed.....	183
Table 8.3: Hot slump results, minimum spacing values where bridging was observed	186
Table 8.4: Hot Slump results for pads with 45 ⁰ orientation (0.28 mm pitch)	188
Table 8.5: Hot Slump results for pads with 45 ⁰ orientation (0.32 mm pitch)	189
Table 8.6: Spread test results (number of bridges) at room temperature (cold) and at alleviated temperature (hot) for different resting periods.	191
Table 8.7: Key results from time-dependent flow characterisation and modelling studies.	195
Table 8.8: Design Principles for new solder paste formulation.	197

CHAPTER 1

INTRODUCTION

Solder joints play an important role in electronics packaging, serving both as electrical interconnections between the components and the board, and as mechanical support for components. One of the key global challenges faced by the electronics manufacturing industry is miniaturization. Over the last fifteen years, the electronic manufacturing industries have experienced tremendous pressure to meet the requirements for miniaturised products, particularly, hand-held consumer products. Functionality of these products has also evolved at the same pace through packing in more and more features. With further reductions in the size of solder joints, the reliability of solder joints will become more and more critical to the long-term performance of electronic products. As these trends are set to continue, there is also an increasing demand for a better understanding of the soldering technology, particularly in the area of solder pastes used in the reflow soldering of surface mount devices.

Another key challenge is the recent world-wide legislation for the removal/reduction of lead and other hazardous materials from electrical and electronic products – which means that the electronics manufacturing industry has been faced with an urgent search for new lead-free solder alloy systems and other solder alternatives. For example, with effect from the 1st July 2006, the European Union's Waste Electrical and Electronic Equipment (WEEE) Directive 2002/95/EC requires the substitution of various heavy metals (lead, mercury, cadmium, and hexavalent chromium) and brominated flame retardants (polybrominated biphenyls or polybrominated diphenyl ethers) in all new electrical and electronic equipment put on the market.

The study of the rheology of paste materials is very important for two main reasons: firstly, paste rheology could be used to determine the process window in which operations such as mixing, transportation, dispensing and storage in the paste production

process could be carried out. In addition, a quantitative description of the paste is essential for developing models of the various paste processing operations; these models can be employed for process optimisation and for predicting the onset of flow instabilities in the paste production processes. Secondly, rheology can be used as a quality control tool in the paste processing and production stages for identifying batch-to-batch variation; and for attempting to reduce the associated printing defects in the paste printing process. As a quality control tool, the sensitivity of rheological measurements to minor structural differences in materials can provide a useful aid for quality control engineers when deciding whether to accept or reject an incoming material. The focus of the work reported in this thesis is the study of the time-dependent rheological behaviour of lead-free solder pastes and flux mediums used for flip-chip assembly applications

1.1 Electronics Packaging – The Challenges

The field of electronic packaging is a complex and highly interdisciplinary sector, which is facing significant technological challenges. To start with, the levels of integration in electronic packaging are doubling on an almost annual basis. This was first stated by the Intel co-founder Gordon Moore in 1964, which is also well known as the Moore's law. The law states that "the number of transistors doubled every 12 months while price unchanged". Although the rate has slowed down in the 1980s to every 18 months, but it is amazingly still correct and is likely to keep until 2010. Chips dissipate more energy, require more inputs and outputs and operate at ever-increasing speeds. But most importantly, electronic products are getting smaller and smaller, but with ever-expanding functionality. One of the primary challenges of modern electronic packaging is to utilize the available functionality in a manner compatible with the application and at a reasonable price.

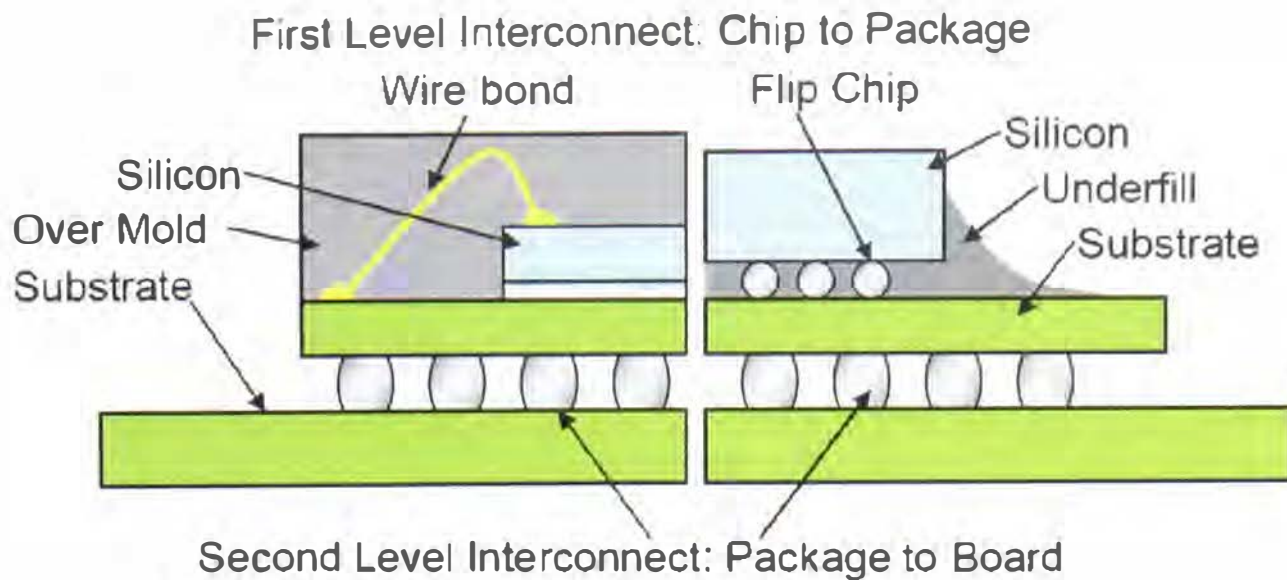


Figure 1.1: Interconnect levels for flip chip and wire bond packages (Garner et al. 2005).

Typical electronic package consists of a hierarchy of interconnections that can be simply divided into first level and second level. The first level connects the silicon die to the package. This may be a wirebond or flip-chip-type interconnect. The second level is the connection between the package and system board. Figure 1.1 shows the first and second level interconnects in a typical electronic package.

First-level Interconnect

Currently, the reliability of the first level interconnect is being challenged by two changes: low dielectric constant (low k) materials and the need to remove lead materials from the package. In order to reduce electrical signal delays and improve the performance of the silicon circuits, the industry in general has shifted toward reduced k material for the inter-layer dielectric in the silicon die. These materials challenge the mechanical reliability since they are substantially weaker than previous materials. This is further compounded by the legislative requirement to remove lead from the package. At present all of the available lead-free materials have unfavourable properties that impose additional stress on the first-level interconnect (Garner et al. 2005). This is because, none of these materials meet all the desirable properties, which include good wetting, low melting temperature, good manufacturability and stable interfaces with metallic surfaces (Suganuma, 2004).

Second-Level Interconnect

At the second-level interconnect there is a distinct set of challenges. Firstly, mobile computing is rapidly increasing in popularity, with both laptops and smart phone/PDAs. As people carry these devices around more frequently they will also drop them more often. This imposes more stringent shock conditions on mobile components. The second challenge arises from the need to switch to lead-free solders. Sn-Ag-Cu (SAC405/305) alloy, the current industry-standard second-level interconnect solution, is significantly worse than eutectic SnPb alloy. With regard to its shock performance, it is as much as 40% lower as compared with eutectic SnPb. SAC405/305 alloys with their inherently low shock resistance are not optimal for next generation, lead-free applications in mobile computing (Garner et al. 2005). Finally, the long-term industry trends always drive for greater integration of functions and features in devices. This implies that a greater number of interconnects are required to facilitate these new features. Mobile computing also exerts down pressure on device size. These two trends combine to constantly reduce the size of the second-level interconnect, thus making each individual interconnect weaker.

1.2 Challenges in Flip Chip Technology

Solder bumped die (flip chips) have been used in electronic devices for over 30 years, but mainly as captive businesses within large companies. Widespread use of flip chip as a surface mount alternative has been slow to develop due to the multi-million dollar investment in capital equipment required to bump wafers using traditional bumping techniques (i.e. vapor deposition, photolithography, electroplating, etc). As new lower cost manufacturing technologies have emerged, the true advantages of solder bumped die have been realized by a much broader community; e.g., low cost, high electrical performance, high I/O density, small package size, and high reliability (Erickson 1998).

Numerous interconnection technologies have been developed within the electronics manufacturing industry in order to provide flip chip interconnection solutions

(Lau 1995 and Rinne 1997), such as vapor phase deposition (including evaporation and sputtering), liquid phase deposition (including immersion soldering and solder jetting), solid phase deposition (e.g. stud bumping and stencil printing), and the electrochemical deposition (electrolytic and electroless plating). Each technique demonstrates favorable attributes in terms of technological capability, yield analysis and processing costs. However, extending traditional surface mount technology (SMT) infrastructure (process capabilities, equipment, and soldering materials) using stencil printing has been proven to be the most economical solution for flip chip interconnection (Huang et al, 2002, Nguty et al, 2001 and Strandjord, 2001). Whilst the stencil printing process is paramount to producing high volume, low cost joints it also accounts for almost 60% of assembly defects within the SMT process (Durairaj et al, 2002). In light of these defect statistics, there is an increased focus to better understand the sub processes involved with stencil printing especially for ultra fine pitch applications (Jackson et al, 2003).

1.3 Driving Forces for Lead-Free Solders

a) Health-Related Aspects

Although lead (Pb) had been used for quite a long time, it is now well recognised that lead can have some serious ill effects on humans. Depending on implications, Pb poisoning is sometime classified as alimentary, neuromotor, or encephalic (Puttlitz and Stalter, 2004). Drinking Pb-contaminated water is regarded as one of the main sources for ingesting Pb. Based on this concern, the electronic industry is rapidly moving ahead with lead-free assemblies and components to avoid potentially Pb-contaminated drinking water. In this case, the source is claimed to be Pb leached from landfills containing electronic wastes (such as lead from component finishes, PCB assemblies etc.) of consumer products such as TVs, PCs, telephones, camcorders, and other household electronic products. It is believed that the Pb-contaminant would find its way into the groundwater system with the potential of contaminating residential water supplies. In Japan, the Pb-elution environmental standard in landfills is 0.3 mg/L and in the US, the regulatory limit for Pb in drinking water is 0.015 mg/L (Puttlitz and Stalter, 2004). The

concentration of lead leached from solders can be several hundred times higher than the acceptable limit (Puttlitz and Stalter, 2004).

b) Legislation on the ban of Pb-based materials

An initial driving force for the movement toward the elimination of Pb in electronic industries is the fear of legislation. The most important of which is the European Union's (EU's) directive on the Restriction of Certain Hazardous Substances (RoHS), which has been implemented in all the 25 EU member states since 1st July 2006. The hazardous substances included in the directive are lead (Pb), cadmium (Cd), mercury (Hg), hexavalent chromium (Cr^{6+}), polybrominated biphenyl (PBB), and polybrominated diphenyl ether (PBDE) flame retardants. The legislation effectively bans the supply and the use of the Pb-containing electronics and electrical products in the European market. As outlined in the directive, the maximum concentration value in materials should be less than 0.1wt% for Pb, Hg, Cr^{6+} , PBB or PBDE and less than 0.01wt% for Cd. The basis for the directive is the claim that Pb could be leached from electronic wastes discarded in landfills, and that the leachate will find its way into the groundwater system, ultimately contaminating the drinking water supplies. Although it only applies to EU countries, the RoHS directive directly affects the electronic industries round the world because of the globalization of the electronics manufacturing industries. Therefore, it is indeed a great challenge for the electronic manufacturers to find viable alternative to Pb-based solders.

c) Market Advantages – Green Marketing

When lead-free issues are concerned, the market-driven aspect is often more important than the legal mandates. The market can force a transition to lead-free solders much more quickly as it can provide substantial marketing advantages, particularly for consumer products. "Green" marketing is rapidly being viewed as a powerful and effective marketing tool. Japanese electronics manufacturers have been in the lead in green marketing and manufacturing. In order to reduce disassembly cost at the end-of-

life, Japanese original equipment manufacturers (OEMs) took the approach of introducing lead-free technology into their assemblies, specially the solders used in reflow-soldering process, and lead-free components and board finishes. This has put Japanese OEMs at the forefront of lead-free implementation. A product bearing a green environmentally safe symbol could gain a significant increase in market share compared to a traditional lead-bearing product. Therefore, more and more electronics manufactures are taking the proactive environmental approach and becoming increasing aware that benefiting the environment can lead to bottom-line benefits, such as reduction in expenses and the creation of new sources of revenue (Puttlitz and Stalter, 2004).

1.4 Lead-free Soldering Issues

The switch from lead to lead-free assembly affects all aspects of electronics manufacturing. This has brought up new challenges in terms of design, formulation, reliability and handling of paste materials. The transition from Pb-based solders to Pb-free solder has raised the following concerns.

a) Higher Cost for Lead-Free Implementation

The adoption of lead free soldering has created unavoidable costs for the global electronics industry. The higher cost of metals used in the lead-free solder alloy has significant effect on the overall cost of lead-free soldering. A mighty 263% increase in base metal cost between the most popular lead-free alloy SAC305 (96.5Sn3Cu0.5Ag) compared to the standard tin-lead (Sn63% Pb37%) alloy has been reported (IPC-SPVC, 2006). According the RoHS directive, the maximum tolerable amount of Pb in Pb-free solder is 0.1% by weight. It is quite difficult to control the Pb contamination and to maintain such amount of Pb during manufacturing of Pb-free materials. The monitoring and control of lead contamination will therefore incur additional cost in the manufacturing process. The higher melting temperature of lead-free solders also means an increase in manufacturing and energy cost. As the lead-free solder alloys are lighter than the lead based alloys (SAC305 is 14.1% lighter than 63Sn37Pb), the manufacturers

will need to produce more solder powder and flux medium to obtain the equivalent batch weight of solder paste product.

b) Higher Processing Temperature

One of the other key challenges with lead-free soldering is the availability of components that can withstand the higher melting temperature required for lead-free manufacturing (with the exception of Bi-Sn alloy, whose melting point is lower than Sn-Pb solder). The liquidus temperature of SnAgCu lead-free alloys is 217 – 220 °C; this is about 34 °C above the melting point of traditional eutectic tin-lead (Sn37Pb) alloy. This higher melting range requires peak reflow temperatures to achieve wetting to be in the range of 235 – 245 °C. Because of these higher lead-free processing temperatures, components and board suppliers need to re-qualify their parts. Considering the range and number of parts available, this is indeed a very lengthy process. Moreover, the higher reflow profile temperature will require the use of new solder paste flux chemistries. Thermal stability of flux ingredients up to 245 °C is essential to avoid issues of decomposition, oxidation, and polymerization of paste flux during reflow (Biocca, 2004).

c) Solderability and Reliability Issues

Lead-free solder does not flow as easily as leaded solder. Lack of lead decreases the flow-ability of solder, resulting in poor solderability. Lead-free solder pastes also show decreased wetting relative to standard Sn/Pb eutectic solder for most common interconnect surfaces. The poor wetting characteristics can have significant impact on the incidence of component tomb-stoning and can dictate re-flow profiles (ramp rates, dwell times, etc.). Tomb-stoned components require hand repair, a costly process that can have detrimental effects on component and product reliability. Besides this, the higher consumption of metallization and formations of thick intermetallic layer are all well-known problems for lead-free materials (Rizvi, 2007). All these issues have made the use of lead-free solders questionable in the sectors where high interconnection reliability is required.

1.5 The Processing of Paste Materials

The electronic industry has seen a rapid growth in various sectors of the market e.g. the computer, telecommunications, automotive and consumer sectors. Some of the key drivers for this growth include the customers demand for portability, flexibility and better performance of the final product. As a result, this imposes tight requirements in terms of size reduction, performance increase, higher reliability and lower cost. As the current product miniaturisation trend is set to continue for hand-held consumer products, area array type package solutions (such as chip scale packages and flip chip) are now being designed into products. The assembly of these devices requires the printing of very small paste (solder paste or ICAs) deposits consistently from pad to pad, and from board to board.

The paste printing process is an important process in the assembly of flip chip devices using the reflow soldering technique. The paste printing process accounts for the majority of assembly defects, and most defects originate from poor understanding of the flow properties and processing of pastes. Paste materials are dense suspensions, which exhibit complex flow behaviour under the influence of stress. The main difficulty, however, of predicting the flow behaviour of paste is the lack of knowledge of their structure and the nature of the interactive forces between the particles.

Implementing effective materials characterisation procedures in product development, process optimisation and quality control can contribute significantly to reducing defects in the assembly of flip chip devices and subsequently increasing the production yield. Rheology can be described as the study of how materials flow in response to the application of external shear. Rheological characterisation is performed on pastes materials for the following reasons: 1) to understand the fundamental nature of a system; 2) for quality control of raw materials, final products, and manufacturing processes such as mixing, pumping, packaging, and filling; and 3) to study the effect of

different parameters such as formulation, storage time and temperature on the quality and acceptance of a final product.

In recent years increasing numbers of researchers, paste manufacturers and contract electronic manufacturers have begun to incorporate rheology as part of their research and quality control tools. The rheological characterisations of pastes for the assembly of flip chip devices provide important information for R&D and production staff to facilitate the manufacture and assembly of their products. Today, most paste formulators also count on rheological results to develop customer focussed products for surviving in the competitive market. For this reason a proper understanding of the rheology of paste material is becoming increasingly necessary for both paste manufacturers and production/assembly line staff.

1.6 Stencil Printing Process

In order to achieve high volume, low cost production, stencil printing process and subsequently wafer bumping of solder paste has become an indispensable part of the flip chip assembly route (Nguty et al. 1999). For this reason, it is essential that production line and R&D staff gain a thorough understanding of the stencil printing process, to ensure that they are able to cope with the change in paste formulation and materials (such as that required for lead-free paste development)

Although the stencil printing process is paramount in producing high volume, low cost production, it does account for some 60% of assembly defects (Mangin et al. 1991), and it is estimated that up to 87% of reflow soldering defects are caused by stencil printing defects (Okuru et al. 1993). It is in recognition of the impact of stencil printing on assembly defects rates that the stencil printing/rheology of solder pastes has been examined in various studies (Bao et al. 1998, Kolli et al. 1991, Nguty et al. 1999, Durairaj et al. 2004). In these studies, the flow characteristic has been investigated in order to understand the causes of printing defect formation such as skipping and the post-

print behaviour of the paste, such as slump. There is however an urgent need to correlate the rheology of the paste to the paste printing performance as this will provide the key to achieving consistently good paste deposition and defect free assembly processes.

In the stencil printing of pastes, illustrated in figure 1.2, the reduction in the size of the stencil apertures such as those required for flip-chip pitch sizes will usually result in increased stencil clogging and incomplete transfer of paste to the printed circuit board pads. The key sub-processes in the solder paste printing process includes the paste roll in front of the squeegee, the aperture filling and aperture emptying stages. During stencil printing the paste develops a rolling action in front of the squeegee, filling the apertures in the stencil some distance ahead of the squeegee. The squeegee then shears off the paste in the apertures as it moves over the stencil. It is known that during the printing process, the squeegee generates hydrodynamic pressures in the paste roll that injects the paste into the apertures.

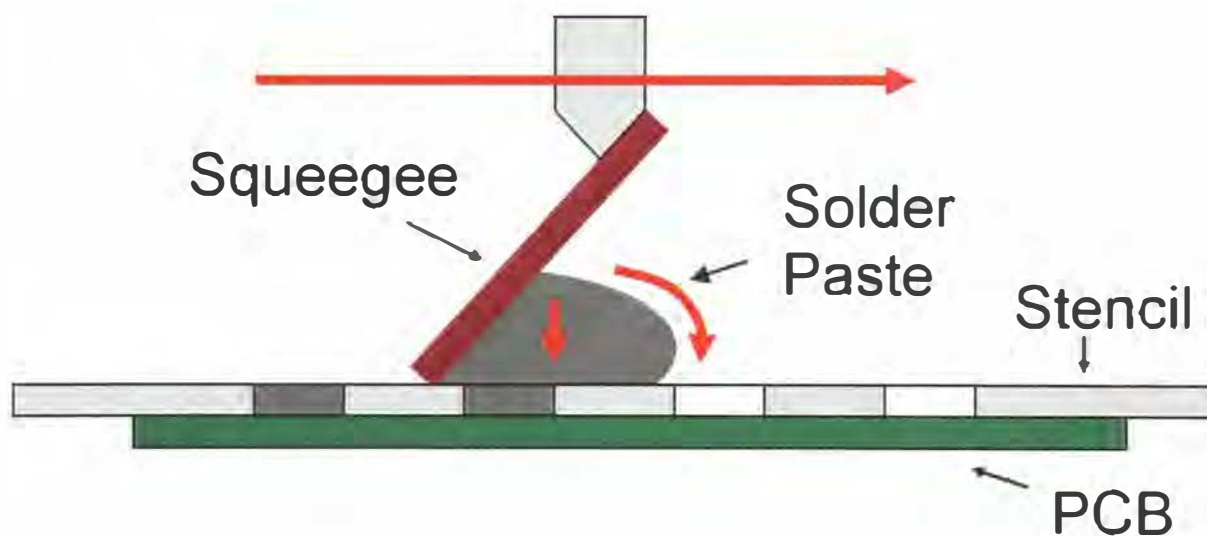


Figure 1.2: The stencil printing process

Once the print stroke is completed, the board is separated mechanically from the stencil (figure 1.2). Separation of stencil and printed circuit board (PCB) or substrate occurs at the end of the squeegee move across the stencil and the substrate is then separated mechanically from the stencil. As the substrate moves away from the stencil, the paste experiences frictional force at the aperture walls as shown in figure 1.3. In order

to achieve a good paste transfer the adhesive force between the substrate and paste must be greater than the frictional forces caused by the roughness of the walls, if not the paste will fracture, leading to incomplete paste transfer.

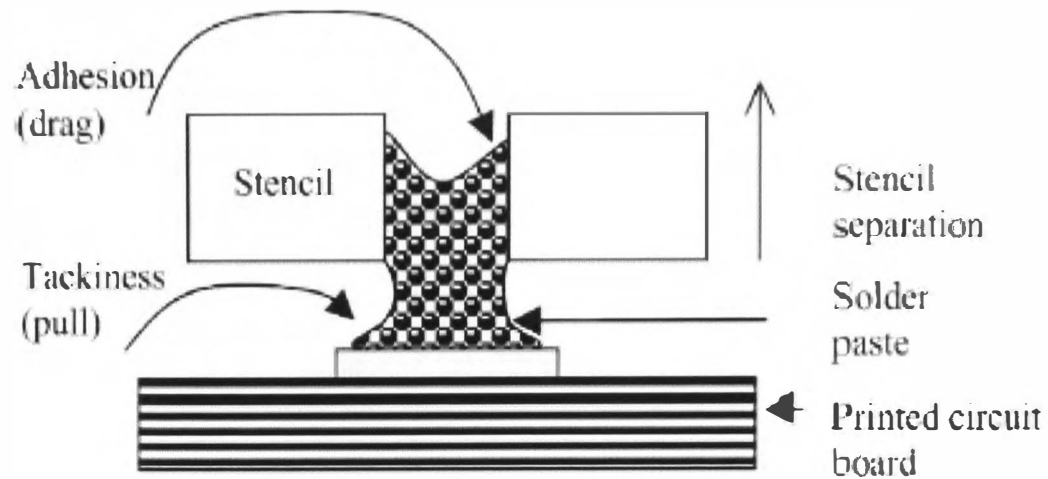


Figure 1.3: Aperture emptying process (Durairaj 2001)

According to Lau and Yeung (1997) in the solder paste printing process, there are five major decisions that determine the quality of the solder joint: (i) the choice of the stencil opening geometry; (ii) the matching of the solder paste; (iii) the fixing of the waiting time; (iv) the selection of the squeegee material; and (v) the parameter setting of the printing machine. The paste printing process is known to be controlled by a number of process parameters, which can be divided into four groups (Haslehurst and Ekere 1996): printer, stencil, environmental, and paste parameters. During the printing process, due to the product requirements, some of these parameters are fixed (e.g. stencil), but the paste properties such as viscosity are changing during the printing process due to the continuous structural breakdown and recovery of the paste material. The key physical sub-processes includes: (a) paste pre-print treatment, (b) squeegee deformation, (c) paste roll (Ekere et al. 1997), (d) aperture filling (Ekere et al. 1994), (e) aperture emptying (Mannan et al. 1994a and 1994b) and (f) paste slump. These sub-processes are linked together by the properties of the pastes such as its flow history and its rheology. The pressure in the paste during and after aperture filling helps determine whether the paste will adhere onto the substrate, stencil or squeegee after aperture emptying.

As stated earlier, the paste rheology dictates the paste's behaviour during the printing process; and for this reason the rheology of solder pastes has been the focus of various studies (Bao et al. 1998; Nguty et al. 1999 and Kolli et al., 1999) and there have been numerous attempts to correlate paste rheological properties with the stencil printing performance. There is however a continuing need for investigating the flow characteristics of the paste under shear conditions to provide a better understanding of defect formation mechanisms in the printing process. Likewise, the post-print behaviour of the paste, such as tack value and slump are known to be dependent on the paste's rheology. Therefore, the correlation of this rheology property to the printing performance is essential for minimising this defect formation.

1.7 Problem statement and Research Objectives

As the demand for smaller and miniature hand-held and pocket electronic consumer products such as mobile phones and camcorders continues, the drive towards further miniaturisation of electronic devices and solder joints will also continue. As stated previously, the assembly of these devices requires the printing of very small paste deposits consistently from pad to pad, and from board to board. The stencil printing of solder paste is a very important stage in the reflow soldering of surface mount devices. There is wide agreement in industry that the paste printing process accounts for the majority of assembly defects, and most defects originate from poor understanding of the effect of printing process parameters on printing performance and paste rheology.

The development of new pastes formulations is a very complex process because the paste rheology is known to be governed by a large number of parameters. These parameters typically include solder powder particle size, flux/vehicle medium, and volume fraction. In addition, the paste manufacturing industry has used viscosity as the key attribute for characterising the flow behaviour of pastes materials. This attribute alone does not adequately describe why a paste prints differently under different conditions. With more extensive chemical and physical characterisation of the properties

of paste it should be possible to understand why certain process parameters and environmental factors cause printing problem at ultra-fine pitch.

Hence, an understanding of the flow behaviour of the paste is important for achieving consistent paste deposit volume and reduction in the printing defects, ultimately increasing production yield. In particular, full characterisation of the visco-elastic properties of pastes is essential for determining the right printing process parameters, and ultimately for achieving proper control of the printing quality. Solder pastes are known to exhibit a thixotropic behaviour, which is recognised by the decrease in apparent viscosity of paste material with time when subjected to a constant shear rate. The proper characterisation of this time-dependent rheological behaviour of solder pastes is crucial to establishing the relationships between the pastes' structure and flow behaviour; and to correlating the physical parameters with paste printing performance. The work reported in this thesis is concerned with the time-dependent rheological characterisation of pastes designed for ultra fine pitch flip chip assembly and their application to the stencil printing process. This study on the time-dependent rheological characterisation of solder pastes and flux mediums has four main objectives, as follows:

1. To study the time-dependent flow-behaviour of solder pastes and flux mediums.
2. To model the break-down of the paste structure using the Structural Kinetic Model.
3. To model the build up of the paste structure using the Stretched Exponential Model.
4. To correlate the time-dependent rheological behaviour of pastes to the paste printing performance through printing trials.

1.8 Overview of the Thesis

The thesis is sub-divided into nine chapters. Chapter 1 provides the introduction to the thesis and gives an overview of the study on the time-dependent rheological

Chapter 1

behaviour of lead-free solder pastes and flux mediums used for flip-chip assembly applications, outlines the aims and objectives of the research work, and presents the thesis overview.

Chapter 2 presents the results of the literature review on solder paste printing process, rheology of pastes and thixotropic behaviour of solder paste and suspensions. The chapter is made up of four main sections. The first section gives a review of previous studies on solder paste printing process. The second section deals with the review of previous work on the rheology of paste materials. The final section of the chapter concerns the review of previous work on the thixotropic behaviour of paste materials.

Chapter 3 provides an overview of the fundamentals and basic concepts used in the study of time-dependent rheological behaviour of suspensions. This chapter is divided into four main parts. The first part of the chapter concerns with the basic definition of rheology. The second part introduces various fluid systems such as viscous and non-Newtonian fluids. The third part presents the introduction to time-dependent behaviour of structured fluids and its influence on the flow behaviour of such fluids. The final part of the chapter 3 presents the measurement techniques used in characterising time-dependent behaviour of suspensions.

Chapter 4 presents an overview of solder pastes and flux mediums and describes the function of their constituents. It also introduces the key concepts used in rheometry, an important experimental technique used in the characterisation of a material. A guideline for measuring the time-dependent rheological properties of pastes reported in this thesis is also outlined in chapter 4.

Chapter 5 outlines the results of an investigation of the time-dependent thixotropic behaviour of solder pastes and flux mediums. The chapter is made up of two main parts: the first part describes the experimental method and parameters used in this study and the second part presents the results from the investigation. Two types of tests were carried out, namely the hysteresis loop test and the step-shear-rate test.

Chapter 6 presents a modelling study of the structural breakdown of paste structure. In this chapter the study the time-dependent rheology of solder pastes and flux mediums has been modelled to evaluate the mechanisms for the break-down of the internal structure of the paste materials. A novel technique has been developed which combines the experimental rheological data with a modified structural kinetic model (SKM) to investigate the rate and extent of structural change of solder paste and flux medium.

Chapter 7 reports on the modelling study of the build-up of paste structure. The short-term build-up of paste structure has been modelled using the stretched exponential model. Experimental studies were also carried out to validate the results from the modelling study. The chapter also presents the experimental study to simulate the long term build-up of solder paste using single-frequency oscillatory test.

Chapter 8 presents the results of the solder paste printing trials. The focus of the study was to validate and correlate the results from the modelling studies to the printing performance of solder paste. The printing trials of four different solder paste samples were carried out to investigate the effect of post-print rest period on slumping behaviour of solder paste.

The final chapter, Chapter 9, presents the summary of the study, the main conclusions from the study and the suggestions for future work.

CHAPTER 2

LITERATURE REVIEW

2.1 Introduction

The electronics industry has experienced tremendous growth and change since the revolutionary invention of transistor in 1947. According to the Semiconductor Industry Association (SIA), worldwide sales of semiconductors grew 3.2% to reach \$255.6bn in 2007, up from the \$247.7bn of 2006, and the figure is expected to rise at the rate of 7.7% in the year 2008. The main sectors for semiconductor demand are personal computers, hand-held mobile phones and consumer electronics. The key challenge in electronics manufacturing in recent years has been related to the use of new materials and new processes driven by increased density and complexity of circuitry (Hwang, 1989), increased functionality of the final products and world-wide legislation on producer responsibility such as WEEE.

Solder paste is the primary joining material used in the electronic assembly process for attaching electronic components/devices directly onto the surface of printed circuit boards. Solder paste serves in three segments of electronic markets : hybrid circuit assembly, printed circuit board (PCB) assembly, and components assembly. In both hybrid and printed circuit assemblies, solder paste is used to interconnect active and passive components/devices, connectors, and other components onto the board; and in component assembly, solder paste serves as a joining material for attaching leads, lead frames, and the structural units to make end-use components (Hwang, 1989). As stated earlier in chapter 1, stencil printing is the most widely used method for depositing solder pastes onto the substrate. The paste printing process is estimated to account for some 60% of the assembly defects (Mangin, 1991) and most defects originate from poor understanding of the flow properties and processing of pastes. The situation has even

become worse with the introduction of regulations governing the ban of traditional lead-based solders in the electronics manufacturing. There is now a greater need for a better understanding of the interaction between new materials and the printing process.

Over the last 10 years, substantial research and development have been reported on attempts to identify viable lead-free solder compositions that meet specific criteria for manufacturing, reliability, toxicity, cost and availability. Although numerous tin-based lead-free solder are now available commercially, none of these meets all the desirable properties, which include good wetting, low melting temperature, good manufacturability and stable interfaces with metallic surfaces (Suganuma, 2004). It is worth noting that the current processing equipments and assembly processes also need to be optimised for new lead-free solders in order to get good yield and reliable product. In addition to the challenge of using new materials such as lead-free solder pastes, there is also an urgent need to understand the rheological behaviour of lead-free solder pastes that will provide a better understanding of the various defect mechanisms occurring during the assembly processes.

This chapter outlines the outcome of a literature review on stencil printing process, solder paste rheology and the time-dependent behaviour of solder pastes and other suspensions. The chapter is made up of three sections; the first section presents a review of previous studies on solder paste and stencil printing process. This section covers an overview of the previous experimental, modelling and design work on solder pastes and printing process. The second section presents a detailed review of the previous works on rheological characterisation and modelling of solder pastes. The third section presents a review of time-dependent thixotropic behaviour of suspensions. The aim of this last section was to identify the experimental and theoretical approaches used in studying the thixotropic behaviour of suspensions.

2.2 Previous studies on solder paste and stencil printing process

The formulation of new solder pastes for surface mount applications require a great deal of expertise and knowledge of the constitution and composition of solder pastes, their processing conditions and the assembly requirement for the target product. In a valuable piece of work, Kozel (1983) outlined the properties desired in the solder pastes and each of its constituents from the formulation point-of-view. The paper provides useful information on the functions of the different constituents of solder pastes: solder powder, rosin/resin, solvent, activator and agents to modify rheological characteristics. The standards and guidelines in selecting the constituents are also discussed. The factors affecting the occurrence of bridging between pads were identified and the effect of drying time on solder paste printing were investigated. It was suggested that the formulator and the user must work together to get optimum result by reaching agreement on each of the four major processing steps: method of application, drying, reflow and cleaning.

In another early study, Owczarek and Howland reported on developing a physical model for the description of screen printing process. Although the work was carried out in 1984, it was published as open literature in 1990 (Owczarek and Howland 1990a, 1990b). The model was based on printing tests on ceramic substrates in which the printing was interrupted after only partial coverage of the substrates. Two different pastes and two squeegees with different hardness values were utilised. It was found out that during printing, the angles of squeegees decrease from the underformed angle of 45 deg by about 20 deg for hard squeegees and by 30 – 40 deg for soft squeegees. Equations were derived from the analysis of the model which allow calculation of the thickness of dry paste deposited on a substrate in the off-contact screen printing process. The model showed that the height of the deposited paste depends on the magnitude of the equivalent paste height under the squeegee and on the paste flow speed under the squeegee.

In another study, Kasturi (1992) carried out experiments on a range of solder pastes with varying viscosities, particle size distributions, flux types, and metal contents. The study used the ANOVA technique to investigate the effect of four printing parameters at

two levels using sensitivity and interaction plots for evaluation. The parameters investigated were: aperture pitch, stencil thickness, snap-off distance and humidity.

In another study, Mannan et al (1993) investigated the role of squeegee plays in the solder paste printing process and proposed a model for predicting the scooping and skipping defects. The interactions between the paste properties and squeegee materials were also investigated. The results of an experimental study using different types of squeegee blades have been used to validate the model. The squeegees tested included one metal squeegee, three simple polyurethane and two composite squeegees. Although the metal squeegee has performed best in reducing scooping defect, the lowest level of skipping were found with the softer blades.

The effect of different types of squeegee blades on solder paste print performance has been outlined in more details in another study by Mannan et al (1994). In addition to reporting experimental test results with six different squeegees, an empirically enhanced model was developed for calculating paste heights as a function of paste viscosity, squeegee loading, speed, and aperture geometry. Their study showed that the cause of the differences in paste heights between perpendicular and parallel pads is the different paste pressures in these apertures. The model also suggested that the viscoelastic nature of the paste plays an important part in creating the large pressure difference.

In another study, the detailed modelling maps for the solder paste printing process was presented by Ekere et al (1994, 1995), giving a clear overview of the paste printing process in terms of the key sub-processes, the process parameters and their interactions. These maps are quite useful and informative in a sense that they indicate how the process parameters interact in the designed experiments as well as the reasons for deviations on the quality of the paste deposited.

A computer simulation of solder paste flowing out of a stencil aperture during stencil printing has been outlined in two linked studies by Mannan et al (1994a, 1994b). The simulation reported is based on lubrication theory and is valid for dense suspension flow

of spherical particles where the volume fraction of particles is higher than 45%. In the first study (Mannan et al, 1994a) detailed the assumptions used in the simulation technique – outlining the methods and procedures required to simulate the motion of a dense suspension containing spherical particles. The results of the simulation for the aperture emptying sub-process are discussed in the second part (Mannan et al 1994b) and the study shows that the simulation technique can be used for finding mechanisms for skipping and general trends. However, the model can not be used for predicting the onset of skipping, as this depends on various paste properties.

One of the key parts of the surface mount assembly process is the reworking of the defective components from the assembly line through desoldering and resoldering of the component. Although rework is time-consuming, labour intensive and adds substantial costs to the manufacturing, it is still an indispensable part of the surface mount assembly process. Having identified the challenges and significance of automated SMD rework, Geren and Ekere (1994) reported on the development of a robotic rework cell for surface mount (SM) and through-hole (TH) boards. The rework cell developed can be used to perform both assembly and rework helping to reduce cost. The paper also outlined valuable information and guidelines on the equipment selection, the integration and interfacing of sub-equipments and process characteristics experiments.

The quality and output from the stencil printing depends on a wide range of factors. In one study, Hwang (1994) provided an overview of the different factors which could contribute to the final printing quality and output. The main factors covered were: stencil printing principles, solder paste rheology, solder powder, paste viscosity, printing parameters and stencil selection. The importance and the challenge of predicting rheology of solder pastes have been identified and briefly outlined. A guideline on setting up and effective use of three major printing parameters, namely squeegee speed, squeegee pressure and snap-off distance, were discussed. Moreover, a guideline for stencil selection and stencil design were also provided.

In one study, Monaghan et al (1995) investigated the effect of stencil aperture wall designs on the paste withdrawal in the stencil printing process. Experiments were conducted to investigate the effect of altering the aperture wall angle and the effect on the paste deposit volume on paste printing performance.

The stencil printing of solder paste is known to be affected by a large number of factors including printer settings, stencil aperture geometry and environmental conditions. Haslehurst and Ekere (1996) reported on a study based on a fractional factorial experiment to investigate the effects and interactions of some of these parameters. A two-level design of eleven factors was used. The main purpose of the experimental study was to determine which of the parameters had a significant effect on solder paste height, as this is an important indicator of print quality. The key results and recommendations from the study are –

- Pressure, speed and separation speed, together with direction of print stroke were identified as the most important printer parameters.
- Many two- and three-way interactions have been identified with the interaction between pressure and squeegee direction being the most significant one.
- It was suggested that the temperature and humidity should be controlled for better yield from the production line. Also the paste should be replenished regularly and the amount used should be kept as consistent as possible in order to print consistently.

In another study, He and Ekere (1996) analysed the performance of the vibrating squeegee in the stencil printing of solder paste. The study showed that the application of vibration produces a liquid-rich layer at the interface between the squeegee leading edge and the paste roll, thus reducing the squeegee resistance on paste roll. It was found out that the application of oscillatory shear may enhance the flow capability of viscoelastic materials like solder paste through reduction in dynamic viscosity. The study also concluded that the careful selection of the kinematic parameters such as the squeegee printing speed, the squeegee vibration amplitude and the vibration frequency can help to improve the paste roll and the quality of the printing process.

Zou et al (2003) reported on a work undertaken to evaluate the performance of a enclosed print head system for fine pitch stencil printing. A fine pitch (down to 300 μm pitch/150 μm line width) printed circuit board and stencil (100 μm thick) were used to evaluate fine pitch printing performance. The enclosed print-head system has been shown to be a robust process and has out performed traditional squeegee printing at increased humidity (to 75%). The enclosed printing system also allowed successful intermittent printing over a 5 day period. From the work, it was concluded that the use of enclosed print-head will significantly reduce past wastage, by reducing atmospheric degradation of the paste.

Because of the current restriction on the use of lead and other hazardous substances in consumer electronic products, electronics manufacturers have been forced to adopt new lead-free technologies. As a result, a substantial amount of research has been carried out in last ten years in different aspects of lead-free soldering technology. In one study, Suganuma (2004) provided a very useful introduction to lead-free soldering technology. The paper discusses the worldwide regulations on restricting the use of lead in electronics manufacturing and presents details of global lead-free solder development projects. It was pointed out that the Japanese electronics manufacturers are the pioneers in adopting lead-free solder for mass production. While outlining the advantages and limitations of different lead-free solder alloys, it was stated that the Sn-Ag-Cu family of solder is the strongest candidate to become the standard lead-free solder, as it is extremely stable and also meets the globally acknowledged standards. In another study, Fujiuchi (2004) outlined the key requirements and the desirable physical and chemical properties of lead-free solder paste in reflow soldering process.

In another article, Price (2005) reported on various important challenges in relation to the transition from lead-based to lead-free soldering. The author has put special emphasis on the need for “higher melting temperature” by lead-free soldering and its consequences on the assembly process and equipments. Sn-Ag-Cu (SAC) alloys with the melting points between 215 – 220 $^{\circ}\text{C}$ were identified as cost-effective and widely-

used alternative to lead-based solders. Moreover, the article outlines separately the issues/challenges in reflow, wave and hand soldering and also how these processes can be optimised for lead-free soldering.

In a recent study, Clements et al (2007) developed a mathematical model to describe the pressure characteristics of paste during the stencil printing process. The derivation of the model was based on the foundations of continuity of fluid flow and shear stresses that are imparted by the squeegee blade movement. The pressure profile generated by the mathematical model showed very good agreement with predicted pressure profiles using experimental data. Furthermore, the mode provided a theoretical framework for a better understanding of how to overcome the failure modes inherent in stencil printing, such as over or under-filled stencil cavities.

In another recent study, Greene and Srihari (2008) reported on a technique for determining the high-speed stencil printing performance of solder pastes. Four different solder pastes (different in alloy composition and melting points) from different vendors were examined. A series of experiments at an increasing print speed (6, 6.5 and 7 inch/sec) was performed to deposit these solder pastes on to PCBs and the printed solder volumes were measured. The maximum acceptable print speed was found different for different solder paste samples. The results from the investigation provide an useful guideline on parameters to use in the stencil printing of lead-free solder pastes at high speeds.

2.3 Previous studies on rheological characterisation and modelling of solder pastes

In a pioneering study, Trease & Dietz (1972) reported on the rheological behaviour of thick-film pastes used in electronics manufacturing. In this study, the viscosity of twelve pastes were investigated and the results were correlated with printing parameters such as squeegee speed, screen or mask size and required line resolution. A

graphical representation of the different flow conditions (viscosity and shear rate) was outlined as shown in figure 2.1.

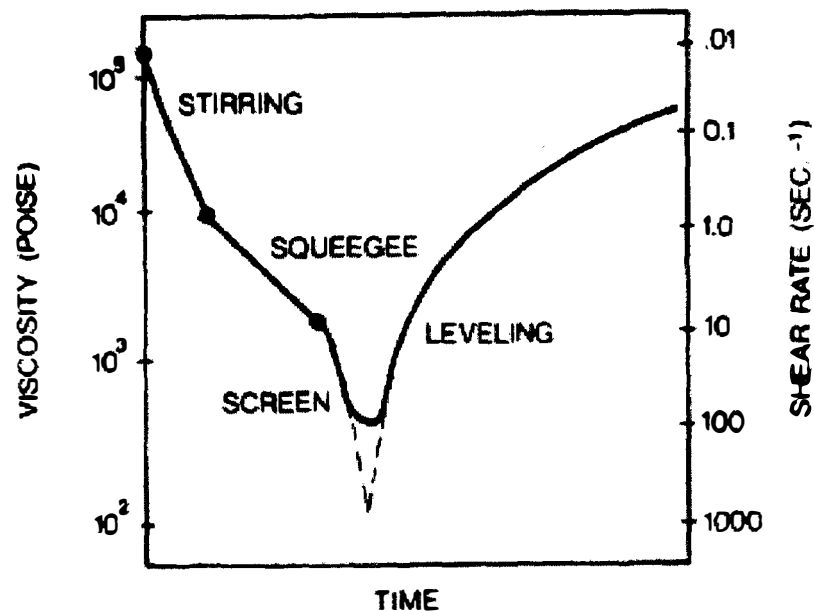


Figure 2.1: Viscosity changes during screen printing (Trease & Dietz, 1972)

Two methods were proposed to relate paste viscosities with print performance. The first was a “screen viscosity index”, which is the ratio of the paste viscosity during screening and levelling of the printed paste on the substrate. In the second method a mathematical description of the paste rheology in terms of viscosity was given, which included the factors of pseudoplasticity and infinite viscosity.

The complete characterisation of the rheological flow properties of paste materials involves measuring response of the paste to different shearing actions experienced by the paste during screening, the effect of continuous shear and the flow behaviour during viscosity recovery. In another early work, Kardashian and Vellanki (1979) presented a method for the rheological characterisation of thick-film pastes. Having identified the limitations and problems of traditional single point viscosity measurements, a set of experimental techniques were outlined for measuring thixotropy, shear-thinning and recovery of pastes as experienced during the screening process.

In another study, Cheng (1984) reviewed the literature on the viscosity measurement of suspensions of spherical particles in a variety of media. The work reported on the results of experiments carried out at Warren-Spring Laboratory (WSL) on various dense suspensions. From the literature review of 40 published work, it was concluded that “the steady shear properties of a dense suspension is not characterised by an unique viscosity or flow curve, but rather it is described by a wide viscosity distribution or a shear stress-shear rate flow band whose mean and standard deviation are functions of solids concentration, particle size distribution and viscometric geometry and dimensions”. It was shown that the reproducibility of viscometric measurement was very poor and became worse and worse as concentration was increased beyond 40 and 50 %. It was stated that the overall flow behaviour of dense suspension is governed by particle migration or changes in local solids concentrations or particle packing density or structure, which occur during flow. It was suggested that the investigation of the dense suspension behaviour should be carried out using a range of viscometers and different sizes of measuring geometries. This is because the viscosity of dense suspension was found to be dependent on the dimensions as well as the geometry of the viscometer used to measure it.

In one study, Ogata (1991) has utilized solder paste rheology as a linking mechanism between the various sub-processes in stencil printing. Solder paste printability was investigated from a combined study of paste viscosity and thixotropy. The work recommended that solder pastes with a viscosity of 1800 Poise and 0.6 Thixotropic Index be used to achieve good printability. It was also argued that the viscosity alone is not sufficient to study printability as the viscosity of solder paste changes with the change in applied pressure and speed.

Lapasin et al (1994) reported a study using three different test methods: constant shear rate test, step shear rate test and hysteresis loop test to characterise the solder paste behaviour. Their study showed that the results of the hysteresis loop test can be influenced by previous shear history and hence may not be suitable for the study of the time-dependent rheological properties of solder pastes. They suggested using stepwise

technique to achieve a thorough characterisation of time and shear-dependent properties. A correlation between rheological parameters and printability was also presented in terms of the viscosity of solder pastes. They concluded that under specific test conditions, only two rheological parameters, the viscosity and yield stress are sufficient for predicting the screening behaviour of solder pastes.

In a study by Mannan et al (1995), the effect of various stages of stencil printing on the rheological properties of solder pastes was reported. Six different commercially available solder pastes were investigated. The study showed that the heat generated inside the solder paste roll during printing is conducted away so that no noticeable temperature rise occurs. From the investigation of particle size distribution, they concluded that to achieve the lowest viscosity, and hence reduce skipping, a wide spread of particle distribution is required. It was also observed that the paste does not flow out of the stencil as a rigid body as the wall drag stresses are too high, but rather the relative movement of the particles produces regions of high particle concentration and stresses leading to stick/slip flow action.

In yet another study, Anderson et al (1995) has reported on the problems encountered in the rheological measurements of solder pastes. Five commercially available lead-based solder pastes were investigated to determine the relationship between various rheological properties including viscosity and the tendency of the pastes to slump. The three major problems encountered during rheological measurements were 1) slippage of the pastes at the interface of the paste with the measurement plates, and/or slippage between internal layers of the pastes, 2) residual stress after shear is stopped and 3) thixotropy. It's been found out that the use of sand paper (by covering the interior side of the measurement plate) delayed the start of the slipping but did not prevent it. Pre-shearing of solder paste samples was found to leave a residual stress in the paste sample, which has made the viscosity measurements even more difficult. In order to cope with the thixotropic tendency of solder paste (change of paste viscosity with time), "absolute viscosity" measurements was suggested by taking into account the previous sample

history. It is also suggested that the printing parameters may need to be changed over the course of a production shift, as the paste is subjected to shear.

In a paper by Bao et al (1998), they reported on a series of tests performed to investigate and determine the rheological properties of a group of solder pastes and fluxes, and the correlation of those properties with paste performance prior to reflow. Their work showed that the rheology of solder paste has a significant effect on its stencil printing performance, in particular on the tack and slump performance and they came up with three major conclusions:

1. solder paste printing defects increase with increasing compliance (J_1 and J_2) and decrease with both higher elastic properties (G'/G'' and recovery) and higher yield stress.
2. slump resistance increases with increasing elastic properties (recovery), solid characteristics and rigidity.
3. high elastic properties (recovery), low compliance (J_1 and J_2), and low solid characteristics are essential in order to achieve a high tack value.

In addition, they also observed a good correlation between fluxes and solder paste properties in terms of yield stress and recovery behaviour.

The difficulties associated with characterising the rheology of the solder pastes has been reported by Kolli et al (1997). They reported that the apparent slip at the walls of measuring geometry, the internal slip in the samples, and the shear fracture could severely influence the determination of the rheological properties of solder pastes. Three different types of tests were performed on five brands of commercial grade pastes, namely the step-shear, thixotropic loop tests, and oscillatory strain sweeps. Both smooth and rough surface (using sand paper) were used to investigate the effect of wall slip. It was found that the slip effect was dominant at low shear rates. It is also concluded that the rough surfaces could be used to prevent wall slip and thus valid data can be obtained before shear fracture occurs in the sample.

In another study, Nguty et al (1999) investigated a range of solder pastes formulated for ultra-fine pitch and flip-chip applications using a wide range of rheological tests; including steady shear rheometry, oscillatory and the creep-recovery test. The paper also provided an overview of the paste printing process and solder paste composition. Their results showed that the estimated viscosities (from model fitting) at zero and infinite shear rates can be used in understanding both the aperture filling and emptying stages in the stencil printing process. The oscillatory test results were used to determine the linear viscoelastic region for the solder paste samples. The effect of creep-recovery index (on the extent of paste recovery after deformation) was investigated and successfully correlated to the aperture filling and slump behaviour of solder pastes.

Shelf life or in other words ‘the paste storage’ is a very important factor in both the manufacturing and application phases of solder pastes. This is because, leaving the solder paste for long periods may lead to separation between the flux medium and solder particles, adversely impacting on the rheological properties of solder paste and ultimately leading to poor print performance. The storage condition of solder paste (specially the temperature and humidity) is also an important issue which directly affects the shelf life of solder paste. In another study Nguty and Ekere (2000a) reported on the effect of storage conditions, and stated that the solder paste reacts with the atmosphere and the degree of reaction was found increasing exponentially with temperature and linearly with time. In a separate study, Nguty and Ekere (2000b) also investigated the effects of storage conditions and duration on the rheological properties of solder pastes. Experiments were conducted on solder paste samples kept both at room temperature and in the fridge over a period of 5 months. Results showed an increase of 60% in paste viscosity for samples kept at the room temperature. A stretched exponential model for the change in viscosity at different storage conditions was also presented. The model can be used to estimate the shelf life of solder pastes and hence can serve as a quality control tool for paste manufacturers. In addition, the paper also provides an overview of solder paste materials and its different constituents.

In another study, Nguty and Ekere (2000) investigated the rheological properties of a tin-lead solder paste and compared that with the behaviour of solar paste (a material used in the manufacture of semiconductor solar cells in the photo-voltaic industry). Steady shear and creep-recovery tests were performed using a rheometer to characterise viscous and elastic behaviours. Existing models were fitted to experimental results to highlight similarities and differences in solder and solar paste flow behaviours. It was concluded the rheological properties such as, zero shear-rate viscosity, shear thinning index and creep compliance will affect the stencil printing process of solar pastes.

In another study, He and Ekere (2001) reported on the development of a relative viscosity model for concentrated bidisperse suspensions of noncolloidal particles. The influences of particle size ratio and the volume ratio of large particles to total particles on the relative viscosity were investigated. The results from the work would be beneficial to many industrial applications where suspensions of high solid volume fractions are demanded but reasonably low viscosities are desirable from the processing viewpoint.

Dusek et al (2002) produced a report outlining the guidelines on different test methods for the rheological measurements of solder pastes and conductive adhesives. Three rheological test methods namely viscometry, Creep-recovery and Oscillation tests were identified as most commonly used and viable methods for characterizing paste flow behaviours. Although the report does not provide in-depth discussion on how to interpret the test results but it gives a good overall guideline on rheological measurements and their importance in characterizing flow-behaviours of solder pastes and isotropic conductive adhesives.

In a recent work, Billote et al (2006) studied the rheological behaviour of a solder flux and its solder pastes containing 64% volume metallic powder. Both the flux and the tin-lead solder paste used in this work were home-made. Instead of using serrated or roughened parallel-plate geometry, six-blade vane geometry was used for the rheological measurements to avoid wall-slip and sample fracture. Results from the study showed that the solder paste was highly shear-thinning and thixotropic in nature and possesses yield

stress. The maximum packing factor was also determined to be $69 \pm 2\%$ for the solder paste sample. While the work presented in this paper would be quite beneficial for the solder paste manufacturers and users, but it would rather be more interesting to see how the results are comparable to lead-free solder paste which are most widely used now-a-days because of environmental concerns.

2.4 Previous studies on thixotropic behaviour of suspensions

The term thixotropy is used to describe the time-dependent reversible change of microstructure of materials under the application of shear. According to Barnes (1997), the origin of thixotropy goes back to early 1920's when the term was originally used to describe an isothermal reversible change between gel (solid state) and sol (liquid state) due to mechanical stirring or shearing. The definition of thixotropy has changed over the years. In a recent study Mujumdar et al (2002) defined thixotropy as "...the term is generally used to describe the reversible breakdown of particulate structures under shear, structures which are frequently associated with a yield stress".

Several experimental techniques have been developed for measuring the thixotropy of suspensions. The classical approach to characterise thixotropic behaviour is the measurement of the hysteresis loop, first reported by Green and Weltmann (1943). In the hysteresis loop test, a sample is sheared at a continuously increasing, then continuously decreasing shear rate, and a shear stress-shear rate flow curve is plotted. The up and down curves do not coincide - if structural breakdown occurs, creating a hysteresis loop. The area enclosed by the loop gives a measure of the thixotropic behaviour of the material. Although hysteresis loop test provides an easy way of qualifying time-dependent behaviour, it has the major disadvantage as the hysteresis is strongly affected by the shearing cycle time, the paste shear history and maximum shear rate selected by the investigator (Mewis 1979, Barnes 1997, Nguyen et al 1998). Barnes (1997) rather suggested a step-wise experiment for characterising thixotropic behaviour, where the shear rate or stress is changed from one constant value to another with a carefully controlled prehistory.

Mewis in 1979, presented a comprehensive review of the thixotropic behaviour of various suspensions. In his careful review, Mewis traced the evolution of the term thixotropy and provided a generalised definition. In the publication, the various approaches such as hysteresis loop and constant shear rate test, which are used to measure thixotropic behaviour of suspensions, were discussed.

Fluids with internal structure e.g. emulsion, suspension and sols, can show time-dependent behaviour under the application of shear and even when shearing ceases. The characterisation of the time-dependent flow properties of these fluids is of intense importance in process design and control, for product development and also to establish relationship between structure and flow. In one earlier work, Figoni and Shoemaker (1983) investigated the time-dependent structural breakdown of commercial mayonnaise. The measured flow curves at constant shear rates were fitted with a series of two first order rate functions. The reproducibility of rheological measurements were evaluated through two-way analysis of variance (AOV) and least significant difference (LSD) tests. It was proved that unlike rheological studies with flow curves and hysteresis loops, steady shear studies could allow for the reproducible calculation of rates of structural breakdown as well as shear stress – shear rate data.

The phenomenon of structural breakdown of time-dependent fluids has been of key interest to a large number of researchers. As identified by Barnes(1997), the micro-structural approach using the structured kinetic model has been used extensively to describe structural decay of many industrial fluids. The structural kinetic theory was originated by Cheng and Evans (1965) which was then extended by Petrellis and Flumerfelt (1973) to describe the time-dependent behaviour of shear degradable crude oils. Since then the theory has been modified and simplified to describe the time-dependent flow behaviour of various materials including mayonnaise (Tiu & Boger 1974), concentrated mineral suspensions (Nguyen & Boger, 1985), starch pastes (Nguyen, Jensen & Kristensen, 1998) and more recently for concentrated yogourt and

semisolid foodstuffs (Abu-Jdayil & Mohameed, 2002; Abu-Jdayil, 2003). A modified version of the structural kinetic model is shown in equation 2.1.

Modified structural kinetic model (Nguyen and Boger, 1985): For constant shear rate condition -

$$\left[\frac{(\eta - \eta_e)}{(\eta_0 - \eta_e)} \right]^{1-n} = (n-1)kt + 1 \quad (2.1)$$

where η_0 is the initial apparent viscosity at $t = 0$ and η_e is the equilibrium apparent viscosity at $t \rightarrow \infty$. n and k are model parameters.

In one study, Ramaswamy et al. (1992) studied the time-dependent structural break-down of stirred yogurts. The two yogurt samples investigated were subjected to different shear rates between $100 - 500 \text{ s}^{-1}$ and temperatures of $10 - 25^\circ\text{C}$. The equilibrium shear stress method was used to characterise the time-dependent thixotropic behaviour of yogurts, where a constant shear rate was applied until the sample reaches equilibrium. It was revealed that shearing the yogurt samples for a period of 60 seconds was not enough to get to the equilibrium stage.

In a work by Usui (1995), a thixotropic model to study the complex rheological behaviour of coal-water mixtures was presented. The model developed was based on the assumption that the thixotropic behaviour of dispersed systems is well described by the coagulation process of the minimum sized particles contained in a dispersion system and the break-up process of coagulated clusters.

In another study, Peret et al (1996) reported on the thixotropic behaviour of fine grained mud for Eastern Canada. The authors used the traditional hysteresis-loop test to characterise the thixotropic behaviour of the mud samples. The calculated areas of the hysteresis loops were used as a measure of thixotropy. It was also shown that the hysteresis loop area could be related to the volume of the sample sheared in a time unit.

In the field of thixotropy – one of the most valuable and comprehensive review was done by Barnes in 1997. The 33-pages of review report with 167 references of published work is regarded as a compulsory reading to understand thixotropic behaviour. The review starts with the history of thixotropy along with a description of how it is evolved and understood now-a-days in different sectors of scientific community. A list of useful definitions of thixotropy has been presented. Then the mechanism of thixotropic behaviour was outlined followed by a description of typical thixotropic experiments used to characterise thixotropic materials. The importance of thixotropy in different engineering applications has been identified and discussed. The author then went on listing a large number of examples of various thixotropic systems. Finally the various kinds of mathematical theories which have been used by researchers over the years to describe thixotropic phenomena were presented.

Majumdar et al (2002) proposed a non-linear rheological model to describe the flow behaviour of thixotropic materials which exhibit yield stress. The two main routes of mathematical modelling of thixotropic behaviour namely “phenomenological” and “microstructural” approaches were reviewed. It was claimed that the proposed model can be used to predict common thixotropic phenomena, such as stress overshoot during start-up of a steady shear flow and stress relaxation after cessation of flow as well as the yielding behaviour of materials. In order to evaluate the accuracy of the model, oscillatory shear experiments were conducted on a series of concentrated suspensions of silicon particles and silicon carbide whiskers in polyethylene. Reasonable agreement between the theory and experimental data was observed.

Jdayil et al (2002) studied the flow curves and time-dependent flow properties of Tehineh, as semi-solid foodstuff. Rheological measurements were carried out using a viscometer equipped with a cup-and-bob system. Flow curves were measured at different temperatures (5 – 45⁰C) by increasing and decreasing shear rates. The time-dependency of tehineh were identified through the presence of hysteresis loops in the measured flow-curves. The flow curves of tehineh were also modelled using the power-law model as shown in equation 2.2, where τ and $\dot{\gamma}$ are shear stress and shear rate, m is consistency

coefficient and n is the flow behaviour index. The time-dependent rheological properties were investigated by shearing tehnieh samples at constant shear rates. The first order stress decay and Weltman models (equations 2.3, 2.4 and 2.5) were used to model the time-dependent flow properties. The thixotropic behaviour observed in tehineh paste was found increasing with increasing temperature. The study showed that the time to reach equilibrium viscosity was about 25 min or less for tehineh paste.

Power law model: $\tau = m(\dot{\gamma})^n$ (2.2)

First-order stress decay (with a zero equilibrium stress value):

$$\tau = \tau_0 e^{-kt} \quad (2.3)$$

First-order stress decay (with a non-zero equilibrium stress value):

$$\tau - \tau_{eq} = (\tau_0 - \tau_{eq}) e^{-kt} \quad (2.4)$$

Weltman model:

$$\tau = A_1 - B_1 \ln t \quad (2.5)$$

Hahns model:

$$\ln(\tau - \tau_{eq}) = A_2 - B_2 t \quad (2.6)$$

In the above models, t is the shearing time, τ_0 is the initial shear stress value, τ_{eq} is the equilibrium shear stress value, k is the breakdown rate constant. The parameter A_1 and A_2 represents the stress at the beginning of shearing and B_1 and B_2 represents the rate of structural breakdown experience by the sample during the shearing process.

In a recent work, Durairaj et al (2004) reported the results on the thixotropic behaviour of two suspensions: solder paste and isotropic conductive adhesive (ICA). The thixotropic behaviour was investigated through two rheological tests: (i) hysteresis loop test and (ii) steady shear rate test. The solder paste was found to exhibit a higher degree

of structural breakdown compared to isotropic conductive adhesive. The well known Weltman and Hahns models (equations 2.5 and 2.6) were applied to study the difference and similarities in thixotropic behaviour between solder paste and ICA. Among the two models Weltman model was reported to show a stronger correlation with the experimental data compared to Hahn model

In one study, the thixotropic behaviour of colloidal dispersions has been modelled by Labanda et al (2004) by taking into account the equilibrium viscosity, structural level, thixotropy time, and elasticity. The proposed model with eight parameters has been satisfactorily used to predict thixotropic behaviour of two colloidal dispersions of different polymers. For the polymers tested it was found that the rate of structural breakdown was greater than the rate of structural build-up.

In a more recent work, Wallevik (2005) presented a rheological model to simulate thixotropic behaviour of cement paste. The model is based on the microstructural approach and can be used to explain transient effects commonly observed in cement pastes. Experiments were carried out by measuring torque under complicated shear flow. Predictions from the model were validated using data/results from these experiments. The results from the work highlighted that the thixotropic behaviour of cement paste mostly governed by a combination of reversible coagulation, dispersion and then re-coagulation of the cement particles.

Maingonnat et al (2005) studied the time-dependent build-up of a thixotropic clay suspension. Rheological test methods were designed in such a way the fluid structure was first broken down with a high pre-shear and then allowed to build-up with a low shear rate. The behaviour was modelled with the stretched exponential model as shown in equation 2.7:

$$\eta(t) = \eta_{e0} + (\eta_{e\infty} - \eta_{e0})(1 - e^{-(t/\sigma)}) \quad (2.7)$$

where σ is a characteristic time. The term $\eta_{e\infty}$ is the viscosity value at equilibrium and the term η_{e0} is the fluid viscosity when the structure is completely broken down. From the observation of experimental and model results it was suggested that the build-up phenomenon was only due to a yield stress development in the fluid.

In a recent study, Choi and Yoo (2005) have investigated the time-dependent flow properties of commercial kochujang (hot pepper – soybean paste), which is a fermented food suspension of solid particles dispersed in a continuous medium. The time-dependency of kochujang was examined at various shear rates (5, 15, 25 and 35 s⁻¹) and temperatures (5, 15 and 25°C). The result showed that the stress decay of the suspension dependent on the shear rate and temperature. To quantify the time-dependency of kochujang samples, shear stress – time of shearing data were fitted to three time-dependent models (Weltman, Hahn and Figoni and Shoemaker models). The results from the model-fitting re-strengthen the fact that the time-dependent flow behaviour of Kochujang samples very much dependent on shear rate and temperature. Among the three models both Weltman and Hahn models gave better overall predictions of the experimental data and hence have been recommended for commercial kochujang.

In another recent work by Roussel (2005), the time-and shear-dependant apparent viscosity of cement paste was experimentally and theoretically analysed. A four-parameter thixotropic model was presented, where the parameters were identified using experimental couette viscometer results obtained for one cement paste. Unlike other models, the proposed model allows the prediction of both steady state and transient flows. Although the model presented have been used to quantify the effect of the thixotropy of cement pastes in several flow conditions, a more complex model with higher parameters was recommended for complete quantitative prediction of flow conditions.

In another work, Labanda & Llorens (2006) proposed a mathematical model to describe the thixotropic behaviour of colloidal dispersions. In contrast to the structural kinetic model (SKM) and stretched exponential model (SEM) used in this thesis work (see chapter 6 and 7 respectively), which describes the kinetic process of structural

breakdown and build-up, the proposed model accounts for the viscoelastic behaviour of the dispersions. Although the model developed would be useful for dispersions and other similar material, its application is rather complicated with too many parameter (a total of 10) to evaluate independently using distinct rheological tests.

In a very recent work, Phair et al (2008) used rheological methods to study the thixotropic characteristics of concentrated zirconia inks for screen printing. Step-shear rate, viscosity, creep-recovery and yield stress experiments were performed and modelled to investigate thixotropic levelling characteristic of the ink. Results from the study showed an increase in yield stress, rate of recovery and extent of recovery with increasing binder (ethyl cellulose) content in the ink. Screen printing results from the study however, revealed that the inks with higher binder content would be more difficult to print.

2.5 Summary

The literature review carried out in this chapter has indicated the importance of solder paste and the stencil printing process in the electronics manufacturing. The significance of studying the time-dependent behaviour of solder pastes has also been demonstrated. But most importantly, the literature presented here has served as a base for this project work, the results of which are outlined in rest of the chapters.

The literature review presented in the first section (section 2.1) highlighted the challenges in the selection and formulation of solder pastes and also the development and optimization of printing process and its parameters. The literatures reported clearly showed that the investigation into the areas of new lead-free solder paste formulations and their effect on the solder paste printing process still remains outstanding. The work presented in this thesis addresses these issues specially the time-dependent characteristics of lead-free solder paste formulations (see chapter 5) and their co-relation to the printing performance (see chapter 8).

Previous studies on the rheological characterisation and modelling of solder pastes have been reviewed in the second part of this chapter. Most of the literatures reported in this section are based on investigation carried out using lead-based solder pastes and till now very little work has been found on rheological characterisation of lead-free solder pastes and new paste formulations for ultra-fine pitch applications.

The literatures presented in the final section on the time-dependent thixotropic behaviour of suspensions have identified the intense need to characterise and model the thixotropic behaviour of solder pastes and flux mediums. Although the study of time-dependent behaviour/properties of solder paste has propound importance in terms of its development and application processes, this has never been explored properly. The lack of data/information in this field has served as the motivation to develop techniques to characterise and model the time-dependent structural break-down and build-up of solder pastes and flux mediums (see chapter 6 and 7).

CHAPTER 3

FUNDAMENTALS OF RHEOLOGY

3.1 Introduction

The term *rheology* is defined as the science of deformation and flow of matter. The word “rheology” was first used by Eugene C. Bingham in 1928 who also described the motto of the subject as *πανταρει* (“panta rhei”, from the works of Heraclitus, a pre-Socratic Greek philosopher active about 500 B.C.) meaning “everything flows” (Steffe, 1996). The field of rheology is very much interdisciplinary and is used to describe interrelation between the applied stress, deformation and time for a wide range of materials such as rubber, oils, molten plastics, inks, polymers, slurries and pastes, blood, clays, paints etc. These materials show remarkably different rheological properties that classical fluid mechanics and theory of elasticity can not describe. In this respect, rheology may also be defined as a science concerned with the behaviour of real materials, which during deformation exhibit more than one fundamental rheological property such as elasticity or viscosity. Thus, rheology describes phenomena which occur in a very broad intermediate range between the solid and fluid states of matter (Ferguson & Kemblowski, 1991)

The main focus of this chapter is to provide an introduction to rheology with an emphasis on suspension rheology. The chapter is made up of four sections. The first two sections outline the fundamentals of various types of materials and the classification of different types of fluids. The third section provides details on fundamental concepts of suspension rheology. The fourth and final section explains the basic mechanism of time-dependent response in suspensions.

3.2 Elastic, viscous and Viscoelastic materials

Elastic materials are those that deform under the application of external stress and returns to their original shape once stress is removed, provided that the applied stress is small enough and does not cause any permanent deformation. When solid materials undergo deformation, under the application of external stress, stretching of intermolecular bonds occurs. The resulting internal stress balances the external stress and an equilibrium can then be achieved (Ferguson & Kemblowski, 1991). The rheological properties of an elastic material may be described by Hooke's Law which states, in its simplest form, that the applied stress is directly proportional to deformation and does not depend on the rate of deformation. If τ_E is the applied stress and γ is the resulting strain, the Hooke's Law can be expressed mathematically as:

$$\tau_E = E\gamma \quad (3.1)$$

The coefficient of proportionality is called the Elastic (or Young) modulus, E . A simple mechanical analogue for elastic materials is that of a spring attached to a rigid wall. Within the elastic limit, the deformation in a spring due to external stresses (or forces) is recoverable. However, if the applied stress (or force) is too great then the material will stretch beyond its elastic limit and will eventually yield. This will cause permanent deformation to the material, known as the plastic deformation.

A *viscous* material is one which undergoes continuous deformation in response to the application of external stress. In contrast to elastic materials, viscous materials will not return to their original state on removal of the stress. The viscous materials deforms even with the application of a small external stress, because of the great mobility of molecules, but internal frictional forces retard the rate of deformation and cause an equilibrium state. In this way constant external stress results in a constant rate of deformation (Ferguson & Kemblowski, 1991). The rheological properties of viscous materials may be described by Newton's Law, which states that the applied stress is

directly proportional to the rate of deformation and does not depend on the deformation itself.

As shown in figure 3.1, in the case of a viscous flow, the fluid layers move at different velocities. The friction between the fluid and the moving boundaries cause the fluid to shear and the force required for this action is a measure of the fluid's viscosity (resistance of a fluid to deformation under shear stress). According to Newton's Law, the applied shear stress, τ , between the liquid layers is proportional to the velocity gradient, $\partial u/\partial y$ and can be expressed as:

$$\tau = \eta \frac{\partial u}{\partial y} \quad (3.2)$$

The proportionality coefficient η is known as the *coefficient of viscosity, viscosity, or dynamic viscosity*. The velocity gradient ($\partial u/\partial y$) across the gap is nothing but the rate of deformation, which is more commonly known as the *shear rate, $\dot{\gamma}$* . The equation 3.2 can therefore be rewritten as:

$$\tau = \eta \dot{\gamma} \quad (3.3)$$

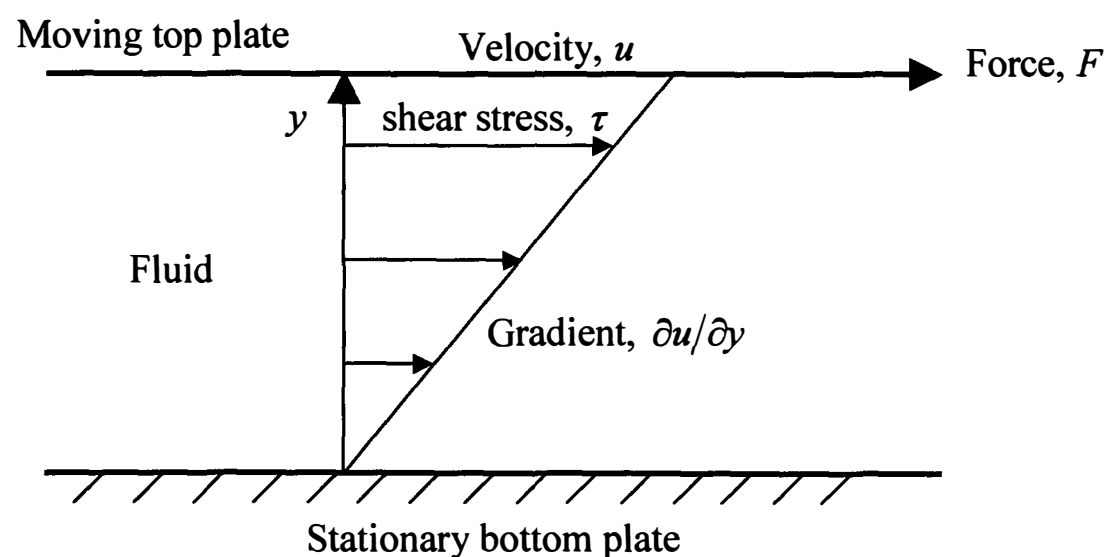


Figure 3.1: Schematic illustration of typical Newtonian fluids flow.

Viscoelastic materials are complex materials which exhibit elastic and viscous behaviours simultaneously. The behaviour of viscoelastic materials may be presented by combining springs, elastic elements and dashpots, viscous ones in series or in parallel. The two simplest models constructed in this way are the Maxwell model and the Kelvin (or Voigt) model.

The Maxwell model consists of a spring (elastic element) and a dashpot (viscous element) combined in series, shown in figure 3.2(a). When a force is applied onto the combined unit, the spring stretches first. If given enough time, the dashpot will also start to deform and the spring will gradually return to its original shape. Upon cessation of the applied force, the element does not necessarily return to its original shape, because of dissipation of energy during the flow. The mathematical presentation of the model, also known as Maxwell equation, has the following form (Macosko, 1994):

$$\tau + \lambda \frac{d\tau}{dt} = \eta \dot{\gamma} \quad (3.4)$$

where λ is the relaxation time; $\tau, \dot{\gamma}, \eta$ are shear stress, shear rate and viscosity respectively.

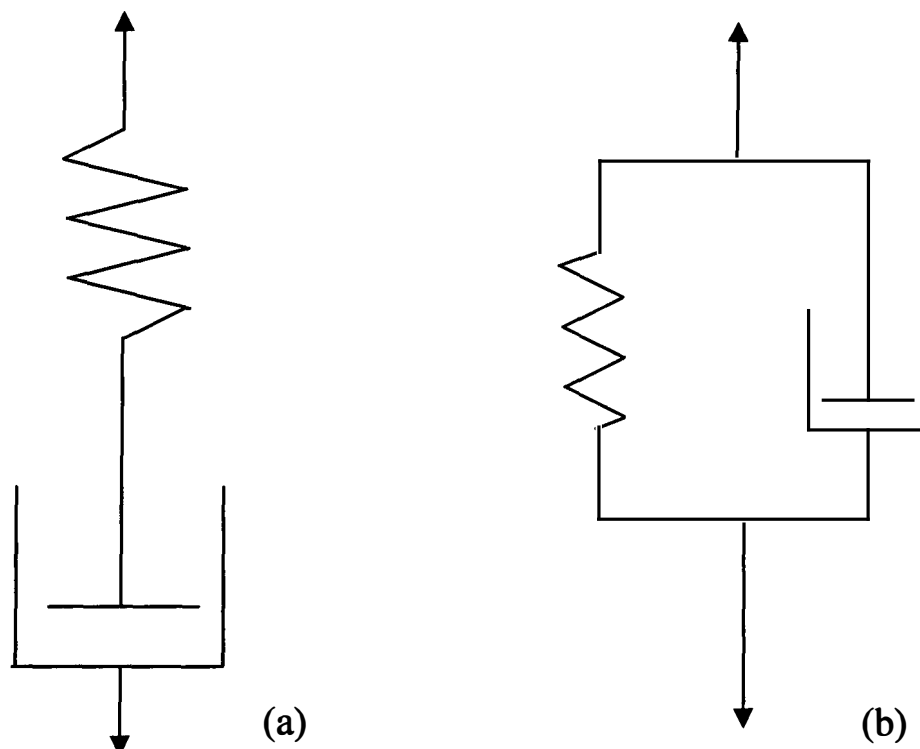


Figure 3.2: Spring and dashpot representation of (a) Maxwell model and (b) Kelvin model.

The Kelvin (Voigt) model is a parallel combination of a spring and a dash-pot, as shown in figure 3.2(b). When an external force is applied to the unit, the stretching of the spring and the flow of the dashpot occur simultaneously. As the flow progresses, the spring tends to increase restoring force to prevent flow. When the force is stopped, the material will ultimately return to its original dimensions. Because of the presence of the dashpot, the recovery process will also be slow. The model can be expressed mathematically (Kelvin equation) in the following form (Ferguson & Kemblowski, 1991):

$$\tau = G\gamma + \eta\dot{\gamma} \quad (3.5)$$

where G is the spring modulus and γ is the strain.

3.3 Non-Newtonian Behaviour of Fluids

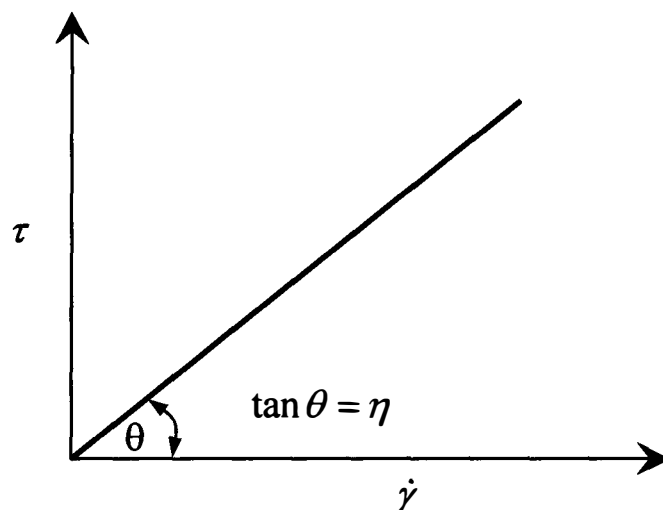


Figure 3.3: Flow curve of a Newtonian fluid

A Newtonian fluid is one which exhibits a linear relationship between the shear stress τ and the shear rate $\dot{\gamma}$. This implies that, for a Newtonian fluid the diagram relating shear stress and shear rate will be a straight line through the origin. Such a plot of τ vs $\dot{\gamma}$ is called the flow curve, figure 3.3 shows an example of a flow curve of a Newtonian fluid. Fluids which do not obey Newton's Law of viscosity or in other words

fluids for which the flow curve ($\tau = f(\dot{\gamma})$) is not linear through the origin at a given temperature and pressure are regarded as non-Newtonian.

Many of the fluids encountered in everyday life (such as water, air, gasoline, and honey) can be satisfactorily described as being Newtonian, but there are even more that are not. Common examples include mayonnaise, yogurt, peanut butter, toothpaste, egg whites, liquid soaps, and multigrade engine oils. Other examples such as molten polymers and slurries are of considerable technological importance. A distinguishing feature of many non-Newtonian fluids is that they have microscopic or molecular-level structures that can be rearranged substantially during the flow (Sci-Tech Encyclopedia, 2005).

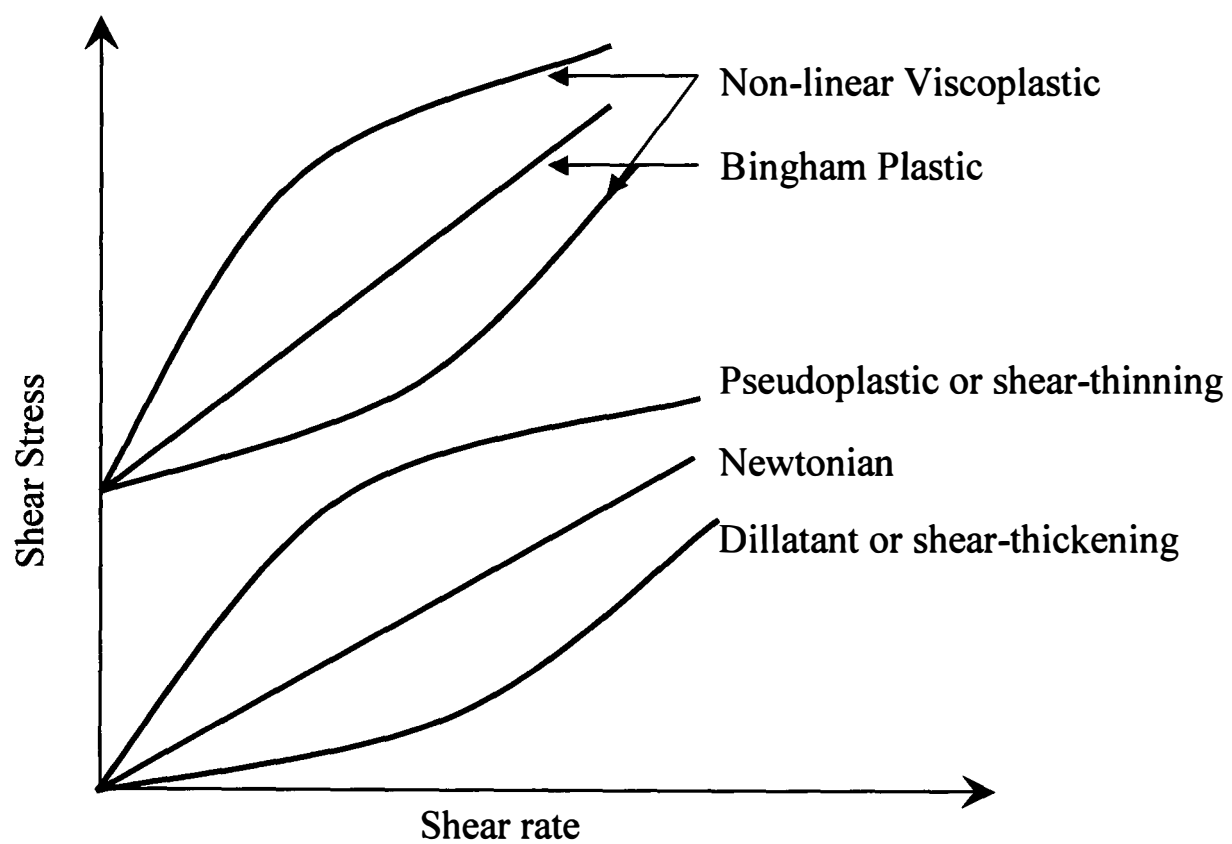


Figure 3.4: Flow curves of fluids without a yield stress and with a yield stress.

3.3.1 Non-Newtonian Fluids without a yield stress

Pseudoplastic Fluids

Pseudoplastic or shear thinning fluids are recognized as fluids for which the shear stress increases less than in proportion to shear rate (figure 3.4). Pseudoplastic fluids may also be identified as fluids whose apparent viscosity or consistency decreases with an increase in shear rate. Fluids of this type are usually suspensions of solids or large polymeric molecules in a solvent with smaller molecules. Pseudoplasticity is regarded as the most common phenomenon of non-Newtonian behaviour among the others. Common examples of pseudoplastic fluids include ketchup, blood, paint, printing ink and nail polish. It is generally assumed that the large molecular chains/particles (of pseudoplastic fluids) will be at completely random position at rest. With increasing shear rate a progressive alignment of the particles/chains along the streamline will occur, which will produce less resistance. Hence, a decrease in viscosity or shear-thinning behaviour will be observed.

Dilatant Fluids

Dilatant or shear thickening fluids are characterized as fluids for which the shear stress increases more than in proportion to the shear rate. This type of fluid also defined as fluid whose apparent viscosity increases with an increase in shear rate. Highly concentrated suspensions of solid particles in liquid are often capable of shear thickening behaviour over certain range of shear rates. The degree of shear thickening and its onsets is a function of the solids concentration, the particle shape and size distribution (Durairaj, 2006). At rest the particles are assumed to be distributed in such a way that the void space, filled with liquid, is at a minimum. At low shear rates the friction between the particles is comparatively low, as the liquid acts as a lubricant. As the shear rate increases the particles becomes more disordered and there may be insufficient liquid to fill the space between the particles leading to direct particle-to-particle contact, which causes an increase in the apparent viscosity of fluid or shear thickening behaviour (Ferguson &

Kemblowski, 1991). A common example of shear-thickening fluid is an uncooked paste of cornstarch and water. Under high shear the water is squeezed out from between the starch molecules, which are able to interact more strongly.

The power law model of Ostwald-de Waale (Ostwald, 1926) can be satisfactorily used to model the rheological behaviour of pseudoplastic and dilatant fluids

$$\tau = k\dot{\gamma}^n \quad (3.6)$$

where the parameter k is defined as the pre-exponential factor or consistency index and n as the exponential factor or the flow behaviour index. The value of constant k gives an indication of the viscous behaviour of the fluid, while the value of the index n describes the extent of the deviation of the fluid behaviour from Newtonian behaviour. For pseudoplastic fluids n must be less than unity. If n is equal to one, then equation 3.6 reduces to the Newtonian model, equation 3.3 and k becomes the Newtonian viscosity, η . When n is greater than one, the fluid is said to exhibit a shear thickening behaviour.

3.3.2 Non-Newtonian Fluids with a yield stress

The yield stress is defined as the limiting shear stress at which the material starts to flow. As outlined by Ferguson and Kemblowski (1991), the phenomenon of yield stress occurs in two- or multi-phase systems, in which one or more phases are dispersed in the form of particles or bubbles in the continuous liquid phase. At high concentration of the dispersion an interaction between the dispersed particles or bubbles may lead to the formation of a three-dimensional structure which is capable of resisting shear stress up to certain value. Below this yield value the material behaves like an elastic solid. It may be assumed that when the yield value is reached, the structure breaks down instantaneously and completely and the material starts to flow as a viscous fluid. On the other hand, an instantaneous and complete build-up of the structure occurs when the shear stress becomes less than the yield value. Fluids with a yield stress are sometimes referred to as

viscoplastic fluids and broadly classified into two types: Bingham plastic and non-linear (or non-Bingham) viscoplastic fluids.

Bingham Plastic fluids

As shown in figure 3.4, Bingham plastic fluid is the simplest type of yield stress fluid represented by a straight line with an intercept τ_y on the shear stress axis. The flow curve of this type is described by the Bingham model (Bingham, 1922):

$$\tau = \tau_y + \eta_p \dot{\gamma} \quad (3.7)$$

Bingham fluids exhibit a yield stress τ_y at zero shear rate, followed by a linear relationship between shear stress and shear rate, the plastic viscosity being the slope of the straight line. If $\tau < \tau_y$, no flow takes place. The behaviour of many real fluids such as slurries, household paints and plastics can be adequately explained with this model.

Non-linear Viscoplastic Fluids

As shown in figure 3.4, non-linear viscoplastic fluids can be of two types: yield pseudoplastic and yield dilatant. Like Bingham plastic these fluids also possess a yield stress. However, the flow curve afterwards is not linear as opposed to Bingham fluids. A yield-pseudoplastic fluid is similar to a pseudoplastic (or shear thinning) fluid except that it requires a minimum shear (yield stress) to behave like a fluid. On the other hand, a yield-dilatant fluid is similar to a dilatant (or shear thickening) fluid but requires a yield stress. The simplest rheological model for the flow curves of non-linear viscoplastic fluids is the Herschel-Bulkley model

$$\tau = \tau_y + k\dot{\gamma}^n \quad (3.8)$$

Equation 3.8 is quite similar to the power law model (equation 3.6) except that it has an additional yield stress term τ_y . Like power law fluid, the value of constant k gives an indication of the viscous behaviour of the fluid, while the value of the index n describes the extent of the deviation of the fluid behaviour from Newtonian behaviour. For yield-pseudoplastic fluids the value of n will be less than unity. If n is equal to one, then equation 3.8 reduces to the Bingham model (equation 3.7). When n is greater than one, the fluid is regarded as yield-dilantant.

3.4 Rheology of Suspensions

Suspensions, an important subdivision of dispersions, consists of solid particles distributed in a liquid medium. The other subdivisions of dispersions are: emulsions (liquid droplets in a liquid medium) and foams (gas in a liquid medium). All these subdivisions have great practical importance in our every-day life and comprise the single most important area of rheological research. The rheological behaviour of dispersions are greatly influenced by the following factors (Mazzeo, 2002):

- Volume concentration of the dispersed phase
- Viscosity of suspending medium
- Size of the dispersed phase
- Size distribution of the dispersed phase
- Surface chemistry of the dispersed phase
- Shape of the dispersed phase

The addition of particles to a liquid not only changes its viscosity but it can also introduce non-Newtonian behaviour. This is illustrated in figure 3.5 (adapted from Mewis and Macosko (1994)) for various concentrations of a polymer latex. The occurrence of shear thinning and shear thickening is quite obvious in this figure. At high concentrations and low shear stress, the Newtonian plateau seems to disappear and to develop into a yield stress. At shear stress exceeding 10^3 s^{-1} , the high concentration samples display shear thickening.

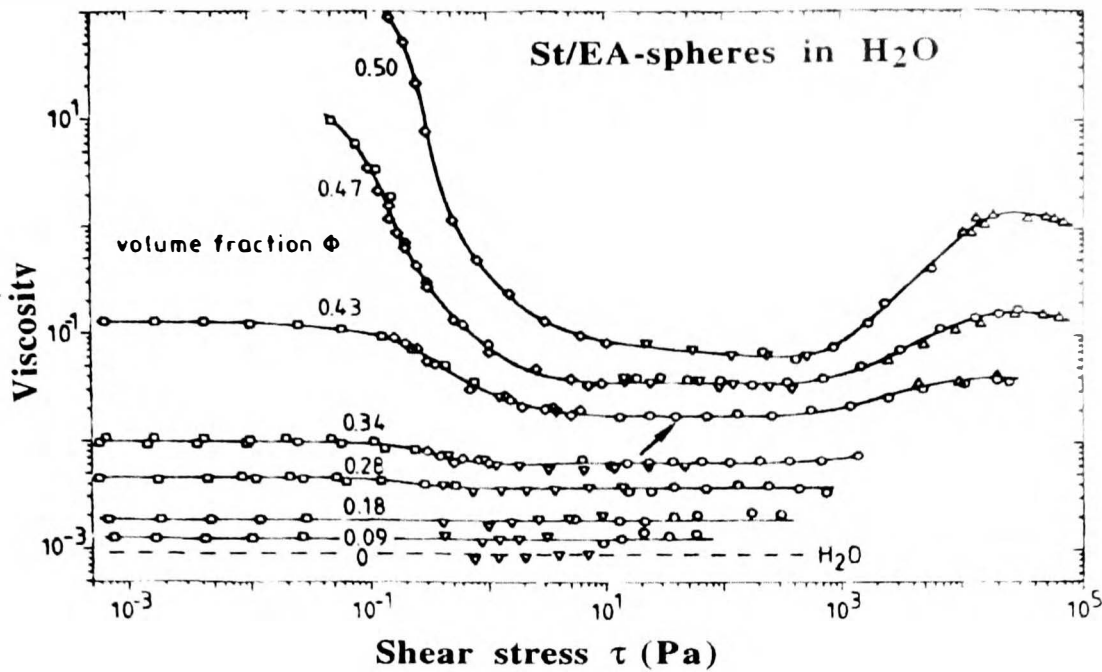


Figure 3.5: Viscosity Vs shear stress for a polystyrene ethylacrylate latex at different volume fractions (Mewis and Macosko, 1994)

3.4.1 Particle-Particle Interactions – Interparticle Forces

The particle-particle interaction in a suspension becomes increasingly significant as the volume fraction grows larger than 0.01 (Macosko and Mewis, 2004). The resulting disturbance of the flow increases the viscosity. At relatively small concentrations only binary interactions are likely to occur. With increasing concentration, more than two particles can interact simultaneously. This causes the viscosity to grow at an increasing rate with concentration. Different kinds of force (described below) are active in particle interactions. Depending on their relative magnitude, the microstructure and the rheology of the suspension can vary widely.

a) *Van der Waals forces*

Van der Waals force refers to the attractive or repulsive forces between molecules (or between parts of the same molecule) of the same substance. They are also known as

intermolecular forces. Van der Waals forces are quite different from the forces that make up the molecule i.e. intramolecular forces (such as covalent and ionic bonds) in that they are not stable and hence relatively weak in nature.

Dispersion forces

Dispersion forces are temporary attractive forces that result when the electrons in two adjacent molecules occupy positions that make the molecules form temporary dipoles. They are also known as London dispersion forces, named after German-American physicist Fritz London who first suggested how they might arise. Both the molecular size and shape significantly affects the strength of the dispersion forces. Larger and heavier atoms and molecules exhibit stronger dispersion forces than smaller and lighter ones. Bigger molecules have more electrons and more distance over which temporary dipoles can develop and therefore the bigger the dispersion forces. The shapes of the molecules also matter. Long thin molecules can develop bigger temporary dipoles due to electron movement than short fat ones containing the same numbers of electrons.

Dipole-dipole forces

Dipole-dipole forces occur in polar molecules, that is, molecules that have an unequal sharing of electrons. For instance, a HCl molecule has a permanent dipole because chlorine is more electronegative than hydrogen. These permanent, in-built dipoles will cause the molecules to attract each other rather more than they otherwise would if they had to rely only on dispersion forces. It's important to realize that all molecules experience dispersion forces. Dipole-dipole interactions are not an alternative to dispersion forces – they occur in addition to them.

b) Electrostatic Forces

Electrostatic forces refer to the attractive or repulsive forces between the charged particles in a suspension, when they are at rest. The relative charges on the two particles

are what determine whether the force between the charged particles will be attractive or repulsive. If the particle surfaces are of opposite charges they attract each other, while if their charges are similar they repel themselves. In the case of a suspension, the electrostatic forces are most important where the continuous phase is polar. The presence of charges on the particle surface often facilitates the formation of a “electrical double layer” around the particle with charges of opposite sign from the continuous phase. The presence of this electrical double layer has a profound effect on suspension viscosity. The following three electroviscous effects may be addressed (Ferguson & Kimblowski, 1991):

1. For very small particles, an enhancement of the viscosity will be observed due to the work required during flow to maintain the distortion of the diffuse (outer) part of the electrical double layer will be observed.
2. Where the particles are of similar charge, the electrical repulsion between the particles will ultimately lead to an increased particle-particle collision. This will result in an increase in viscosity.
3. Coating of particle surface with polyelectrolytic stabilizers could also affect the suspension viscosity. Because the pH and electrolyte concentration in an aqueous continuous phase change, the polyelectrolyte conformation will alter in response, changing the viscosity.

c) Steric Forces

Steric forces refer to the interparticle forces which arise due to the presence of polymer layer onto the particle surface. A stable structure within suspension can be produced (in polar and non-polar media) by coating the particles with polymer molecules (Ferguson & Kimblowski, 1991). The coating on the particle surface can be held either by absorption or by chemical grafting. Main effects contributing to steric repulsion are (Paunov, 2002): i) excess osmotic pressure due to overlapping of polymer segments and ii) elastic effect due to deformation of polymeric chains. When two polymeric chain molecules comes close to each other, the limited interpenetration of the long chain

molecules attached to the opposite surfaces leads to effective repulsion due to osmotic pressure and elastic effects. The potential energy allows a stable particle-particle distance to be established.

3.4.2 Factors Influencing Suspension Rheology

In addition to the interparticle forces discussed in the previous section, the particle size, volume fraction, particle size distribution and particle shape can have significant effect on the rheological behaviour of suspensions. The details of these factors are outlined below:

a) Particle Size

Experimental and theoretical studies reported by Mcketta and Cunningham (1990) has shown that the absolute size of particles has no effect on suspension rheology provided that the particles are well dispersed in suspension and are influenced by hydrodynamic forces only. However, these two assumptions do not hold for solder paste samples reported in this work. The particles in a solder paste are not perfectly dispersed as they always tend to flocculate themselves on rest and are influenced by various forces including hydrodynamic, Brownian forces and electrostatic forces. Mcketta and Cunningham (1990) also found that in reality, the rheological data of suspension do vary with the variation in particle size, due to various reasons, such as:

- The presence of an absorbed layer of molecules on the particle surface, in the case of stabilized aqueous solution. The additional layer will increase the solid volume. This will result in a increase in viscosity with decreasing particle size, if the particle volume concentration and shear rate are constant.
- The effect of Brownian movement forces on flow properties when the particle size is reduced down to micron sizes. Owing to particle collisions arising from Brownian motion, the suspension viscosity tends to increase with decreasing particle size.

- The increased importance of electrostatic forces, when the particle size is reduced to the order of μm or below.

If the mass of particles in a suspension is kept constant, reduction in particle size will lead to an increase in the number of particles in the system. The effect of this change on viscosity is illustrated in figure 3.6 for a system of latex particles in a pressure sensitive adhesive. A higher number of smaller particles results in more particle-particle interactions and an increased resistance to flow due to structure formation. As shear rate increases, this effect becomes less obvious, suggesting that any particle-particle interactions are relatively weak and can be broken down at high shear rates.

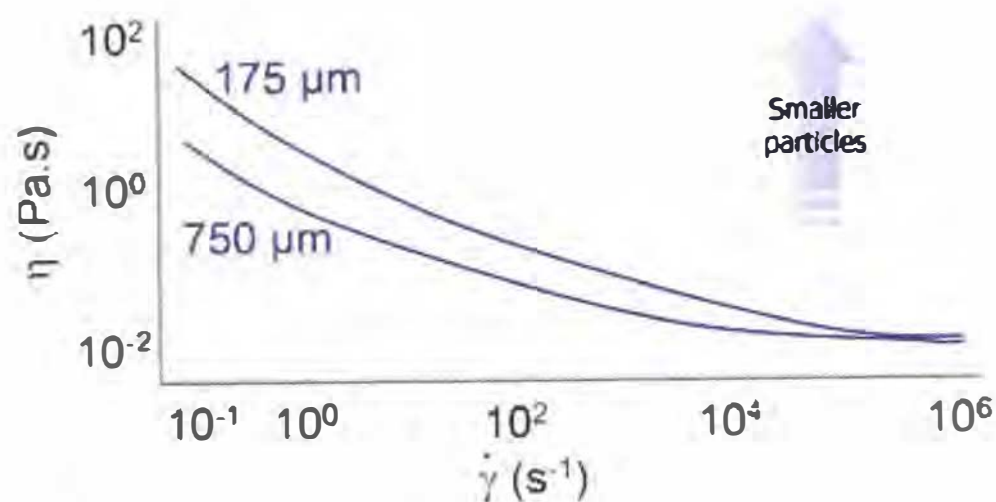


Figure 3.6: The effect of particle size on viscosity (from Fletcher and Hill, 2008)

b) Volume Fraction

The viscosity of the suspension normally increases with increasing volume fraction of particles. This is illustrated in figure 3.7 in a relative viscosity V_s volume fraction plot for a silica suspension in cyclohexane. At higher values of volume fraction, the particles become more closely packed together. The interaction between the particles will increase as their movement becomes more restricted, which leads to an increase in viscosity. Also a rapid increase in viscosity can be observed as the particle concentration

approaches the maximum volume fraction (ϕ_m) of particles that can be accommodated in the suspension before flow ceases.

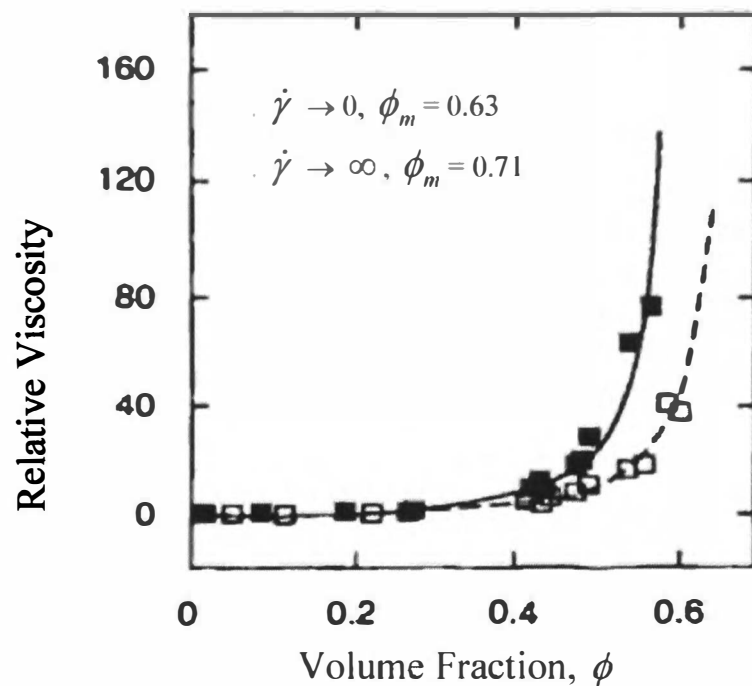


Figure 3.7: Relative viscosity versus volume fraction of particles for sterically stabilized suspensions of silica spheres (radius = 110 nm) in cyclohexane, for low and high shear rates (from Rahaman, 2003)

In addition to the influence on the value of viscosity, volume fraction also affects the nature of the relationship between the shear rate and viscosity (i.e. the flow behaviour) for suspensions (Fletcher and Hill, 2008). Suspensions with relatively low volume fraction tend to behave like Newtonian fluids, with viscosity independent of shear rate. Increasing volume fraction leads to shear-thinning behaviour. The transition is illustrated in Figure 3.8 for a latex/pressure-sensitive adhesive system.

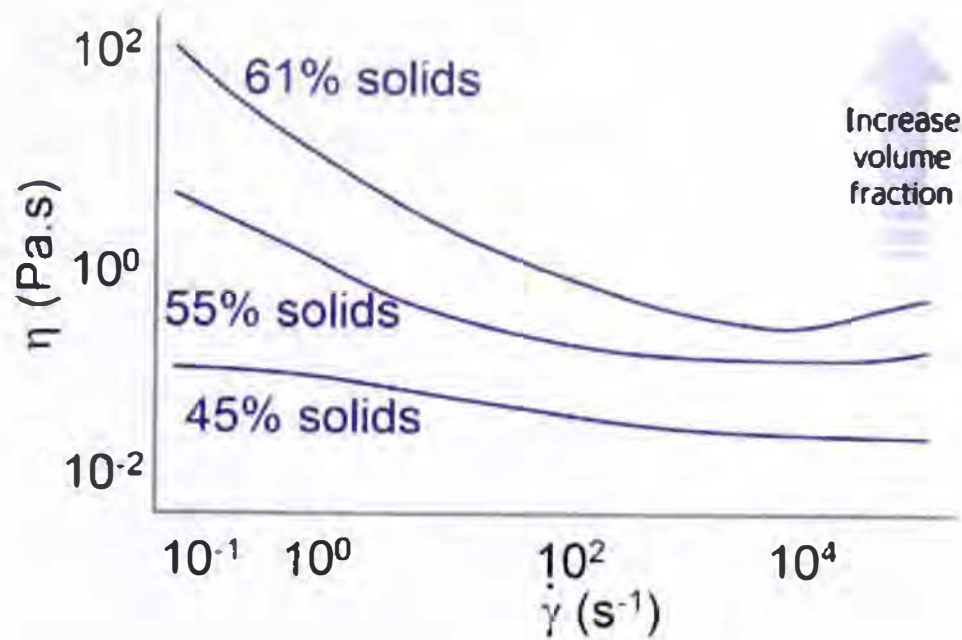


Figure 3.8: Viscosity as a function of shear rate for different volume fractions, for a latex/pressure-sensitive adhesive system (from Fletcher and Hill, 2008)

c) Particle Size Distribution

The packing of particles can be significantly improved by mixing spheres of two different sizes (bimodal distribution) or by using a broad, continuous particle size distribution (Rahman, 2003). The maximum packing fraction for monodisperse suspension lies at around 62%. A polydisperse suspension, on the other hand, could have a maximum packing fraction of around 74%, as smaller particles can effectively fill the gaps between larger ones. The viscosity of a suspension is generally reduced by increasing the particle size distribution (PSD) for a given volume fraction of solids. The PSD can be used as an effective tool for controlling the viscosity of a system that has a fixed volume fraction. Up to 50-fold reductions in shear viscosity due to changes in PSD, whilst maintaining the same solid content, have been reported (Barnes et al., 1989)

Viscosity as a function of fraction of large or small talc particles is shown for an epoxy in figure 3.9. The viscosity at maximum volume fraction (for bimodal dispersion) is lower than that can be achieved using a monodisperse sample of either sized talc. These results show how particle size distribution can be used to manipulate viscosity. If

the requirement is for a higher solids loading but the same viscosity, then this can be achieved by broadening the particle size distribution. Conversely, viscosity can be increased by using particles with a narrower size distribution.

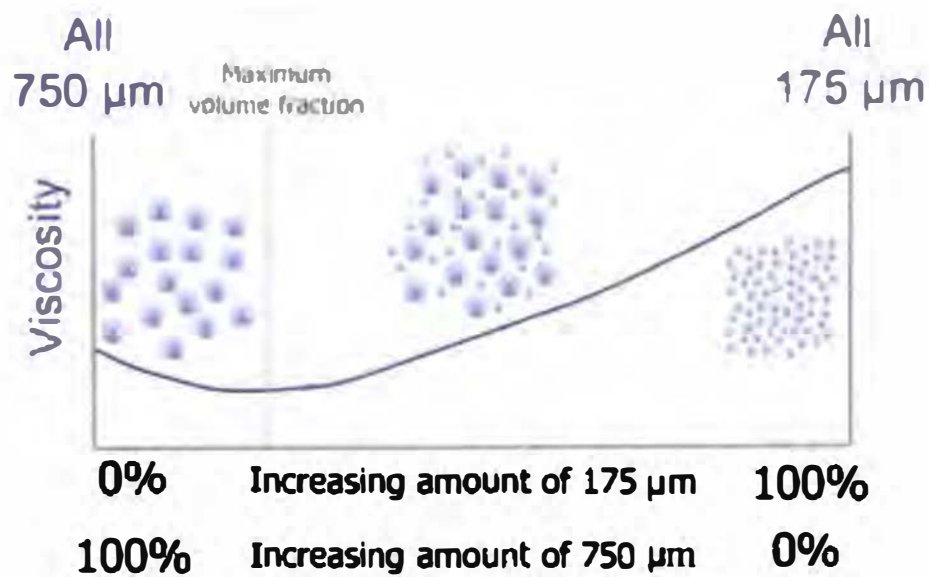


Figure 3.9: Viscosity as a function of polydispersity (from Fletcher and Hill, 2008)

d) Particle Shape

The viscosity of suspension is generally known to increase if the shape of suspended particles is changed from spherical to non-spherical (Macosko & Mewis, 1994). The Maron-Pierce equation can be used to describe a large number of suspensions (Ferguson & Kemblowski, 1991):

$$\eta_r = \frac{1}{(1 - c/c_{max})^2} \quad (3.9)$$

where η_r is relative viscosity (ratio of system viscosity to the continuous phase viscosity) and c is a constant representing the packing geometry. The maximum packing value c_{max} , varies from between 0.74 and 0.63 for monodisperse spheres, to 0.18 for fibres with an aspect ratio (ratio of major axis to minor axis) of 27 (Ferguson & Kemblowski, 1991). Thus, for a given volume concentration c , η_r will increase as particle aspect ratio increases.

3.5 Time-dependent Behaviour of Suspensions

The rheological properties of concentrated suspensions often depend not only on the shear rate but also on the length of time. When the viscosity decreases with time under shear but recovers to its original value after flow ceases, the behaviour is known as thixotropic. This type of behaviour is more often observed in flocculated suspensions and colloidal gels (Rahman, 2003). When the suspension is sheared, the flocs are broken down leading to a distribution of floc sizes. Often the regeneration of the flocs is slow which causes the resistance to flow to decrease. The opposite behaviour, when the viscosity increases with shear rate and is also time dependent, is known as rheopectic. In practice, rheopectic behaviour is often undesirable because at high shear rates the suspension becomes too stiff to flow smoothly.

As stated by Barnes (1997) – “all liquids with microstructure can show thixotropy, because thixotropy only reflects the finite time taken to move from any state of microstructure to another and back again”. Characterising the degree of thixotropy in pastes such as solder pastes and flux mediums is an important step in understanding the rheological behaviour of the material during stencil printing. According to Ferguson and Kemblowski (1991), a thixotropic fluid is one that is characterized by the following features:

1. Structure develops while the fluid is at rest.
2. The structure can be destroyed by the application of shear.
3. The process of destroying and rebuilding of the structure is reversible and occurs isothermally.
4. In laminar shear flow, under conditions of constant shear rate, the fluid behaves as follows:
 - The shear stress decreases with time if the fluid was previously at rest or was sheared under conditions of lower shear rate.
 - The shear stress increases with time if the fluid was previously sheared under conditions of higher shear rate.

- No matter what were the previous shear conditions, if an applied shear rate is maintained constant for sufficiently long time, shear stress approaches an equilibrium value dependent only on the shear rate.
5. The response of shear stress to an abrupt change of shear rate is immediate (there is no delay characteristic of elastic response).

All these thixotropic characteristics are quite desirable for solder pastes in relation to the stencil printing process. During stencil printing, solder paste's structure breaks down under the application of shear and it behaves like a fluid so that it can flow through holes and produces good deposits. However, when printing ceases the solder paste needs to recover its structure in order to prevent slumping.

The mechanism of thixotropy may be explained as the result of aggregation of the suspended particles (Ferguson & Kemblowski, 1991). In a typical suspension system, interaction between the particles occurs as a result of the attraction due to van der Waals forces and also the repulsion due to electrostatic and steric forces. Because of the presence of repulsive forces, a potential barrier forms which prevents the particles from approaching close to one another. The comparatively weak physical bonds between the particles developed in this way give rise to aggregation. When no force is exerted on the suspension, the particle aggregation can form a spatial network and the suspension develops an internal structure. If the suspension is sheared, the weak physical bonds are disrupted and the network breaks down into separate aggregates which can disintegrate further into smaller fragments or flocs. A structural build-up also occurs at the same time due to thermal motions which cause collisions between the flow units, and a consequent growth in the number of aggregates. After some time at a given shear rate, a dynamic equilibrium is established between aggregate destruction and growth, and at higher shear rates the equilibrium is shifted in the direction of greater dispersion.

A qualitative way of testing for the existence of thixotropy is the "hysteresis loop test". A typical test procedure involves exposing a mechanically stable (rested for long

period of time) thixotropic fluid to a shear rate which increases continuously from a low value to some maximum value, and after reaching this point starts to decrease continuously back to the low shear rate value. Because of the breakdown of the fluid structure which occurs during the experiment a flow curve with a hysteresis loop is usually observed. Figure 3.10 shows a typical example of flow curve with a hysteresis loop, with the arrows indicating the chronology of the process. The area between the hysteresis loop is sometimes used as a measure of the ‘amount’ of thixotropy. From the figure 3.10, it can be derived that the unit of the area between the hysteresis loop is Jules/sec². Therefore, the area between the hysteresis loop represents change in the rate of energy to breakdown the material structure with time. In other words, the hysteresis loop area gives an indication of the strength of the materials under the application of shear. A high value of the area would usually mean that the material possesses a weak structure and is quite easy to breakdown when shear is applied. A low value of the area, on the other hand, represents a strong material structure and is therefore, less prone to collapse under the application of shear. The gap ‘x’ in the figure represents the unrecovered stress due to the structural breakdown of the material.

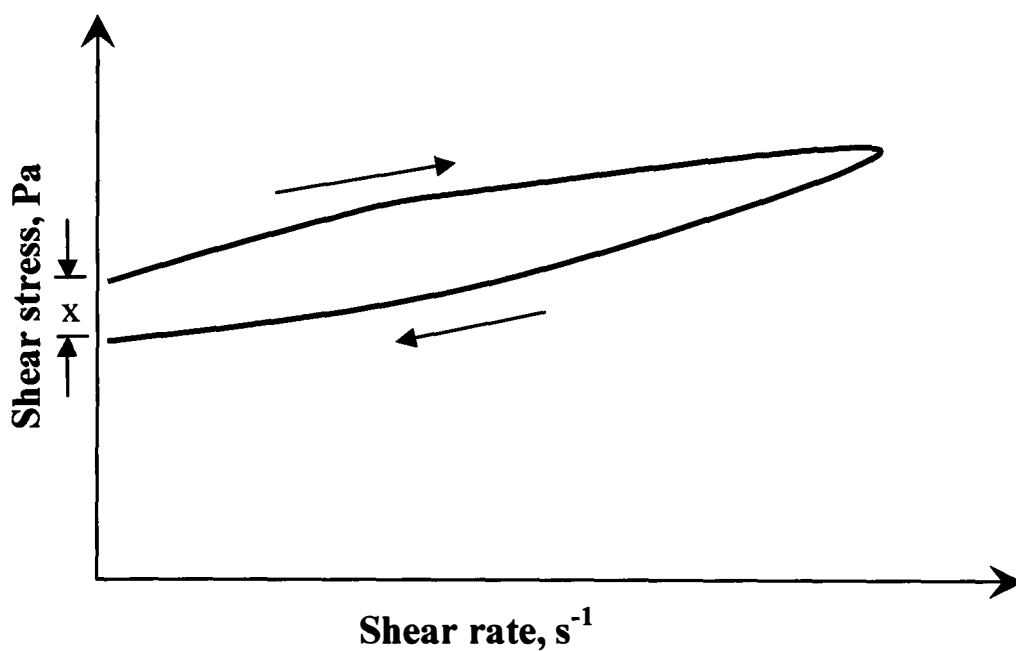


Figure 3.10: The flow curve of a thixotropic fluid with a hysteresis loop

3.6 Summary

The basic concepts used in the study of the rheology of materials have been introduced in this chapter. The chapter has covered an introduction to elastic, viscous and viscoelastic materials, as well as non-Newtonian behaviour of different fluid materials. A great emphasis was also given in identifying and understanding the factors which affect the rheology of suspensions. Finally the time-dependent behaviour of suspensions and the mechanism of thixotropic response were also outlined.

Thixotropy or the time-dependent behaviour is regarded as one of the most important rheological property of solder pastes. A proper characterization and modelling of this thixotropic behaviour would be very useful in the manufacturing and application phases of solder paste. The work reported in chapter 5 of this thesis is dedicated to the characterization of time-dependent behaviour of solder pastes and flux mediums. Modelling of the time-dependent structural breakdown and build-up of solder pastes and flux mediums are presented in chapter 6 and 7. Chapter 8 reports on the results from the printing trials carried out to correlate experimental and modelling results to the printing performance.

CHAPTER 4

MATERIALS AND METHODS

4.1 Introduction

Solder paste is one of the most widely used interconnection materials in the electronic assembly process. Solder pastes can be categorised as a homogeneous and dense suspension of solder alloy particles suspended in a flux medium. The metal content of a typical solder paste lies between 88 – 91% by weight (Currie, 1997). The main constituent of flux medium is a naturally occurring rosin or resin. A number of different ingredients including solvents, activators, thickeners, thixotropic agents and tackifiers are normally added to the flux to achieve the desired flow properties.

To measure flow and deformation behaviour (i.e. the rheological behaviour), there are several techniques that can be used. The term *rheometry* refers to a set of standard techniques used to measure rheological properties. For solder pastes, rotational rheometry is the most popular technique for the measurement of rheological behaviour (Currie, 1997).

This chapter presents an overview of the materials and experimental techniques used in the study reported in this thesis. The chapter is made up of two main sections. The first section provides an overview of solder pastes and flux mediums used in the electronics assembly process. The second section introduces the experimental techniques used in the rheological characterisation of the paste materials.

4.2 Solder Paste Characteristics

Solder paste can be defined as a dense suspension and/or a homogeneous mixture of solder alloy powder, flux and vehicle. In the electronic assembly process, solder paste plays the crucial role by providing electrical, mechanical, and thermal bonds between the electronic components and the substrate. As a dense suspension of 50% solid and 50% liquid (by volume), solder paste will have attributes such as volume fraction, size distribution, metal content, inter-particle forces and possible particle flux interactions (Currie, 1997). When considered as a homogeneous and kinetically stable mixture (Hwang, 1989), solder paste can be recognised by the properties such as viscosity, normal forces, density and surface tension.

Solder pastes are made up of three primary components (Hwang, 1989):

1. Solder alloy powder which melts to form the bond between the components and the substrate.
2. The flux system which helps the alloy powder and the surfaces to be joined to maintain a clean and metallic state, so that good wetting and metallic continuity between solder alloy and the surfaces joined can be formed.
3. The vehicle carrier system which is primarily a carrier for solder powder and provides a desirable rheology.

In addition to metallurgy and particle technology, the physical, chemical, thermal, and rheological properties of vehicle/flux systems are equally important to the performance and characteristics of the resulting paste (Hwang, 1989). Based on the performance, solder paste can be categorised into four areas (Hwang, 1989): applicability, solderability, residue characteristics, and joint integrity. Applicability refers to the ability of a paste to adapt to a specific paste-application process such as dispensing, screen printing, or stencil printing. Solderability refers to the ability of a paste to wet the surfaces to be joined with complete coalescence of solder powder particles, and to

achieve a reliable metallurgical bond. Residue characteristics covers the physical and chemical properties of the resulting chemical mixture after soldering, such as corrosivity, activity, tackiness, hardness, and compatibility with cleaning process. Solder joint integrity is the ultimate purpose of the solder joint after the soldering process in terms of mechanical properties, resistance to adverse environment, and its compatibility with service conditions.

4.2.1 Solder Alloy Powder

The elements commonly used in solder alloys are tin (Sn), lead (Pb), silver (Ag), bismuth (Bi), indium (In), antimony (Sb), and cadmium (Cd) (Hwang, 1989). Solder alloy powder can be produced from bulk solder alloy by different techniques: chemical reduction, electrolytic deposition, mechanical processing of solid solder, and atomization of liquid solder. Among these, atomization is the most widely used technique for making solder paste powder. Atomization involves disintegrating the liquid solder metal under high pressure through small orifices into water or into a gaseous chamber or vacuum chamber. The process is capable of producing solder powders of high density, good flow rate and spherical shape, which are all desirable properties for solder pastes.

An alternative method of producing solder powders involves the use of a spinning disc. The molten metal is fed to the centre of a spinning disc and spread by centrifugal force into a continuous circular film that thins as it spreads, and at or just beyond the edge of the disc, the liquid solder becomes thin enough for surface forces to form small drops that solidify into fine spherical shaped powder particles. Although the process parameters (such as temperature and size of the chamber, velocity of the disc, and feed rate) can be adjusted to produce spherical particles, a considerable number of elongated particles tend to be produced during the process (Pecht, 1993).

a) Alloy composition

Sn-Pb solder alloys, specially the eutectic 63Sn 37Pb have been used extensively in electronic applications for more than 30 years until the introduction of environmental legislations banning the use of lead in electronic assembly. The eutectic composition (with 63Sn 37Pb solder alloy) gives the lowest melting temperature (183⁰ C) in the Sn-Pb range. The lower melting point helps to minimise the thermal damage to the components during the soldering process. The excellent wettability of 63Sn-37Pb alloy also leads to a lower soldering defect rate (Fujiuchi, 2004).

In contrast, for lead-free soldering, the solder alloy can be made from the combination of a wide range of elements, including Sn, Ag, Bi, Cu, In, Sb, Zn in binary, ternary, or multi-component systems (Nimmo, 2004). The tin-silver-copper (SAC) alloy combination is one of the most commonly used lead-free solder alloy system. Three compositions in the Sn-Ag-Cu system have been chosen as replacements for Sn-Pb eutectic solders (Handwerker, 2004). The preferred solder compositions are: Sn-3.0Ag-0.5Cu (Japan), Sn-3.5Ag-0.9Cu (EU), and Sn-3.9Ag-0.6Cu (US).

The selection of solder alloy depends on the following factors (Hwang, 1989):

- Metallurgical compatibility, consideration of leaching and potential formation of intermetallic compounds.
- Environment or service compatibility, consideration of silver migration.
- Temperature capability, consideration of service temperature, process
- Wettability on substrate

Various recommendations have been made by organisations within the electronics industry since the first research program on lead-free electronic solders were completed in the early 1990s. Table 4.1 summarises the world-wide research activities on lead-free solder paste selection.

Table 4.1: Summary of major research carried out world-wide for lead-free solder selection (Nimmo 2004; IPC-SPVC, 2005)

Time	Project Details	Results/Recommendations
1991 – 1994	<ul style="list-style-type: none"> – U.K. Government (DTI) sponsored project. – Companies involved: GEC-Marconi, BNR Europe, ITRI, and Multicore. – Made initial investigations on a range of alloys including Sn-Ag-Cu-Bi, Sn-Ag-Bi, Sn-Zn-Bi, and others. 	<ul style="list-style-type: none"> – Findings were used as a basis of European-funded IDEALS program.
1996 – 1999	<ul style="list-style-type: none"> – European-funded program – IDEALS (Improved Design life and Environmentally aware manufacture of Electronic Assemblies by Lead-free Soldering) – Companies involved: GEC-Marconi, Philips, Siemens, Witmetaal, Multicore, and NMRC. – Investigated lead-free solders for both reflow and wave soldering. 	<ul style="list-style-type: none"> – Sn-3.8Ag-0.7Cu was found as the optimum lead-free alloy functionally equivalent in performance to Sn-Pb. – Sn-Ag-Bi and Sn-Ag-Cu-Sb were also reported to be suitable for use in single-sided reflow soldering and all wave soldering processes, respectively.
1993 – 1997	<ul style="list-style-type: none"> – NCMS (National Center for Manufacturing Sciences) lead-free program in United States – Involved 11 corporations, academic institutions, and national laboratories and examined about 	<ul style="list-style-type: none"> – A series of application-specific alloy choice recommended. – Bi-42Sn, Sn-3.5Ag-4.8Bi, and Sn-3.5Ag were recommended.

	70 solders.	– Sn-Ag-Cu alloys were not examined in detail.
January 2000	<ul style="list-style-type: none"> – NEMI (National Electronics Manufacturing Initiative) Consortium in United States. – Involving 50 companies, suppliers, government agencies, and universities. 	<ul style="list-style-type: none"> – Sn-3.9Ag-0.6Cu recommended as the primary choice for reflow soldering. – Sn-0.7Cu was favoured for wave soldering with Sn-3.5Ag as a secondary alternative
2000	– JEIDA Roadmap on Lead-Free Soldering, Japan	– Sn-3.0Ag-0.5Cu was recommended with two other notable solder alloys, the Sn-Zn-Bi for low temperature use and Bi-Sn-Ag for very high temperature use.
May 2002	<ul style="list-style-type: none"> – Research by the IPC Solder Products Value Council (SPVC) – 18 companies were involved and nearly \$ 1 million has been spent on the program. 	– Sn-3.0Ag-0.5Cu was recommended as the “lead-free solder paste alloy of choice” for the electronic industries due to its lower cost and equivalent performance to Sn-Pb solder.

b) Particle Shape

The powder particles in a solder paste are usually almost spherical in shape. This allows for greater reproducibility in terms of rheological properties for the paste system (Park, 1992) and also improves the ability of the paste to be dispensed and minimizes the potential damage that can be caused to stencils by forcing irregular particles through the apertures. The three-dimensional shape with the minimum surface area is a sphere. A solder paste sample with excessive amounts of fines and irregular shaped particles would

have a higher surface area of particles in a given volume of paste. This will eventually accelerate the evaporation rate of volatiles in the flux/vehicle system and cause increased oxidation of the powder particles. This evaporation may result in printing problems associated with clogging of stencil apertures, poor paste deposit and skipping or incomplete paste withdrawal (Jirenic, 1984).

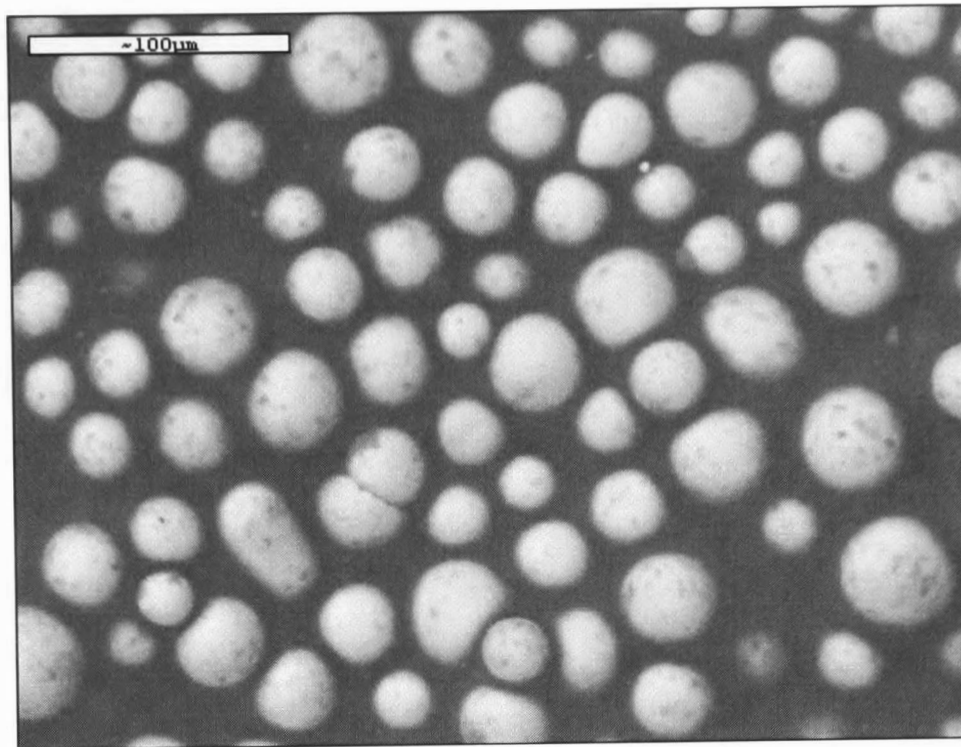


Figure 4.1: SEM micrograph of a typical lead-free solder paste in a flux medium.

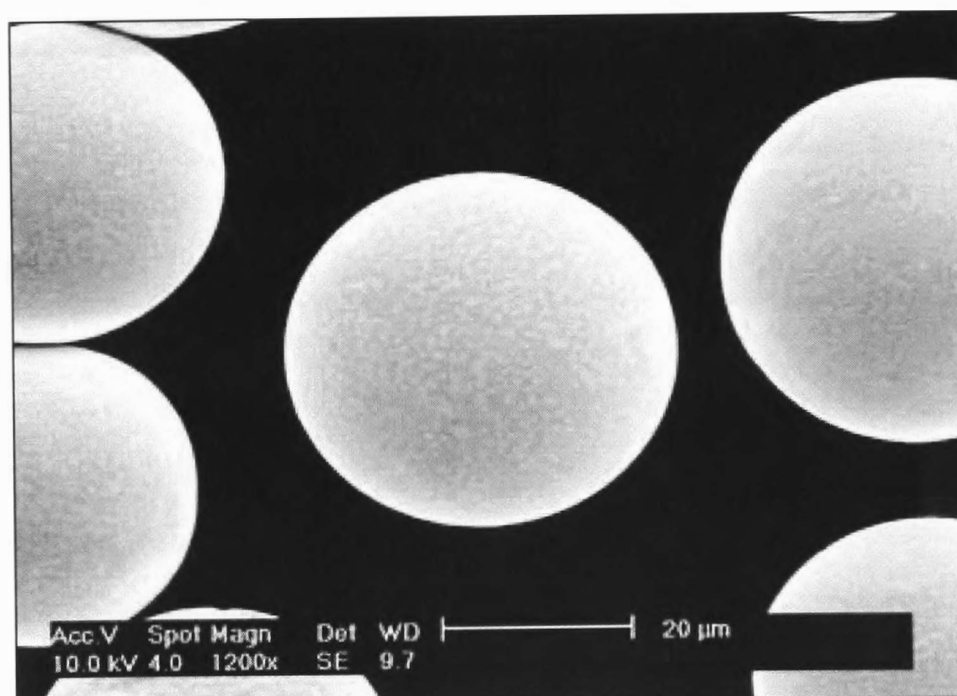


Figure 4.2: SEM micrographs of spherical solder powders (Mitsui-kinzoku, 2002)

c) Particle size and distribution

The trend towards the use of more fine pitch electronic devices has made new demands on the properties and performance of solder paste. Fine pitch starts with 0.875 mm (35 mil), progressing via 0.750 mm (30 mil) and 0.625 (25 mil) to 0.5 mm (20 mil) and 0.3 mm/12 mil (ultra-fine pitch) (Strauss, 1998). However, now-a-days ultra-fine-pitch (UFP) is defined as the pitch size of less than 120 micron (0.12 mm) (Pudas et al, 2005). In a recent study, Koo et al (2007) investigated the reliability of Ni flip-chip with the bump and pitch size of 30(W)×30(D)×10(H) μm^3 and 60 μm respectively. A method to fabricate flip-chip bonds to sub-micron sizes (in nanoscales) has also been proposed (Orendoff et al, 2008). For such fine pitch applications, improving paste printing quality is critical to achieve further reductions in soldering defects. In general, the smaller the pitch size, the smaller the solder alloy particles required to minimize the potential of clogging the stencil apertures. As a rule of thumb, the maximum particle diameter in a given paste should be less than 1/3 of the width of the narrowest aperture through which the paste has to pass.

The particle size distribution (PSD) of solder paste is also very important. As the trend towards miniaturization is continuing, solder paste manufacturers are facing the challenge of making solder particles with increasingly narrower PSD. Particle sizes are usually expressed in microns (μm) diameter, with one micron equal to 0.04 mils. There are two main standards used for classifying the solder alloy particle sizes used in solder pastes: (a) joint industry standard (J-STD-005) from the Association Connecting Electronics Industries (IPC) and (b) DIN 32 513 from the Deutsches Institut Fur Normung (DIN). The J-STD-005 recommends screening, microscopy or optical image analysis as suitable methods for determining the PSD for solder pastes, whilst the DIN standard only suggests the use of microscopic measurement for measuring particle sizes. Tables 4.2(a) & (b) and 4.3 presents six specific types of PSD for solder alloy powders for J-STD-005 standard and three specific types of PSD for solder alloy powders under the DIN 32 513 standard.

Table 4.2a: Solder powder particle size distribution for solder paste: type 1 to 3 (J-STD-005)

Type	None Larger Than (microns)	Less Than 1% Larger Than (microns)	80% Minimum Between (microns)	10% Maximum Less Than (microns)
1	160	150	150-75	20
2	80	75	75-45	20
3	50	45	45-25	20

Table 4.2b: Solder powder particle size distribution for solder paste: type 4 to 6 (J-STD-005)

Type	None Larger Than (microns)	Less Than 1% Larger Than (microns)	90% Minimum Between (microns)	10% Maximum Less Than (microns)
4	40	38	38-20	20
5	30	25	25-15	15
6	20	15	15-5	5

Table 4.3: Solder powder particle size distribution for solder paste (DIN 32 513)

Powder Type	Min. 85% Between (microns)	Max. 10% Between (microns)	Max. 3% Below (microns)	Max 3% Between (microns)	No Particles Over
1	75 – 125	63 – 75	63	125 – 140	140
2	45 – 75	32 – 45	32	75 – 80	80
3	20 – 45	15 – 20	15	45 – 50	50

d) Oxide content

Solder powders are generally manufactured in inert atmosphere (e.g. using nitrogen gas) in order to minimize surface oxide formation. Because of the higher surface area, solder powders with irregular shapes will tend to oxidize faster than those with spherical powder, which in most cases will lead to an increase in solder balling (Bauer and Lathrop, 1998). The total surface area for the solder alloy particles within the paste may also increase rapidly if the PSD of the solder powder particles is reduced. Poor rheological properties and associated poor printing performance can often be attributed to heavily oxidized solder alloy powder particles. For example, the formation of surface oxide on the particles is known to facilitate early dry out of the solder paste, leading to an increase in paste viscosity. To reduce or eliminate possible oxides formation on the surface of the particles, a Parylene (poly-para-xylylene) conformal coating process has been suggested as a viable remedy (Currie, 1997). This material is known to reduce the reactivity of the powder with the flux as well as extending the tack time, shelf-life and stabilization of the viscosity of solder paste. The oxide content and contamination level are usually measured by fusion tests and oxygen detectors (Pecht, 1993).

4.2.2 Flux/vehicle System

Flux/vehicle system selection for a new solder paste formulation is very important as the flux/vehicle system composition plays a key role in determining the soldering defect rate and the ultimate solder joint reliability. The composition and formulation of flux/vehicle system directly affect the deformation and flow characteristics of the paste and its printing performance. The inherent chemical nature of flux/vehicle system also greatly controls the reflow soldering performance and determines the nature and extent of soldering defects.

The composition of a typical vehicle/flux has some 5 – 20 constituents. Each ingredient, or group of ingredients, provides a necessary function such as binding agent, fluxing agent, rheological controller, suspending agent, or specific function modifier.

Every ingredient plays a role in the final performance of the paste. Most of the time, all ingredients are interrelated with respect to performance (Hwang, 1989).

a) Fluxes

The flux is the substance used to facilitate the joining process (soldering, brazing or welding) by chemically cleansing the surfaces to be joined. The flux is very important for metallurgical bonding, as the formation of the intermetallic bond requires the production of two fresh metallic surfaces to be in contact. For soldering, brazing and welding processes, one of the key functions of the flux is to facilitate the removal of the surface oxide from the base and filler materials to help form a good and reliable intermetallic bond.

In soldering, the functions of flux are threefold: it removes oxides and tarnish from surfaces to be soldered, increases wetting of surfaces by decreasing surface tension, and seals out air thus preventing re-oxidation of surfaces during the soldering process. In addition to these essential functions, the flux must flow out of the way of the molten solder so that intermetallic bonding can take place, and must be stable enough to withstand high soldering temperatures without chemically breaking down. Moreover, the flux residue left behind after soldering must be non-conductive and non-corrosive, or else be easy to wash away (Pecht, 1998). Tackiness of flux (in solder paste) is also essential to prevent part movement during handling between placement and reflow soldering operations (Hwang, 1989).

There are two major considerations in selecting a flux for electronic assembly: flux activity and cleanability. Flux activity refers to the ability of the flux to wet and clean surfaces. The activity in a soldering flux is generally provided by halides (chlorides, bromides) present in the flux, although there are some halide-free fluxes containing amino acids or other organic acids (Prasad, 1997). The higher the flux activity, the more corrosive flux residues will be left behind after soldering, potentially causing reliability

problems in the assembly. Surfaces with poor solderability requires highly active flux so that acceptable wetting of the surfaces can be achieved.

The cleanability of the flux refers to the simplicity and effectiveness with which residues can be removed after soldering and is measured by the degree of solubility of flux in water and solvents. Rosin-based fluxes are soluble in chlorofluorocarbon solvents. These fluxes can be made soluble in water by saponification (conversion into soap). The tackiness of residues is also an important factor in determining flux cleanability. For applications requiring cleaning, soft residues are desirable; for no-clean applications, hard, non-tacky residues, which encapsulate the contaminants, are desirable (Pecht, 1998).

Flux Classification

The composition and formulation, the level of activity of the residue, and the cleaning requirements are all important in classifying fluxes. A number of standards exist defining the various flux types. According to the old MIL QQS standard, fluxes can be grouped into four classes:

R	(Rosin)
RMA	(Rosin Mildly Activated)
RA	(Rosin Activated)
WS	(Water Soluble)

Any of these categories (except WS) may be classified as no-clean or water-soluble depending on the chemistry selected and the standard that the manufacturer requires.

The most recent and widely used standard is the J-STD-004A from IPC (2004) which superseded MIL QQS standard. J-STD-004A addresses all forms of fluxes used in electronic assembly: paste, liquid, flux-cored solder wire, and flux-cored or flux-coated preforms. The new standard categorizes all fluxes into one of four groups based on their composition. The flux composition categories and their symbols are:

Rosin	(RO)
Resin	(RE)
Organic	(OR)
Inorganic	(IN)

Each of the four groups in the J-STD-004A standard can be subdivided into six further flux activity levels according to the corrosive or conductive properties of the flux and its residues. The flux activity levels are determined by results from copper mirror testing, corrosion testing, surface insulation resistance (SIR), electrochemical migration (ECM) and halide content. The three main activity levels are:

- L Low or no flux/flux residue activity
- M Moderate flux/flux residue activity
- H High flux/flux residue activity

These three activity levels are further characterized by using a 0 or 1 to indicate the absence or presence of halides in the flux. This results in six classifications.

- L0
- L1
- M0
- M1
- H0
- H1

When the 4 composition classes and 6 activity levels are taken together, the J-STD-004A standard results in 24 different classifications. Table 1, taken from J-STD-004 lists the 4 composition categories in the first column and the 6 flux activity levels/flux types in the second column, and their resulting 24 classifications with their “flux designator” symbols in the third column.

Table 4.4: Classification of fluxes to J-STD-004

Flux Materials of Composition	Flux Activity Levels (% Halide)/ Flux Type		Flux Designator
ROSIN (RO)	Low (<0.05%)	L0	ROL0
	Low (<0.5%)	L1	ROL1
	Moderate (<0.05%)	M0	ROM0
	Moderate (0.5-2%)	M1	ROM1
	High (<0.05%)	H0	ROH0
	High (<2.0%)	H1	ROH1
RESIN (RE)	Low (<0.05%)	L0	REL0
	Low (<0.5%)	L1	REL1
	Moderate (<0.05%)	M0	REM0
	Moderate (0.5-2%)	M1	REM1
	High (<0.05%)	H0	REH0
	High (<2.0%)	H1	REH1
ORGANIC (OR)	Low (<0.05%)	L0	ORL0
	Low (<0.5%)	L1	ORL1
	Moderate (<0.05%)	M0	ORM0
	Moderate (0.5-2%)	M1	ORM1
	High (<0.05%)	H0	ORH0
	High (<2.0%)	H1	ORH1
INORGANIC (IN)	Low (<0.05%)	L0	INL0
	Low (<0.5%)	L1	INL1
	Moderate (<0.05%)	M0	INM0
	Moderate (0.5-2%)	M1	INM1
	High (<0.05%)	H0	INH0
	High (<2.0%)	H1	INH1

Rosin/Resin Fluxes

Rosin or colophony is a natural product that is extracted from the stumps or bark of pine trees and then refined. Resins are similar compounds to rosins that are either completely synthesised, or are highly processed rosins (Shea et al., 2007). Although the J-STD-004A classification system (table 4) differentiates rosin-fluxes from resin-fluxes, in the following discussions both are referred to as “rosin-fluxes” for simplicity. The composition of rosin may vary from batch-to-batch, but mainly consists of several rosin acids, rosin acid esters, rosin anhydrides, and fatty acids. The major components of unmodified rosin are abietic acid (70 – 85 % depending on the source), primaric acid (10 – 15 %), isoprimary acid, neoabietic acid, and dihydroabiatic acid with a general formula $C_{19}H_{29}COOH$ (Hwang, 1989; Prasad, 1997).

The addition of rosin to a flux formulation determines the nature of its residue from both electrochemical and aesthetic point of view. Rosin fluxes are inactive at room temperature but become active when heated to soldering temperatures. When heated in the soldering process it becomes molten and reacts with metal oxides, when cooled it solidifies to act as a hydrophobic encapsulant to any ionically active ingredients (such as chlorides, bromides, or unreacted acids left in the residue), which may otherwise cause reliability problems (Shea et al., 2007). Rosin fluxes are not soluble in water and require the use of solvents, semi-aqueous solvents or water with saponifiers to remove them. Rosin fluxes are generally weaker when compared to other flux types, and activators are required to improve their activity level. The removal of oxide by rosin can be expressed by the following general formula (Prasad, 1997):



where RCO_2H is rosin in the flux ($C_{19}H_{29}COOH$)

$M = Sn, Ag, \text{ or } Cu$

$X = \text{Oxide, Hydroxide or Carbonate}$

One of the common concerns associated with the use of rosin fluxes is the physical appearance of their residue. Residues from rosin fluxes are typically sticky or tacky requiring cleaning. Therefore, when using rosin fluxes a proper cleaning process needs to be adopted; otherwise the reliability of assemblies may be compromised, because the sticky rosin residues may attract dust and harmful contaminants whilst in service.

Organic Fluxes

Organic fluxes contain the acids commonly found in food and dairy products, such as citric acid, lactic acid, and oleic acid. In terms of flux activity, organic fluxes are more active than rosin fluxes but less active than inorganic fluxes. They provide a good balance between flux activity and cleanability, especially if their solids content is low (1-5%). These fluxes contain polar ions, which are easily removed by a polar solvent such as water. Because of their solubility in water, the OR fluxes are preferred due to their environmental friendliness. Organic fluxes have been successfully used on military programs and have been found to meet both military and commercial requirements for cleanliness. Due to the environmental concerns associated with the cleaning of rosin-based fluxes/pastes with chlorofluorocarbon (CFCs), water soluble fluxes such as organic fluxes have become even more popular for applications that require cleaning or in applications where there are soldering defect rate concerns with low residue or no-clean pastes and fluxes (Prasad, 1997).

Inorganic fluxes

Fluxes based on inorganic acids, alkalies, and their salts are highly corrosive in nature. Inorganic fluxes are typically made up of inorganic acids and salts such as hydrochloric acid, hydrofluoric acid, orthophosphoric acid, zinc chloride, ammonium chloride and other halides (Prasad, 1997; Pecht, 1993). Because of their high corrosivity, inorganic fluxes are not used in electronic assemblies because of their potential reliability concerns. They are generally used for hard-to-solder materials such as stainless steel, kovar, and nickel irons (Prasad, 1997).

Water soluble and No-clean Fluxes

In terms of the electrochemical activity of flux residues, fluxes can be further categorized as water soluble or no-clean. By definition, a “water soluble” flux is one whose soldering residue can be removed by water or saponified water. Water soluble fluxes are generally non-rosin based and both organic and inorganic fluxes falls into this category. Organic fluxes are more active than rosin-fluxes but less active than the inorganic fluxes. As stated earlier, inorganic fluxes are not recommended for electronic applications because of their high corrosive nature (Prasad, 1997). However, as a viable commercial alternative to non-rosin flux, water soluble fluxes are estimated to account for about 50% of total soldering flux in electronic assembly (Currie, 1997). Because of the presence of strong acids (tartaric, di-, tri-functional organic acids), halides, amines and amides, water soluble fluxes are regarded as “most highly active” (Currie, 1997; Shea et al., 2007). Water soluble fluxes contain a high percentage of solvents, such as methanol, isopropanol, ethylene glycol, mono-butyl ether and polyethylene glycol. So, to improve the printing performance of water soluble paste, a controlled environment is advised to minimize solvent evaporation (Currie, 1997). The obvious disadvantage of using water soluble fluxes is that their residues require cleaning - which adds to the cost of the assembly process. Secondly, if the residues are not cleaned off properly, the residues/contaminants left behind may lead to long-term reliability problems.

In order to reduce the residue levels and to eliminate the cleaning operation altogether, no-clean flux based solder pastes were developed in late 1980's (Currie, 1997). The main driver for the development of no-clean fluxes/solder pastes is the cost savings from eliminating the residue cleaning stage (and the associated equipment and floor space costs). In addition to these savings, environmental regulations, such as the ban on the use of CFCs, have also persuaded many companies worldwide to adopt no-clean fluxes in their production process. Rosin based fluxes generally fall into the no-clean flux category because of their ability to produce low levels of residues. If not cleaned, rosin flux residues may become sticky but do not usually pose any reliability concern, specially if they are halide free. The resin content (also referred to as solid content) in a no-clean

flux determines the amount of postsoldering residue left on the board. The use of high solid content in no-clean fluxes can lead to excessive residues if too much resin is used. The trend is to use low solid content fluxes (with between 1% to 5% solid content) to minimize residue levels and the associated corrosion related reliability problems (Prasad, 1997). It is also worth noting that due to low activity of no-clean fluxes and solder pastes, they require a very clean assembly environment and solderable boards and components. Compared to water-soluble fluxes, the options for no-clean flux formulation is limited by the smaller number of allowable constituents.

b) Vehicle constituents

The vehicle is a complex formulation of different ingredients designed to provide the desired rheological properties to the solder paste. A typical vehicle/flux system may consist of between 5 to 20 ingredients. The vehicle system serves as a carrier for the solder particles, provides the desirable rheology, coats the surface of the solder alloy particles and provides a good heat transfer path between substrate and component (Currie, 1997). The three most important ingredients in flux/vehicle systems used in solder pastes are: activators, solvents and rheological additives.

Activators

Activators are often added to the rosin-based fluxes to increase their cleaning activity at the soldering temperature. Activators are polar, mostly high weight molecular organic compounds, which may or may not contain a halogen atom (Strauss, 1998). An ideal activator will be fully soluble in the rosin (and also in the flux solvent) and must not separate out when the rosin solidifies. Frazier et al. (1990) have identified five different types of organic compounds used as activators in solder paste, these are: acids, halogens, amines, amides and rosin (which consists of diterpenoid acids). Judd and Brindley (1999) have also outlined the activators used in soldering fluxes as follows:

- certain organic halide salts such as dimethylammonium chloride (DMA HCL), and diethylammonium chloride (DEA HCL).

- organic mono-basic acids such as formic acid, acetic acid, and propionic acid.
- organic di-basic acids such as oxalic acid, malonic acid, sebacic acid.

Activators can be classified as “halide activators” and “halide-free activators”, based on the presence of halogen. The first tier of activators listed above i.e. organic halide salts are regarded as halide activators as they are based on halides of chlorine or bromine. It is generally believed that a halogen activated rosin flux could cause a higher corrosion damage and of lowered surface insulation resistance (SIR) than halogen free one, and some soldering documentations specially outlaw the use of halide-activated fluxes (Strauss, 1998). The development of halide-free activators has also been influenced by environmental legislations such as the Montreal Protocol. Organic mono- and di-baic acids (as listed above) are used as halide-free activators. However, because of their low activity, a higher concentration is required to get the same effect as halide-activators (Currie, 1997).

Solvents

Solvents are used to dissolve the flux and other active constituents in the solder paste and acts as a carrier system for the solder paste. Choosing the right solvent or solvent blends is vital as they affect the work life, tack time, slump and the temperature profile requirements of solder paste. A low volatile solvent can provide increased work life and tack time. On the other hand, a solvent with a low boiling point (highly volatile) can vaporize explosively during reflow and may cause excessive solder balling. Solder pastes need to be carefully formulated to utilize the solvents that give excellent tack and work life but do not require excessive preheat or soak times (Brian and Lathrop, 1998).

Table 4.5 presents the most commonly used solvents in solder paste formulations. Amongst these all the solvents, the glycols/glycol family are the most widely used solvent because of their balanced solvency power, soldering aid performance and viscosity (Lee, 2000). Alcohols, especially the terpineol solvent are also widely used due to their superior solvency for rosin. The selection of solvent for a flux system depends on

the flux chemistry, the odour of solder paste, target stencil life and the tack time of solder paste (Lee, 2000).

Table 4.5: Commonly used solvents in fluxes of solder paste

Solvent Family	Examples
Alcohols	Isopropanol, n-butanol, isobutanol, ethanol, terpineol
Amines	Aliphatic amines
Esters	Aliphatic esters
Ethers	Aliphatic ethers
Glycols	Ethylene glycol, propylene glycol, triethylene glycol, tetraethylene glycol
Glycol ethers	Aliphatic ethylene glycol ethers, aliphatic propylene glycol ethers
Glycol esters	Aliphatic ethylene glycol esters, aliphatic propylene glycol esters
Hydrocarbons	Aliphatic hydrocarbons, aromatic hydrocarbons, terpenes
Ketones	Aliphatic ketones
Pyrols	M-pyrol, V-pyrol

Rheological Additives

The flow and deformation behaviour of solder paste changes continuously at different stages of the assembly process. For example, the solder paste is required to flow easily (acts like a liquid) during the printing process, but not to flow at all afterwards (acts like a solid). Therefore, the rheology of solder paste has to be tailored to meet the various processing requirements. This can be achieved by adding appropriate rheological additives in the flux system. Table 4.6 outlines some commonly used rheological additives.

The most commonly used rheological additives are castor oil derivatives (Currie, 1997). This chemical family is highly hydrocarbon in nature, and is typically used in no-clean or rosin fluxes. For water-soluble fluxes, polyethylene glycols or derivatives of polyethylene glycols are the popular choices due to their high solubility in water (Lee, 2002).

Table 4.6: Some commonly used rheological additives (Lee, 2002)

Rheological Additives	Examples	Note
Castor oil derivatives	Castor oil is triglyceride of fatty acids Fatty acid composition is approximately 87% ricinoleic, 7% oleic, 3% linoleic, 2% palmitic, 1% stearic, and trace amounts of dihydroxystearic. Modification of castor oil may be hydrogenation, etc. The nature of modification is very proprietary.	No-clean/Rosin fluxes
Petroleum-based waxes	Petrolatum	No-clean/Rosin fluxes
Synthetic polymers	Polyethylene glycols (water soluble) Derivatives of polyethylene glycols Polycethylene	Water-soluble fluxes No-clean/Rosin fluxes
Natural waxes	Vegetable wax	No-clean/Rosin fluxes
Inorganic thixotropic additives	Activated silicate powders Activated clays	No-clean/Rosin fluxes

4.2.3 Materials Used in the Experimental Studies

Two fluxes F1 and F2 and four commercially available lead-free solder pastes P1 to P4 prepared from those fluxes were used in the experimental studies reported in this thesis. Both F1 and F2 fluxes are classified as water-based, rosin-containing, no-clean and halide free. The solder particles for all the paste samples are made of the same tin-silver-copper alloy (95.5 Sn 3.8 Ag 0.7 Cu) with a melting point of 217⁰C. All the solder paste samples had the same metal content of 88.5% by weight. The details of these samples are provided in table 4.7 below. The particle sizes are acquired for the manufacturers acquired data sheet.

Table 4.7: Test materials

Paste Sample	Flux Type	Particle size (µm)
P1	F1	25 – 45
P2	F1	20 – 38
P3	F2	25 – 45
P4	F2	20 – 38

Measurements of the particle size distributions (PSD) were also carried out using Malvern's Mastersizer 2000 PSD measuring instrument. The results are shown in table 4.8 and figure 4.3.

Table 4.8: Particle size distribution for the solder paste samples

Solder Pastes	10% Below [d(0.1), micron]	50% Below [d(0.5), micron]	90% Below [d(0.9), micron]	Particles at the peak, micron
P1	25.97	38.14	56.91	34.67 – 39.81
P2	17.91	34.18	100.16	30.20 – 34.67
P3	25.07	37.09	55.22	34.67 – 39.81
P4	9.46	26.15	47.41	26.30 – 30.20

Chapter 4

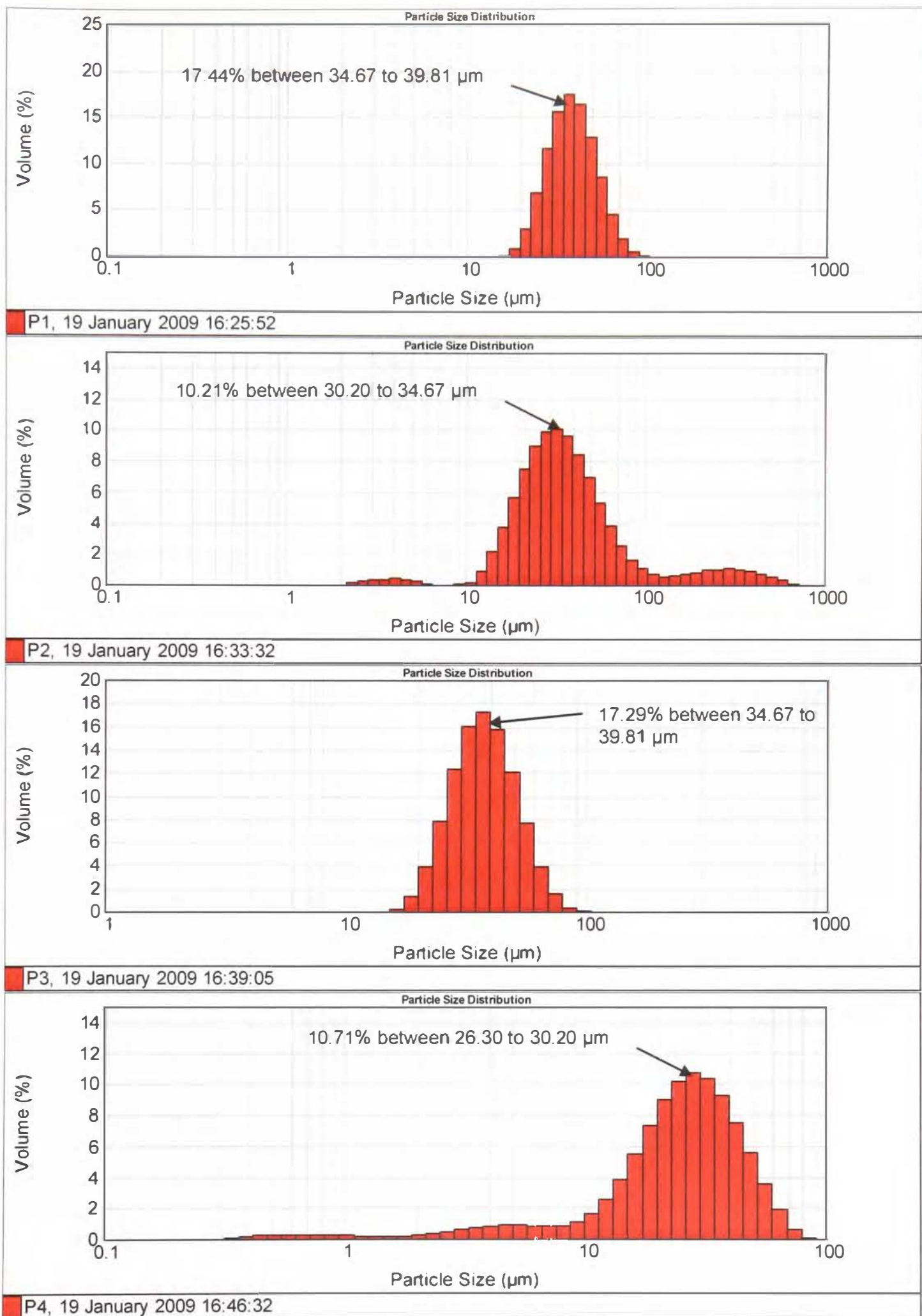


Figure 4.3: Particle Size Distribution for pastes P1 to P4.

4.3 Rheometry

Rheometry can be defined as the science of making rheological measurements. It is an extremely useful tool for determining the flow properties of various materials by measuring the relationships between stress, deformation, temperature and time.

As in the food industry (Steffe, 1996), there are a number of areas where rheological data are needed in the solder paste manufacturing process:

- Process engineering calculations involving a wide range of equipment such as pipelines, pumps, mixtures, heat-exchangers and on-line viscometers.
- Determining constituent functionality in product development.
- Intermediate or final product quality control.
- Shelf-life testing.
- Analysis of rheological equations of state or constitutive equations.

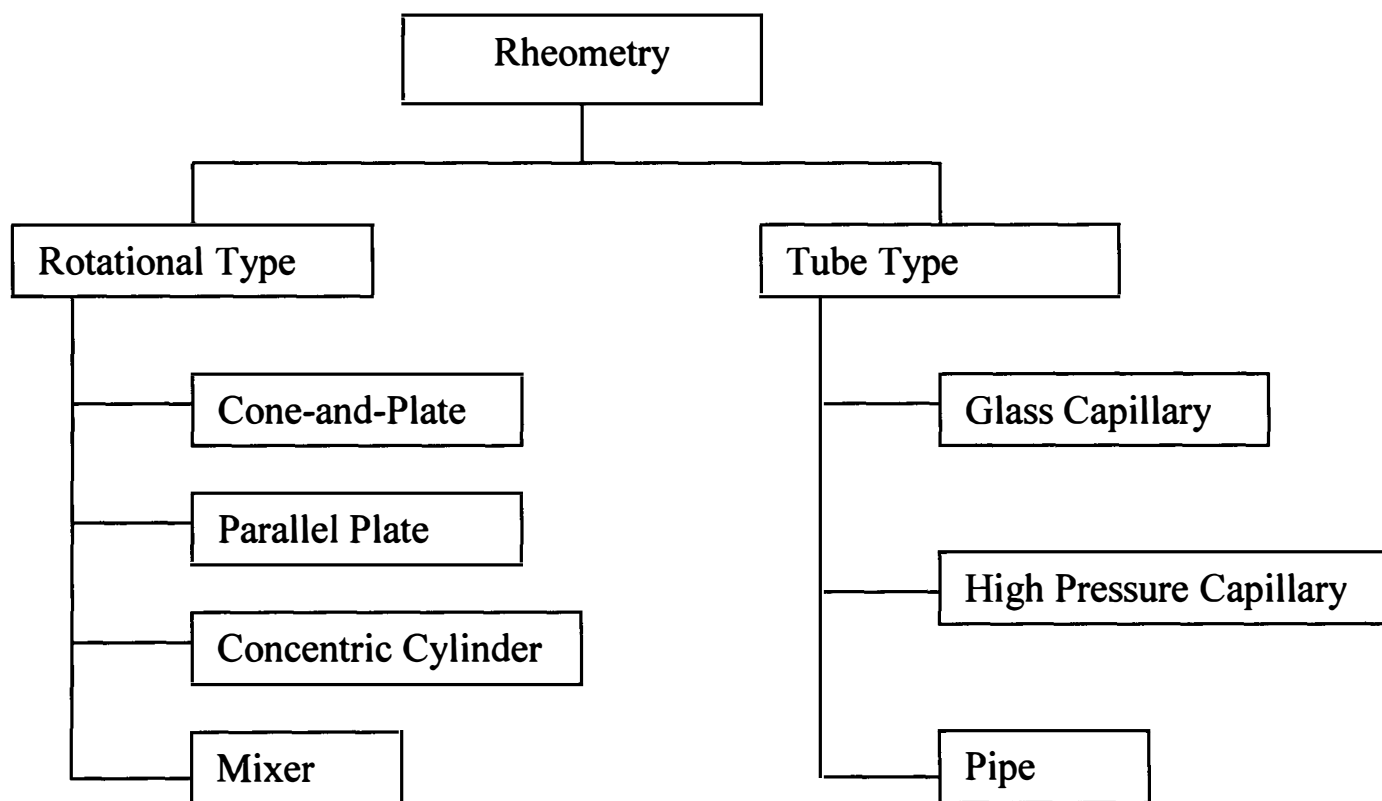


Figure 4.4: Classification of rheological measuring instruments.

Rheological instruments can be broadly classified into two general categories (Steffe, 1996): rotational type and tube type. Based on measuring geometries used, rotational rheometers can be further divided into four sub-categories: cone-and-plate, parallel plate, concentric cylinder, and mixer. The Tube type can also be divided into three sub-categories: glass capillary, high pressure capillary, and pipe. The classification of the rheological instruments is presented in figure 4.4.

Base on their mode of operation, rotational rheometers can also be categorized in two groups: controlled stress and controlled rate rheometers. Controlled stress rheometry is useful in the study of the internal structure of materials as it facilitates the analysis of materials at very low shear stress (creep-testing) as well as the investigation of yield stresses. The controlled rate mode is most useful in obtaining data required in process engineering calculations (Steffe, 1996).

There are advantages and disadvantages associated with each instrument. Gravity operated glass capillaries are only suitable for Newtonian fluids because the shear rate varies during discharge. Cone and plate systems are limited to moderate shear but calculations (for small cone angles) are simple. Pipe and mixer viscometers can handle much larger particles than cone and plate, or parallel plate devices. Problems associated with slip and degradation in structurally sensitive materials are minimized with mixer viscometers. High pressure capillaries operate at high shear rates but generally involve a significant end pressure correction. Pipe viscometers can be constructed to withstand the rigors of production or pilot plant environment (Steffe, 1996).

a) Tube Rheometry

Tube rheometers are based on “Poiseuille flows” (figure 4.5) where the walls of the system (cylindrical tube) are stationary and the flow is caused by the application of external pressure to the fluid. Knowing the dimensions of the tube (i.e. its diameter and length), the functional dependence between the volumetric flow rate of the fluid and the pressure drop due to friction can be determined. If the measurements are carried out so

that it is possible to establish this dependence for various values of pressure drop (or flow rate), then one is able, after performing proper calculations, to determine the flow curve of the investigated fluid (Ferguson & Kemblowski, 1991).

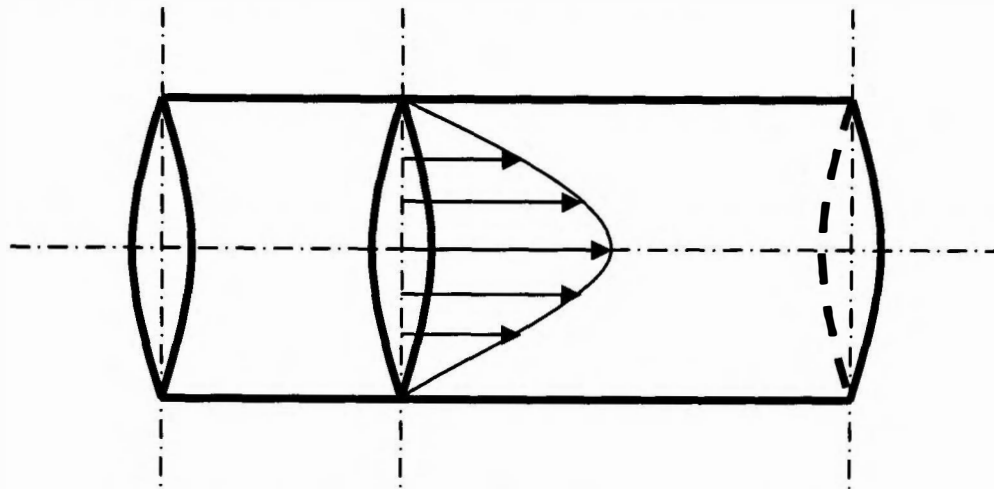


Figure 4.5: Poiseuille flow in a cylindrical tube

Tube rheometers can be placed into three basic categories: glass capillaries, high pressure capillaries, and pipe viscometers. The main difference between a capillary and a pipe viscometer is the diameter of the tube. Diameters for capillary rheometers vary in the range from 0.1 to 4 mm. The size of pipe viscometer diameter varies widely typically in the range of 7 to 32 mm. Glass capillaries (figure 4.6) are designed as gravity operated instruments. High pressure capillaries (figure 4.7 and 4.8) are typically piston driven or gas operated. A pump or gas system can be used to create a driving force in piston viscometers (Steffe, 1996).

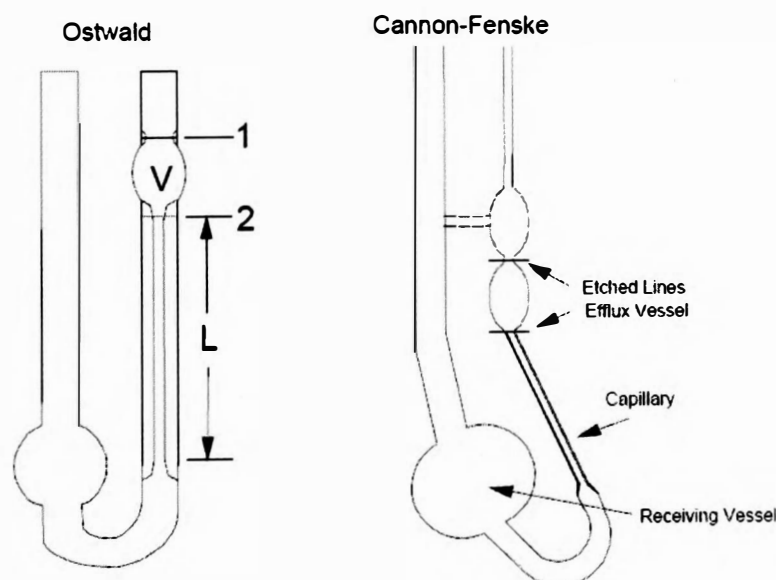


Figure 4.6: Ostwald and Canon-Fenske glass capillary viscometer (Steffe, 1996)



Figure 4.7: High-pressure Capillary Viscometer (Steff, 1996)

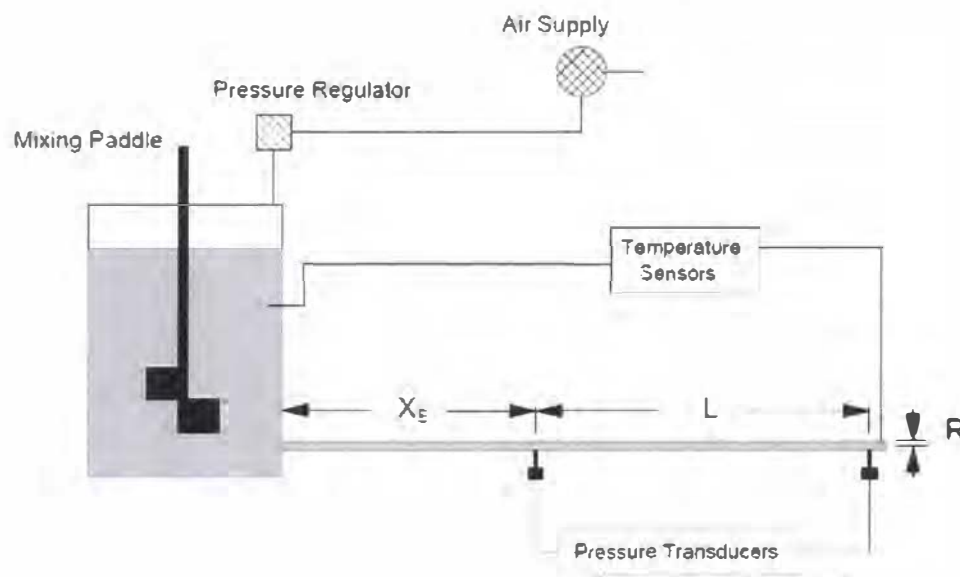


Figure 4.8: Gas driven Pipe viscometer (Steff, 1996)

There are advantages and disadvantages of using tube/capillary rheometers. The advantages are (Ferguson & Kemblowski, 1991):

- The basic instrument is relatively inexpensive, easy to construct and simple to use experimentally.
- Higher shear rates can be obtained than those available in rotational rheometers.
- Temperature control is easy, and the capillary flow process resembles many industrial processes extrusion and injection moulding.
- Two very important fields of rheological research which can only be investigated by this type of instrument namely die-swell and melt fracture.

Although capillary rheometry appears simple, there are some obvious drawbacks as well. The accurate determination of the pressure gradient in capillary rheometers is quite difficult because of the following end effects (Ferguson & Kemblowski, 1991):

- Kinetic energy effects, which are due to acceleration of the fluid at the entrance to the capillary.
- Entrance effects, which result from the development of either a viscous or an elasticoviscous boundary layer in the entrance region of the capillary.
- Exit effects, which result from disturbances of the fully developed laminar flow at the capillary end where an abrupt change of the flow conditions occurs.

b) Rotational Concentric Cylinder (Coaxial) Rheometry

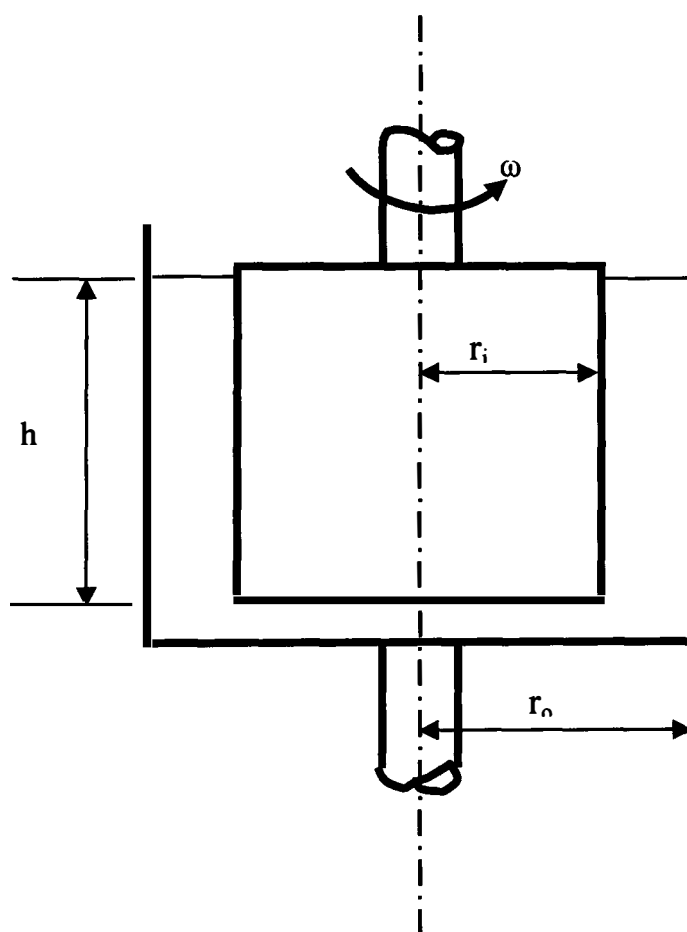


Figure 4.9: Schematic of a concentric cylinder system where the inner cylinder is rotating at a speed of ω rad/sec.

In a concentric cylinder rheometer the shearing occurs in a gap between two cylinders, one of which is rotating and the other stationary. The principle of measurement in concentric cylinder is based on the simultaneous determination of the rotational speed of the rotating element and the torque resulting from this rotation. Experimental data are collected by changing the speed of the rotating element and then processed to determine the flow curve.

Figure 4.9 shows the schematic diagram of the concentric cylinder rheometer. If T is the torque on the inner cylinder and r_i and r_o are inner and outer cylinder radius respectively, then the basic formulae for concentric cylinder rheometer can be given as:

$$\text{Shear stress } \tau = \frac{T}{2\pi r_i^2 h} \quad (4.2)$$

$$\text{Shear rate } \dot{\gamma} = \frac{2V_r r_o^2}{r_o^2 - r_i^2} \quad (4.3)$$

where V_r = velocity at r and the ratio $\tau/\dot{\gamma}$ provides shear dependent viscosity. A number of theoretical problems arise with non-Newtonian fluids as equation 4.2 and 4.3 are only valid for Newtonian fluid. However, correction can be made to help minimize these problems by using very narrow gaps between the two cylinders, so that $r_i/r_o \geq 0.95$ (Ferguson & Kemblowski, 1991).

Advantages

- Able to work with low viscosity materials and mobile suspensions.
- Large surface area provides greater sensitivity in producing reliable data at low shear rates and viscosities.

Disadvantages

- Require relatively large sample volumes and more difficult to clean.
- Performing high frequency measurements may be of problem because of large mass and large inertia of the measuring system.

- Volatile test materials may be prone to ‘skinning’ with time due to sample evaporation.

c) Cone and Plate Rheometry

Figure 4.10 shows the schematic of the cone and plate rheometer. In the cone and plate rheometer the fluid is sheared between a flat plate and a cone with a low angle. The sample is usually placed in slight excess on the lower surface and the gap adjusted so that the apex of the cone just touches the lower plate. The apex of the cone is normally removed (truncated) to help minimize the friction between the apex and the surface of the parallel plate. These types of cone are positioned such that the theoretical (missing) apex would touch the lower plate. The error caused by this is negligible and a more robust measuring geometry is produced (Bohlin, 1994).

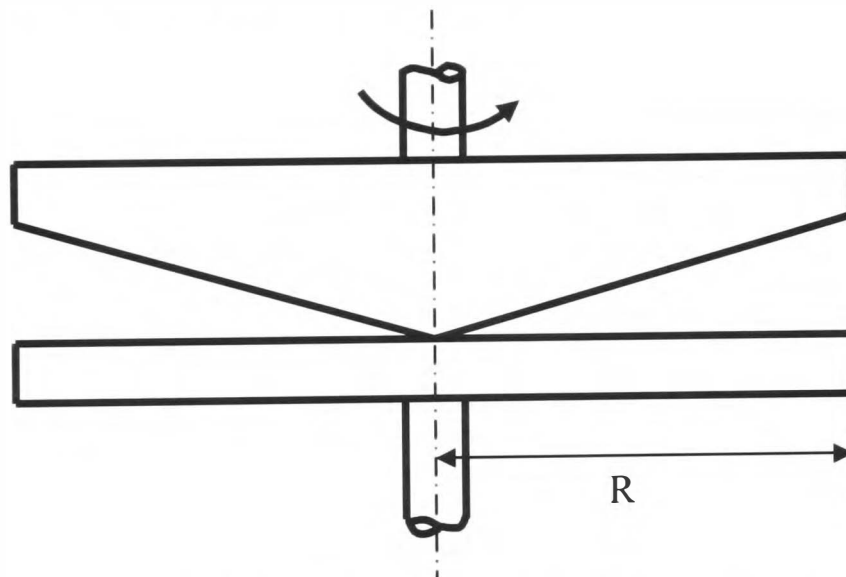


Figure 4.10: Cone-and-plate arrangement

For a cone-and-plate arrangement (see figure 4.10), the angular velocity at any point on the cone surface is proportional to its distance from the centre and the gap width also varies linearly with distance from the tip of the cone. If ω (rad/sec) is the angular velocity and θ is the cone angle, then the shear rate at radius r can be calculated as:

$$\dot{\gamma} = \frac{r\omega}{r \tan \theta} = \frac{\omega}{\tan \theta} \quad (4.4)$$

Chapter 4

Equation (4.4) indicates that the shear rate is constant throughout the gap. For small cone angle, $\tan\theta = \theta$.

In order to develop an expression for shear stress, let's consider the differential torque on an annular ring of thickness dr :

$$dT = (2\pi r dr)\tau$$

This can be integrated over the radius to find the total torque response:

$$\int_0^T dT = \int_0^R (2\pi r^2 \tau) dr \quad (4.5)$$

As the shear rate is constant in the gap, the shear stress is also constant in that area therefore, $\tau = f(r)$. Then, equation (4.5) can be simplified to

$$T = 2\pi\tau \int_0^R r^2 dr$$

hence,

$$\tau = \frac{3T}{2\pi R^3} \quad (4.6)$$

Advantages

- Uniform shear can be achieved across the sample.
- Very easy to clean
- Requires relatively small sample volumes
- Can be used on materials having a viscosity down to about ten times that of water (10 mPas) or even lower.

Disadvantages

- Gap setting for truncated cones at low angles could be problematic and hence not recommended for doing temperature sweeps.

- Particles from the test sample can jam at the cone apex resulting in unreliable data being produced.

d) Parallel Plate Rheometry

Figure 4.11 shows schematic of the parallel plate rheometer. In contrast with cone and plate rheometers, shear rate in a parallel plate rheometer is a function of radius (r)

$$\dot{\gamma} = f(r) = \frac{\omega r}{h}$$

so the shear rate at the perimeter of the plate ($\dot{\gamma}_R$) is

$$\dot{\gamma}_R = \frac{\omega R}{h} \tag{4.7}$$

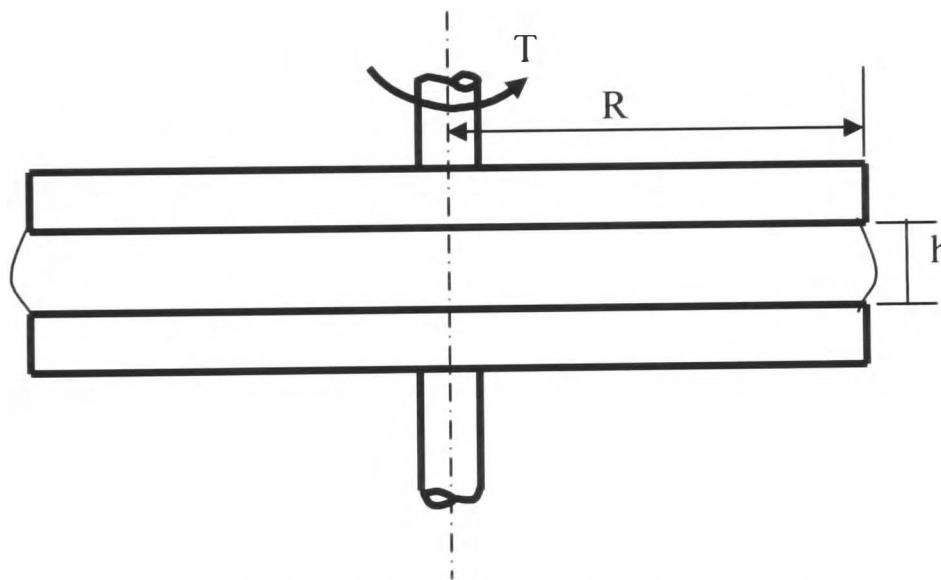


Figure 4.11: Typical parallel plate geometry

The shear stress τ will also vary with radius, and at the perimeter, for a Newtonian fluid this can be calculated as:

$$\tau = \frac{2T}{\pi R^3} \tag{4.8}$$

where T = total torque, and for a non-Newtonian fluid the shear stress is

$$\tau = \frac{2T}{\pi R^3} \left[3 + \frac{d(\log T)}{d(\log \dot{\gamma}_R)} \right] \tag{4.9}$$

Advantages

- Like cone and plate system, it is easy to clean and requires a small sample volume
- Not so sensitive to gap setting, gap can be varied within the limit.

Disadvantages

- The shear rate produced varies across the sample, rheometer only takes an average value for the shear rate.
- The wider the gap between the plates, the more chance there is of forming a temperature gradient across the sample.

4.3.1 Anomalous Effects in Rheometry

In rheometry, many disturbing effects may be encountered in practical situations. They often result from microstructural changes such as sample fracture, sedimentation and migration of particles. Problems may also arise from the type of rheometer or measuring geometries used such as end effects and wall slip. The common anomalous effects found in rheometry are explained below:

a) End and Edge Effects

In practice, every rheometer is subjected to end effects and edge effects, which have to be corrected or taken into account in the derivation of the flow relations. For instance, the basic formulae for concentric-cylinder rheometers were derived under the assumption that the cylinders are of infinite length. But in a real rheometer, the cylinders are always of finite length. The finite length of the cylinders as well as the sidewalls and the bottom of the inner cylinder cause potentially significant variations in the flow depth (Aucey, 2005). In a concentric cylinder rheometer, significant amount of shear can take place between the bottom of the inner cylinder and the cup. Two ways have been suggested (Ferguson & Kemblowski, 1991) to tackle this problem: (i) by trapping air at the bottom of the cylinder by having the shape of an inverted cone on the bottom, and (ii) by making the end into a cone-and-plate geometry. Edge effects are caused by the edges

of the measuring surfaces; the disturbances may become more significant at high values of Reynolds number, when turbulence might occur (Ferguson & Kemblowski, 1991). For parallel-plate rheometer, at moderate to high shear rates, the test sample at the peripheral free surface may bulge out or creep due to the development of centrifugal force. This may introduce a significant variation in the measured torque, possibly varying with time (Ancey, 2005).

b) Wall Effects

Substantial errors in rheological measurements could be introduced because of the presence of wall slip at boundaries of the measuring geometries. This phenomenon can be outlined in the light of explanation given by Ferguson & Kemblowski (1991). For a particle suspension, the concentration of particles at the wall must always be smaller than in the bulk of the fluid. As a result, the layer of fluid adjacent to wall will be of lower viscosity than the bulk of the suspension. When flow starts, this layer will be subjected to relatively higher shear, distorting the velocity profile across the sample. The situation becomes even worse as the particles tend to migrate towards the centre of the measuring system. Both low particle concentrations and particle migration lead to development of a lubricated fluid layer close to the solid boundary and to the slipping of the bulk.

According to Barnes (1995), the following conditions usually lead to large and significant slip effects:

- large particles as the disperse phase (flocs are large particles);
- a large dependence of viscosity on the concentration of the dispersed phase, smooth walls and small flow dimensions;
- usually low speeds/flow rates (although centripetal artifactual effects can be seen at high speeds of rotation), and
- walls and particles carrying like electrostatic charges and the continuous phase is electrically conductive.

Where appropriate, the following solutions/methods can be adopted for correcting wall effects:

- A method of using data from two gap widths and the same torque (for parallel plate rheometers), as proposed by Yoshimura and Prudhomme (1988). This method enables measuring the slip velocity and then computing an effective shear rate.
- Using the “different-gap-size” method, first proposed by Mooney (1931) for concentric cylinder systems. For this method, data are collected at the same wall shear stress and correlated with the slip and bulk flows, using data from different size bobs and various speeds.
- Using roughened surfaces such as grooved or corrugated geometries (Buscall et al., 1993; Franco et al., 1998). Sandblasting with a coarse grit or gluing a sand paper can also be used to roughen a metallic surface.
- Use of Vane Geometry instead of the inner cylinder (bob) in the concentric cylinder system. This method is quite popular, as the vanes are easy to make and clean and have been used successfully for many polymer solutions (Barnes, 1995).
- When there are chemical interactions (chemical attack with ion production) or physical interactions (van der Waals force) between the fluid constituents and the walls, specific surface treatment must be used (Ancy, 2005).

c) Flow instabilities

At high rotational speeds of one of the cylinders (in concentric cylinder arrangement) or for fluids of low viscosity flowing at high volumetric rate through capillaries of large diameters (in capillary rheometer), the laminar shear flow in the gap may become distorted (by the occurrence of secondary flow, eddies and Taylor vortices), and part of the mechanical energy of the fluid would be dissipated by the random movement of fluid elements. The basic flow equations, which were derived on the assumption of laminar flow, will then become invalid. The flow curve tends to bend toward the shear stress axis and will not represent the real rheological properties of the fluid. For concentric cylinder rheometer, an increased turbulence was observed if the inner cylinder is rotating and the outer cylinder is stationary (Ferguson & Kemblowski, 1991).

The possible solutions to the flow instability problems of rheometers have been listed by Ancey (2005), these are:

- Visualizing the internal flow structure to detect secondary flow;
- Placing traces in the fluid to determine their trajectory, then the streamlines;
- Checking the consistency of the collected data. For example, for a parallel plate rheometer, the viscometric treatment is valid provided centrifugal forces are negligible compared to the second normal stress difference. Such an effect can be detected experimentally either by observing secondary flows or by noticing that doubling both the gap and the rotational velocity (thus keeping the shear rate constant) produces a significant variation in the measured torque.

d) Heat Effects

For capillary rheometers, if a fluid of high viscosity is forced through a capillary at high flow rates a significant dissipation of viscous energy may result. The resulting temperature increase changes the rheological properties of the fluid. Because of the decrease of viscosity, the flow curve determined in non-isothermal conditions will tend to bend towards the shear rate axis. Heating effects are even more significant in a coaxial-cylinder rheometer than in a capillary rheometer (Ferguson & Kemblowski, 1991). In this case viscous energy dissipation is caused by shearing the same sample over a period of time, which ultimately results in a rise in temperature. In capillary rheometry, a simple way of minimizing heating effects is by using smaller diameter capillaries. For coaxial-cylinder rheometers, theoretical treatment of the viscous energy dissipation may be appropriate (Ferguson & Kemblowski, 1991).

4.3.2 The Rheometer and the Peripherals

The Bohlin Gemini-150 controlled-stress/strain rheometer (Malvern Instruments Ltd., Worcestershire, U.K.) (figure 4.12) has been used for the work reported in this thesis. The capabilities of the rheometer include:

- Good control on sample temperature;
- Convenience of using a wide range of measuring geometries (parallel-plate, cone-and-plate and cup-and-bob);
- Allows wide shear-rate range (> 10 orders of magnitude);
- Supports both controlled-stress (CS) and controlled-rate (CR) mode;
- Allows both viscometric and oscillatory flow measurements;
- Provides high accuracy and resolution;
- Provides software support and direct monitoring via computer interface.

The main features of Bohlin Gimini-150 rheometer are:

- Torque range: 0.05 μNm to 150 mNm
- Torque resolution: Better than 1nNm
- Position resolution: 50 nano radians
- Frequency range: 1 micro Hz to 150 Hz
- Controlled speed range (CR mode): 0.01 milli rad/sec to 600 rad/sec
- Measurable speed range (CS mode): 10 nano rad/sec to 600 rad/sec
- Normal force measurement range: 0.001 to 20 N
- Step change in strain: <10 ms
- Temperature range: -30°C to 200°C

Figure 4.13 is showing the total rheometer system that is, the rheometer and the supporting peripheral equipments. As shown in figure, the main peripheral equipments comprised of compressed air supply, Peltier temperature control unit, cooling system and the computer unit. The compressed air is mainly used for the air bearing operation, which facilitates friction-less measurements and also controls the movement of the measuring plates. The peltier temperature control unit controls the temperature of the sample being tested with the aid of the water cooling system. The computer unit provides output from the tests in a graphical user interface and also helps in controlling and monitoring the rheometer operation through the software provided.



Figure 4.12: Bohlin Gemini-I50 Controlled-stress/strain rheometer.

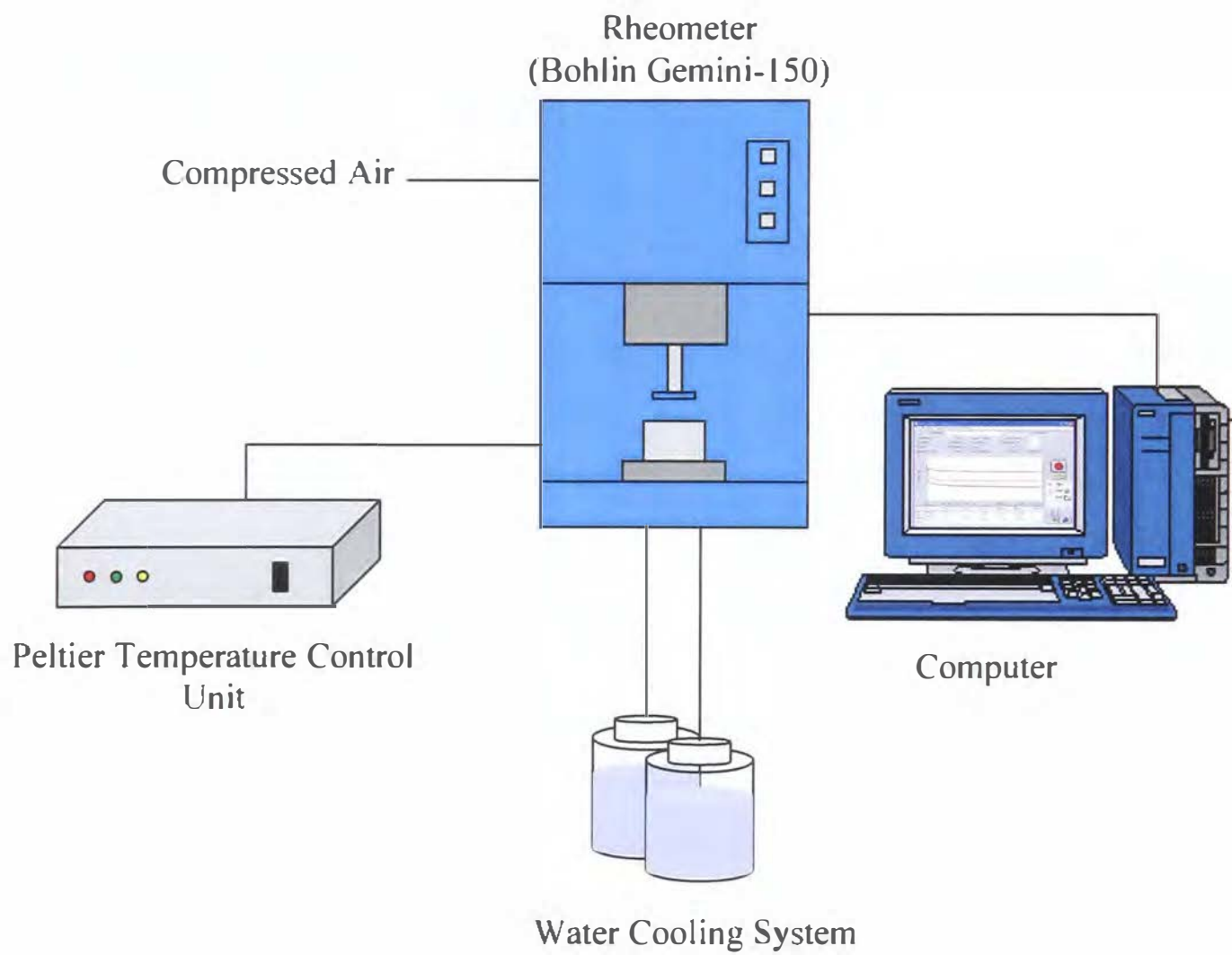


Figure 4.13: The Rheometer Measuring System

4.3.3 Geometries used for rheological measurements

A serrated parallel plate geometry (with serrations on both upper and lower plates) of 20 mm upper plate diameter and 0.5 mm gap width was used for all the rheological measurements reported in this thesis (figure 4.14, Table 4.9). Other measuring geometries such as cone and plate systems while noted for their high accuracy and ability to produce constant shear rates, might be of questionable use in the case of solder paste due to the high metal loading of the relatively “large” solder particles which may cause problems in the narrow gap at the cone tip due to grinding and deformation (Ferguson 1991, Johnson and Kevra 1989, Riedlin 1998). One of the advantages of parallel plate is that the gap can be varied within limits to accommodate the solder pastes. Moreover, parallel plate geometry was highly recommended by Walter and Kemp (1969) for oscillatory measurements because of the fact that the gap can be changed easily and the derived flow equations are precise compared to the cone and plate and concentric cylinder.

Barnes (1995) suggested that the gap heights (between the parallel plates) should be set about 10 times the largest particle size diameter in order to avoid any anomalous effect due to particle jamming and deformation. Taking this as a guideline, a 0.5 mm gap between the parallel plates was used for the all the measurements. Although there are no clear guidelines on selecting plate diameter (specially the upper plate), a smaller diameter (20 mm) was chosen, as it requires less sample volume and can produce higher shear rates (Bohlin, 1994). The serrations on the upper and lower plate were used to minimize the effect of wall slip during rheological measurements. In separate studies by Anderson et al(1993) and Kolli et al(1997), the difficulty of rheological measurements of solder paste due to formation of wall slip have been reported. They also suggested the use of rough surfaces (for measuring geometries) in order to obtain valid rheological data. The roughness values were measured using a Surtronic 3+ (Rank Taylor Hobson Ltd., UK) portable roughness measurement device. As presented in table 4.9, the roughness parameter Ra shows the arithmetic mean of the roughness profile.



Figure 4.14: Serrated Upper Plate (left) and Lower Plate (right) geometries.

Table 4.9: Details of the measuring geometry used

Measuring Geometry	Dimensions	Roughness (Ra), μm	
		Upper Plate	Lower Plate
Serrated parallel plate	Upper serrated plate diameter \approx 20 mm Lower serrated plate diameter = 40 mm Gap width between the plates \approx 0.5 mm	13.7	17.6

4.3.4 Rheological test methods used in this study

a) *Thixotropic/hysteresis loop test*

In the hysteresis loop test, the applied shear rate was increased from an initial low value to a maximum value, and then reversed back to the initial shear rate as shown in figure 4.15. Figure 4.16 shows a typical result of a hysteresis loop test presented in a shear rate versus shear stress plot. According to Trease and Diets (1972), solder paste could experience a shear rate of 0.01 to 1000 sec^{-1} during the printing process. In this

study, the thixotropic loop tests were conducted by increasing the shear rate from 0.01 to 10 s^{-1} in a logarithmic progression and then decreasing the shear rate back to 0.01 s^{-1} . The total duration of each hysteresis loop was 600 sec or 10 minutes.

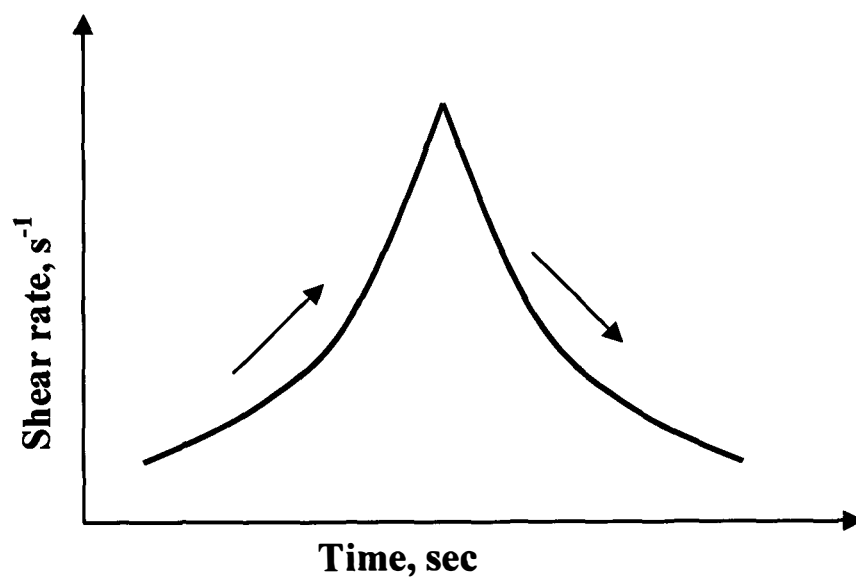


Figure 4.15: Hysteresis loop test

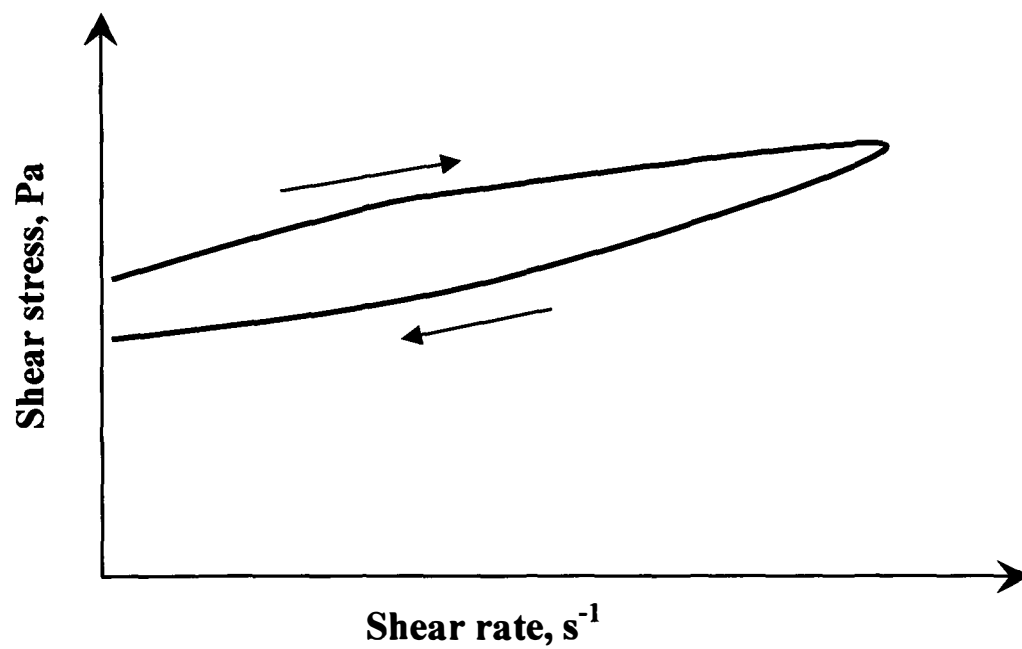


Figure 4.16: Typical hysteresis loop test result

b) Step-shear-rate test

In the step shear test, the shear rate or stress is changed from one constant value to another. In its simplest case, a step shear test is performed by the sudden imposition of the high shear rate or stress on a sample at rest, with intermediate rest periods at zero or very low shear rate. Figure 4.17 shows a typical step shear experiment in a controlled rate mode where the time-dependent response of sample is presented in shear stress values for a step-wise application of shear rates.

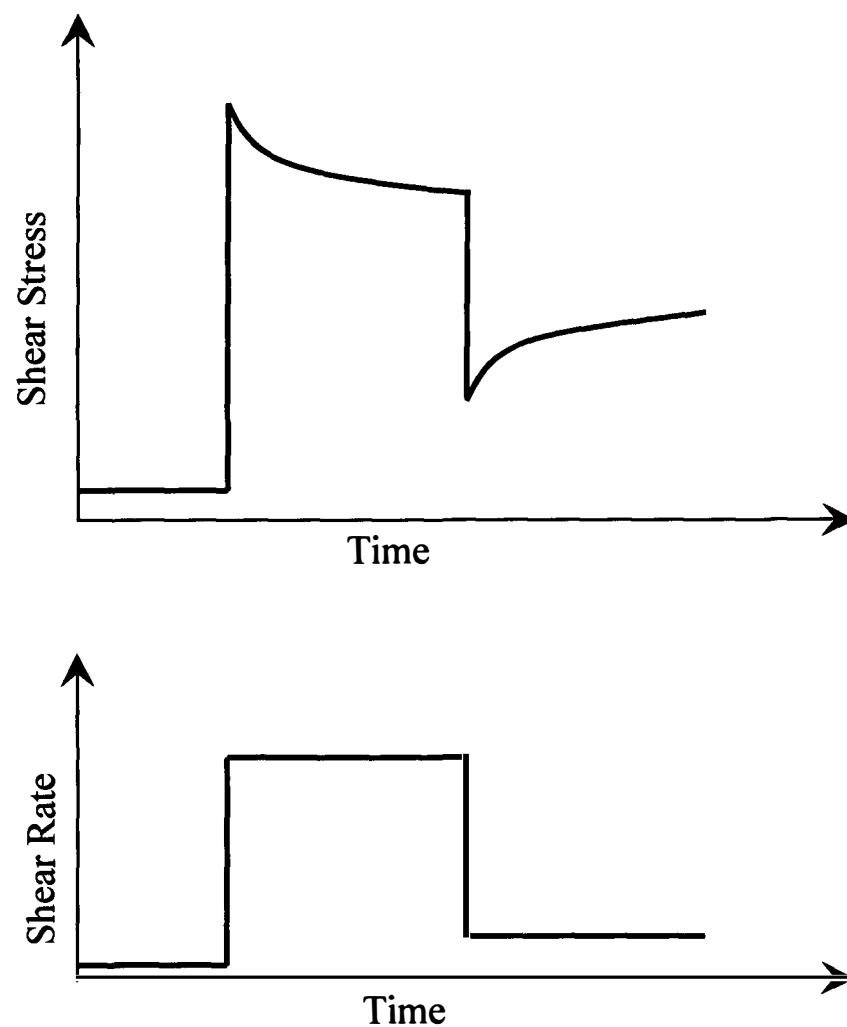


Figure 4.17: Typical step-shear experiment

c) Constant Shear Rate Test

The constant shear rate tests were performed to investigate the break-down of sample's structure with time. The paste structure eventually breaks down under the application of a constant high shear rate and thus result in reduction in viscosity with the time of shear, as shown in figure 4.18. If the experiment is repeated by subjecting the sample to higher shear rates, then a series of curves would be obtained, each curve being successively lower than the previous one (Nguen & Boger, 1985; Johnson et al., 1989). For the constant shear rate tests reported in this thesis, the solder paste and flux samples were sheared for a period of 8 hours at different values of constant shear rates: 2, 4, 6, 8 and 10 s⁻¹. The shear rates values were chosen carefully so that they are high enough to break down sample's structure and also low enough to avoid creeping out from between the parallel plate measuring geometries.

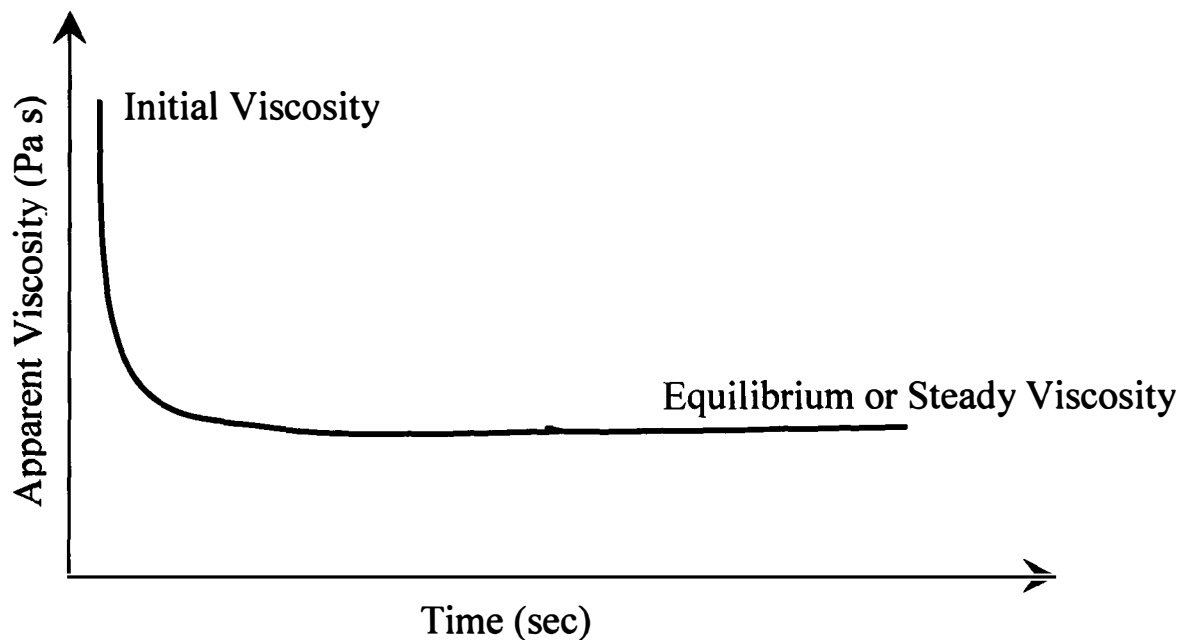


Figure 4.18: Typical response of a constant shear rate test, in apparent viscosity vs time plot.

d) High Shear – Low Shear Test

The primary objective of the High Shear – Low Shear (HSLs) test is to examine the structural buildup of solder pastes and flux mediums. The design of the test involves

applying a preshear (high shear value) to break-down the sample's structure followed by the application of a low shear to observe the recovery of the structure. Figure 4.19 is showing the schematic of the HSLS test design. Time t_1 and t_2 represent the application time the high shear (preshear) and low shear rates respectively. Figure 4.20 is showing a typical result of a HSLS test in apparent viscosity versus time plot.

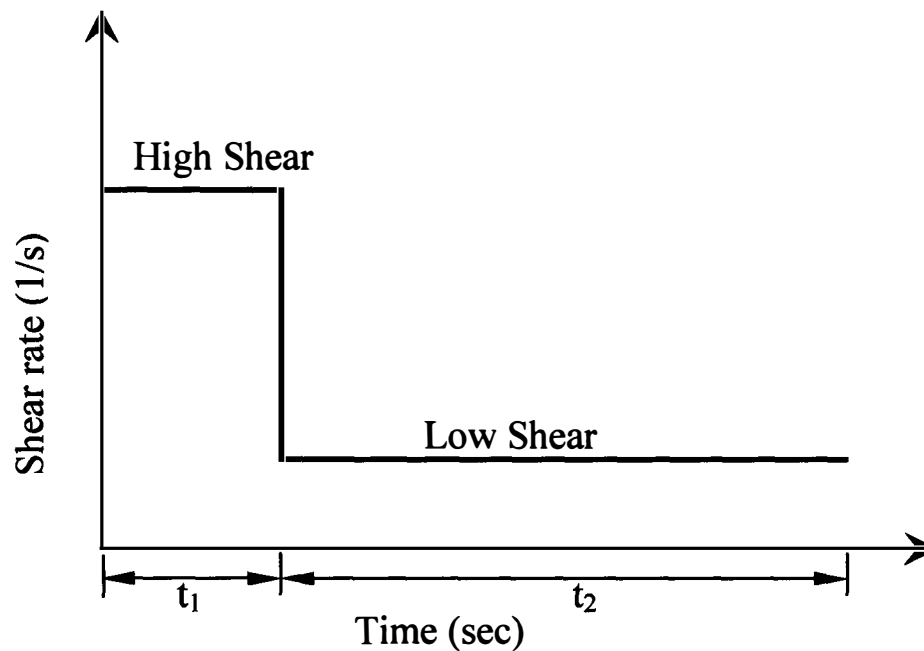


Figure 4.19: High Shear-Low Shear (HSLS) test design

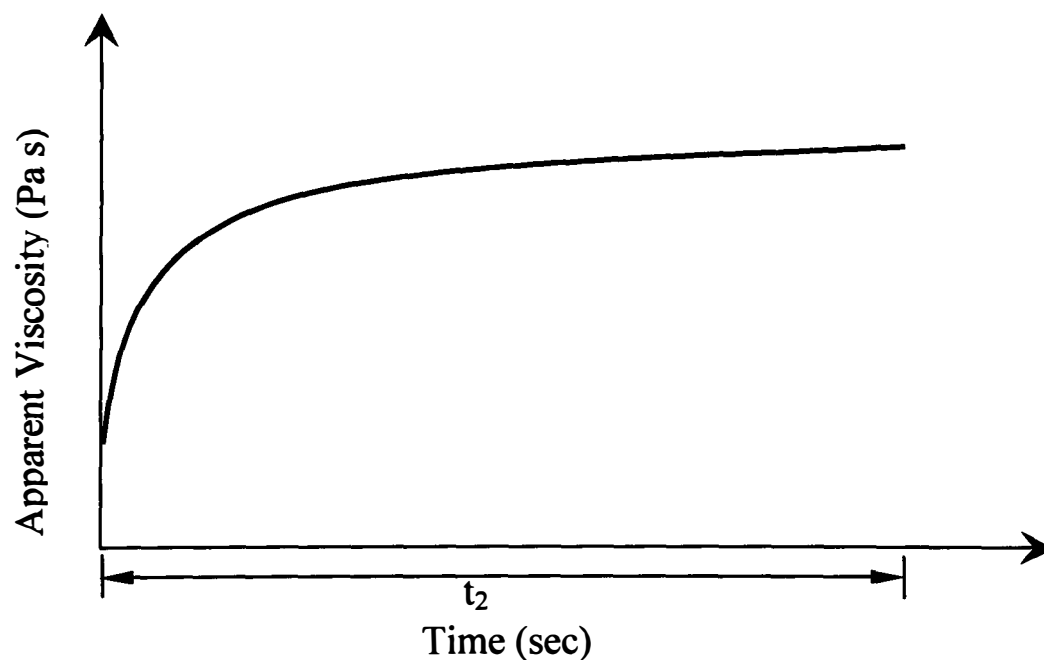


Figure 4.20: Typical result of a high shear – low shear test.

The high shear – low shear test carried out in this study consisted of a preshearing step at 10 s^{-1} for a duration of 30 seconds and then applying a low shear rate for another 900 seconds (15 minutes). A total of five tests were performed on each sample corresponding to the five low shear rates: 0.001, 0.0015, 0.002, 0.0025 and 0.003 s^{-1} . Preliminary tests showed that the paste structure recovers (builds-up) under these low shear conditions.

e) Dynamic Oscillatory Tests

This is done by applying a sinusoidally varying stress (or strain) to the sample and measuring the induced sinusoidally varying strain (or stress) response. Suppose that the applied stress to the material is function of time defined as (figure 4.21)

$$\tau = \tau_0 \sin(\omega t) \quad (4.10)$$

where τ_0 is the amplitude of the stress, ω is the frequency expressed in rad/sec which is equivalent to $\omega/2\pi$ Hertz.

With a small stress amplitude (so the material will behave in a linear viscoelastic manner), the following shear strain is produced by the stress input:

$$\gamma = \gamma_0 \sin(\omega t + \delta) \quad (4.11)$$

where γ_0 is the amplitude of the shear strain and δ is the phase lag or phase shift relative to the stress.

The response from the oscillatory measurements is often measured in complex modulus, G^* , which is the ratio of the stress amplitude to the strain amplitude and is a measure of a material's resistance to deformation

$$G^* = \frac{\tau_0}{\gamma_0} \quad (4.12)$$

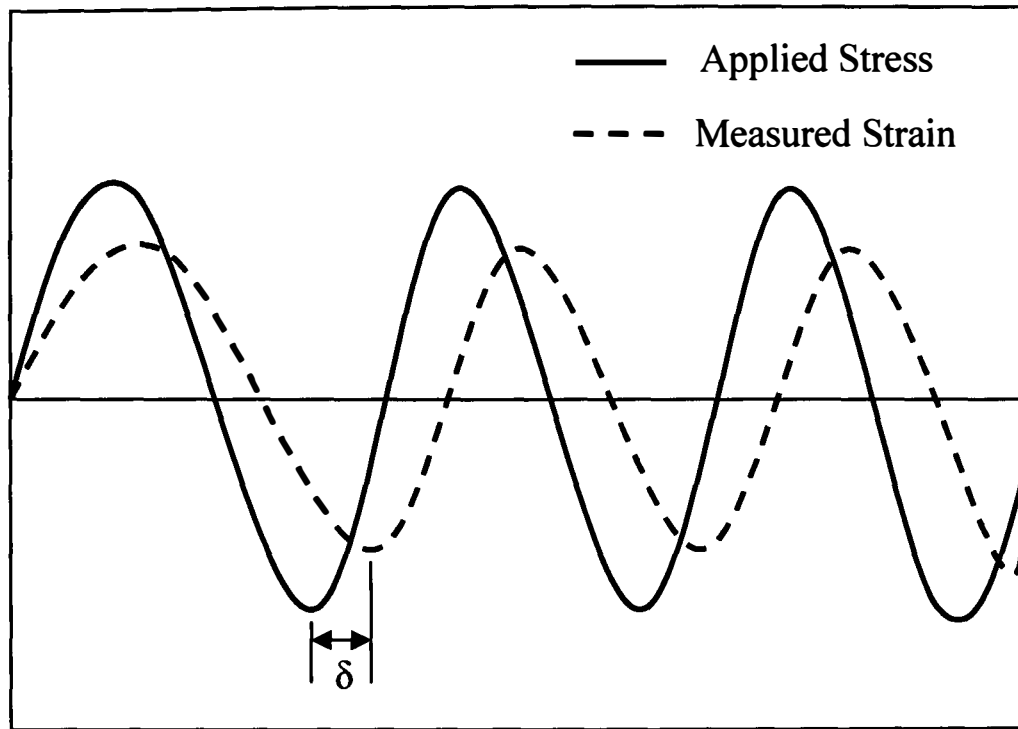


Figure 4.21: Applied oscillatory stress and resulting strain for a typical visco-elastic material.

The complex modulus can be divided into elastic and viscous portions representing the magnitude of the strain in-phase and out-of-phase with the applied stress respectively. The elastic component is called the “storage modulus” and is defined as:

$$G' = \left(\frac{\tau_0}{\gamma_0} \right) \cos(\delta) = G^* \cos(\delta) \quad (4.13)$$

The viscous component, or “loss modulus” is defined as:

$$G'' = \left(\frac{\tau_0}{\gamma_0} \right) \sin(\delta) = G^* \sin(\delta) \quad (4.14)$$

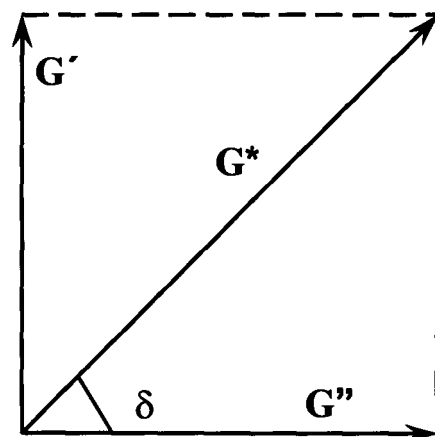


Figure 4.22: Complex modulus and its components

The complex modulus and the tangent of phase angle can be expressed as functions of the storage and loss modulus (figure 4.22):

$$G^* = G' + iG'' \quad (4.15)$$

$$\tan(\delta) = \frac{G''}{G'} \quad (4.16)$$

Two types of oscillatory tests were performed in the course of the study, these are:

Oscillatory Stress Sweep Test (Amplitude Sweep Test)

Executing the stress sweep is normally the first step in oscillation tests. The test is performed by varying the applied stress with the frequency being constant. The primary purpose of the stress sweep test is to determine the linear viscoelastic region (LVR). Before performing oscillation tests on a material it must be verified that the test conditions fall into the LVR. This is because the mathematical calculations are only valid in this linear response region and also within this region the sample structure remains undamaged. Within the LVR, the applied stress and the measured strain follow a linear

relationship. For the oscillatory stress sweep tests reported in this thesis, the applied stress was varied from 0.5 to 500 Pa at a constant frequency of 1 Hz.

Oscillatory Time Sweep Test (Single Frequency Test)

Dynamic oscillatory time sweep tests were performed on solder paste samples to investigate the structure formation during the recovery process. Oscillatory time sweep test provides useful information about how a sample's structure changes with time. As the test was designed to examine the structural recovery of the paste samples, the paste structure was first broken down with a preshear (10 s^{-1} for 30 sec). The structural build-up (or ageing) was then observed at a constant frequency of 1 Hz and with a applied strain value of 0.05% (lies in the LVR), for a period of 8 hours.

4.4 Summary

A detailed overview of major ingredients of solder pastes and flux mediums have been presented. The research and development in the selection of lead-free solder alloys at different parts of the world have been traced back to early 1990s. Although the lead-free Sn-Ag-Cu (SAC) alloy has been widely accepted as the best alternative to lead-based alloys, the use of alloy composition is different in different regions. The chapter also covers the subject of fundamental rheometry explaining details of different types of rheometers and measuring geometries used and also the errors encountered in practical rheological measurements. The chapter also introduces the rheological measurement techniques used in the work reported in this thesis.

CHAPTER 5

INVESTIGATION OF THE TIME-DEPENDENT BEHAVIOUR OF SOLDER PASTES AND FLUX MEDIUMS

5.1 Introduction

Fluids with internal structure can demonstrate time-dependent behaviour upon the application of shear, which can also continue after the shearing has stopped. The most common time-dependent behaviour in which the fluid viscosity decreases with the time of shearing and in which the viscosity gradually recovers when shear is removed – is known as thixotropy and such fluids are called thixotropic fluids. From the structural point of view, thixotropic behaviour takes place when the fluid microstructure changes, under the application of shear, from one state to another in a reversible way. As suggested by Barnes (1997), this microstructural change in the fluid is mainly the result of the competing action between break-down due to flow-stresses and build-up due to in-flow collisions and Brownian motion.

This chapter outlines the results of a study of the time-dependent thixotropic behaviour of solder pastes and flux mediums. The chapter is made up of two main parts: the first part describes the experimental method and parameters used in this study and the second part presents the results from the investigation. Two types of tests were carried out, namely the hysteresis loop and the step-shear-rate test.

5.2 Experimental Test Method

This section presents the details of the test methods used to characterize the thixotropic behaviour of solder pastes and flux mediums. The information on the material and the rheometer used in this study can be found in chapter 4 (see section 4.3.2).

a) Thixotropic/hysteresis loop test

One of the favourite and traditional ways of measuring thixotropic behaviour is to carry out a loop test. In the loop test, the applied shear rate is increased from an initial low value to a maximum value, and then reversed back to the initial shear rate as shown in figure 5.1. Figure 5.2 shows a typical result of a hysteresis loop test presented in a shear rate versus shear stress plot. The area between the up and down curve can be calculated as a measure of thixotropy. However, as calculated area of hysteresis loop depends on the sample shearing history, a coefficient of thixotropy (K_t) is sometimes used which is defined as the ratio of the hysteresis loop area to the highest applied shear rate, see equation 5.1. This way of measuring thixotropy through the coefficient of thixotropy, K_t provides a relative and much more comparable result.

$$K_t = \frac{\text{Thixotropic loop area}}{\text{Highest applied shear rate}} \quad [5.1]$$

The common mode of the thixotropic-loop is the triangular loop mode, wherein the shear rate linearly increases from zero to a maximum value within a set time range, and then linearly drops within the same time range to zero (Huang & Lu, 2005). In this study, the thixotropic loop tests were rather conducted by increasing the shear rate from 0.01 to 10 s⁻¹ in a logarithmic progression and then decreasing the shear rate back to 0.01 s⁻¹. The total duration of each hysteresis loop was 600 sec or 10 minutes.

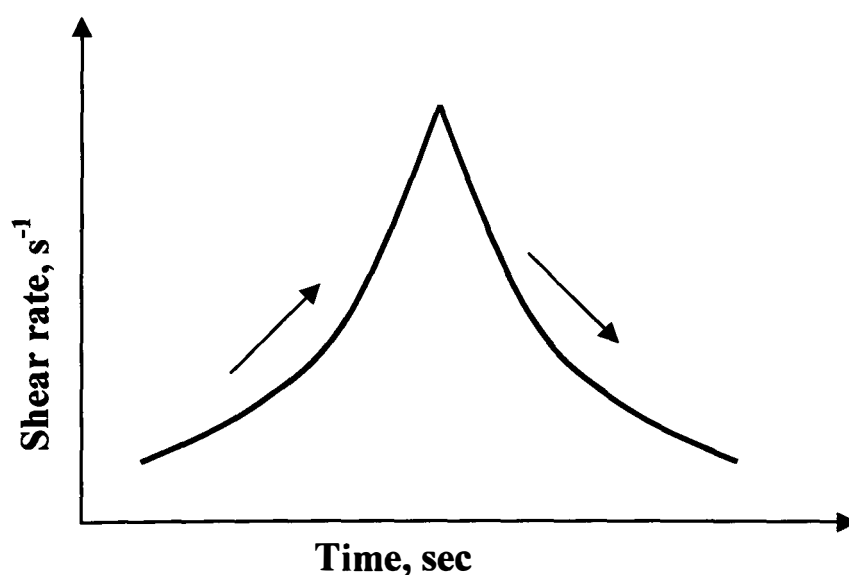


Figure 5.1: Hysteresis loop test

Although thixotropic-loop test provides a quick, qualitative indication of the thixotropic nature of the sample, it has some obvious drawbacks (Barnes, 1997):

- the thixotropic-loop test is often carried out too quickly. This may introduce inertia effects due to the measuring geometries, which is not always recognized or corrected for.
- the response of the material such as the thixotropy itself is a function of both shear rate and time. However, in the thixotropic-loop test both shear rate and time are simultaneously altered. So the response cannot then be resolved into separate effects as it is arising from both variables.

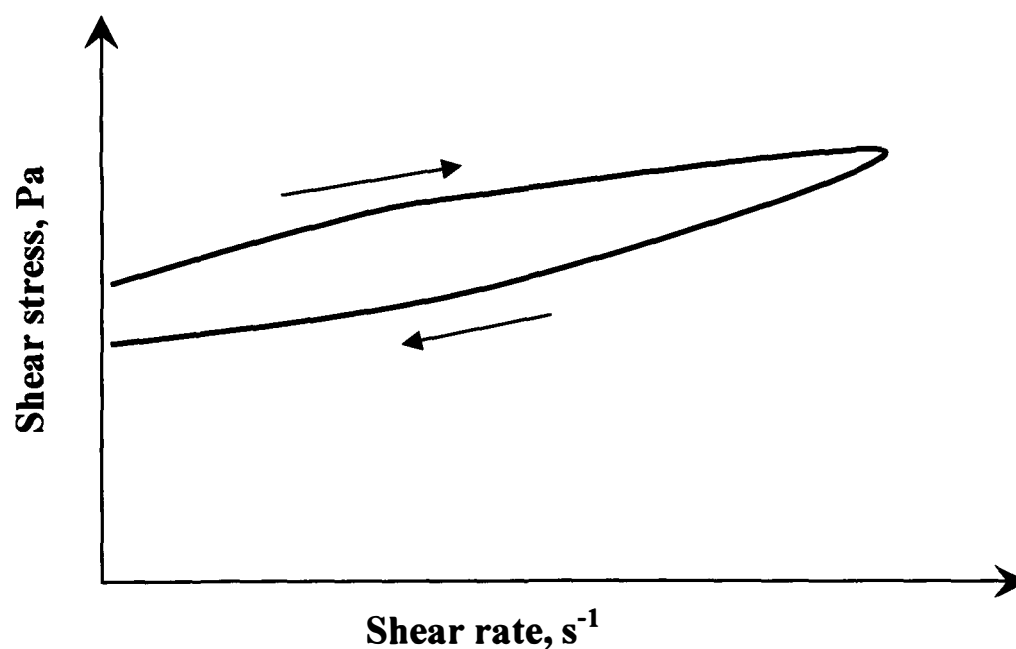


Figure 5.2: Typical hysteresis loop test result

b) Step-shear-rate test

A much simpler and more sensible test for investigating thixotropic behaviour is to perform step shear tests where the shear rate or stress is changed from one constant value to another. The two shear rate or stress values are normally chosen in such a way that one of them would be high enough to break the sample structure, while the other one would be very low (zero or near-to-zero) to allow the sample to build-up (Kolli et al, 1997, Barnes, 1997). In its simplest case, a step shear test is performed by the sudden

imposition of the high shear rate or stress on a sample at rest, with intermediate rest periods at zero or very low shear rate. Figure 5.3 shows a typical step shear experiment in a controlled rate mode where the time-dependent response of sample is presented in shear stress values for a step-wise application of shear rates.

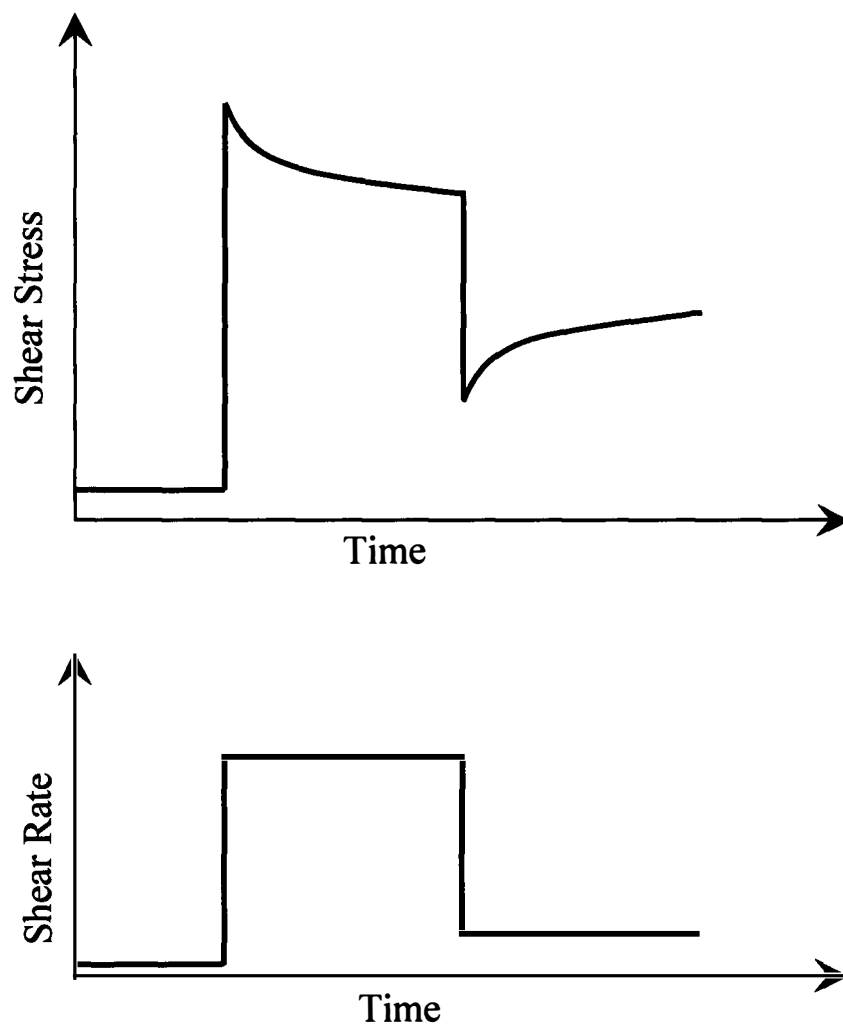


Figure 5.3: Typical step-shear experiment

In this investigation, step shear tests were performed on solder pastes and flux mediums by applying a sequence of step-wise increase in shear rates. Each step consisted of applying a constant high shear rate over 60 sec followed by a low shear rate for 60 sec. The high shear rates were spaced into four steps at 1, 2, 4 and 6 s^{-1} . The low shear rate was a constant value of 0.05 s^{-1} . Time-dependency of the samples was investigated from the continuous recording of the shear stress response. Figure 5.4 shows a schematic presentation of the shear rate values applied during the step shear experiment.

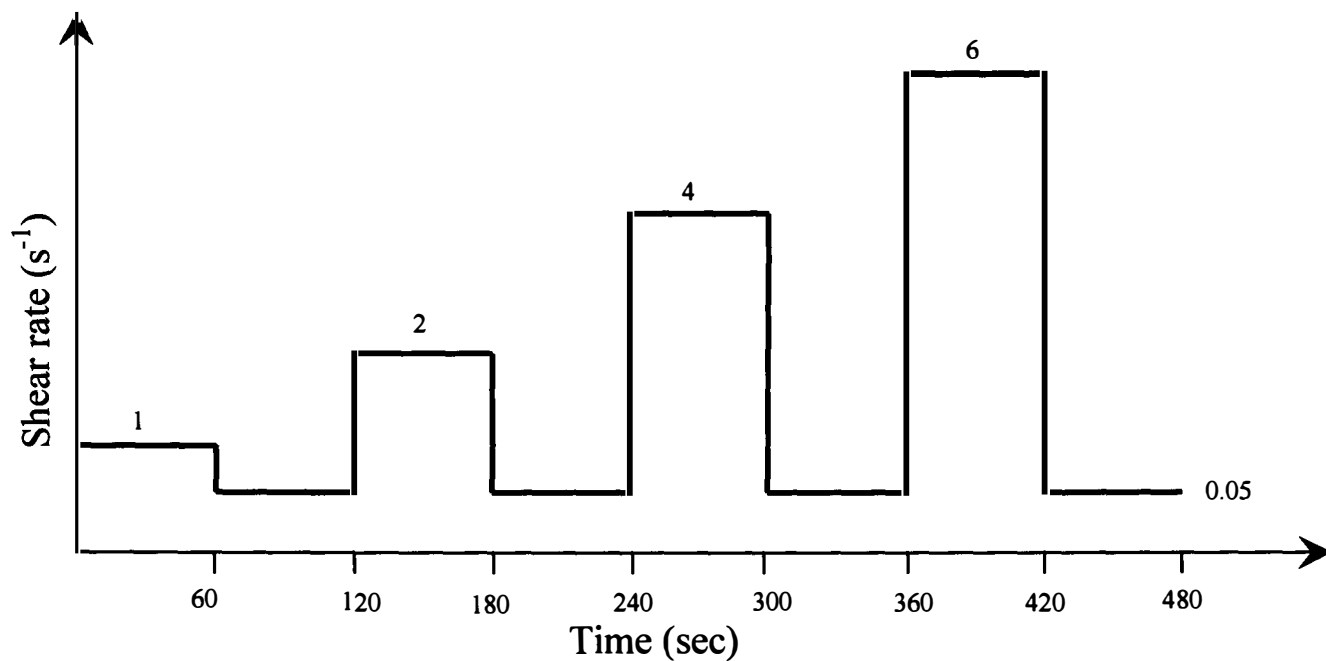


Figure 5.4: Shear rate values used in the step-shear-rate test.

5.3 Experimental Results and Analysis

Section 5.3 presents the results of the hysteresis loop tests and step-shear-rate tests for the solder paste samples and the flux mediums.

5.3.1 Hysteresis loop test results

This section presents the results of the hysteresis loop tests carried out on the solder pastes and flux samples. As was stated earlier in section 5.2 (a), the tests were conducted by increasing the shear rate from 0.01 to 10 s⁻¹ in a logarithmic progression and then decreasing the shear rate back to 0.01 s⁻¹. The total cycle time for each hysteresis loop was 10 minutes. The response of the samples is recorded in shear stress values and the results are presented in shear stress versus shear rate plots. Two types of hysteresis loop tests were carried out namely “single-hysteresis-loop test” and “multiple-hysteresis-loop test”

In the single-hysteresis-loop test the samples were subjected to a cycle of increasing and decreasing shear rates for a period of 10 minutes. The hysteresis loop curve obtained in this way is made up of two parts; the first part of the curve (up curve) represents the increase in shear stress due to the increasing shear rate, which indicates the structural breakdown of the samples. The second part of the curve (down curve) shows the drop in shear stress values, which indicates the recovery of the sample structure, when the shear rate is decreased gradually. The area between the up and down curve was measured using the Bohlin Gemini-150 software as a measure of thixotropy.

Previous studies have shown that solder pastes are thixotropic in nature (Otaga et al. 1991, Lapasin et al. 1994, Nguty et al. 1999 and Durairaj et al 2004). Figure 5.5 shows the shear stress response of pastes P1 to P4 to single-hysteresis-loop test. The hysteresis in the shear-stress response was observed for all the solder paste samples. That is to say that the shear-stress response during the periods of increasing and decreasing shear rates did not match. The figure shows that all the solder paste samples possess yield stress. This is evident from the high, non-zero value of shear stress value at the beginning of shear. It was generally observed that the shear stress values increased parabolically during the period of increasing shear rates. This can be explained by the fact that the initial response of the paste at the start-up of the shear was Newtonian in nature. This was obvious from the monotonous increase in shear stress values at the first part of the curve. As the applied shear increases, a transition from Newtonian to shear-thinning behaviour can be observed. With further increase in shear rates, the shear-thinning behaviour of paste samples become more apparent as the curve tends to flatten out. Towards the end of Newtonian response when the shear rate is large enough, the solder paste structure begins to break down. This ultimately gives rise to the more viscous behaviour of the paste samples. As the shear rate increases further, the solder paste samples start to shear-thin. The structural break-down of the paste is also evidenced by the fact that the down curve of the loop was under the up curve. The rebuilding of the paste structure takes place during the period of decreasing shear rates (down curve). This rebuilding process normally takes time and depends on the intensity of breakdown and the applied shear rate.

The area between the up and down curves of the hysteresis loop can be used as a measure of thixotropy (Barnes 1997). For this study the area between the curves is obtained directly from the software provided with the rheometer. As the calculated area of hysteresis loop depends on the sample shearing history, a coefficient of thixotropy (K_t) is sometimes used (Djakovic et al 1990) which provides a much better and more comparable results. The coefficient is the ratio of the hysteresis loop area and the highest applied shear rate (equation 5.1) and represents the increment of the thixotropic loop area per unit of the applied shear rates intervals. The values of hysteresis loop area and the thixotropic coefficient for the solder paste samples are presented in table 5.1. Of the four pastes tested in the study, paste P1 has showed the highest values for both the hysteresis loop area and thixotropic coefficient. This means that the paste P1 has experienced the highest rate of structural breakdown under the applied shear. In contrast, paste P4 has produced remarkably low values for the area and the coefficient which indicates that the paste P4 is quite strong and is much less prone to collapse under the application of shear.

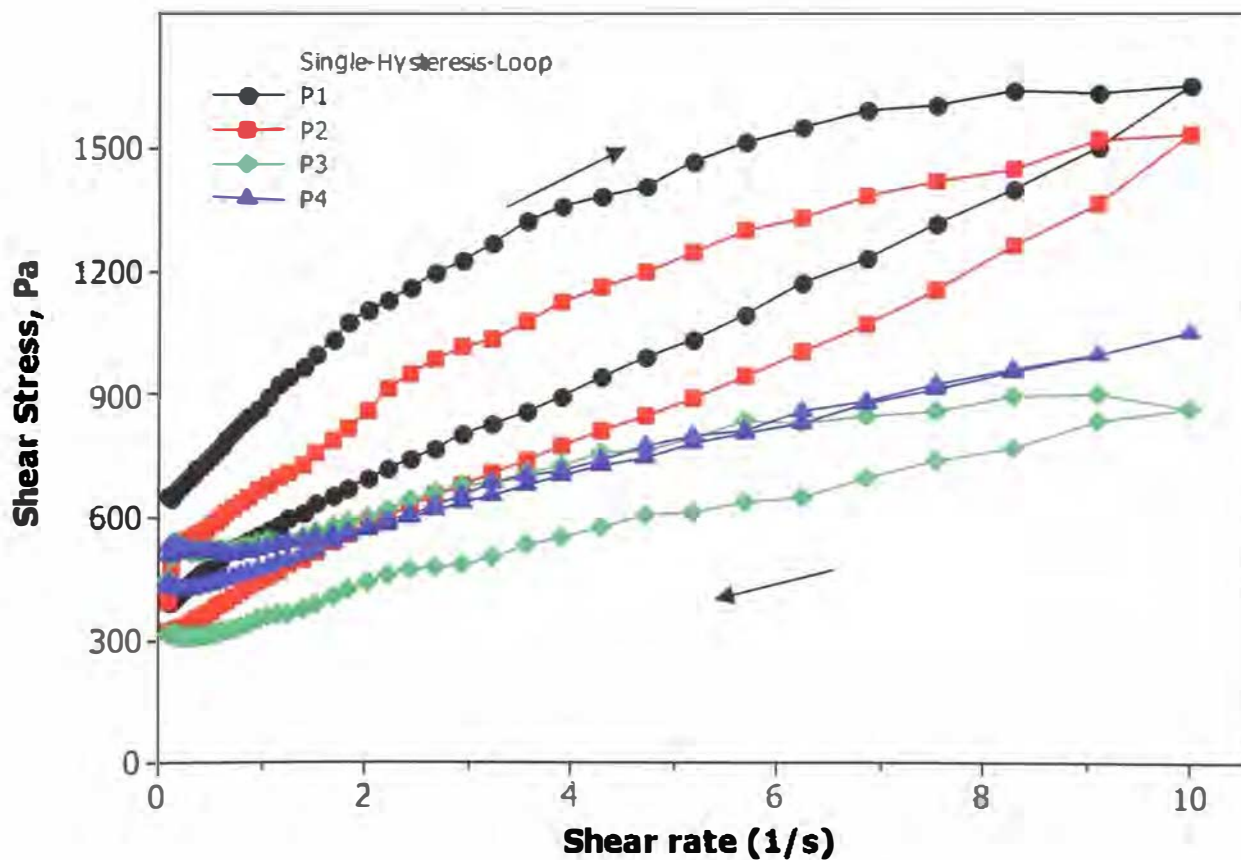


Figure 5.5: Single-Hysteresis-Loop test results for the solder paste samples (P1 to P4)

Table 5.1: Hysteresis loop area (A_t) and thixotropy coefficient (K_t) for solder paste samples

Solder paste	Hysteresis loop area (A_t)	Thixotropy coefficient (K_t)
P1	3300.7	330.7
P2	2648.6	264.9
P3	1515.7	151.6
P4	187.84	18.8

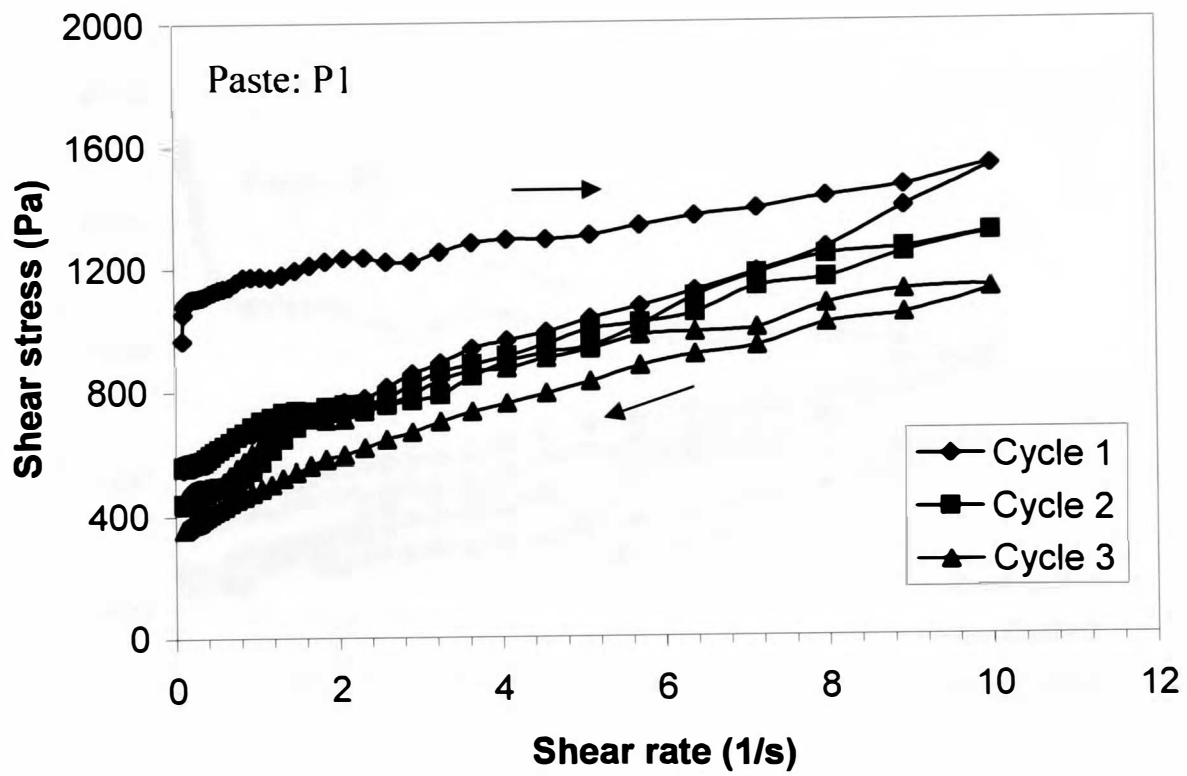


Figure 5.6: Multiple-hysteresis-loop test result for paste P1

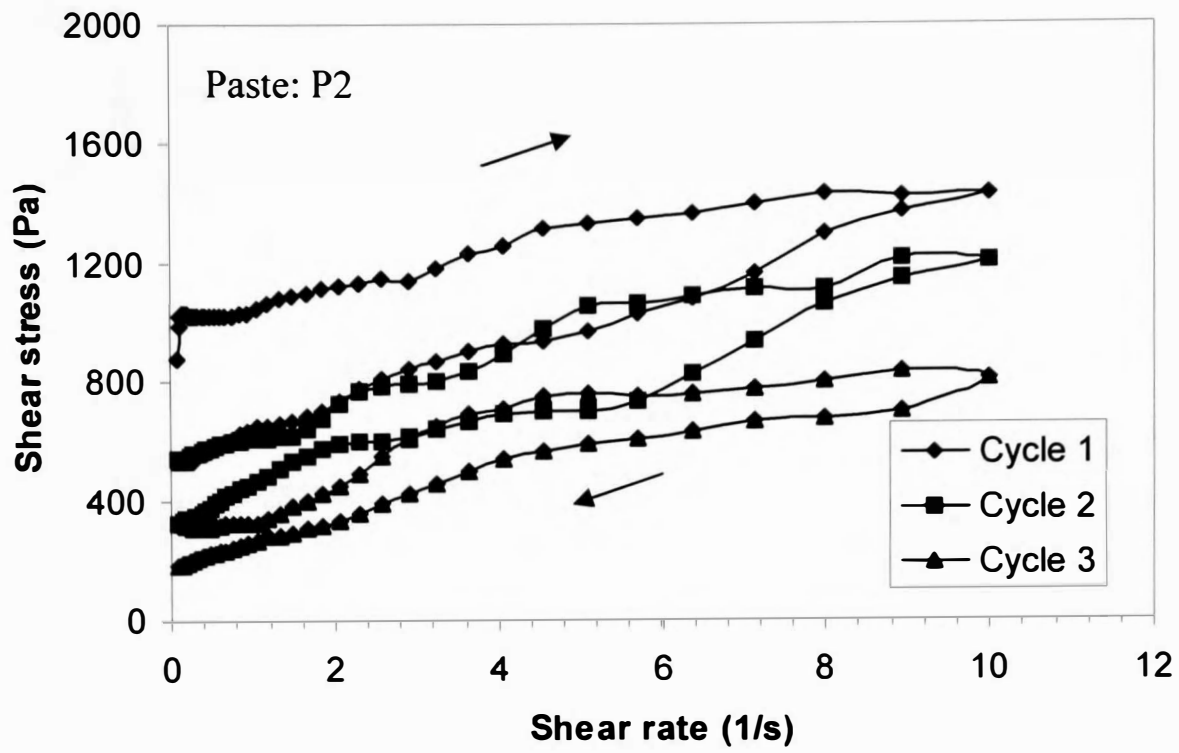


Figure 5.7: Multiple-hysteresis-loop test result for paste P2

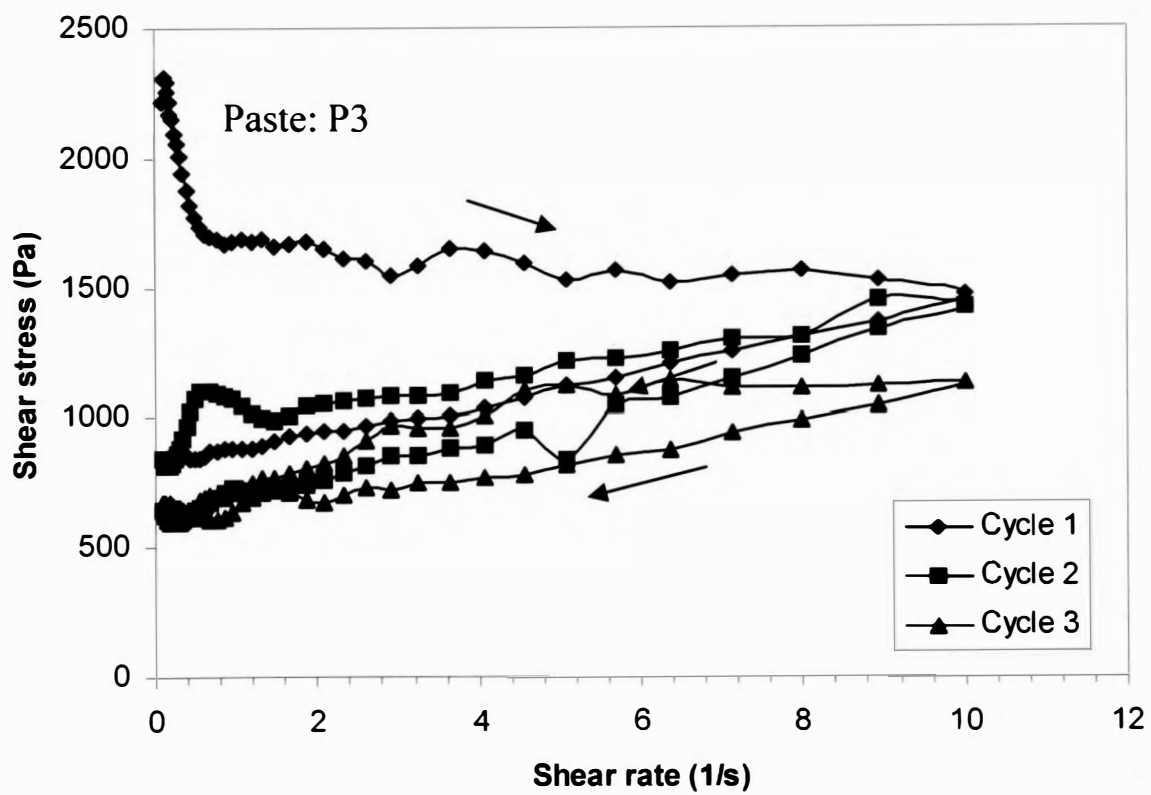


Figure 5.8: Multiple-hysteresis-loop test result for paste P3

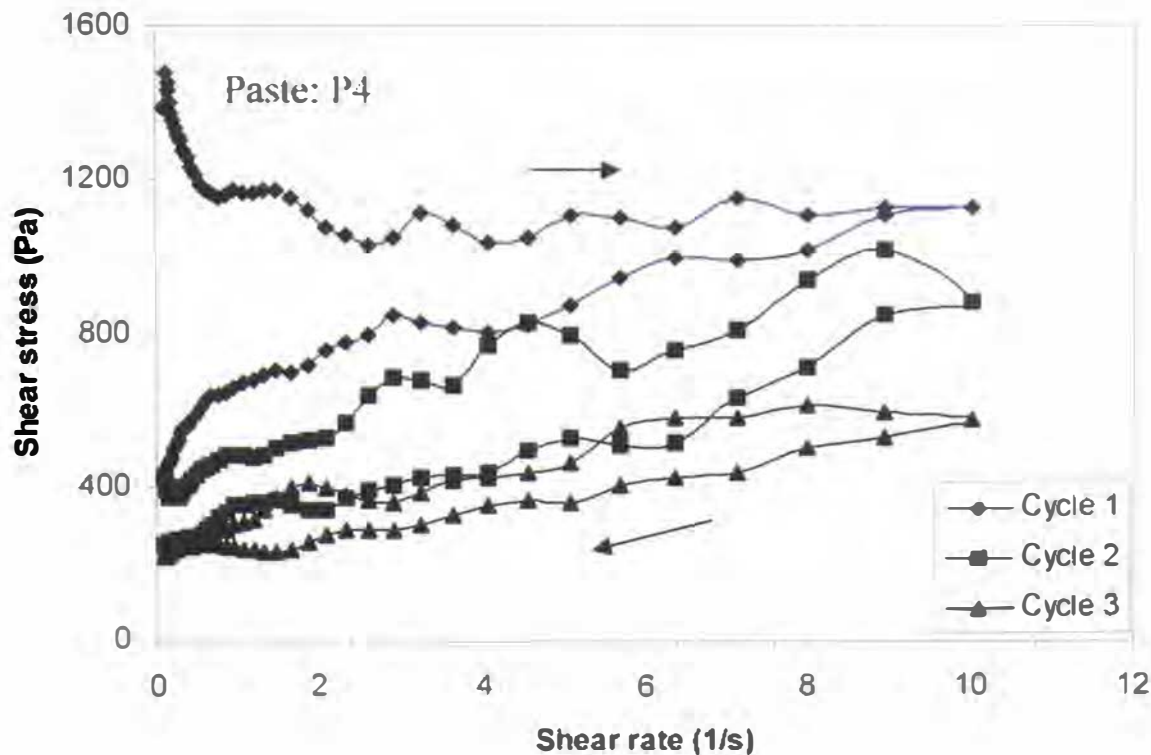


Figure 5.9: Multiple-hysteresis-loop test result for paste P4

In the multiple-hysteresis-loop test a sequence of three hysteresis cycles were applied on the same sample. The shear rate range used for each cycle was the same as the single-hysteresis-loop test (0.01 to 10 s^{-1}). Figures 5.6 – 5.9 gives the results of the multiple-hysteresis-loop test for all the solder paste samples. When the results of single and multiple hysteresis loop tests are compared (figures 5.5 and 5.6 to 5.9), variations in shear stress response can be observed for the same shear rate values. This could be due to effect of “previous shear-history” and “paste-handling” on solder paste flow behaviour. During the continuous shear from 0.01 s^{-1} to a final shear rate value of 10 s^{-1} , the shear stress values in the increasing ramp were greater than those in the decreasing ramp for all solder paste samples (figures 5.6 – 5.9). When more than one thixotropic loop cycle was run on the same sample, the thixotropic loops shifted downward. That is to say that the application of second and third increasing and decreasing cycles shows a lower shear stress of second and third hysteresis loops, suggesting an incomplete recovery of paste structure leading to thixotropic behaviour. It is also observed that the area enclosed between the curves (up and down curve) decreased with each new cycle. The results from the multiple-hysteresis loop test suggest that the paste rheological behaviour can be

strongly affected by the previous shear history and the duration and intensity of the applied shear rate. The changing nature of the solder paste response with increasing hysteresis cycle also suggest that the hysteresis loop can only be used as a qualitative measure of thixotropy as it is highly influenced by the shearing cycle time and the selected shear rates.

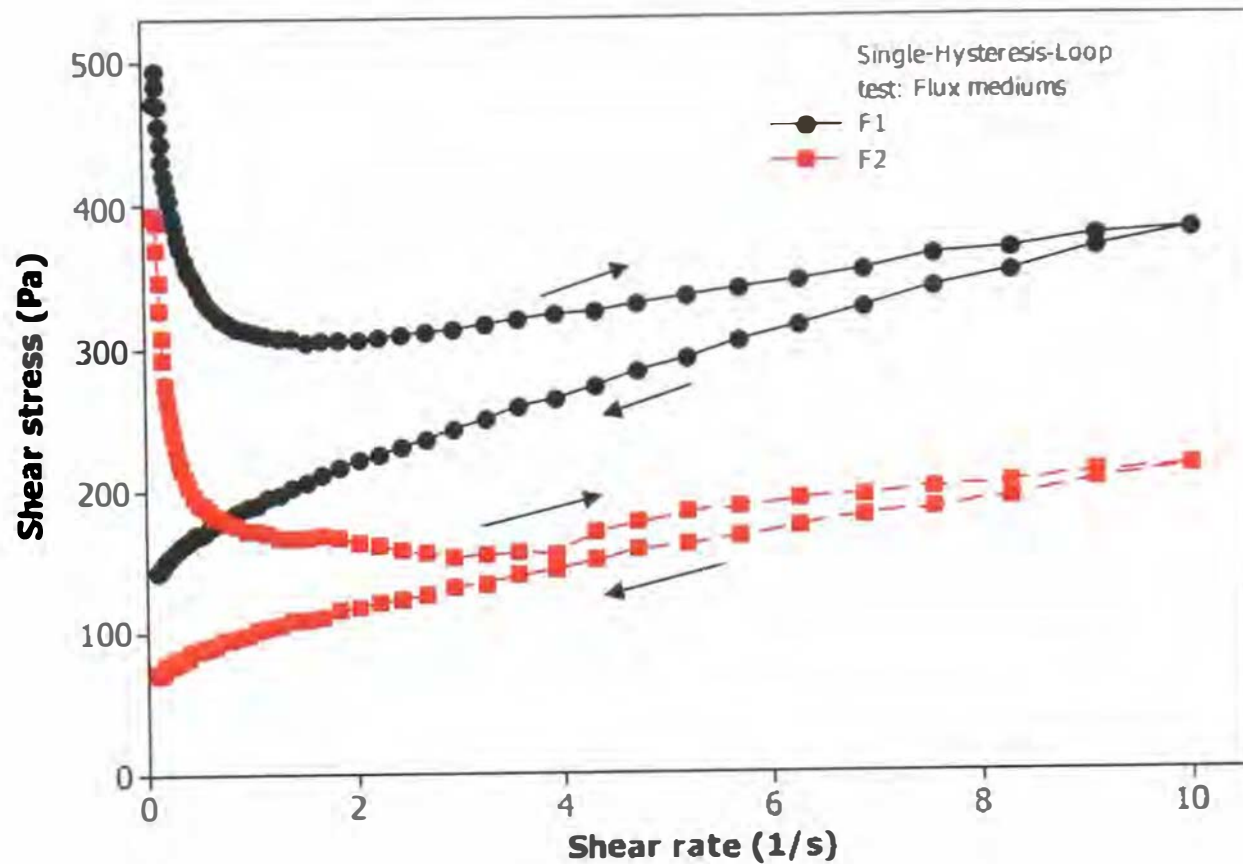


Figure 5.10: Shear stress response to single-hysteresis-loop test for F1 and F2 flux mediums

Table 5.2: Hysteresis loop area (A_t) and thixotropy coefficient (K_t) for flux mediums

Flux mediums	Hysteresis loop area (A_t)	Thixotropy coefficient (K_t)
F1	568.88	56.89
F2	299.77	29.97

The results of the single-hysteresis-loop test for the flux mediums are presented in figure 5.10 and table 5.2. As expected the flux mediums also have shown hysteresis behaviour under the application of shearing cycle. Comparing the results of the single-hysteresis-loop test of solder pastes and flux mediums (figures 5.5 and 5.10), it may be noticed that values of the shear stress for flux mediums were much lower than the solder

pastes. This indicates that the addition of solder particles to the flux medium has made the solder paste stronger. Also the initial elastic response as observed at the beginning of the shearing cycle for solder paste was not observed for flux mediums. This suggests that the flux mediums are more viscous in nature and more shear thinning in nature than solder pastes. The intensity of thixotropic behaviour is also less for flux mediums as evidenced by the lower values of thixotropic loop area and coefficient of thixotropy shown in table 5.2.

Figures 5.11 and 5.12 shows the results of the multiple-hysteresis-loop tests carried out on flux mediums. Flux mediums show a similar behaviour as solder pastes under the application of multiple hysteresis loop cycles. Shear stress values were found to decrease with higher shearing cycle showing an incomplete recovery of flux mediums. As expected, the area of the thixotropic loop (between the up and down curves) was observed to decrease in value for the higher hysteresis loop cycles – the rate of decrease is much more than what was observed for the solder paste samples.

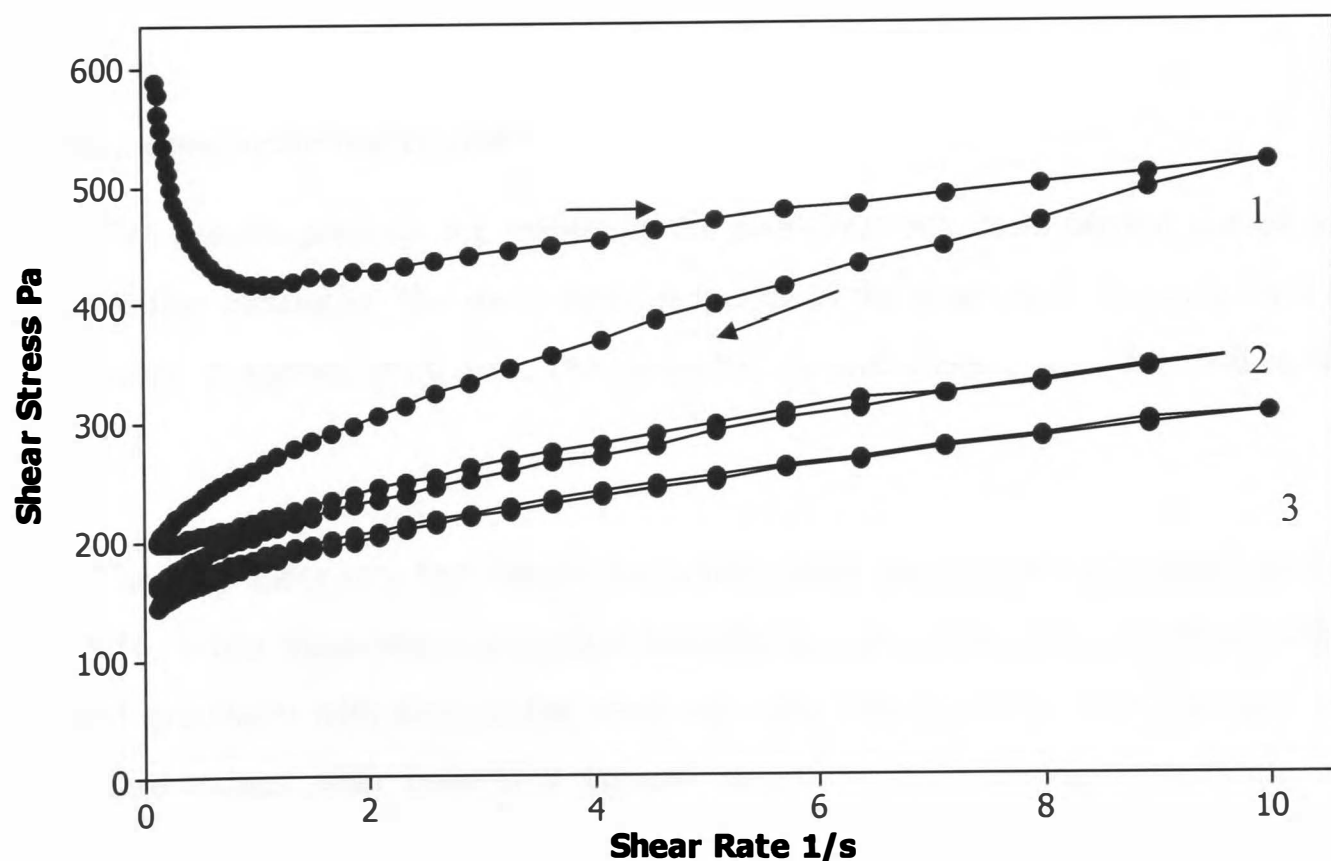


Figure 5.11: Multiple-hysteresis-loop test (3 cycles) results for F1 flux medium.

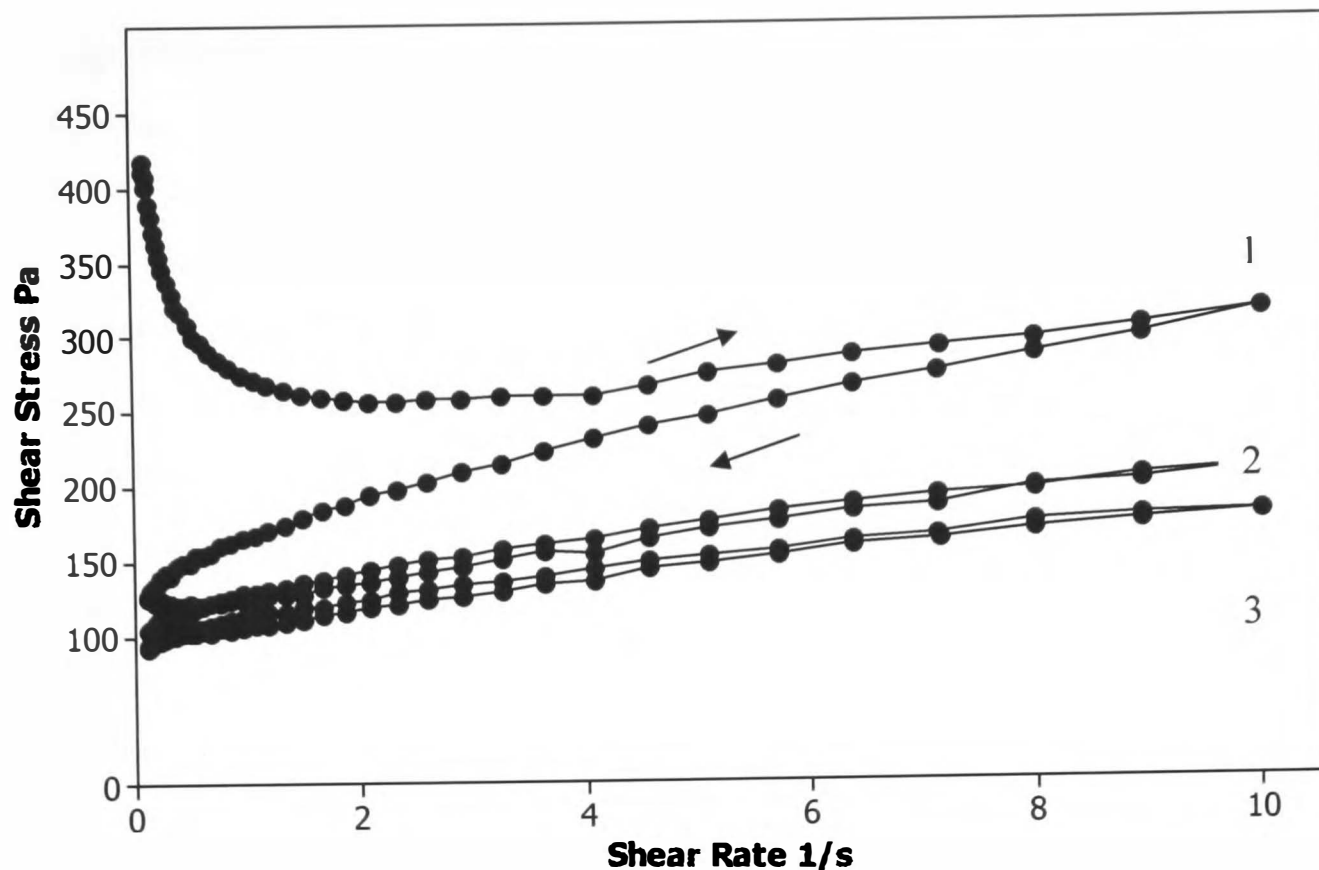


Figure 5.12: Multiple-hysteresis-loop test results for F2 flux medium

5.3.2 Step-shear-rate test results

This section presents the results of the step-shear-rate tests carried out on solder pastes and flux mediums. The shear stress response of the samples is recorded for a step-wise increase in applied shear rate. The details of the test method were outlined earlier in section 5.2.

The step-shear-rate test results for solder paste samples are presented in figures 5.13 – 5.16. When shear rate was applied initially, the stress grew to a maximum and then decreased gradually with time as the shear rate was kept constant. This decrease in the shear stress values with time is a typical behaviour of thixotropic materials which demonstrates a time-dependent breakdown of the sample structure. However, when the shear rate was decreased suddenly, the shear stress decreased to a lower value very quickly, but thereafter increased (first rapidly, then slowly) towards an equilibrium. This type of behaviour can be attributed to the thixotropic build-up of paste structure. When

the shear was increased again to a higher value in the next step, a sharp peak in the shear stress was followed by a steep decrease at first and then a gradual decrease in shear stress was observed.

The step-wise increase in shear rate has influenced the thixotropic behaviour of solder paste samples. This was more obvious during the structural build-up stages when a lower shear rate was applied. As stated earlier (section 5.2 , figure 5.4), during the test period the high shear rate was increased in four steps (1, 2, 4 and 6 s⁻¹), but the low shear rate value was kept constant at 0.05 s⁻¹. As the shear rate values increased, the extent of the structural breakdown also increased. This is demonstrated by the increase in magnitude of drop in shear stress values (when shear rate instantaneously decreased to a lower value) i.e. each time the higher shear rate value increased, the initial shear stress has gone down to a further lower value as soon as the shear rate changed to the lower value. The rate of thixotropic build-up of solder paste structure during the low shear period has also increased with the increase in higher shear rate values. Moreover, although the low shear rate value was same for every step, the equilibrium level reached after each build-up stage was not same and was indeed found decreasing as the step progresses. This implies that the build-up of solder paste structure depends largely on both the previous shear history and the intensity of structural break-down.

This time-dependent behaviour of solder pastes can be explained at the micro-structural level – using the concepts first suggested by Barnes (1997) for thixotropic materials behaviour. In this case, solder pastes can be considered as a flocculated suspension of solder particles in a flux medium. At the start of the test the solder paste microstructure was at rest and hence was only made up of a series of large flocs. When the shear rate was applied suddenly, the floc size changes instantaneously to match with the applied shear rate. But as the shear rate was kept constant, the microstructure begins to break-down and the floc size decreases, until it reaches an equilibrium size appropriate to the applied shear rate. For solder paste this process could take hours (see chapter 6). Now if the shear rate is decreased suddenly to a lower value, the solder particles begin to align once again to re-start flocculation; which continues until the floc size exactly match

with the lower shear rate. Eventually a new equilibrium is attained in this way. This process of structural build-up also takes time. Based on the time-scales involved, solder paste shows two types of build-up phenomena: immediate or short-term build-up (between stencil printing and reflow) and long-term build-up (during storage and idle time), see chapter 7 for more details. As the shear rate is increased with each step, the solder paste sample experiences further structural breakdown, resulting in further decrease in the floc size, and hence lower shear stress values. The level of structural breakdown is a function of the extent of the re-alignment of the solder particles in the low shear stage.

Figures 5.17 and 5.18 shows the results of the step-shear-rate tests carried out on the flux mediums. As with the solder paste samples, both flux mediums show thixotropic behaviour under the step-wise application of shear. As was noted for hysteresis loop test results (section 5.3.1), the step-shear-test results also shows that the flux mediums are more viscous in nature and more shear-thinning compared to solder pastes. This is demonstrated by the higher rate of decrease in shear stress values at higher shear rate values in the steps.

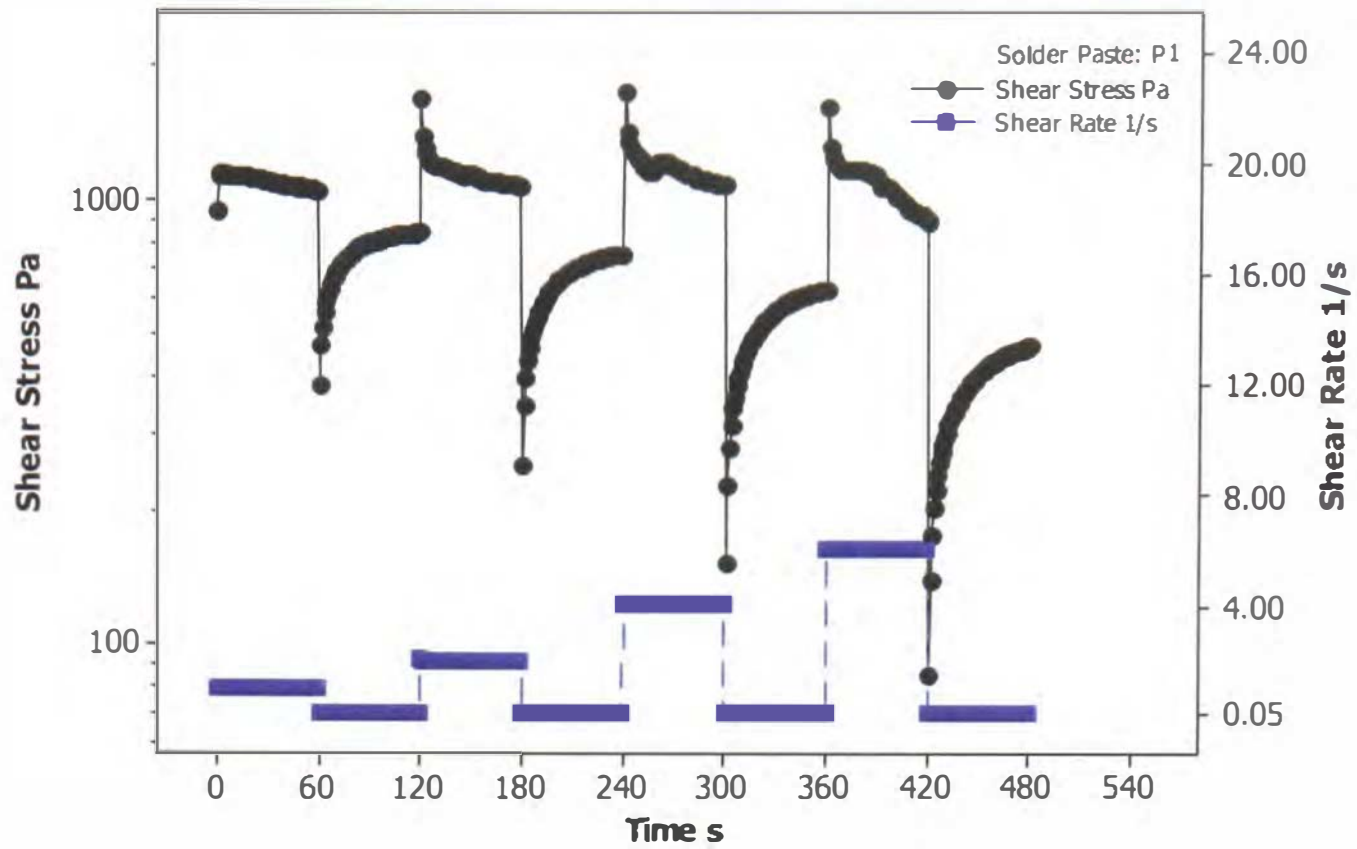


Figure 5.13: Shear stress response for a step-wise application of shear rates on paste P1.

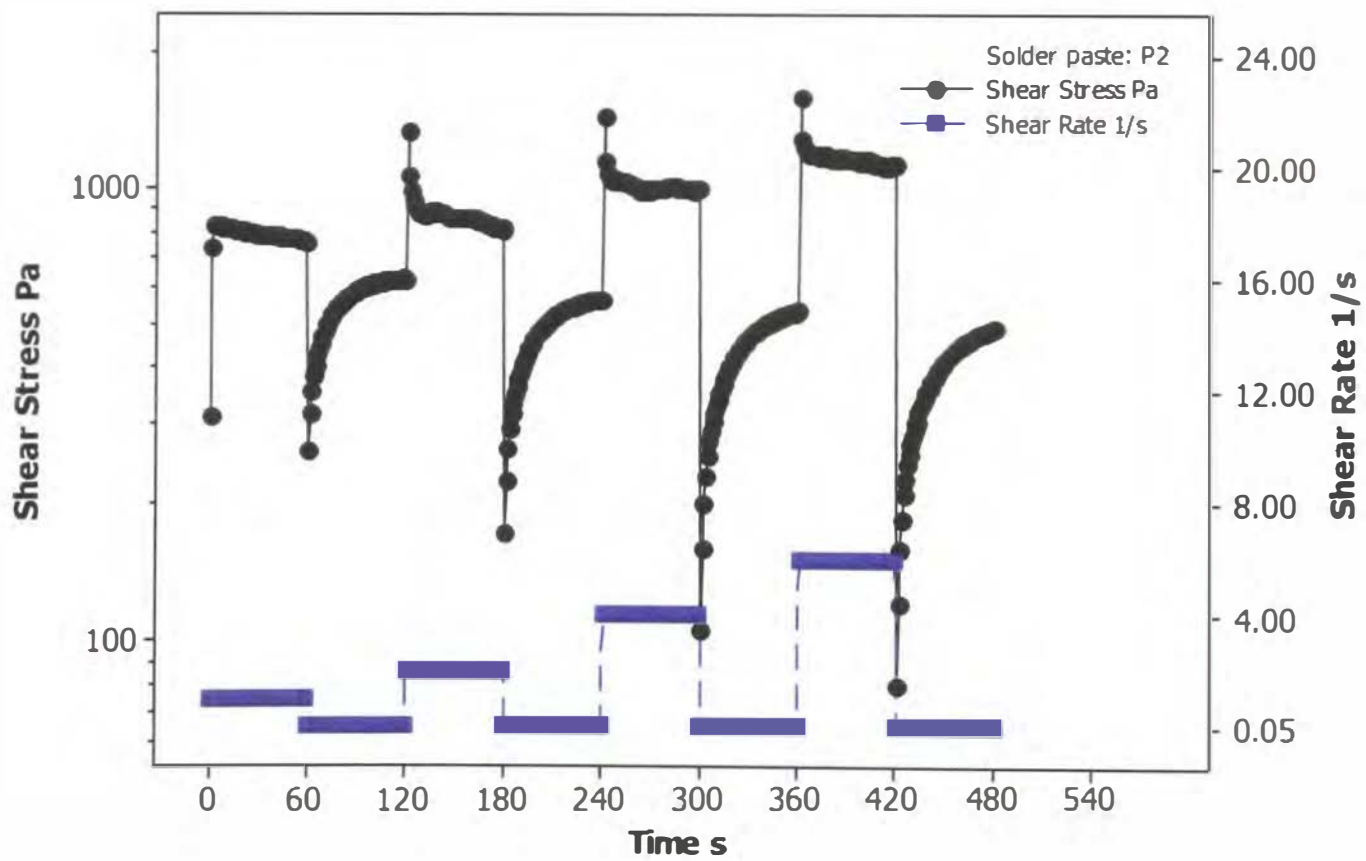


Figure 5.14: Shear stress response for a step-wise application of shear rates on paste P2

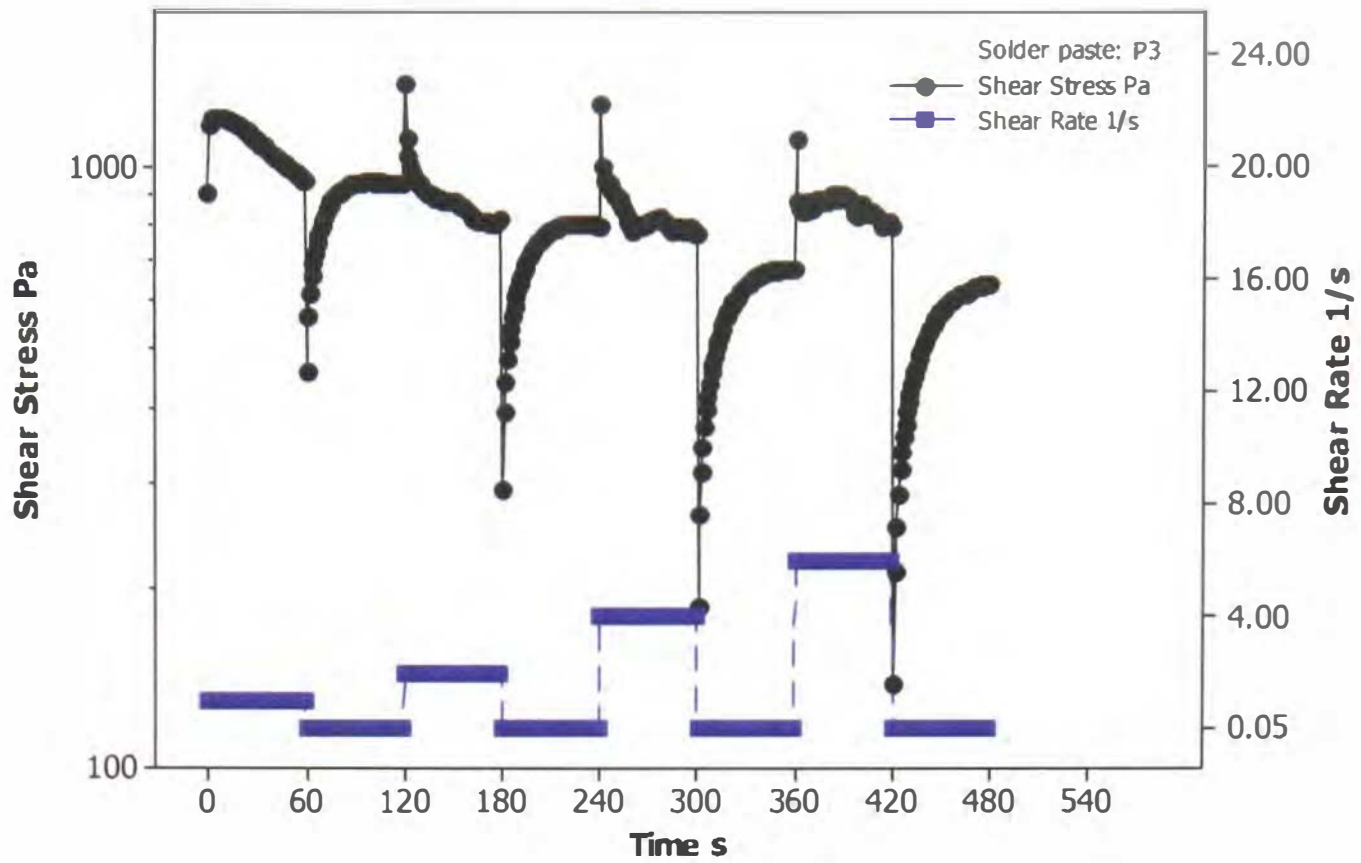


Figure 5.15: Shear stress response for a step-wise application of shear rates on paste P3.

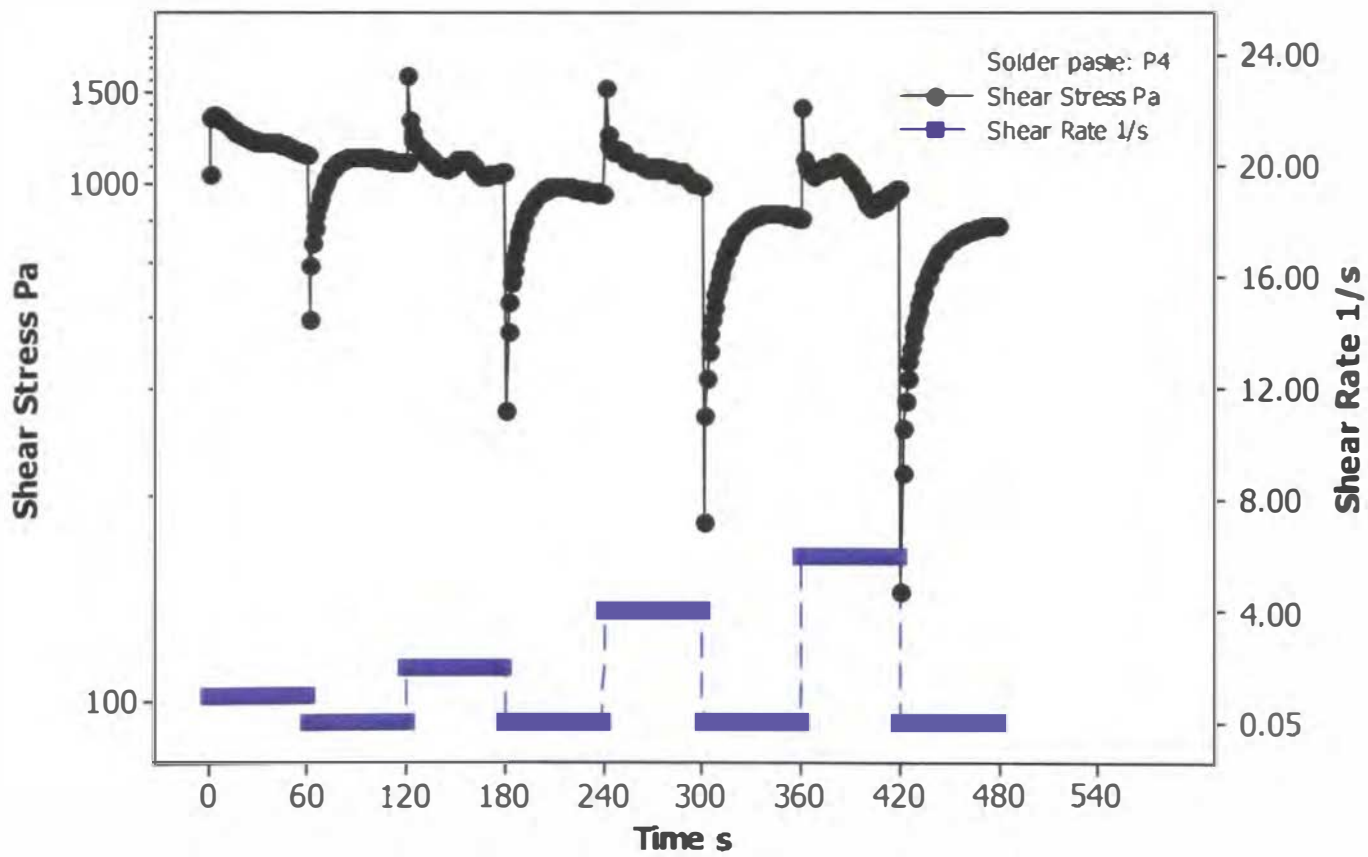


Figure 5.16: Shear stress response for a step-wise application of shear rates on paste P4.

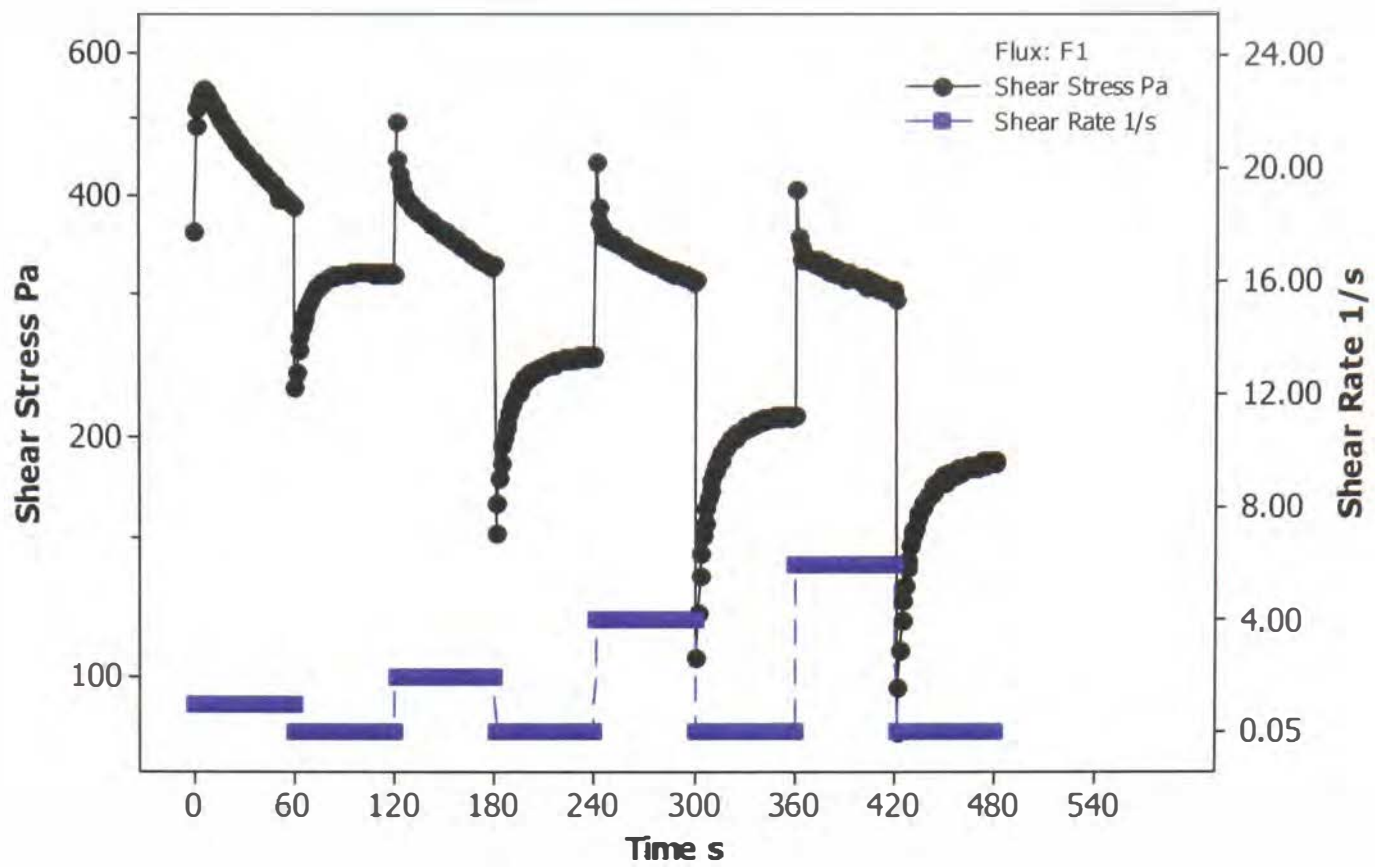


Figure 5.17: Shear stress response for a step-wise application of shear rates on paste P1.

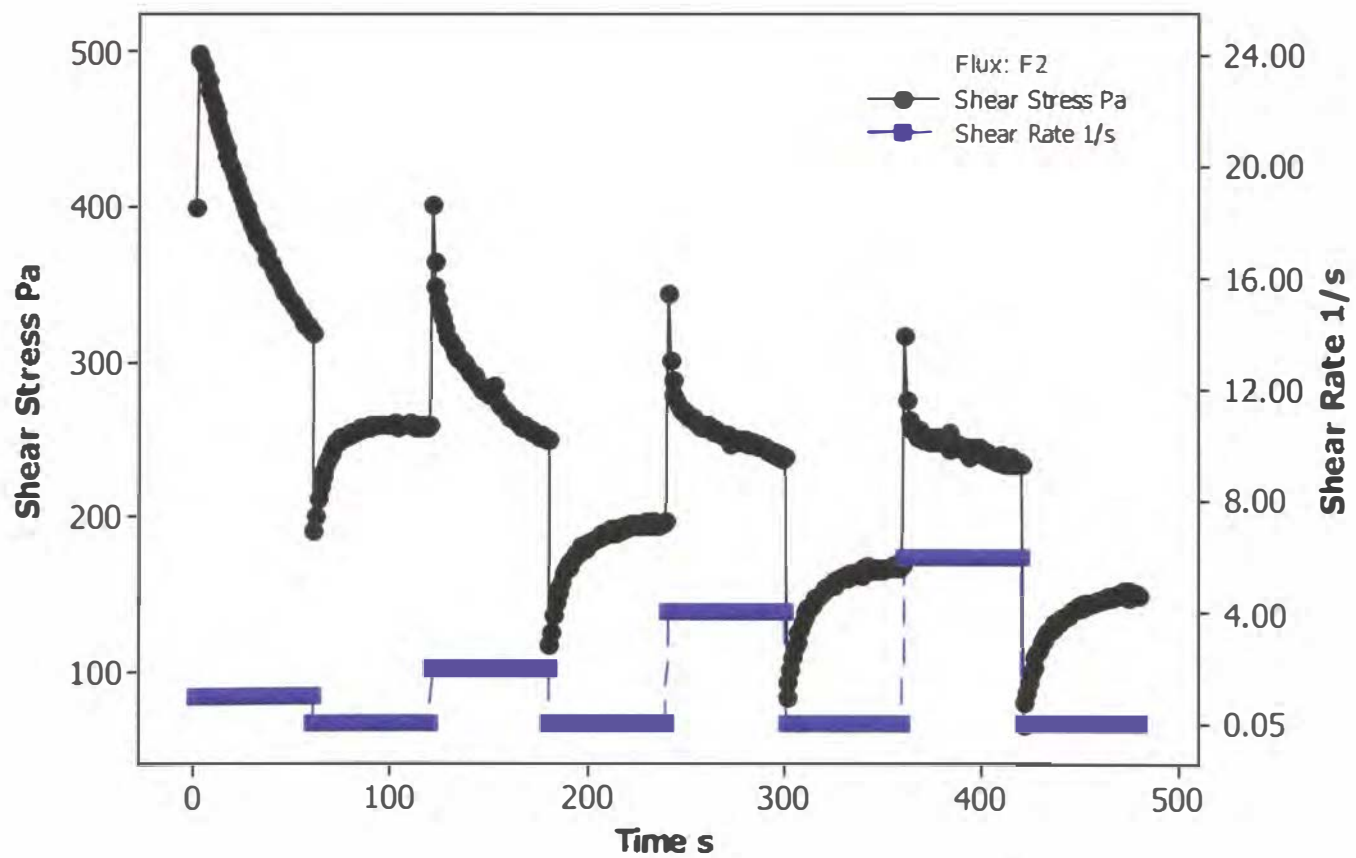


Figure 5.18: Shear stress response for a step-wise application of shear rates on paste P1.

5.4 Summary

The thixotropic flow behaviour of solder pastes and flux mediums have been studied through hysteresis loop tests and step-shear-rate tests. The objectives of these tests were to qualify and characterize the thixotropic behaviour of solder pastes and flux mediums. As expected, all the solder paste samples and flux mediums have shown thixotropic behaviour under the application of shear. From the hysteresis loop test results, paste P1 showed the largest area between the up and down curve followed by P2, P3 and P4 solder pastes. The large area observed for P1 paste suggests a higher rate of structural breakdown and poor recovery behaviour. When correlated to the paste printing process, this implies that while the paste P1 would flow more easily during the aperture-filling and aperture-emptying sub-processes, it would also be more prone to slumping if compared to other paste samples. With the multiple-hysteresis-loop test, the shear stress values was found decreasing (hysteresis loop moved downward) for both solder pastes and flux mediums. This indicates an incomplete recovery of sample structure due to consecutive shearing cycles. Because of this incomplete structural recovery, one should expect variations in printing results from consecutive solder paste printing. From the hysteresis loop test it was also concluded that the hysteresis loop test can only be considered as qualitative because the hysteresis is strongly affected by the shearing cycle time, the paste shear history and maximum shear rate selected.

Step shear tests were performed on solder pastes and flux mediums by applying a sequence of step-wise increase in shear rates. The two shear rates values were chosen in such a way that one of them was high enough to break the sample structure, while the other one was very low to allow the sample to build-up. The step-wise increase in shear rate has influenced the thixotropic behaviour of solder paste samples and flux mediums. This was more obvious during the structural build-up stages when a lower shear rate was applied. The rate of structural breakdown and build-up was found increasing with the increase in higher shear rate values. The result from the step-shear-test implies that the build-up of solder paste structure depends largely on both the previous shear history and the intensity of structural break-down.

CHAPTER 6
MODELLING OF THE BREAK-DOWN OF THE PASTE STRUCTURE
USING THE STRUCTURAL KINETIC MODEL

6.1 Introduction

The non-Newtonian flow properties exhibited by solder pastes during its manufacturing and application phases have been of practical concern to R&D scientist and process engineers for many years. With the increased miniaturisation of the electronic products and the need to meet the challenges of making greener products a number of formulation, processing and application problems have arisen which can, directly or indirectly, be related to the complex rheological behaviour of solder pastes. A better understanding of the rheological properties of the solder pastes (and associated flux mediums) and their effect on pastes processing performance is key to minimizing manufacturing defects – and improve yield.

In order to understand rheological phenomena associated with the flow of solder pastes, it is necessary to understand time dependent rheological behaviour. Such behaviour is common to many industrial fluids and consequently has been of interest to rheologist for many years.

Solder pastes experience a continuous change in terms of break-down and build-up of its internal structure during its manufacturing/packaging and also during its processing phases. This shear induced breakdown of solder paste structure involves two contrasting processes. The application of shear force acts to break down the bonds between the primary solder particles or the aggregates of such particles. At the same time however; shear-induced collisions of the separated structural elements tend to reform part of the broken bonds. The two opposite time-dependent phenomenon gives rise to overall break-down of the paste structure and thus result in reduction in the viscosity over time.

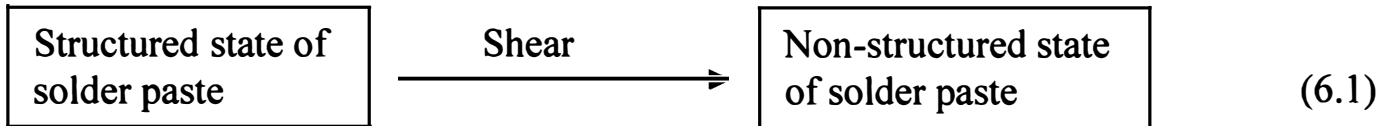
A state of equilibrium can be attained if sufficient time is allowed, at which point the rate of the breakdown of the paste structure and the rate of the pastes structural build-up will be in balance.

The chapter presents a quantitative evaluation of the thixotropic breakdown of the structure of solder pastes and flux mediums under shear, using a rotational rheometer. The structural kinetic model (SKM) has been used to investigate the rate of structural breakdown of solder paste and to correlate the experimental kinetic data with the model parameters. The chapter is made up of three parts: the first part provides a theoretical background on the structural kinetic model used for modelling the breakdown of paste materials, the second part outlines the materials and experimental methods used in this study and the final part presents the results of the investigation.

6.2 Theory - Structural Kinetic Model

The time-dependent flow behaviour of solder pastes can be modelled using the structural kinetic approach. The structural kinetic theory was originated by Cheng and Evans (1965) and was then extended by Petrellis and Flumerfelt (1973) to describe the time-dependent behaviour of shear degradable crude oils. Since then the theory has been modified and simplified to describe the time-dependent flow behaviour of various materials including mayonnaise (Tiu & Boger, 1974), concentrated mineral suspensions (Nguyen & Boger, 1985), starch pastes (Nguyen, Jensen & Kristensen, 1998) and more recently for concentrated yogourt and semisolid foodstuffs (Abu-Jdayil & Mohameed, 2002; Abu-Jdayil, 2003). Although the SKM has been successfully used to model the time-dependent behaviour of different suspensions, there are however, no reports of using the model to study the time-dependent flow behaviour of solder pastes and flux mediums.

As postulated by the structural kinetic model the change in the time-dependent rheological properties of solder paste is associated with shear induced breakdown of the internal structure. This structural change is quite analogous to that of a chemical reaction and the mechanism can be expressed as:



If λ is a dimensionless time-dependent structural parameter the above reaction can be expressed as:

$$\frac{d\lambda}{dt} = f(\lambda, \dot{\gamma}) \quad (6.2)$$

The rate equation states that the rate of change of structure, or alternatively the structure parameter is a function of the shear rate as well as of the structural parameter. The model also assumes that the structure recovery after shear is negligible and the degradation of structure is irreversible.

According to Nguyen et al (1998), the decay of the structural parameter with time is assumed to obey an n-order kinetic equation:

$$\frac{d\lambda}{dt} = -k(\lambda - \lambda_e)^n \quad (6.3)$$

where the rate constant, k , is a function of shear rate to be determined experimentally, and n is the order of the breakdown reaction. Initially, at the fully structured state, $t = 0 : \lambda = \lambda_0$ and at equilibrium state, $t \rightarrow \infty : \lambda = \lambda_e$.

Integration of equation (6.3) can only be achieved in certain special cases. One of these is the case of constant shear rate degradation. Under such conditions k and λ_e are constant and equation (6.3) can be integrated from $\lambda = \lambda_0$ at $t = 0$ to $\lambda = \lambda$ at $t = t$ to yield:

$$\begin{aligned} \int_{\lambda_0}^{\lambda} \frac{1}{(\lambda - \lambda_e)^n} d\lambda &= \int_0^t k dt \\ \Rightarrow \frac{1}{-n+1} (\lambda - \lambda_e)^{1-n} \Big|_{\lambda_0}^{\lambda} &= -kt \Big|_0^t \\ \Rightarrow \frac{1}{(1-n)} [(\lambda_0 - \lambda_e)^{1-n} - (\lambda - \lambda_e)^{1-n}] &= kt \end{aligned}$$

After rearrangement, we have:

$$(\lambda - \lambda_e)^{1-n} = (n-1)kt + (\lambda_0 - \lambda_e)^{1-n} \quad (6.4)$$

The determination of the rate constant k in equation (6.4) as a function of shear rate is not easy because of the fact that the structural parameter λ cannot be acquired explicitly from the experimental measurements. To overcome this difficulty, the structural parameter λ is defined in terms of apparent viscosity.

The apparent viscosity may be defined for any fluid by the equation:

$$\eta = \frac{\text{Shear stress, } \tau}{\text{Shear rate, } \dot{\gamma}} \quad (6.5)$$

where η is a function of both shear rate $\dot{\gamma}$ and time of shear t .

Again, according to Nguyen et al (1998), the structural parameter λ may be defined in terms of apparent viscosity as

$$\lambda(\dot{\gamma}, t) = \frac{(\eta - \eta_e)}{(\eta_0 - \eta_e)} \quad (6.6)$$

where η_0 is the initial apparent viscosity at $t = 0$ and η_e is the equilibrium apparent viscosity at $t \rightarrow \infty$. It should be noted that, both η_0 and η_e are functions of applied shear rate only.

Substituting equation (6.6) into equation (6.4) we get, for a constant shear rate:

$$\left[\frac{(\eta - \eta_e)}{(\eta_0 - \eta_e)} \right]^{1-n} = (n-1)kt + 1 \quad (6.7)$$

Equation (6.7) is only valid only under the constant shear rate condition. The form of equation (6.7) is particularly useful for testing the validity of the model by checking the linearity of the $\left[(\eta - \eta_e) / (\eta_0 - \eta_e) \right]^{1-n}$ and t data and also for determining the model parameters n and k .

6.3 Experimental design

6.3.1 Materials and preparation

Two fluxes F1 and F2 and four lead-free solder pastes P1 to P4 prepared from the fluxes are investigated. The details of these fluxes and the solder paste samples are provided in section 4.2.3 of this thesis.

6.3.2 Rheological measurements

The rheological measurements were carried out using a Bohlin Gemini-150 controlled-stress/strain rheometer. A roughened or serrated parallel plate geometry (with serrations on both upper and lower plates) of 20 mm upper plate diameter and 40 mm lower plate diameter was used in order to minimize the effect of wall-slip. The roughness values (R_a) for the upper and lower plate were 13.7 and 17.6 respectively. Prior to loading a sample onto the rheometer, the solder paste samples were stirred or hand mixed with a plastic spatula for about 30 seconds. The sample is loaded on the bottom plate and the top plate is then lowered to the desired gap height of 500 μm by squeezing the extra paste out from between the plates. The excess paste at the plate edges is trimmed off neatly with a plastic spatula. Then the sample is allowed to rest for about 1 min before starting the test. Identical loading procedures were followed in all the tests. All tests were conducted at $25^\circ\text{C}(\pm 0.1^\circ\text{C})$ with the temperature being controlled by a Peltier-Plate system. The reproducibility of the experimental results were assured by doing two replicates for each of the tests and the results were fairly reproducible with $\pm 5\%$ variation on average.

6.4 Results and discussion

The solder paste samples and the fluxes used in this investigation were subjected to prolonged shear at constant shear rate values. This is to ensure that the samples are able to reach an equilibrium state at which the rheological behaviour is no longer dependent on shear time.

6.4.1 Results and Discussion for Solder Paste Samples

Solder paste samples were sheared for a period of 8 hours at different values of constant shear rates, namely 2, 4, 6, 8 and 10 s⁻¹. The effect of shear rate on the thixotropic behaviour of solder paste samples were investigated. The results are presented as a series of apparent viscosity versus shear time curves as a function of shear rate (figures 6.1 – 6.4). The results show that the rate of change in viscosity increases with increase in shear rate for all the paste samples. At a constant shear rate, the apparent viscosity decreases rapidly with time in the initial stages and is then followed by a constant flat plateau region. The results also show that for all the paste samples, no significant change was observed after 60 minutes of shearing. This indicates that the solder paste is at an equilibrium state. The results clearly demonstrate that the apparent viscosity can be drastically reduced from the initial unperturbed (structured) state to an equilibrium (de-structured) state with the application of shear. This indicates that the solder paste samples are highly shear-thinning in nature. The rate of decay is quite rapid in the first hour of shearing, but reduces in magnitude as shearing is prolonged to approach the equilibrium state.

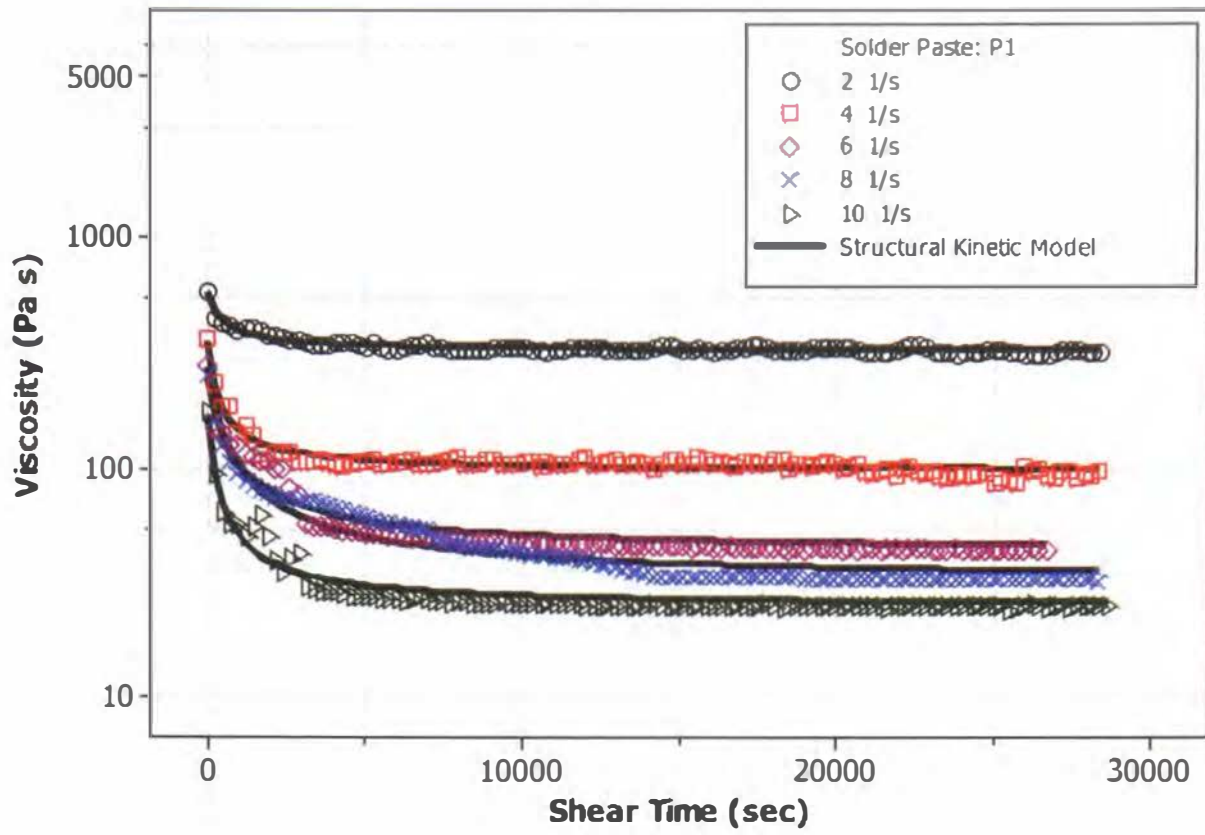


Figure 6.1: Effect of shear rate on apparent viscosity for paste P1 at 25⁰C.

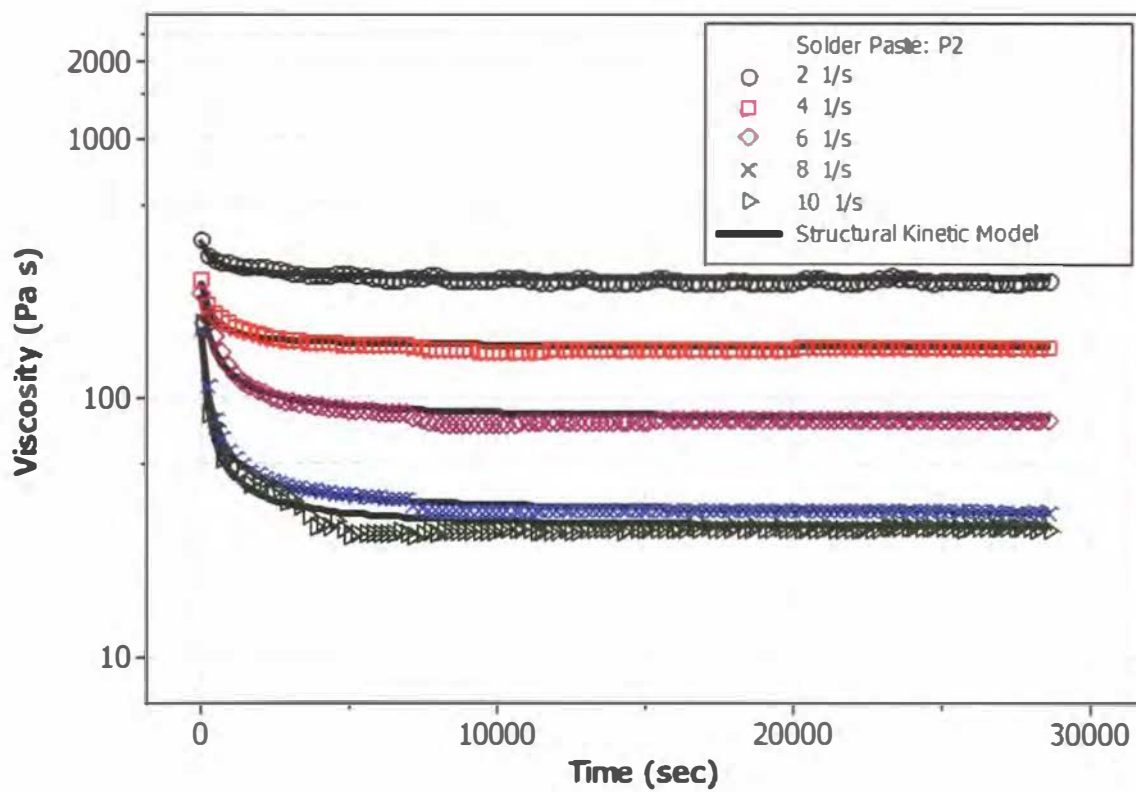


Figure 6.2: Effect of shear rate on apparent viscosity for paste P2 at 25⁰C.

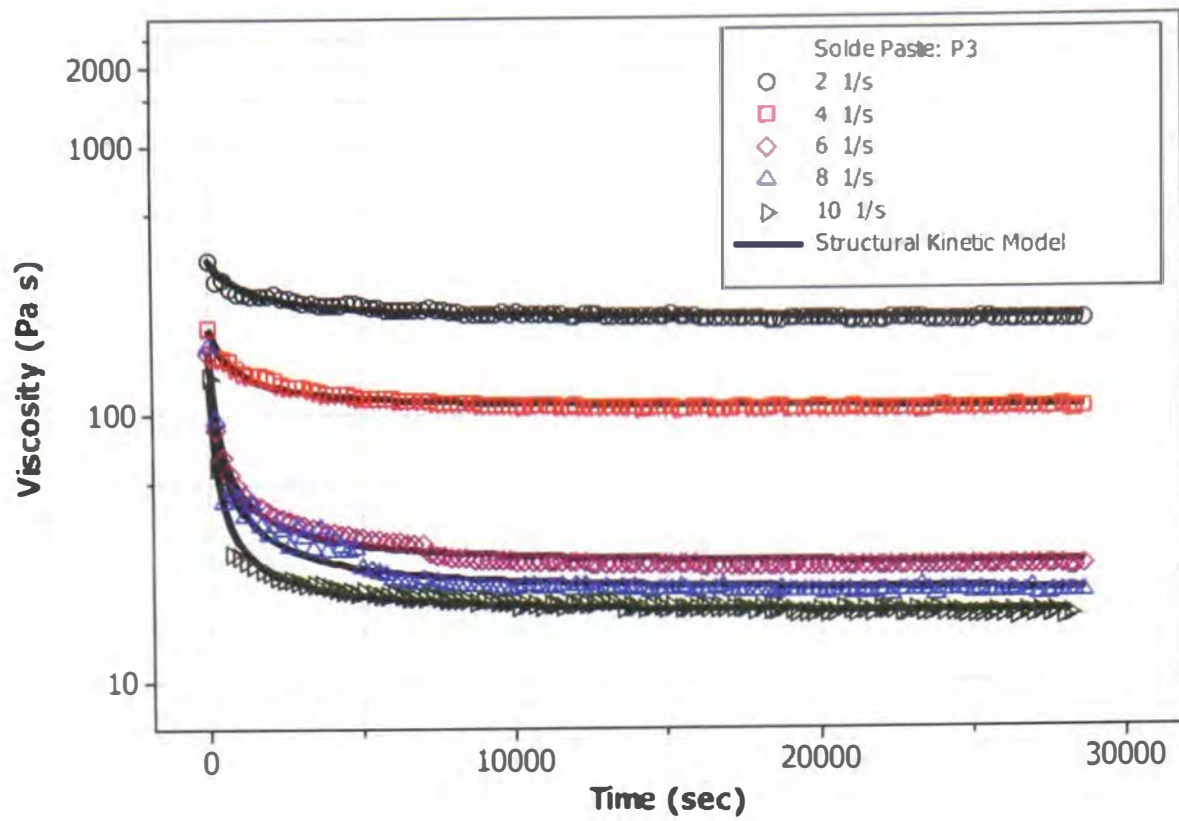


Figure 6.3: Effect of shear rate on apparent viscosity for paste P3 at 25°C.

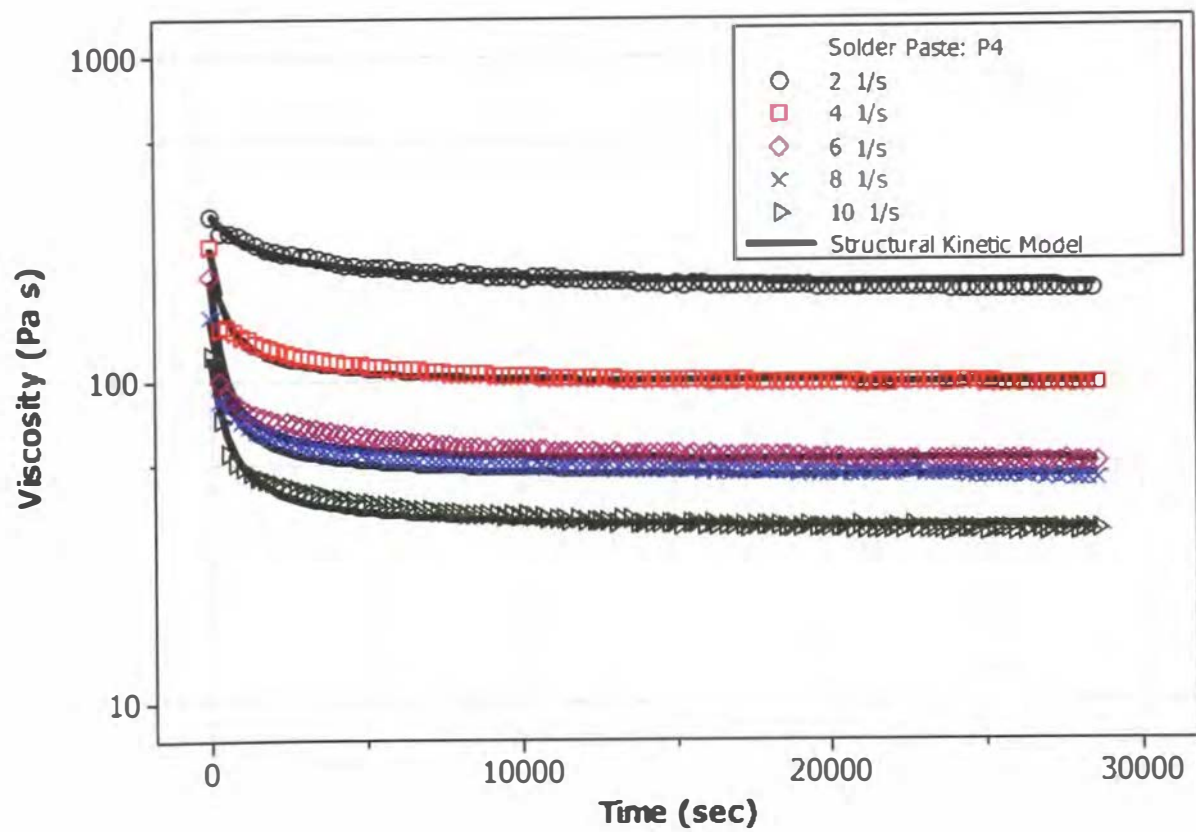


Figure 6.4: Effect of shear rate on apparent viscosity for paste P4 at 25°C.

Samples of the pastes (P1, P2, P3 and P4) all exhibited thixotropic behaviour for the shear rate values tested. The observed thixotropic flow behaviour of solder pastes was modelled using the structural kinetic approach. For all solder paste samples studied, it was found that their apparent viscosity at constant shear rates could be satisfactorily correlated using $n = 2$ in Eq.(6.7), i.e., with a second-order structural kinetic model. Figure 6.5 shows the plots of $[(\eta - \eta_e)/(\eta_0 - \eta_e)]^{-1}$ vs. t for different solder paste samples. All the pastes demonstrate linearity, which confirms the applicability of the structural kinetic model given by equation 6.7.

Figures 6.1 to 6.4 show a good correlation between the structural kinetic model fitted result (solid line) and the apparent viscosity-time data for all the solder paste samples tested. Table 6.1 presents the values of rate constant, k , the ratio of initial to equilibrium viscosity, η_0 / η_e , initial viscosity, η_0 and the correlation coefficient, r as a function of the applied shear rate for the solder paste samples. The rate constant, k , is a measure of rate of structural breakdown. The ratio of initial and equilibrium viscosity (η_0 / η_e) on the other hand shows the extent of structural decay with shear. For materials which exhibit time-dependent flow behaviour, the rate constant k is expected to increase with increasing shear rate, as was observed for starch pastes (Nguen et al 1998) and for yogurt (Abu-Jdayil, 2002). Examination of Table 6.2 shows that only paste P3 show this increase in the rate constant k – the other pastes do not show a definite trend. One of the reasons of this behaviour might be because the constant shear rate values applied on the solder paste samples were quite close to each other and hence were not able to produce any big difference in terms of the k values. The other reason of variation could be because of the “experimental scattering” of the test data. However, although the k value for these pastes did not follow the expected trend, it should be noted that the ratio of the initial to equilibrium viscosity (η_0 / η_e) was generally found to increase with increasing shear rate, demonstrating shear thinning behaviour. For example, for solder paste sample P2, the apparent viscosity was found to decrease from 194 Pas for a shear rate of 10 s^{-1} to a value of 31 Pas when the shear rate reached an equilibrium state. The shear thinning nature of

these solder pastes was also evident from the initial apparent viscosity values (η_0) which were generally found to decrease with increasing shear rate values.

Table 6.1: The parameters from the second-order kinetic model for solder paste samples evaluated at different shear rates.

Solder Paste	Shear rate (1/s)	k ($\times 10^{-3}$)	η_0 / η_e	η_0	Correlation coefficient, r
P1	2	2.360	1.789	584.9	0.960
	4	4.441	3.779	369.3	0.980
	6	2.735	6.448	279.3	0.970
	8	2.182	7.994	255.8	0.979
	10	4.766	7.118	176.8	0.984
P2	2	2.371	1.421	406.4	0.946
	4	3.874	1.808	282.0	0.977
	6	2.962	3.064	250.0	0.988
	8	4.736	5.184	183.0	0.999
	10	6.765	6.274	193.8	0.990
P3	2	1.029	1.710	379.7	0.970
	4	1.586	2.021	209.2	0.983
	6	4.560	6.353	169.0	0.996
	8	5.296	8.638	180.1	0.988
	10	6.627	7.945	138.4	0.995
P4	2	0.680	1.721	328.1	0.984
	4	3.427	2.722	261.4	0.963
	6	4.937	3.849	211.4	0.973
	8	3.475	3.234	157.7	0.975
	10	3.158	3.554	120.2	0.984

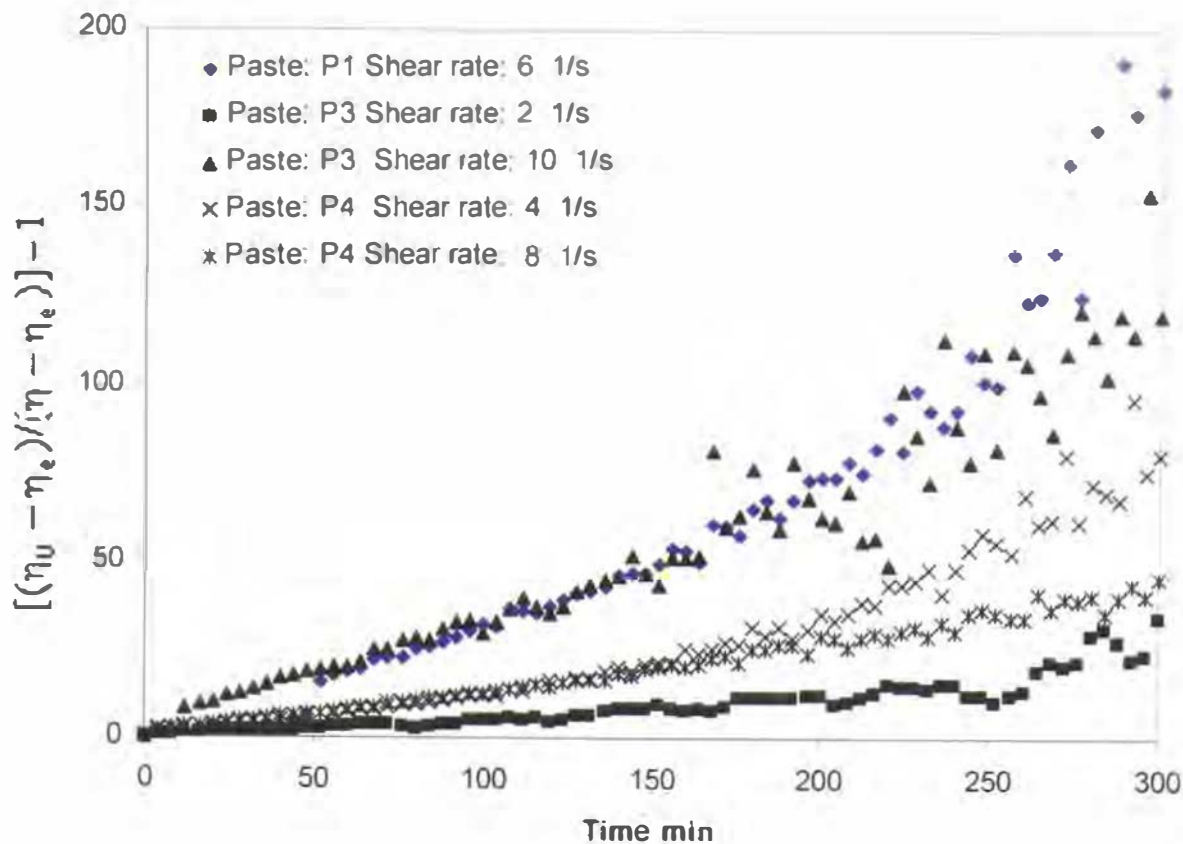


Figure 6.5: Testing of the structural kinetic model with different solder paste samples at 25°C.

As stated earlier (section 6.3), the kinetics of structural breakdown of solder paste can be linked to that of red mud suspension as observed by Nguyen and Boger (1985). Based on this study, we can assume that there are two main types of bonding in the internal structure of solder pastes: (i) bonds between the particles or inter-particle bond and (ii) bonds between the aggregates or inter-aggregate bond. The inter-aggregate bonds are thought to be responsible for maintaining the strength and integrity of the system. When shear is applied in excess of the yield stress the inter-aggregate bonds first breaks down irreversibly. This leads to a collapse of the network and concurrently a dramatic reduction in the viscosity with time. The inter-particle bonds, however, break down reversibly in a way that they can both be broken and reformed during shear to an extent depending on the applied shear rate. The breaking of these inter-particle bonds results in breaking down of the aggregates into smaller flocs or particles and causing the system to be more dispersed with a further decrease in the viscosity. The results also show that after prolonged shearing, the solder pastes still exhibited finite viscosity and shear thinning

behaviour. Similar structural behaviour has been observed for red mud suspension (Nguyen and Boger 1985), starch pastes (Nguyen et al 1998) and semisolid foodstuffs (Abu-Jdayil 2003). This type of behaviour may indicate that the original solder paste structure can not be destroyed completely by long-time shearing (unless the paste is subjected to a very high shear rate) but may only be broken down to a certain minimum or equilibrium state.

6.4.2 Results and Discussion for Flux samples

This section presents the results and discussion for the rheological time-dependent behaviour of two fluxes (F1 and F2). As stated earlier in section 4.2.3, these fluxes were used to prepare the solder paste samples as outlined in table 4.7. So, one of the key issues in this investigation was to find out if there is any correlation between paste and flux rheology with regards to break-down behaviour.

As with the solder paste samples, the two fluxes were sheared for a period of 8 hours at constant shear rate values of 2, 4, 6, 8 and 10 s⁻¹. The results presented in figure 6.6 and 6.7, show the effect of shear rate on the time-dependent rheological properties of flux mediums. Although the fluxes showed similar breakdown behaviour to the solder paste samples under the application of constant shear rates, the flux samples exhibited a sharper rate of decrease in viscosity compared to those for solder paste samples. It should also be noted that the flux samples took much more shearing time before they attained the equilibrium states, when compared to the solder paste samples.

The results show that the second order structural kinetic model provides a satisfactory fit for the time-dependent behaviour of the flux samples. Figure 6.8 shows the applicability of the model to the time-dependent rheological data of fluxes, where the plots of $[(\eta - \eta_e)/(\eta_0 - \eta_e)]^{-1}$ versus t are linear. Figure 6.6 and 6.7 illustrates that the second order structural kinetic model provides very good fit (solid lines) with the apparent viscosity versus time data for the flux samples. Table 6.3 presents the values of rate constant, k , the ratio of initial to equilibrium viscosity, η_0 / η_e , initial viscosity, η_0

and the correlation coefficient, r as a function of the applied shear rate for the flux samples. It was expected that the rate of structural breakdown, k would increase with increasing shear rate. The value of k , however, generally found to decrease with increasing shear rate for both of the flux samples. A similar trend was observed for the ratio of initial to final viscosity (η_0/η_e). These sort of quantitative behaviours rather unexpected and do not match with the thixotropic behaviour of the flux samples. As mentioned earlier this might be due to the closeness of the chosen shear rate values. Further study needs to be carried out with a wider range of applied shear rate. The aim of the further study would be to verify and confirm the findings from the present study using a different and wider range of shear rate values. Table 6.2 also shows that the initial viscosity values (η_0) for fluxes F1 and F2 decreases with increasing shear rate values – indicating shear thinning nature of the flux samples.

An examination of the data presented in Table 6.1 and 6.2 suggests that the rate of structural breakdown (as measured by the values of k) for fluxes is greater than the corresponding solder paste samples for the same shear rate. In addition, the values of η_0/η_e reported in table 6.1 and 6.2 indicate that the amount of structural breakdown of the fluxes is generally higher than the values for the solder pastes. The flux samples also show lower values for the initial viscosities (η_0). These results imply that the addition of solder particles to the flux medium makes the system more viscous and more resistant to breakdown under the application of shear.

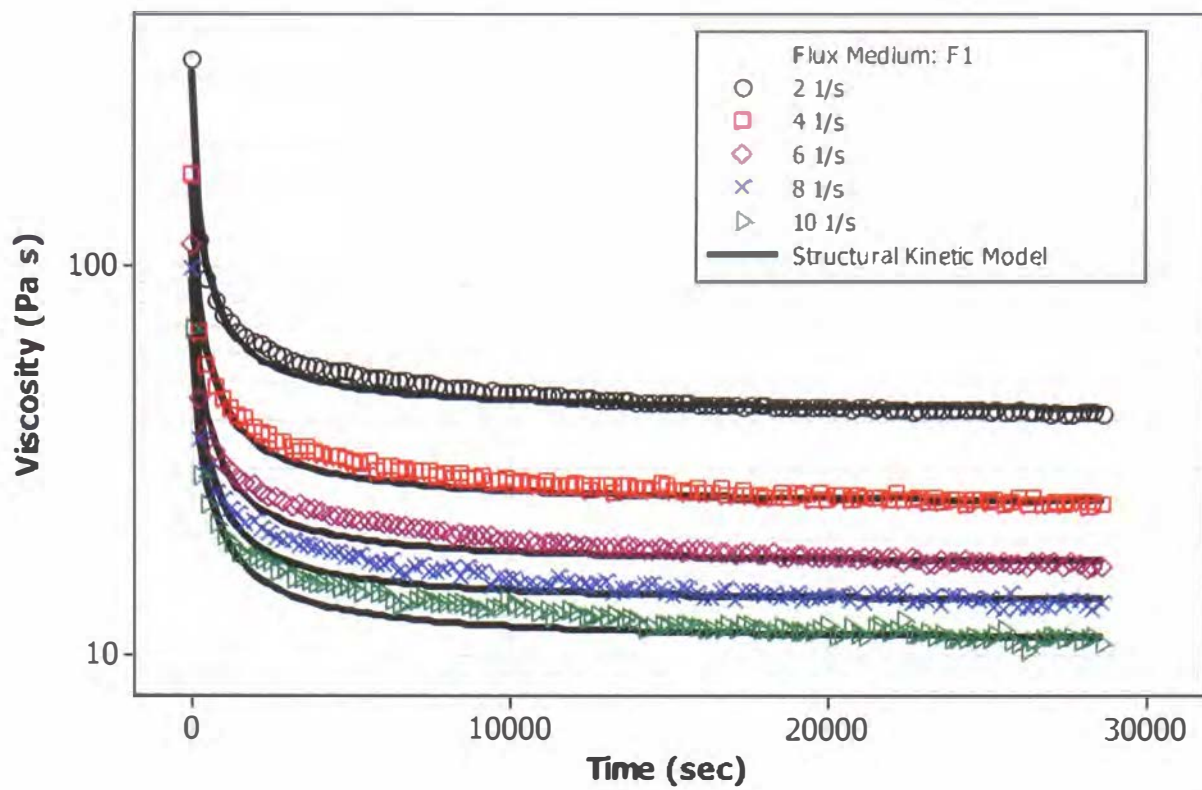


Figure 6.6: Apparent viscosity data at constant shear rates for flux medium F1 at 25°C.
Effect of shear rate.

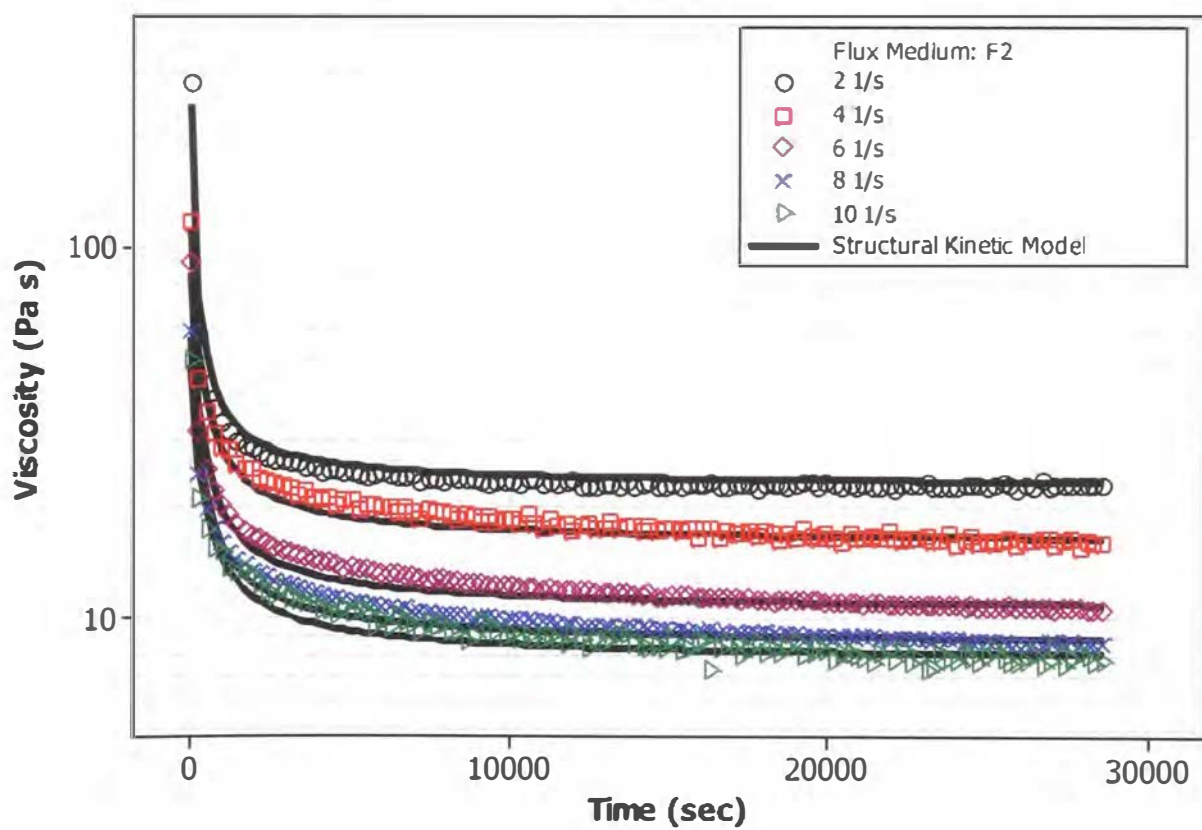


Figure 6.7: Apparent viscosity data at constant shear rates flux medium F2 at 25°C.
Effect of shear rate.

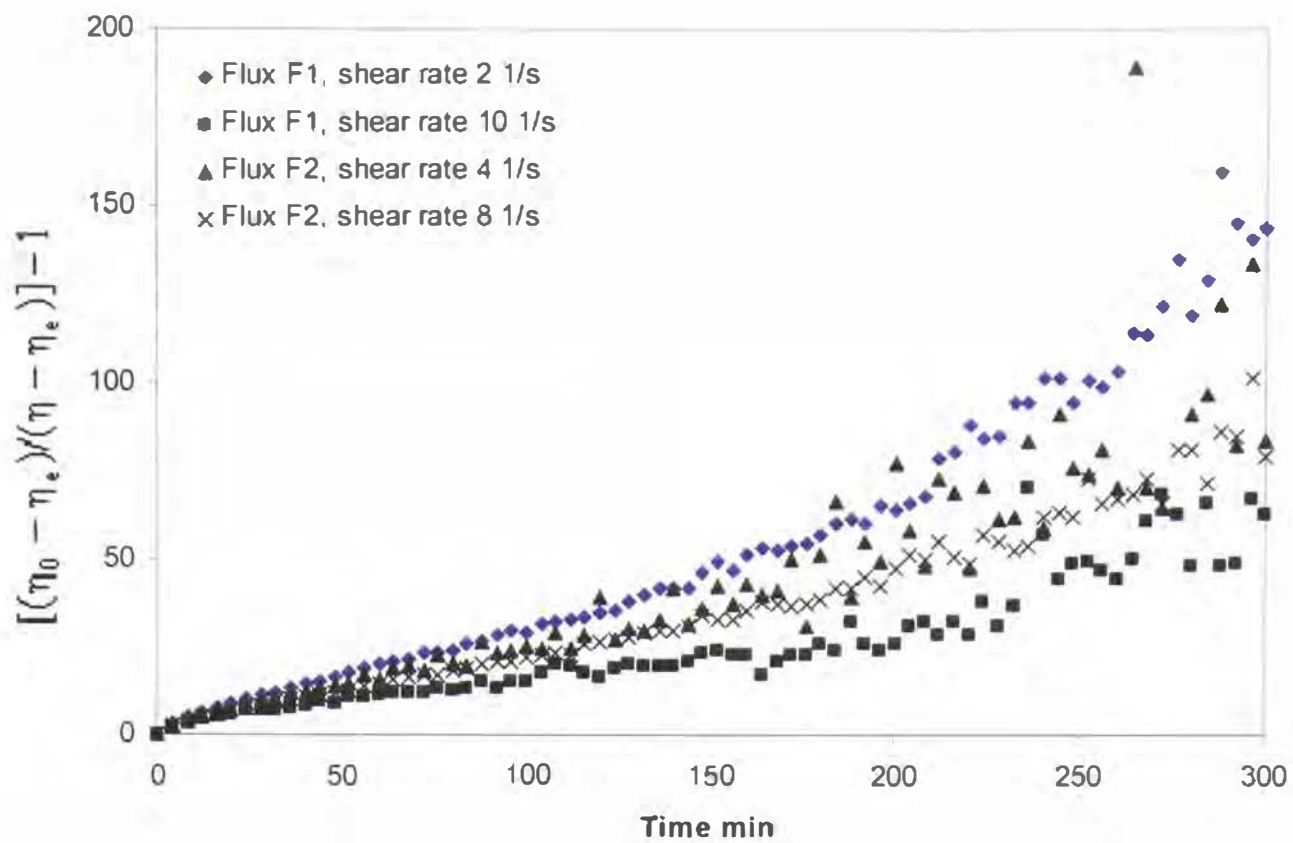


Figure 6.8: Testing of the structural kinetic model with different flux samples at 25°C.

Table 6.2: The parameters from the second-order kinetic model for flux samples evaluated at different shear rates.

Flux Medium	Shear rate (1/s)	$k (\times 10^{-3})$	η_0 / η_e	η_0 (Pas)	Correlation coefficient, r
F1	2	8.296	7.995	335.3	0.993
	4	6.228	7.034	170.3	0.990
	6	6.053	6.698	113.4	0.987
	8	6.903	7.245	97.81	0.986
	10	5.042	6.437	69.07	0.981
F2	2	16.837	12.291	280.6	0.995
	4	7.121	7.326	116.7	0.991
	6	7.934	8.647	90.97	0.994
	8	6.130	7.007	59.46	0.991
	10	5.307	6.488	49.98	0.983

6.5 Summary

The time-dependent break-down behaviour of solder pastes and flux mediums has been analysed in this chapter. The objective of the study was to quantitatively evaluate the structural breakdown of solder pastes and flux mediums using the structural kinetic model (SKM). A novel technique has been developed which combines the experimental rheological data with the theoretical structural kinetic approach. Upon analysing the experimental data, the rheological behaviour of solder paste and flux mediums can be characterised as thixotropic and shear-thinning. As expected, for the solder paste samples studied the rate and extent of thixotropy was generally found to increase with increasing shear rate. The thixotropic rheological behaviour of solder paste and fluxes has been satisfactorily modelled using a second-order structural kinetic model which demonstrates that the internal structure of solder paste and flux mediums breaks down irreversibly under the application of shear. A comparative study of the thixotropic breakdown behaviour of solder paste and flux medium was also presented.

The results from this study can be of great help for the solder paste manufacturers and formulators in quantifying and predicting the effect of long time shearing on solder paste samples. The technique developed may also be utilized for other similar materials like solar pastes and conductive adhesives.

CHAPTER 7

MODELLING OF THE BUILD-UP OF THE PASTE STRUCTURE USING THE STRETCHED EXPONENTIAL MODEL

7.1 Introduction

Solder pastes generally have a flocculated structure (show aggregation of solder particles), and hence are known to exhibit thixotropic behavior. Difficulties arise in mixing and handling of solder paste materials because thixotropic structures progressively break-down on shearing and slowly rebuild at rest. For thixotropic materials, the time-scales for structural breakdown and build-up can range from a couple of minutes (for structural breakdown) to several hours (for the rebuilding of the material structure) (Barnes 1997).

For solder pastes, thixotropy is designed into the formulation to meet specific processing requirements, for example to make the pastes shear thinning under shear application (e.g. squeegee action during stencil/screen printing) and to facilitate structural build-up after the application of shear. However, thixotropy is not always desirable, especially in the case of mixing, handling and experimentation – hence the need for a balance in terms of the rate and extent of thixotropy as this can also adversely impact other sub-processes in the stencil printing process. Because of the presence of thixotropic structure, solder paste behaviour is highly influenced by the previous shear history. It is the thixotropy, which is the main cause of the “batch-to-batch variation” in solder paste manufacturing. The poor-reproducibility of experimental results of solder paste is also caused by thixotropic nature of solder paste.

The objective of the study reported in this chapter is to investigate the thixotropic build-up behaviour of solder paste and flux mediums. The stretched exponential model (SEM) has been used to model the structural changes during the build-up process and to correlate model parameters with the paste printing process. The chapter is divided into three main parts. The first part focuses on the theoretical aspect of the stretched exponential model. The second part presents the details of materials and methods used in this study and the final part outlines the results from the investigation.

7.2 Modelling the build-up of thixotropic fluids

A review of mathematical models for time-dependent behaviour of thixotropic fluids was reported by Barnes in 1997 (Barnes, 1997). One of the models outlined in this review is the stretched exponential model (see equation 7.1), which has been suggested as a suitable model for predicting the structural build-up in suspensions such as solder pastes and flux mediums.

$$\eta = \eta_{e,0} + (\eta_{e,\infty} - \eta_{e,0})(1 - e^{-(t/\tau)^r}) \quad (7.1)$$

In this equation, $\eta_{e,0}$ is the viscosity at the commencement of shearing, $\eta_{e,\infty}$ the viscosity after shearing for an infinite time, τ is a time constant and r is a dimensionless parameter with values between 0 and 1 and is referred to as the stretched parameter. Equation 7.1 can be used to model both the build-up and break-down in step-up or step-down tests, with the values of τ and r depending on both the level and the direction (Barnes, 1997).

In another study, Heymann et al (1996) used an equation similar to equation 7.1 to investigate the build-up of newsprint inks. Instead of using viscosity, they used a yield stress σ_y to describe the rebuilding of printing inks:

$$\sigma_y(t) = \sigma_y^0 + [\sigma_y^\infty - \sigma_y^0](1 - e^{-(t/\tau)}) \quad (7.2)$$

The form of stretched exponential model used in this work is a simplified version of eq. 7.1 with $r = 1$. This has also been used by Maingonnat et al (2005) to describe the build-up phenomenon of colloidal clay suspensions and can be rewritten in the following way:

$$\eta(t) = \eta_0 + (\eta_\infty - \eta_0)(1 - e^{-(t/\psi)}) \quad (7.3)$$

where ψ is a characteristic time. The term η_∞ is the viscosity value at equilibrium and η_0 is the viscosity when the structure is completely broken down. The three parameters $(\psi, \eta_0, \eta_\infty)$ are calculated as fitting parameters of the model described by equation 7.3. In the work reported in this chapter, the MATLAB software system was used for performing the regression analysis and model fitting (see section 7.4).

7.3 Experimental Design

7.3.1 Materials

Two fluxes F1 and F2 and four lead-free solder pastes P1 to P4 prepared from the fluxes are investigated. The details of these fluxes and the solder paste samples are provided in section 4.2.3 of this thesis.

7.3.2 Rheological measurements

The rheological measurements were carried out using the Bohlin Gemini-150 controlled-stress/strain rheometer with a serrated parallel plate geometry of 20 mm upper plate diameter. As outlined in chapter 6 (section 6.3.2), an identical sample loading procedure was followed.

In order to investigate the build-up phenomena, the fluid structure had to be broken first. Based on the experience from previous experimental studies, applying a

preshear of 10 s^{-1} for 30 seconds is adequate for partially breaking down the paste's structure. One of the problems of applying high shear rate is that the sample tends to spill out from between the parallel plate measuring geometry due to centrifugal force, leaving an undesirable gap between the upper plate and the sample. This ultimately leads to unreliable measurement data being produced. So, the rate and duration of the preshear was carefully chosen in such a way that the applied shear would not force the sample out of the gap and therefore, will provide reliable rheological data.

Having decided on the preshear, a rheological high shear – low shear test method has been designed. This consists of a preshearing step at 10 s^{-1} for a duration of 30 seconds and then applying a low shear rate for another 900 seconds (15 minutes). A total of five tests were performed on each sample corresponding to the five low shear rates: 0.001 , 0.0015 , 0.002 , 0.0025 and 0.003 s^{-1} . Preliminary tests showed that the paste structure recovers (builds-up) under these low shear conditions.

Dynamic oscillatory tests were performed on solder paste samples to investigate the structure formation during the recovery process. The tests were performed in two steps. First, oscillatory stress sweep test was carried out, by varying the stress from 0.5 to 500 Pa at a frequency of 1 Hz, to determine the linear viscoelastic region (LVR). Within the LVR, the applied stress and the measured strain follow a linear relationship. Before performing oscillation tests on a material it must be verified that the test conditions fall into the LVR. This is because the mathematical calculations are only valid in this linear response region and also within this region the sample structure remains undamaged. It was observed that all the samples were within the LVR at 0.05 – 0.07% strain. Secondly, to observe structural build-up, time sweeps were performed on the paste samples. Paste structure was first broken down with a preshear at 10 s^{-1} for 30 sec, then a constant frequency of 1 Hz was applied with a strain value of 0.05% for 8 hours.

7.4 Results and Discussion

The result section is comprised of three parts. The results from the preliminary investigation of long-term build-up behaviour of paste samples are reported in the first part. The second part outlines the results from the experimental and modelling studies of the short-term build-up of solder paste and flux samples. The final part presents the results of the oscillatory time sweep experiments carried out on solder paste samples to examine structural changes during the build-up process.

7.4.1 Preliminary investigation of build-up phenomenon

In this part of the investigation, solder paste samples were subjected to a constant low shear rate for 8 hours after being presheared for 30 seconds at 10 s^{-1} . Figure 7.1 shows the results of the investigation for P1 and P4 solder pastes for the apparent viscosity versus time plot. The low shear rate used in this case was 0.0005 s^{-1} . The intention here was to examine the time-dependent build-up of solder paste (over a long period of time) after breaking down its structure. The observations made in this preliminary investigation have helped in designing the experiments for remainder of the study reported in this chapter.

For solder pastes, when they are allowed to recover their structure following preshear (at low shear rate), the paste viscosity will tend to increase with shearing time. The recovery data shown in figure 7.1 shows that the rate of increase in viscosity is fairly rapid at first and then decreases with further shearing time. This type of behaviour is quite similar to the behaviour of bauxite residue (red mud) suspension as observed by Nguyen and Boger (1985). They measured the yield stress instead of viscosity to observe the recovery behaviour. Two important observations can be made when the data presented in figure 7.1 are analysed. First, after breaking down the paste structure with the preshear a remarkable increase in viscosity occurs in a short time scale – of the order of several minutes. Secondly, the viscosity value starts to decrease slowly in longer term after reaching an equilibrium state. These observations strongly suggest that the solder

paste possesses a yield stress. Lapasin et al (1994) also identified yield stress as one of the important properties of solder paste. The initial build-up of the solder paste structure (as may be seen in figure 7.1) can be attributed to the development of yield stress in the solder paste. The decrease in viscosity value after a short time period (after reaching an equilibrium state) also suggest that the developed yield stress is quite weak in nature and was not sufficient to hold the solder paste structure for a long time even at a very low shear rate.

The short-term build-up of solder paste structure is quite significant from the application point of view. In the reflow soldering stage of the SMT assembly process, this prevents the slumping of solder paste deposit after stencil withdrawal and during component placement. The time-frame involved in this short-term build-up represents the time required for component placement and the start of the reflow soldering process. Therefore, a clear understanding of this structural build-up behaviour is of immense importance to both the solder paste manufacturers and the end-users.

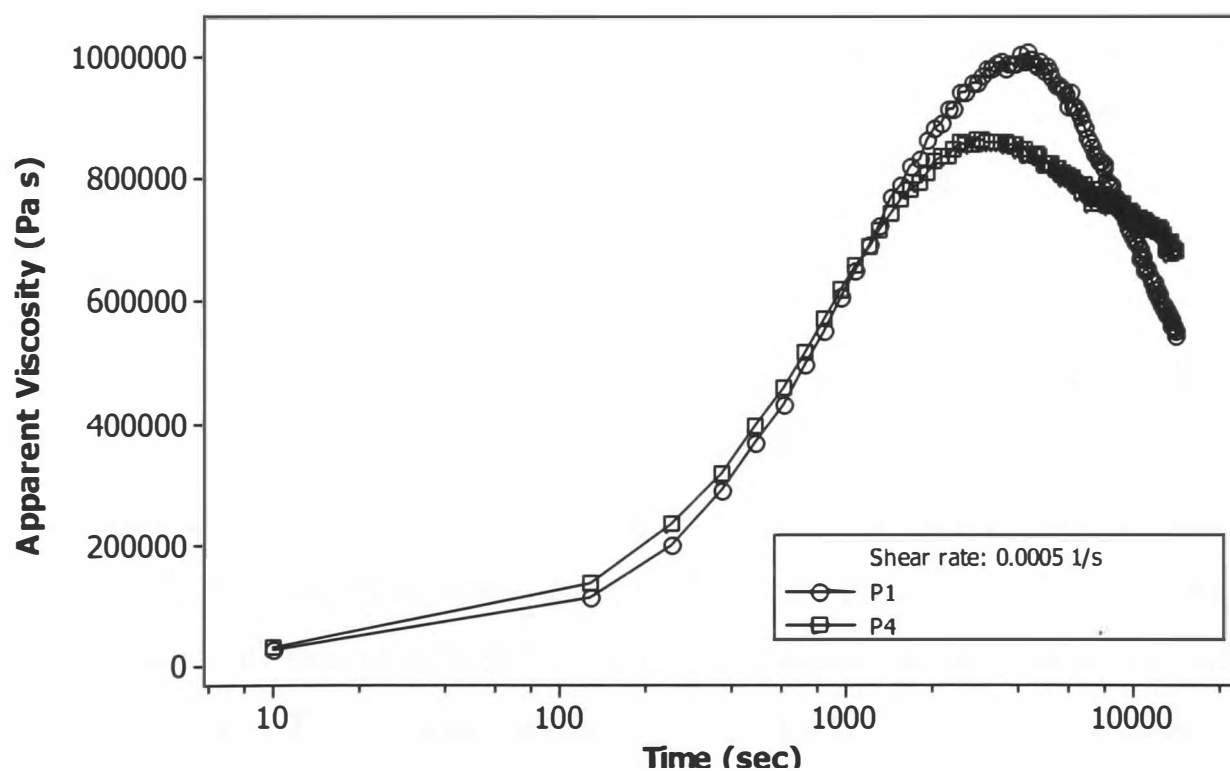


Figure 7.1: Apparent viscosity data of solder pastes as a function of time at a shear rate of 0.0005 s^{-1} .

7.4.2 Results from the investigation of short-term build-up behaviour

7.4.2.1 Solder Paste Samples

This section outlines the results obtained from the experimental and modelling studies of short-term build-up of solder pastes. Four different commercially available lead-free solder paste samples (P1, P2, P3 and P4) were investigated; the details of these pastes were described in section 6.3.1.

The structural build-up of the solder paste samples at different low shear rates is presented in figure 7.2 to 7.5 in terms of viscosity versus time plot. The solder paste samples were first broken down with a preshear and then allowed to build up at low shear rates. The applied low shear rate values were 0.001, 0.0015, 0.002, 0.0025, 0.003 s⁻¹. The increase in apparent viscosity value was used as a measure of thixotropic build-up of solder paste structure. This is because, the viscosity is the most important, widely used and easily measurable rheological property of solder paste. In a previous study, Maingonnat et al. (2005) also used viscosity to represent the structural build-up of a colloidal suspension of clay. Nguyen and Boger (1985) rather used the yield stress value to represent the recovery of red mud suspension.

All the solder paste samples have shown similar build-up behaviour under the shear rate range investigated. A careful observation of experimental results (figure 7.2 to 7.5) demonstrates that for any applied low shear rate - the rate of structural build-up was quite rapid at first and then slows down as it approaches an equilibrium state. Another important point to notice is that the rate of structural recovery was dependent on the applied shear rate. This is more obvious at the equilibrium end of the build-up curve. Within the low shear rate range examined, the equilibrium viscosity was found decreasing with increasing shear rate.

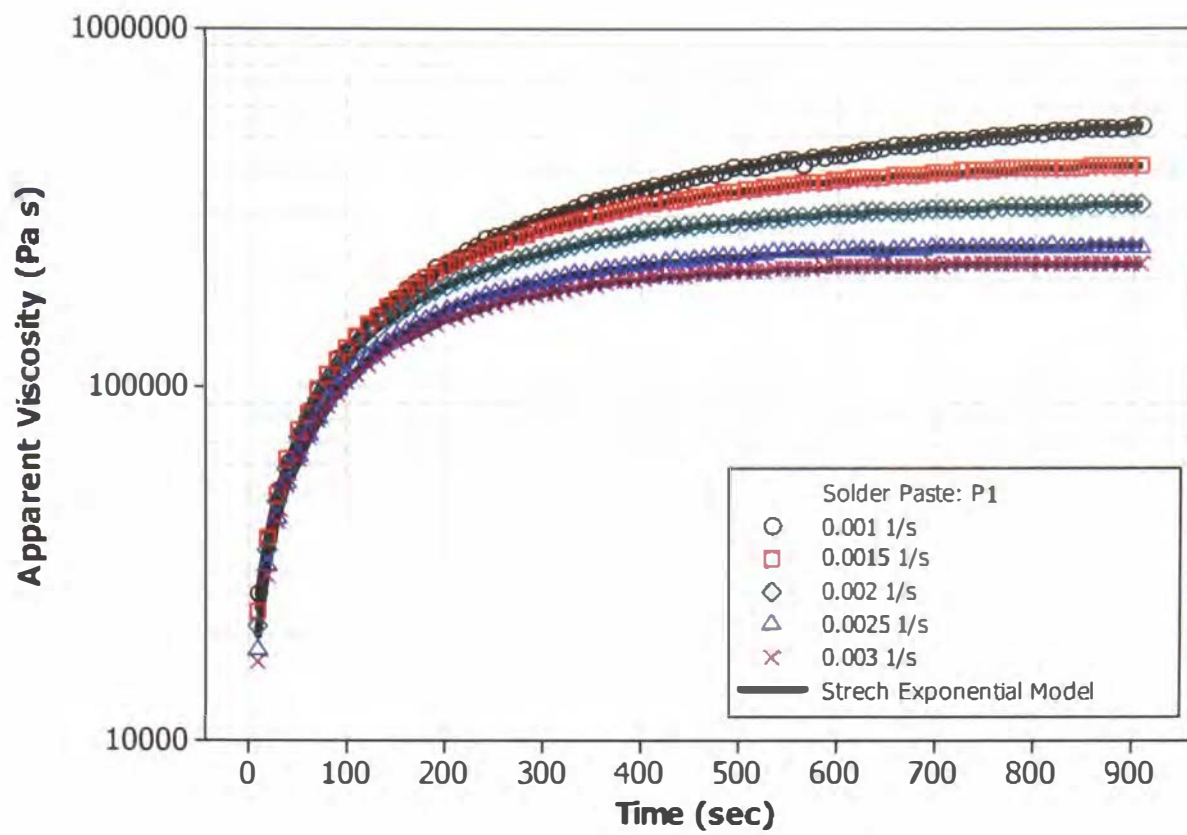


Figure 7.2: Apparent viscosity of solder paste P1 as a function of time at low shear rates.

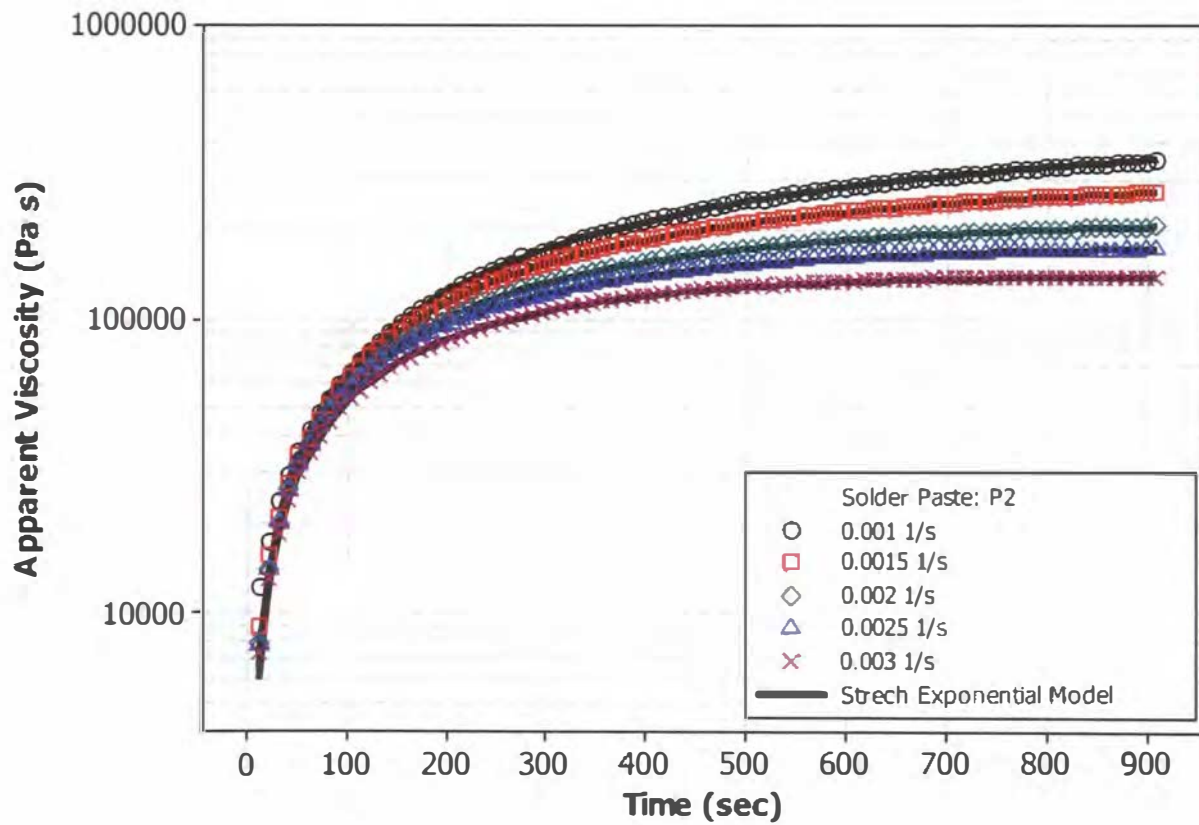


Figure 7.3: Apparent viscosity of solder paste P2 as a function of time at low shear rates.

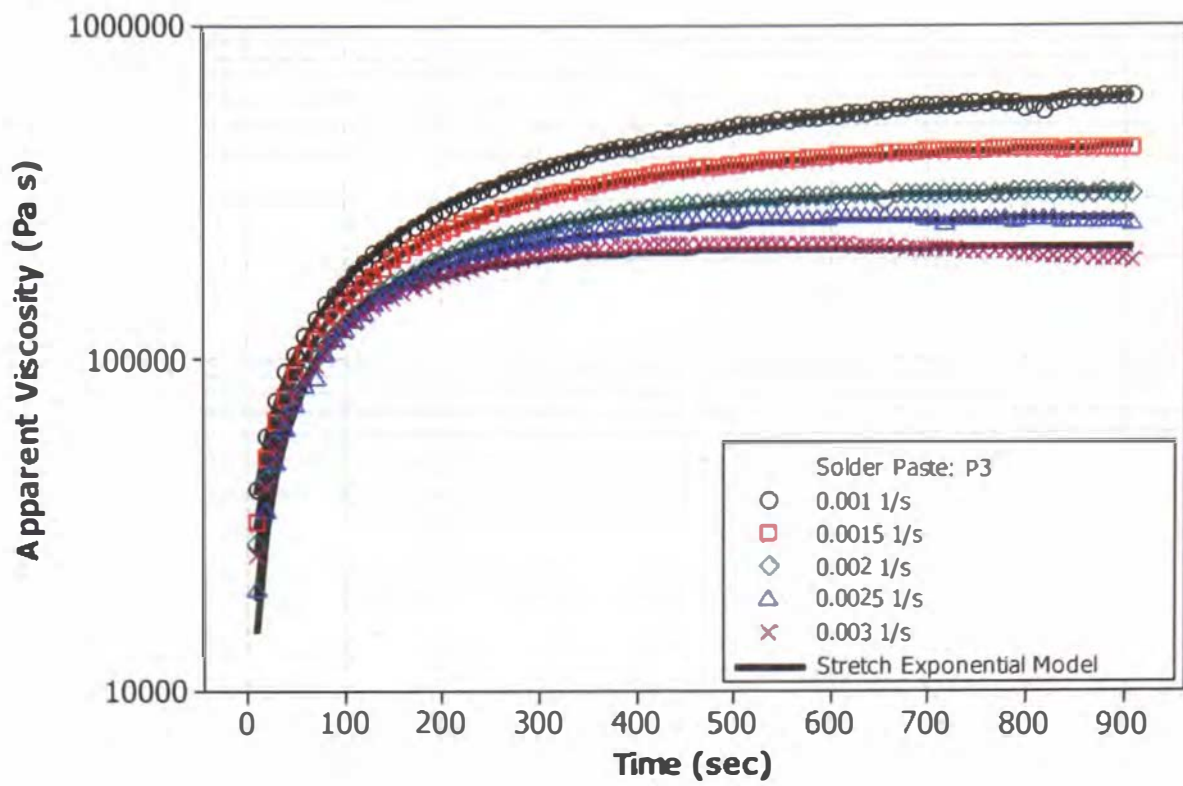


Figure 7.4: Apparent viscosity of solder paste P3 as a function of time at low shear rates.

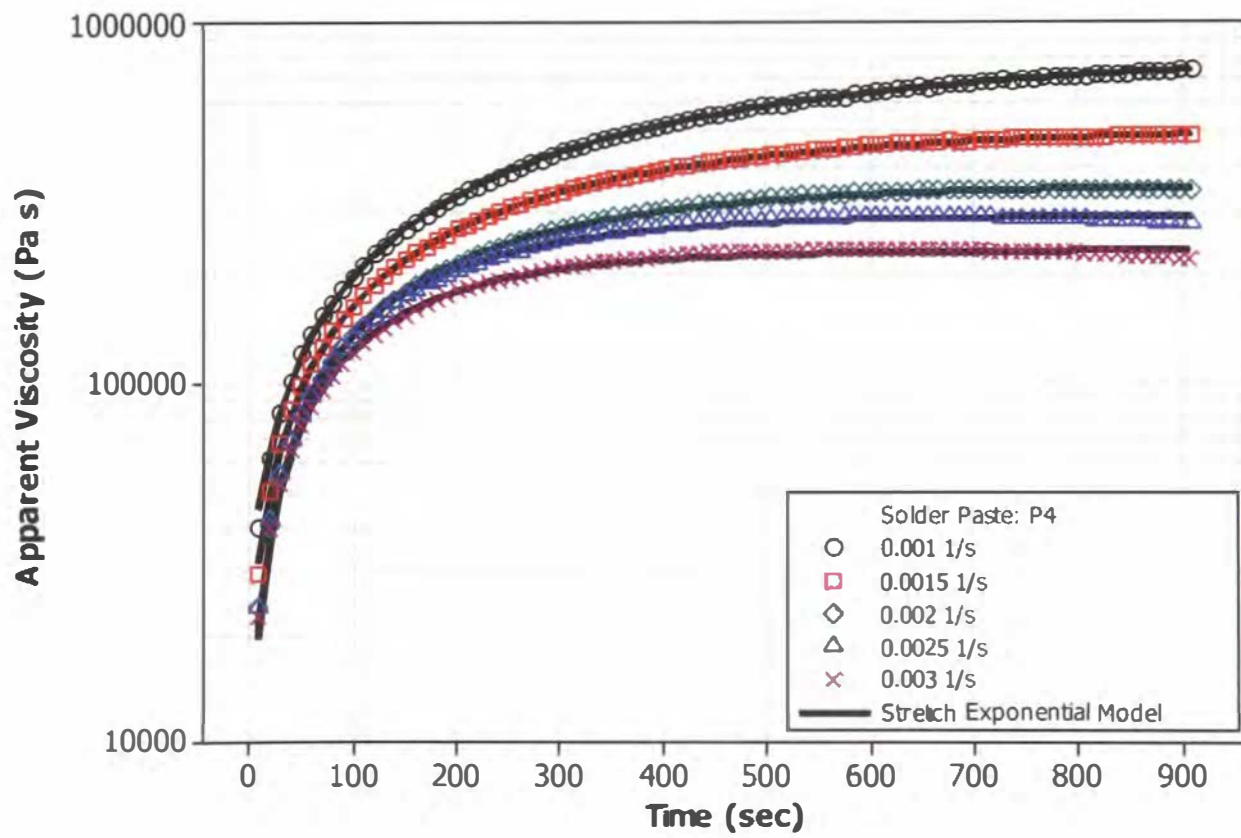


Figure 7.5: Apparent viscosity of solder paste P4 as a function of time at low shear rates.

The observed thixotropic build-up behaviour of solder paste samples was modelled using the stretched exponential model (equation 7.3). Figures 7.2 – 7.5 shows a good correlation of the model fitted result (full solid line) and the apparent viscosity – time data for all the solder paste samples. Table 7.1 presents the calculated values of equilibrium viscosity (η_{∞}), characteristic time (ψ) and correlation coefficient (r) as a function of applied shear rate for the paste samples, when fitted to the stretched exponential model. The model was originally fitted with three parameters, including the initial viscosity (η_0). The initial viscosity η_0 was included as a model parameter, because this viscosity value is strongly influenced by the rheometer inertia-effect (Maingonnat et al. 2005) as well as the pre-shear history. However, in the model fitting negative values were obtained for η_0 . This is most likely due to insufficient data at the beginning of shear (Chamberlain and Rao, 1999). Negative values for η_0 is quite unrealistic and does not make any sense in this context, hence the values are not shown in table 7.1. The equilibrium viscosity (η_{∞}) and the characteristic time (ψ) are presented in figure 7.6 and 7.7 respectively as a function of applied shear rates. Both η_{∞} and ψ were found decreasing with increase in shear rates. Figures 7.6 and 7.7 suggested that both the equilibrium viscosity (η_{∞}) and characteristic time (ψ) can be fitted by power functions as given in equation 7.4 and 7.5.

$$\eta_{\infty} = a\dot{\gamma}^b \quad (7.4)$$

$$\psi = c\dot{\gamma}^d \quad (7.5)$$

Table 7.1 and 7.3 presents the estimated values of parameters from equation 7.4 and 7.5 respectively.

The equilibrium viscosity and the characteristic time are of great importance to the actual solder paste assembly process. A higher equilibrium viscosity value for a solder paste at a given shear rate would mean that the solder paste will be less susceptible to slumping. Therefore, paste P4 would show the highest resistance towards slumping

followed by P3, P1 and P2, according to table 7.2 and figure 7.6. The characteristic time here represents the time window between the stencil printing and reflow soldering of solder paste - when slumping must be avoided. A higher characteristic time means more time for component placement and reflowing the circuit board to make solder joints.

Table 7.1: Estimated values of stretched exponential model parameters for the build-up of solder paste samples.

Solder Paste	Shear rate (1/sec)	Equilibrium Viscosity η_{∞} (kPa s)	Characteristic time ψ (Sec)	Correlation Coefficient, r
P1	0.001	638.503	497.769	0.999
	0.0015	440.656	317.360	0.999
	0.002	329.605	243.681	0.999
	0.0025	248.933	195.962	0.999
	0.003	221.490	179.286	0.999
P2	0.001	454.847	610.978	0.999
	0.0015	309.198	429.052	0.999
	0.002	221.011	323.304	0.999
	0.0025	179.572	261.415	0.999
	0.003	142.506	215.697	0.999
P3	0.001	681.475	395.402	0.999
	0.0015	449.619	273.675	0.999
	0.002	323.290	211.967	0.999
	0.0025	264.311	159.287	0.997
	0.003	215.344	115.022	0.986
P4	0.001	843.855	425.078	0.999
	0.0015	512.762	282.108	0.999
	0.002	356.786	216.180	0.999
	0.0025	291.839	160.530	0.997
	0.003	233.795	137.156	0.996

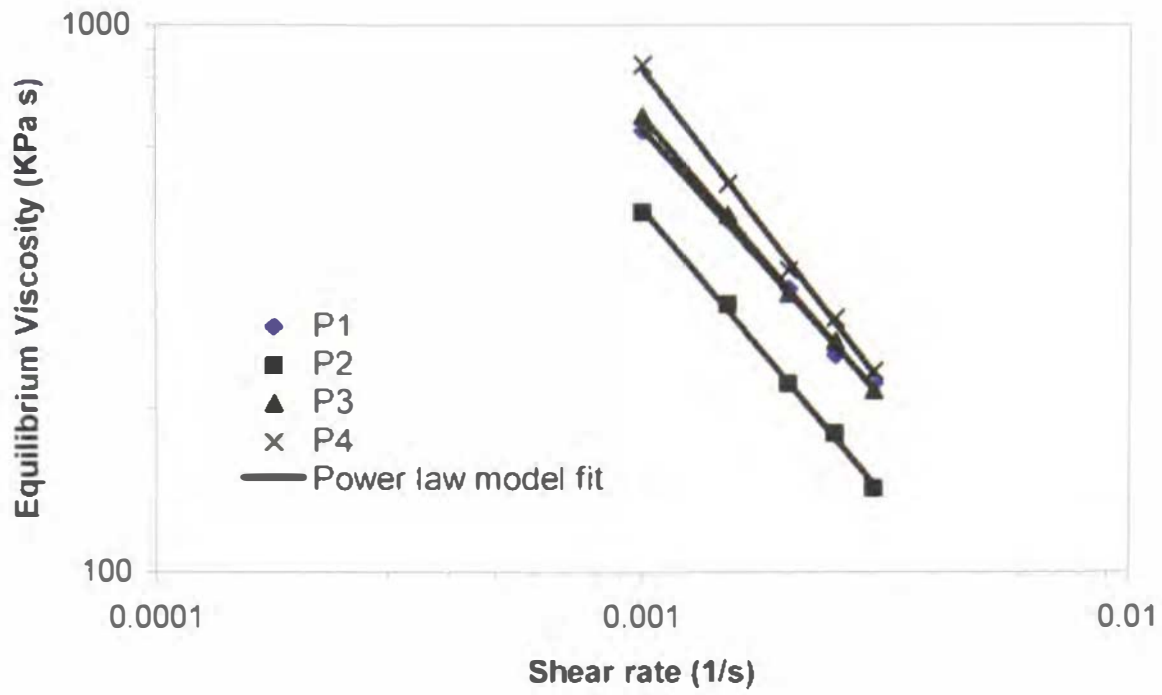


Figure 7.6: Equilibrium viscosity from the stretched exponential model for the solder paste samples.

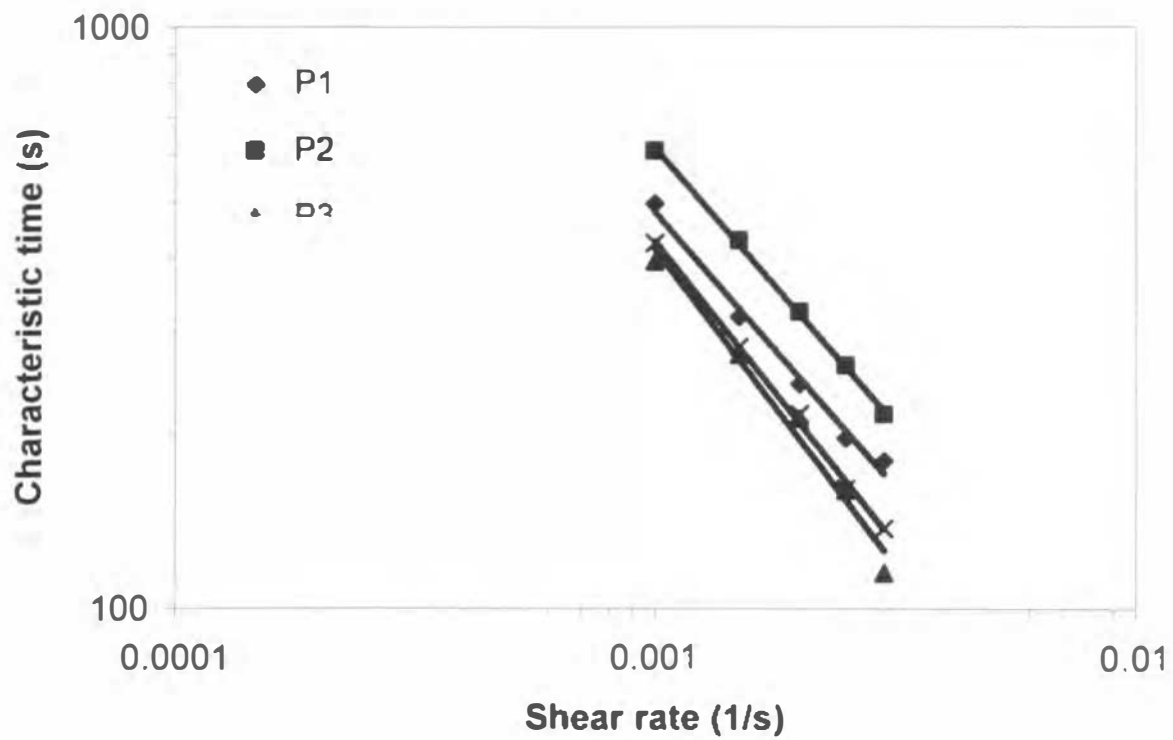


Figure 7.7: Characteristic time of the stretched exponential model for the solder paste samples.

Table 7.2: Estimated values of parameters for the equilibrium viscosity model fit for solder paste samples

Solder paste	Model parameters for Equilibrium Viscosity		Square of Regression Coefficient, R^2
	a	b	
P1	0.683	-0.992	0.996
P2	0.321	-1.053	0.998
P3	0.490	-1.048	0.999
P4	0.269	-1.163	0.998

Table 7.3: Estimated values of parameters for the characteristic time model fit for solder paste samples

Solder paste	Model parameters for Characteristic time		Square of Regression Coefficient, R^2
	c	d	
P1	0.697	-0.946	0.990
P2	0.893	-0.947	0.998
P3	0.227	-1.087	0.979
P4	0.325	-1.040	0.997

While resting, the undisturbed solder paste structure may take the form of a three dimensional continuous network throughout the whole material volume (Nguen and Boger 1985). The network may be a matrix of aggregates and/or flocs of primary particles held together by the intermolecular forces, also known as van der Waals forces (Durairaj 2004). This intermolecular bonding is caused by momentary polarization of particles and are quite unstable in nature compared to chemical bonding. The intermolecular forces consist of repulsive forces e.g. electrostatic interaction forces,

which prevent collapse of the molecular structure and attractive forces due to induction and dispersion forces. When the suspension is sheared, these weak intermolecular forces break down causing the network to break-down into smaller flocs. In experimental studies, this breakdown behaviour is generally manifested by the decrease in viscosity value, the detailed mechanism of which is outlined in chapter 6 of this thesis. When the solder paste structure is allowed to recover at low shear rate, the damaged inter-particle bonds tends to restore by themselves. The mechanism may involve reorganisation and reflocculation of disrupted structural elements under the action of diffusion (Nguen and Boger 1985, Barnes 1997). The diffusion in turn is the result of Brownian motion. Brownian motion is the random thermal agitation of atoms and molecules that results in elements of the microstructure being constantly bombarded, which causes them to move to a favourable position where they can – given the necessary attractive force – attach themselves to other parts of the microstructure (Barnes 1997). The Brownian rebuilding forces are quite small and weak compared to the shearing forces. This implies that the recovering process for solder paste structure could be very long, as this small, random force may take a long time to rearrange particles into flocs.

7.4.2.2 Flux Samples

This section presents the results of the investigation of build-up behaviour of the two flux samples (F1 and F2). These fluxes were used to prepare the four solder pastes. As with the solder paste samples, a preshear (10 s^{-1} for 30 sec) was applied to break-down the flux structure. Then the fluxes were allowed to recover at low shear rates. The shear rate values applied were $0.001, 0.0015, 0.002, 0.0025, 0.003 \text{ s}^{-1}$.

Figures 7.8 and 7.9 show the results of the investigation of apparent viscosity versus time plots. The build-up of the flux structure is obvious from the continual increase of apparent viscosity value with shearing time. A careful observation of figures 7.2 - 7.5, 7.8 and 7.9 reveals that the build-up phenomenon was more pronounced for solder paste samples compared to flux mediums. At 0.001 s^{-1} , for P1 solder paste the

viscosity increased from 25.8 to 537.7 kPa s during the experiment (figure 7.2). Whereas, for F1 flux the increase in the apparent viscosity was 82 – 358 kPa s (figure 7.8), for the same shear rate. Moreover, the rate of increase in viscosity was quite gradual for flux samples as opposed to the initial rapid increase observed for solder paste samples.

It was found that the stretched exponential model satisfactorily fits the build-up data of flux samples. Figure 7.8 and 7.9 illustrates that the stretched exponential model provides a very good fit (solid lines) of the apparent viscosity versus time data for the flux samples. This is also evident from the values of correlation coefficient being close to one, as presented in table 7.4. Table 7.4 also presents the estimated values of the three parameters ($\eta_0, \eta_\infty, \psi$) of the model for the flux samples. Unlike solder paste samples, the model fitting for flux samples did not produce any negative values for the initial viscosity (η_0). The parameters – initial viscosity, equilibrium viscosity and characteristic time are presented in figures 7.10, 7.11 and 7.12 respectively as a function of applied shear rate. All three parameters were found to fit nicely using power law relations:

$$\eta_0 = m\dot{\gamma}^n \quad (7.6)$$

$$\eta_\infty = k\dot{\gamma}^l \quad (7.7)$$

$$\psi = q\dot{\gamma}^r \quad (7.8)$$

The estimated values of the parameters of these equations are given in table 7.5, 7.6 and 7.7 respectively.

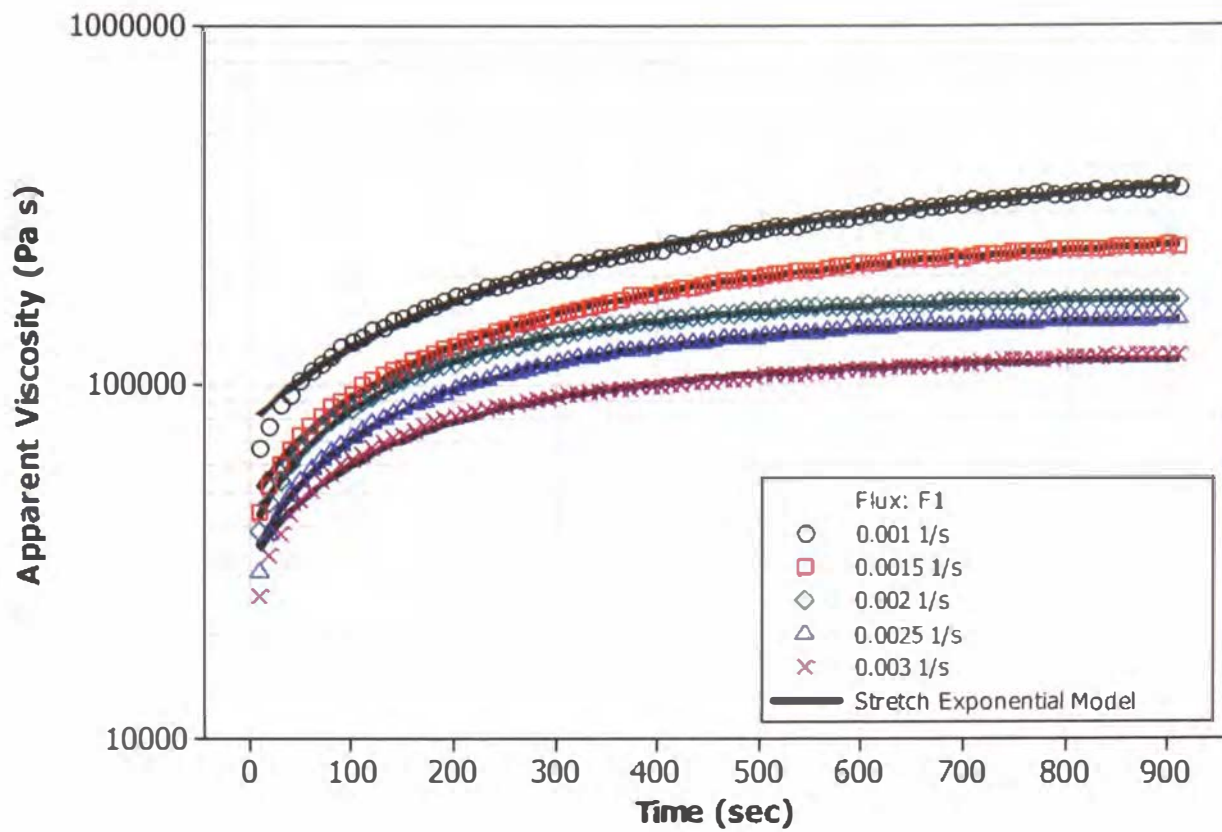


Figure 7.8: Apparent viscosity of flux F1 as a function of time at low shear rates.

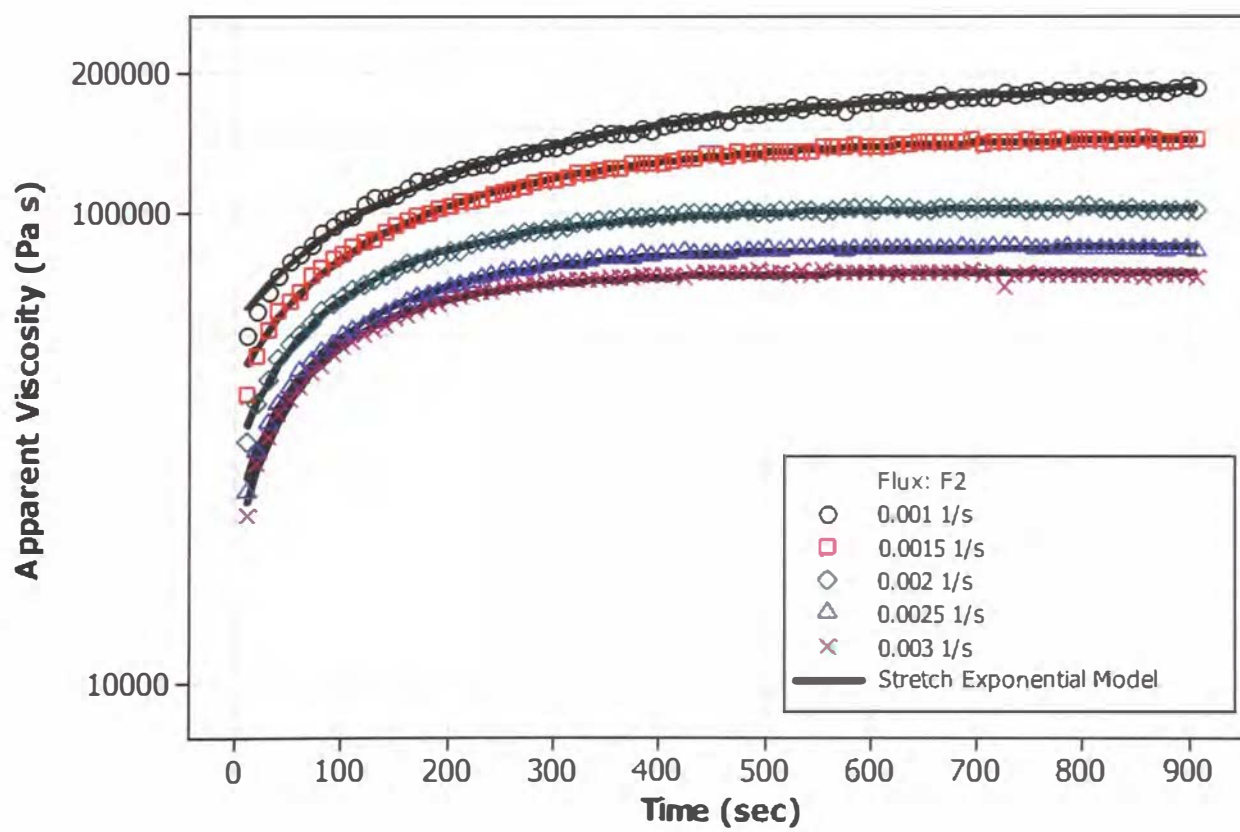


Figure 7.9: Apparent viscosity of flux F2 as a function of time at low shear rates.

Table 7.4: Parameters of the stretched exponential model for the flux samples

Fluxes	Shear rate 1/sec	Initial Viscosity η_0 kPa s	Equilibrium Viscosity η_∞ kPa s	Characteristic time ψ sec	Correlation Coefficient R
F1	0.001	76.795	481.211	763.963	0.9990
	0.0015	46.031	275.110	456.849	0.9995
	0.002	36.782	174.420	235.514	0.9996
	0.0025	30.670	153.636	263.718	0.9996
	0.003	31.271	119.481	262.885	0.9953
F2	0.001	58.085	192.926	319.642	0.9984
	0.0015	42.792	145.750	224.385	0.9988
	0.002	30.245	102.402	149.606	0.9985
	0.0025	22.676	84.414	139.052	0.9990
	0.003	19.164	74.361	110.930	0.9970

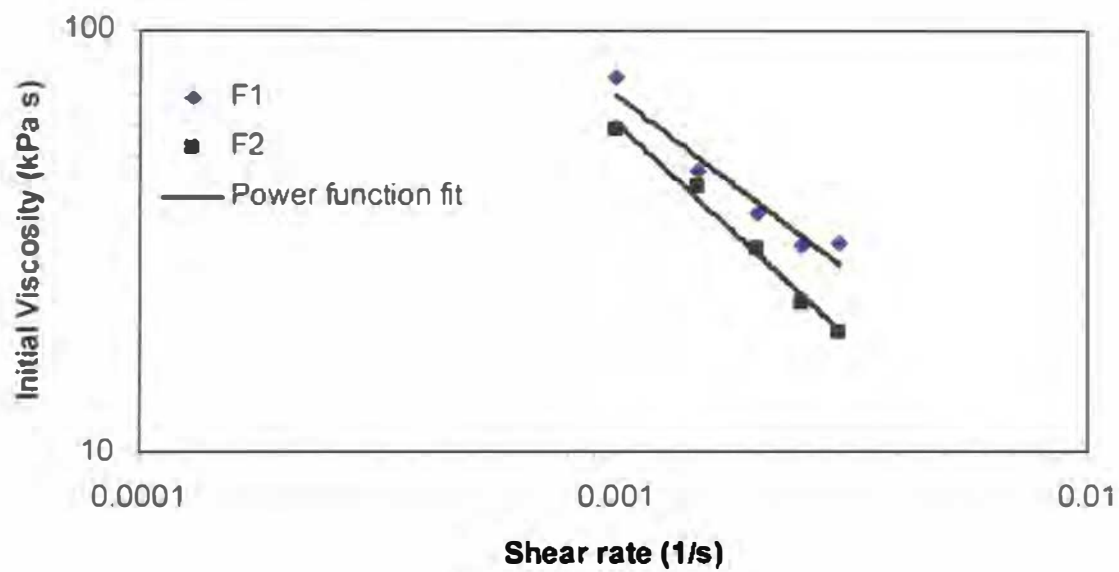
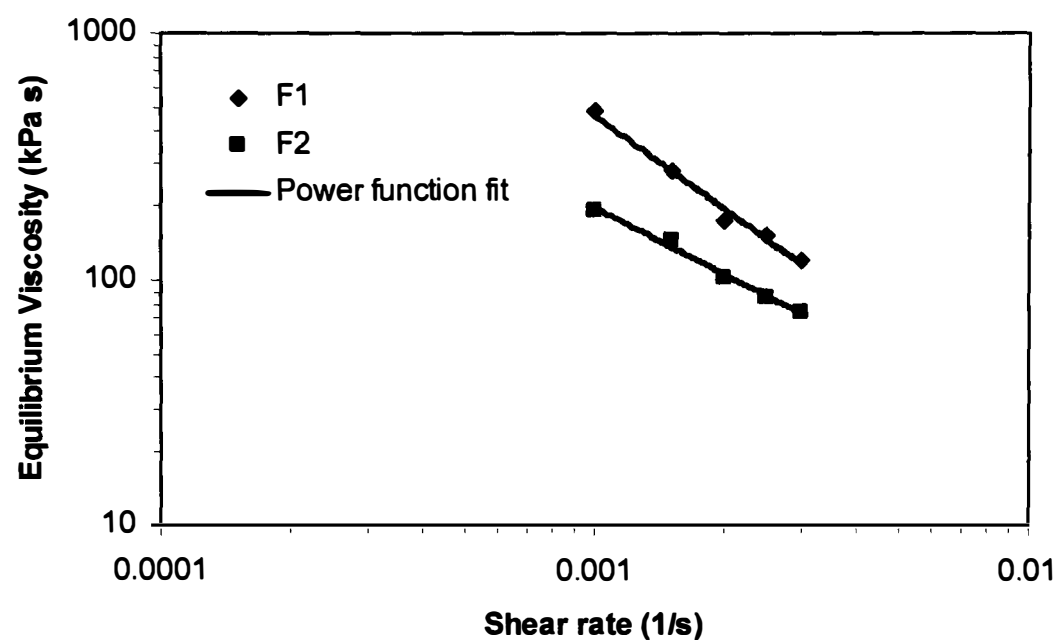


Figure 7.10: Initial viscosity of the stretched exponential model for flux samples.

Table 7.5: Estimated values of parameters for the initial viscosity model fit for flux samples.

Flux Mediums	Model parameters for Initial viscosity		Square of Regression Co-efficient, R^2
	m	n	
F1	0.202	-0.847	0.938
F2	0.046	-1.041	0.989

**Figure 7.11:** Equilibrium viscosity of the stretched exponential model for flux samples.**Table 7.6:** Estimated values of parameters for the equilibrium viscosity model fit for flux samples.

Flux Mediums	Model parameters for Equilibrium viscosity		Square of Regression Co-efficient, R^2
	k	l	
F1	0.077	-1.259	0.987
F2	0.384	-0.904	0.990

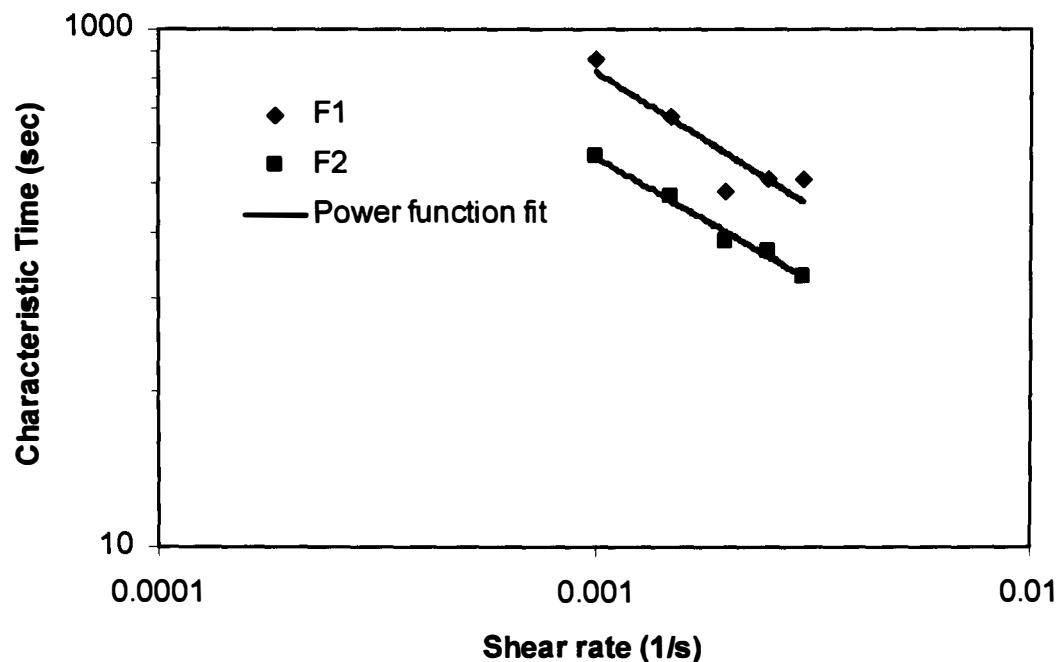


Figure 7.12: Characteristic time of the stretched exponential model for flux samples.

Table 7.7: Estimated values of parameters for the characteristic time model fit for flux samples.

Flux Mediums	Model parameters for Characteristic time		Square of Regression Coefficient, R^2
	q	r	
F1	0.480	-1.051	0.833
F2	0.413	-0.963	0.983

7.4.3 Study of the structural build-up using oscillatory time sweep data

In this section, the time-dependent structural build-up of solder pastes has been investigated using oscillatory time sweep measurement. In contrast to conventional controlled shear rate measurement, which can only characterise viscous behaviour of materials, oscillatory measurements can be used to know both the viscous and elastic properties of materials. This is done by applying a sinusoidally varying stress (or strain) to the sample and measuring the induced sinusoidally varying strain (or stress) response.

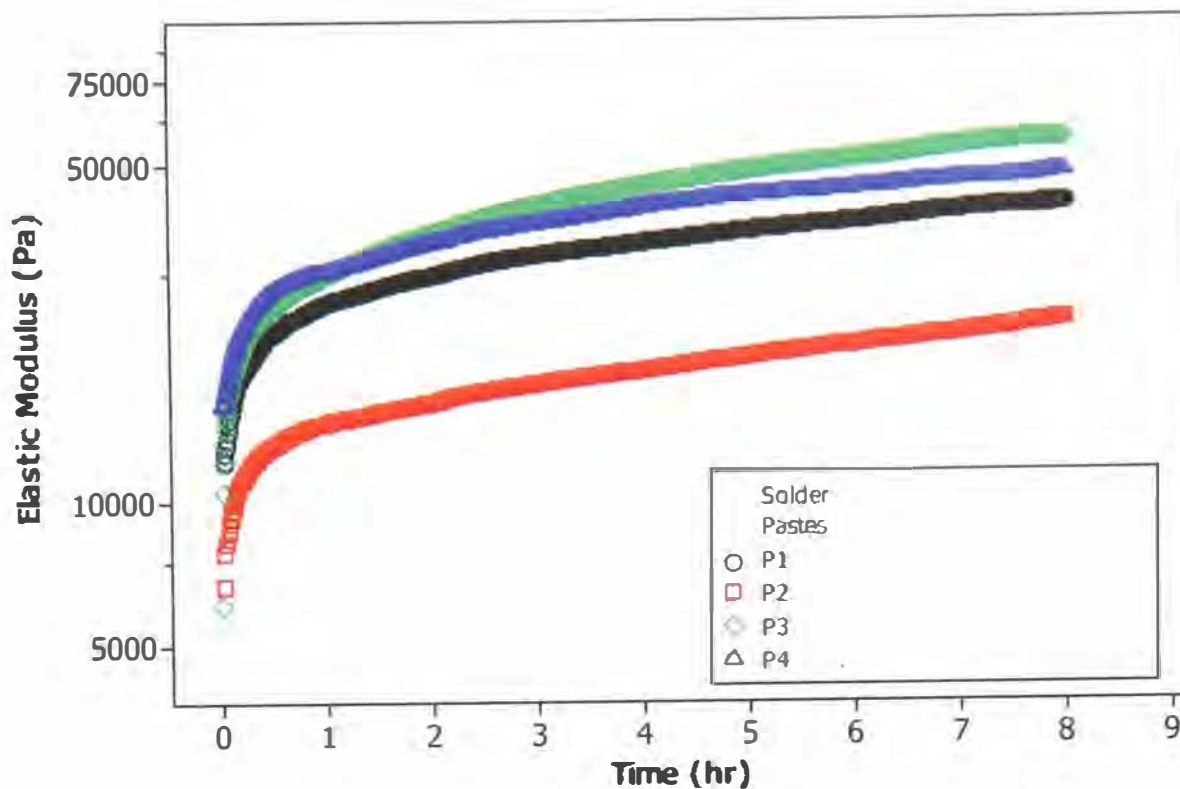


Figure 7.13: Changes in storage modulus (G') during ageing at 25°C for 8 hours.

As mentioned earlier (section 7.3.2), oscillatory time sweep tests were performed on presheared samples for a duration of 8 hours at 0.05% strain and 1 Hz frequency. The results from the tests are presented in figures 7.13 and 7.14, demonstrate the variation in elastic modulus (G') and phase angle (δ) as a function of time. Figure 7.13 is showing the changes in elastic modulus (G') as a function of aging time of 8 hours at 25°C for all the solder paste samples. It may be seen that for all solder paste samples G' is increasing rapidly in the first hour of aging and then continued to increase steadily without any plateau region. A similar behaviour was observed by Chang et al (2004) for corn starch-sugar composites. From the change in G' values during the aging two different rate of structural development can be observed for the solder paste samples. The initial rapid increase in G' value could be attributed to the rapid aggregation of the solder paste particles at the early stage of aging. This is a quite important behaviour of solder paste in terms of solder paste printing which refrain solder paste from slumping and helps it to retain its shape after the printing. As suggested by Kim & Yoo (2006) the later monotonous steady increase in G' value could be due to the slow formation and

rearrangement of the molecular networks within the solder paste structure at the late stage.

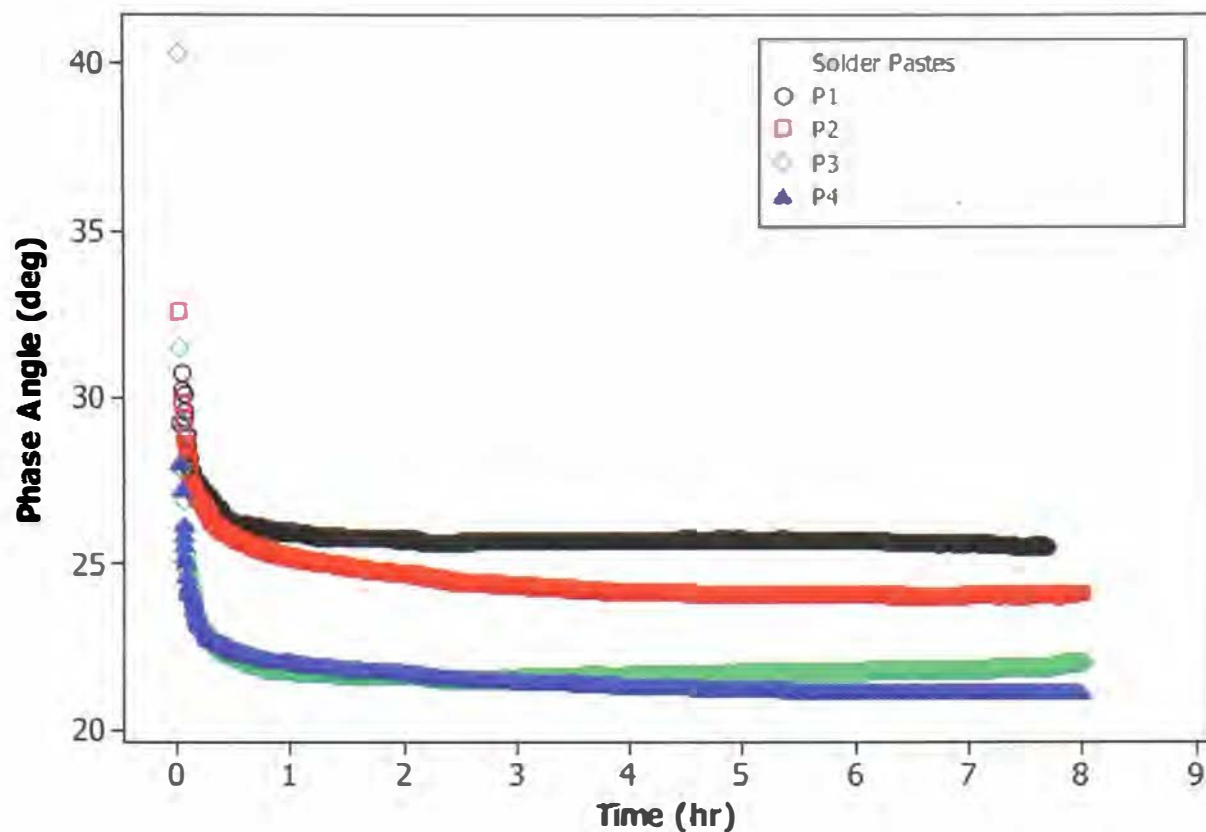


Figure 7.14: Phase angle (δ) as a function of time, measured at 25°C for different solder paste samples.

The effect of build-up time on phase angle (δ) is presented in figure 7.14. Phase angle is the phase in degrees between the stress and strain values. In dynamic oscillatory testing, phase angle provides a useful way of measuring the solidity and liquidity of any material. In the case of a pure solid, the strain (or stress) response will be totally in phase with the applied stress (or strain), that is, the phase angle is equal to 0° . For pure viscous liquid the resultant strain (or stress) will be totally out of phase to the applied stress (or strain), therefore, the phase angle is equal to 90° . The structural build-up of solder paste samples is evident from the decrease in phase angle with the time, as shown in figure 7.14. From the time-dependent change of phase angle for the solder pastes samples, it can be clearly observed that the phase angle reduced drastically in the first hour of ageing. Later, the decrease of phase angle became slower and reached a plateau region in long term. The rapid decrease and plateau of δ re-strengthen the earlier finding that the aggregation of

solder paste structure was quite fast initially and then followed by a slow aggregation at long time. Previous research carried out on various starch paste suspensions (Ravindra et al, 2004, Chang et al, 2004) have shown similar build-up behaviour under the application of oscillatory shear.

7.5 Summary

The time-dependent structural build-up of solder paste and flux mediums has been investigated in this chapter. The objective of the study was to quantify and model the structural build-up of solder pastes and flux mediums using the stretched exponential model (SEM). Experiments were designed to examine both short-term and long-term build up behaviour of paste materials. The stretched exponential model has been used satisfactorily to fit the short-term structural re-building of solder paste and flux mediums. As expected, for solder paste samples, the rate of structural recovery was found dependent on the applied shear rate. The model parameters, such as, equilibrium viscosity and characteristic time, have been correlated to the shear-thinning and slumping behaviours of solder paste during the stencil printing process. A higher equilibrium viscosity of solder paste would mean a higher resistance towards slumping. The characteristic time, on the other hand, represents the time frame from the end of stencil printing to the beginning of reflowing process. A higher characteristic time for solder paste would therefore, means more time for component placement by avoiding slumping of the solder paste. The results from the oscillatory time sweep measurements have also provided useful information regarding the structural changes of solder paste during an 8 hour long build-up process.

The results from these experimental and modelling studies of the build-up of solder paste structure would be quite useful to both the solder paste manufacturers and end-users. The paste manufacturers and formulators can use the technique developed to predict and quantify the slumping behaviour of solder paste. The end-users, for example the electronics assemblers/manufacturers can also use the technique to optimize their assembly process by minimising/preventing slumping of solder paste.

CHAPTER 8

EVALUATION OF SLUMP AND SPREAD BEHAVIOUR OF SOLDER PASTES AND THEIR CORRELATION TO THE RHOLOGICAL PROPERTIES

8.1 Introduction

The solder paste printing process is widely recognised as the primary source of soldering defects in the surface mount assembly. Previous studies show that more than 60% of the assembly defects can be traced to solder paste and the printing process (Mangin, 1991; Jensen & Lasky, 2006), and up to 87% of reflow soldering defects are caused by printing problems (Okuru et al., 1995). One way of understanding the various defect mechanisms occurring during the assembly processes and hence increasing the yield is by understanding and characterising the flow and deformation behaviour that is, the rheology of solder pastes. Rheology is regarded as one of the vital characteristics of solder paste with respect to the printing process, as the flow and deformation behaviour of solder paste directly affects the quality of paste deposition onto the substrate. Therefore, the correlation of paste rheology to the applications and its specific parameters is of paramount importance to the control of rheological quality when manufacturing paste, as well as to the setting and control of application parameters when using paste (Hwang, 1996).

This chapter presents the results of the printing process trial focused on the evaluation of the shear thinning and slumping behaviour of four commercially available solder pastes. The objective of the study is to correlate the solder paste properties (shear

thinning and slumping behaviour as measured by rheological characteristics) with the pastes printing performance at the ultra-fine pitch level. The chapter is organised in four main parts. The first part of the chapter presents the details of the printing parameters, equipments and materials used in the study. The second part outlines the step-by-step procedure, which been followed during the printing test experiments. The third part presents the slump and spread test results. The last part of the chapter investigates the correlation of the printing results to the time-dependent rheological properties and modelling studies carried out in the previous chapters.

8.2 Experimental Equipment and Materials

8.2.1 Printing Parameters

Selecting the correct printing process parameter values is crucial in achieving optimum print performance. Several investigations have been carried out in optimising process parameters (Morris and Wojcik, 1990; Ismail et al., 1993; Ekere et al., 1993; Poon and Williams, 1999; Lau, 2000 and Durairaj et al., 2000). The printing parameter values used in this study is based on the results of the previous work reported by Marks et al. (2007). The details of these parameters are listed in table 8.1.

Table 8.1: Printing parameters

Printing Parameters	Values Used
Printing/Squeegee Speed	20 mm/sec
Squeegee Loading (or pressure)	8 kg
Separation Speed	100 % (3 mm/sec)
Snap-off/Print-Gap	0.0 mm (On-contact printing)

Printing or squeegee speed is the rate at which the squeegee moves across the stencil and squeegee pressure or loading represents the vertical force applied to the

squeegee during the print stroke. These two parameters are directly proportional to each other and must be optimised in order to achieve a good clean wipe of the top side of the stencil surface. Using higher squeegee speed and pressure will increase the heat generation at the squeegee/stencil interface. This will create greater paste shear and may therefore lead to problems like slumping, under stencil bleed-out and pad-to-pad bridging (Seelig et al 2000). Separation speed can be defined as the rate at which the substrate is pulled away from the stencil after the completion of a print stroke. The ideal separation depends on the solder paste and stencil aperture wall smoothness. A too fast separation speed will result in stencil clogging and solder paste skipping. A slow separation speed on the other hand will increase the print cycle time (Verboven 2008). Snap-off or print-gap is the distance between the substrate and the stencil. An on-contact printing (with snap-off set to zero) may prevent bridging related to paste bleed-out and also provides for a more uniform paste deposition and more consistent paste height (Seelig et al 2000).

8.2.2 Printer

The DEK 260 semi-automatic printer, shown in figure 8.1, was used for the experiments reported in this chapter.



Figure 8.1: DEK 260 Stencil Printing Machine

The printer mainly consists of the stencil frame holder, the squeegee system, the substrate holder, the motor and the stencil/substrate alignment system. The substrate is held by using edge-clamp and/or vacuum created by air suction and it can be supported by magnetic pins or tooling pins. In order to operate the printer, the printing parameters can be changed by using the PC interface as shown in the figure 8.1. The printer can support a maximum printing stroke (squeegee travel distance) of 450 mm. The print speed can be varied from 10 to 250 mm/sec in both forward and reverse directions with 1 mm/sec increments. The print gap between the stencil and the substrate can be adjusted between 0 – 5 mm in 0.1 mm increments.

8.2.3 Squeegee System

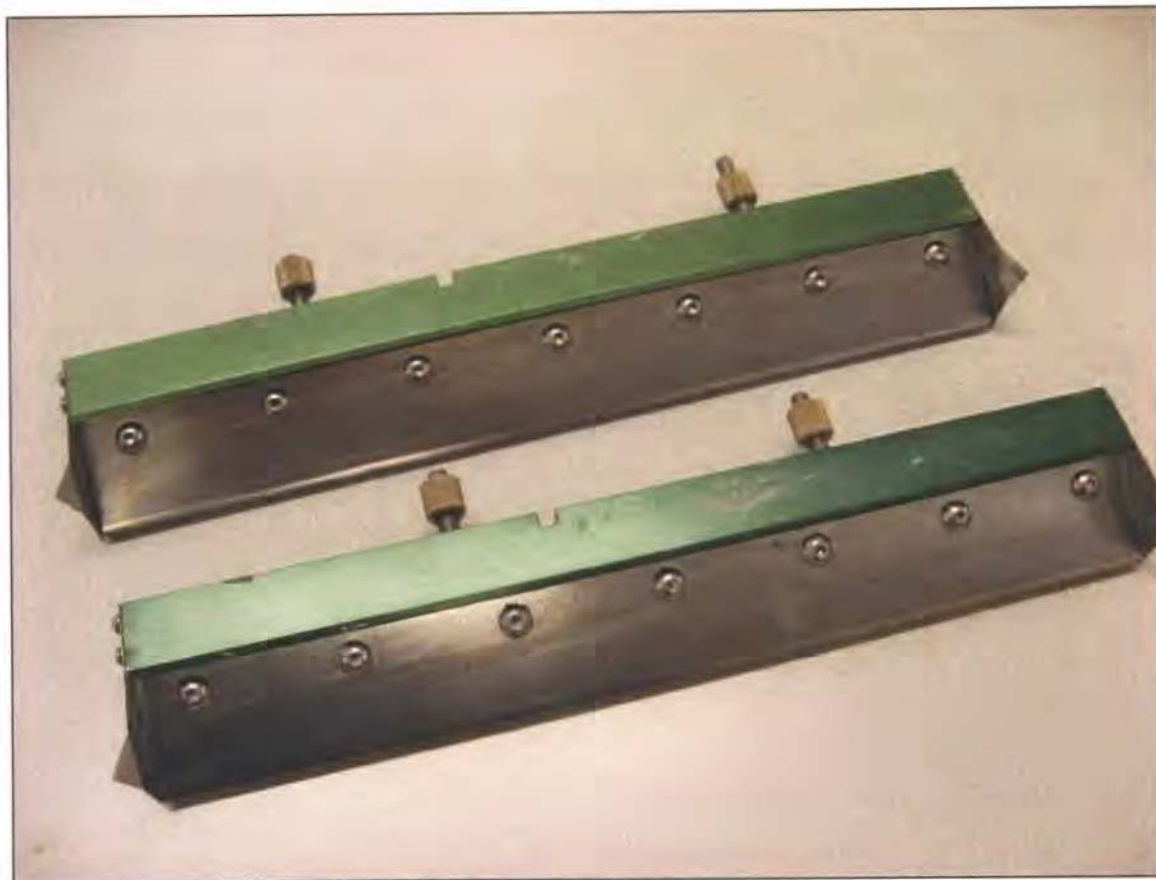


Figure 8.2: Metal Squeegees

The main function of the squeegee is to help transfer the solder paste from the stencil into the aperture. When the squeegee moves across the stencil, it creates a paste

roll in front of the squeegee. The hydrodynamic pressure created by the paste roll helps to force the solder paste into the apertures. Two metal squeegees have been used throughout the experiment, one for forward printing and another one for reverse printing. The squeegee blades are made of stainless steel with an angle of 60° with the vertical axis. The squeegees were 300 mm in length.

Among the two common types of squeegees: rubber or polyurethane and metal, metal squeegees are more popular for fine pitch applications. Because lower pressure is used, metal squeegees do not scoop paste from apertures, and because they are metallic, they do not wear easily like rubber squeegees and hence do not need to be sharpened. However, metal squeegees cost significantly more than rubber squeegees, and can cause stencil wear (Prasad 2000).

8.2.4 Test Board

The printing tests were conducted using the “Benchmark II” test board designed by Heraeus (figure 8.3). This specially designed test board combines numerous test features and can be used for different purposes such as printability test, slump test, spread test, test for wettability and solder ball formation and many others.

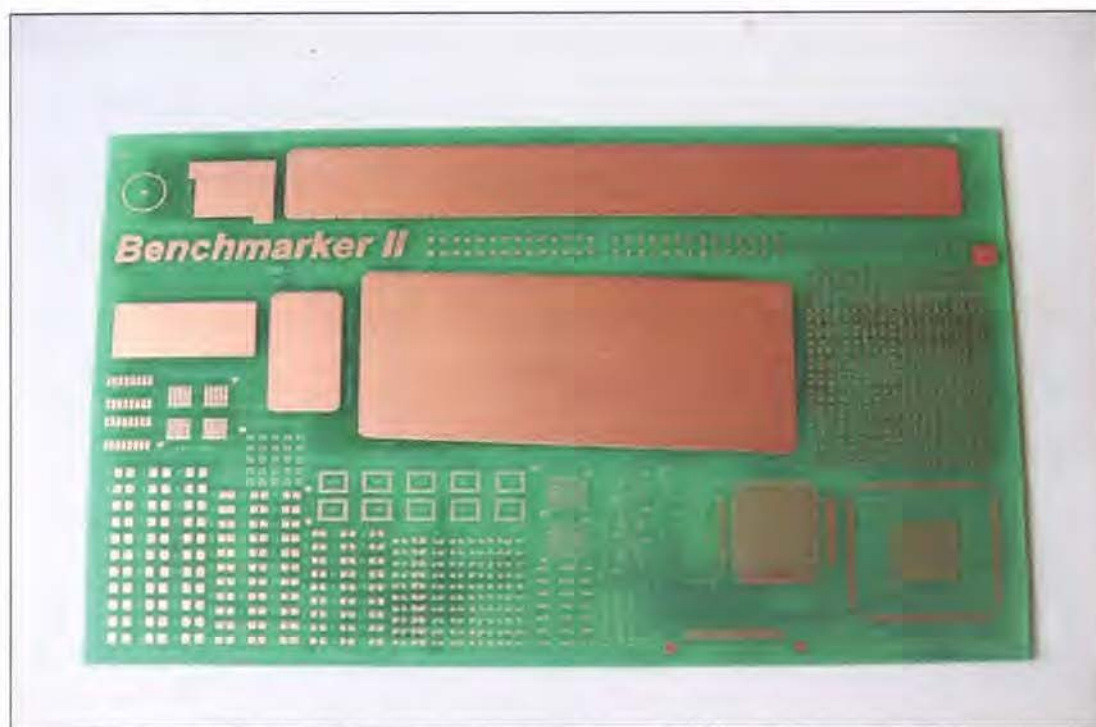


Figure 8.3: Heraeus Bechmarker II test board

8.2.5 Stencil



Figure 8.4: Benchmarker II laser-cut stencil

A stencil provides the openings for all the components on the board or substrate so that the paste can be printed through. The number of openings on the stencil matches the number of openings required for the surface mount components on the board. Stencils are uniquely made to match specific printed circuit board (PCB) design and hence can not be used for others. As shown in figure 8.4, a laser cut stencil with a thickness of 0.125 mm was used in this investigation. A closer view of the stencil openings is shown in figure 8.5. The stencil is made to match the Benchmarker II test board design (figure 8.3). According to Prasad (2000), laser cut stencils provides improved aperture accuracy (capable of producing aperture widths as small as 0.004" with an accuracy of 0.0005") and therefore, are very suitable for ultra-fine-pitch component printing. The other common processes of making stencils are chemical etching and eletroforming.

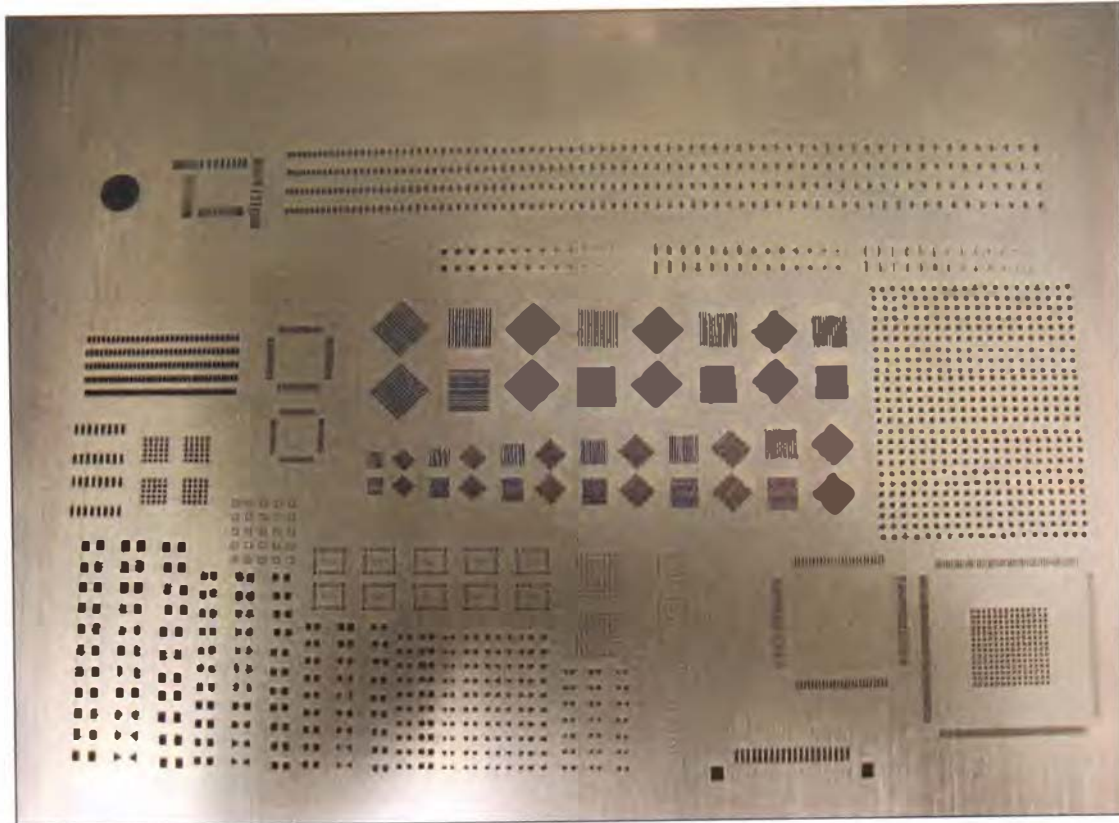


Figure 8.5: Close up view of openings on the stencil

8.2.6 Inspection

The Leica S6D zoom stereomicroscope, shown in figure 8.6, was used for inspecting solder paste deposits for slump and spread behaviours. The microscope can provide a zoom of 6.3:1 and a magnification from 6.3X to 40X. The camera exit of the microscope was fitted with a high resolution video camera (JVC KY-F55), as shown in figure 8.6. The output from the camera was fed into a computer where live images can be observed and/or saved for further analysis.



Figure 8.6: Lica S6D zoom stereomicroscope with the camera kit

8.2.7 Batch Reflow Oven

A forced-convection batch reflow oven (Model SM500 CXE, Reddish Electronics), as shown in figure 8.7, was used to study the hot slump and spread behaviours of solder paste samples. According to the manufacturer, the Reddish forced convection reflow oven incorporates two heating elements, one at the front and the other at the rear of the chamber, to heat up the air inside the oven. The temperature of these heating elements can be adjusted and set in four different time zones, so that, a temperature profile can be produced over time. A forced convection process, produced by a fan, circulates the hot air, thus equalising the temperature inside the oven. Setting the temperature of the heating elements for four time windows simulates the four zones. The

oven also includes a gas inlet valve so that reflow in nitrogen atmospheres can be obtained.



Figure 8.7: Reddish forced convection reflow oven

8.2.8 Areas of Observation/interest

In order to examine the slump and spread behaviours of solder pastes, three areas were selected for observation. These three areas are levelled as Slump Location-1, Slump Location-2 and Spread Location, as shown in figure 8.8. The details of these locations are given in the following sections.

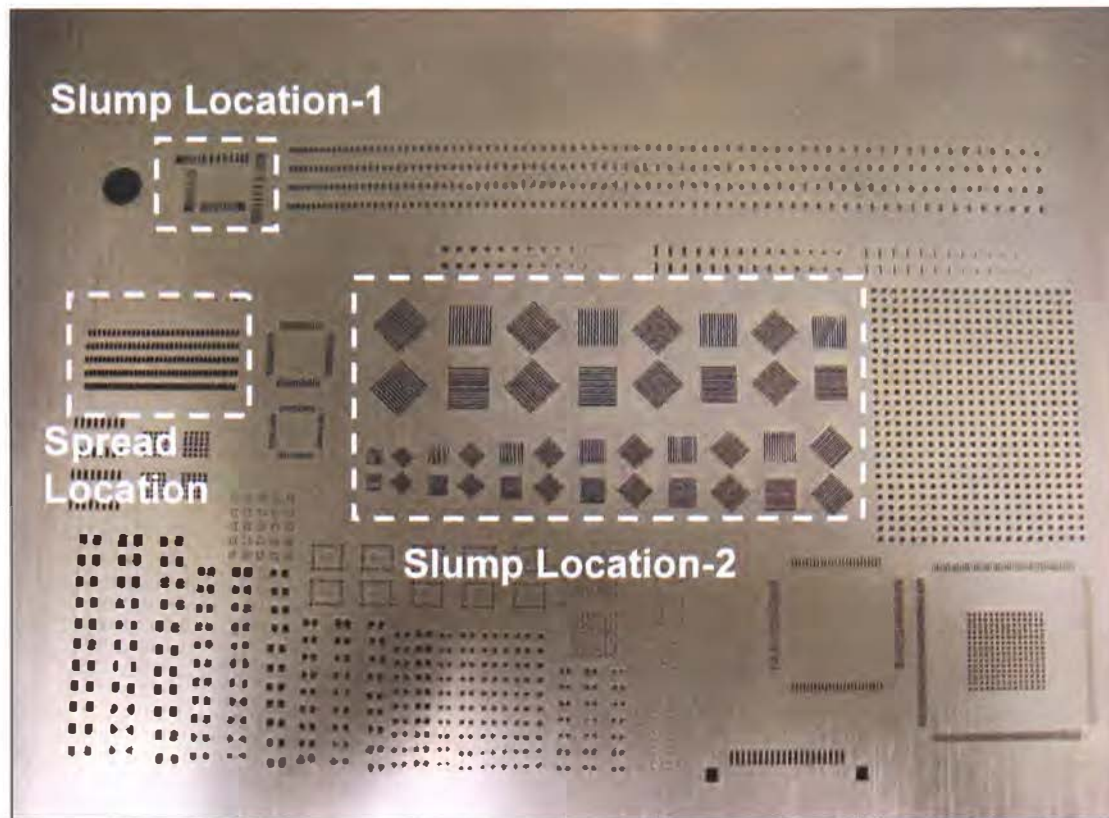


Figure 8.8: The three areas of interest on the Benchmarker II stencil.

a) Slump Location-1

This area of the Benchmarker II stencil/test board was specially designed to examine the slump characteristics of solder paste printing. The apertures in this area are designed by integrating the IPC-A-20 and IPC-A-21 stencil patterns (IPC, 1998). The details of the apertures/pad sizes and the spacing are shown in figure 8.9. Three different pad sizes with different spacing are available in both horizontal and vertical directions to examine slumping behaviour. In this investigation, Slump location 1 was examined for both cold and hot slump.

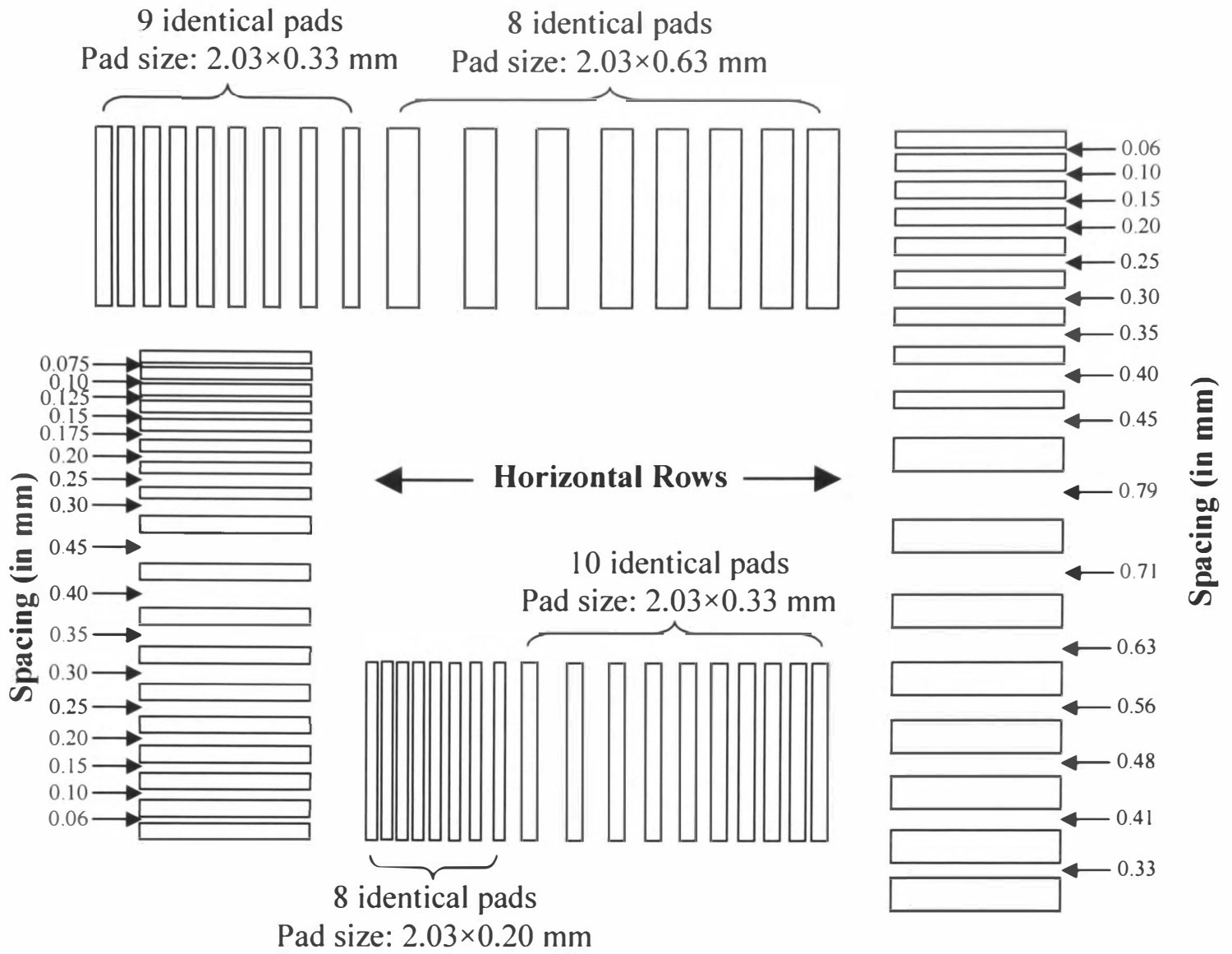


Figure 8.9: Slump Location-1

b) Slump location-2

Slump location-2 is consist of 10 groups of fine pitch apertures with same width ranging from 120 μ m to 300 μ m in 20 μ m steps. For each pitch there are 4 groupings of 13 lines and 12 spaces with one grouping horizontal, one vertical and two oriented at 45⁰ to the print direction.

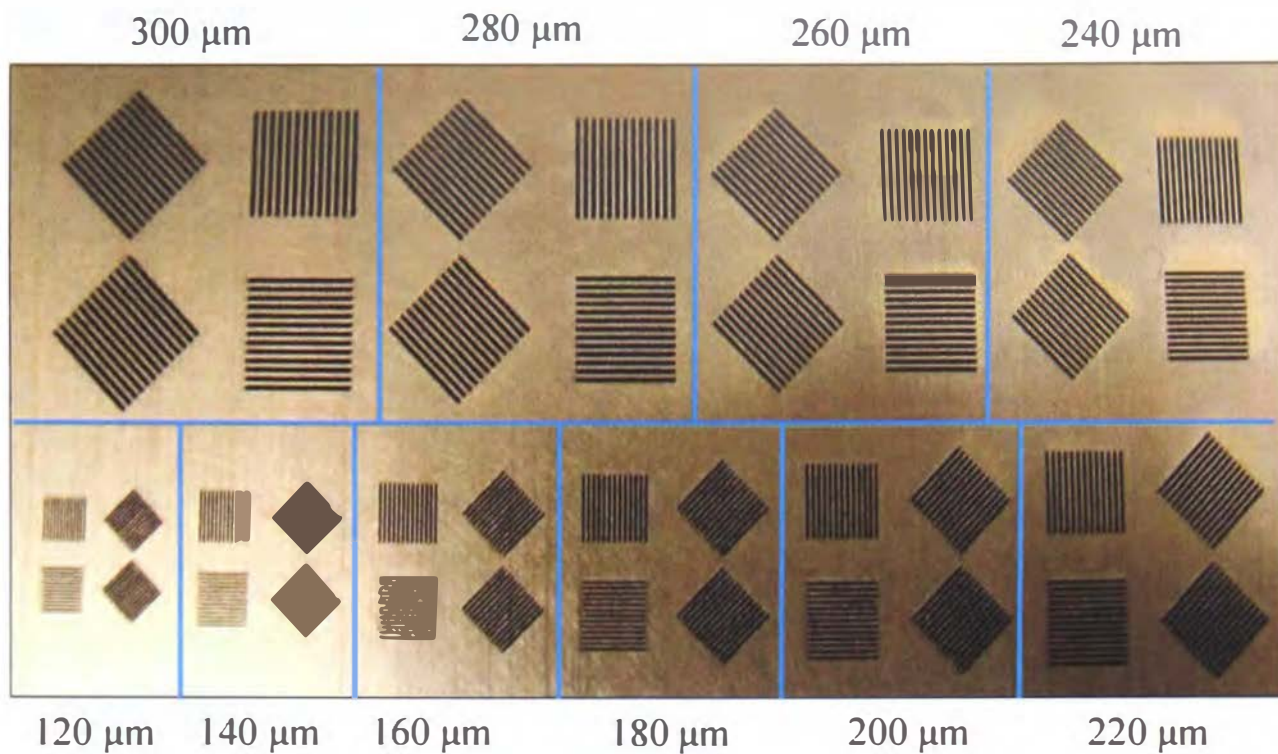


Figure 8.10: Slump location-2

c) Spread Location

This area of the Benchmarker II is specially designed to examine spreading behaviour of solder paste. There are five rows of relatively wide pads of 25×50 mil (0.625×1.25 mm) size with different gaps between the pads in each row, ranging from 4 mils to 12 mils ($100 \mu\text{m}$ to $300 \mu\text{m}$). There are 31 pads at the top row and the number increased in a step of two with the bottom row having a maximum of 39 pads.

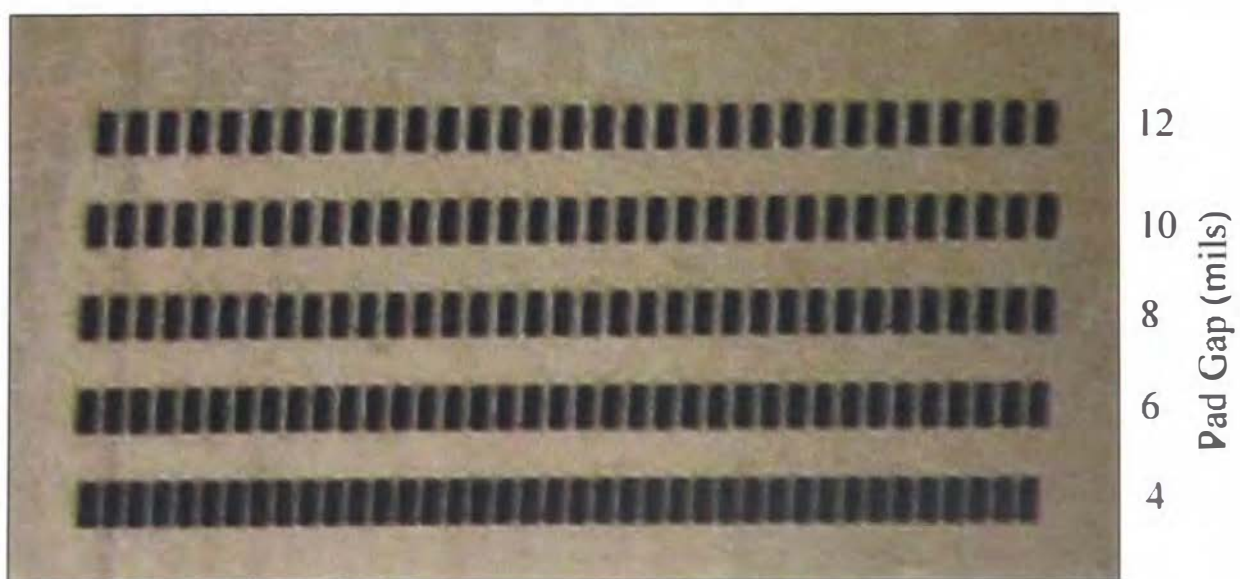


Figure 8.11: Spread test location on the Benchmarker II stencil

8.3 Experimental Procedure

This section outlines the experimental procedure which been followed for the printing experiments carried on the solder paste samples.

- a) The Benchmark II stencil was placed in the stencil holder compartment of the printer. The stencil was firmly secured in the compartment by touching the 'stencil lock' button on the computer screen.
- b) The stencil was then thoroughly cleaned using Iso-propanol (IPA) solvent which readily evaporates.
- c) The squeegees were cleaned using IPA before being placed in the squeegee holder. The screw on the squeegee easily secures the squeegee. Double squeegees were used in this experiment. One for forward printing and the other for reverse printing.
- d) The printing process parameters required for the experiment such as squeegee speed, separation speed and print-gap were entered into the computer according to the values provided in table 8.1.
- e) The squeegee pressure was adjusted manually to the required value of 8 Kg.
- f) The Benchmark II board was placed onto the table supported by the magnetic tooling pins.
- g) The solder paste was applied manually onto the stencil in a central position just before the squeegees. This is to allow paste elongation during the printing process.
- h) The printer was set to 'step-mode'. This mode allows the user to input the required data in step by step through a series of questions. In this mode the input data can be changed/alterd before the printing commences.
- i) The 'print stroke' (distance travelled by the squeegee during the printing) was set to cover the whole length of the stencil aperture pattern.
- j) Once the table was brought mechanically underneath the stencil, it was aligned (using the x, y and theta alignment screws) so that the board design matches exactly the openings on the stencil.

- k) As suggested by Morris and Wojcik (1990) a cycle of ten consecutive prints were performed and the eleventh and twelfth prints were taken for examination. The initial 10 prints were carried out to allow the paste to reach the equilibrium viscosity.
- l) The bottom side of the stencil was then dry-cleaned. Since the apertures are small, clogging is a major problem. Therefore this step is very important to ensure good paste deposit.
- m) The two prints (eleventh and twelfth) were marked as specimen #1 and specimen #2 and were stored for 5 minutes at room temperature. Specimen #1 was examined for cold slump and spread.
- n) Specimen #2 was heated to 150⁰C for 10 minutes, cooled to ambient and examined for slump and spread.
- o) The same procedure was repeated (from (a) to (n)) after 10 and 15 minutes of rest/storage time on separate days.

A total of 12 experiments (each of 12 runs) were conducted during the course of the investigation for the four different solder paste samples.

8.4 Discussion of the printing test results

8.4.1 Slump Test Results

Lee (2002) has defined slump as “a phenomenon where the paste viscosity is not high enough to resist the collapsing force exerted by gravity, and consequently results in spreading beyond the area to be deposited”. Slump is identified by a decrease in height and an increase in length and width of the solder paste deposit. Based on the temperature condition, slump can be categorised as cold and hot slump. Cold slump refers to the slumping behaviour at room temperature and hot slump refers to slumping during reflow. Although Lee (2002) has probably misinterpreted “yield stress” as the “thixotropy”, he highlighted some of the important causes of cold slump, which include: a) low yield

stress (was actually “thixotropy” in Lee’s book), b) low viscosity, c) low metal or solid content, d) small particle size, e) wide particle size distribution, f) low surface tension of flux, g) high humidity, h) hygroscopic paste, and i) high component placement pressure. In addition, hot slump is also affected by the ramp-up rate of the reflow cycle.

This section outlines the results of cold and hot slump tests carried out on the four solder paste samples – P1, P2, P3 and P4. The IPC slump test procedure outlined in “IPC-TM-650 Test Methods Manual” was followed. The detailed experimental procedure is provided in the previous section (section 8.2). The slump tests were performed with 5, 10 and 15 minutes of resting time. The resting time here represents the time between the printing step and the reflow. The objective of the investigation was therefore to find out how different resting periods affect the cold and hot slump behaviour of solder pastes.

a) Cold Slump Results

Table 8.2 and figures 8.12 to 8.15 show the cold slump results for all the solder paste samples, examined at slump location 1 (figure 8.8). At slump location 1 (figure 8.9), solder paste deposits were obtained for three pad sizes: 2.03×0.63 mm, 2.03×0.33 mm and 2.03×0.20 mm, both in horizontal and vertical directions. The spacings between the pads were variable, as shown in figure 8.9. Slumping was examined/evaluated by noting the maximum spacing which has bridged for a particular pad size in horizontal and vertical directions. It is worth mentioning here that none of the paste samples has shown slump for the pad size of 2.03×0.63 mm. Table 8.2 is showing the minimum spacing where slumping occurred for the pad sizes of 2.03×0.33 mm and 2.03×0.20 mm for different rest periods (5, 10 and 15 minutes). “H” and “V” in table 8.2 represent the horizontal and vertical rows. The results are also presented in bar graphs (figures 8.12 to 8.15) with the spacing in y-axis and solder pastes in x-axis. Different solder pastes have shown different cold slump behaviours with increasing rest periods. In most cases there was no change/difference observed in cold slump behaviour with the rest periods. However, in some instances cold slumping was found increasing with the increase in rest period.

For 2.03×0.33 mm pads in horizontal rows/arrangement (figure 8.12), cold slump behaviour remain unchanged with the increase in resting time for most of the solder paste samples. This is an indicative of good slump resistant behaviour of the solder paste samples by showing that the solder paste deposits can retain their shape even after 15 minutes of resting time. This broader time-window (between the printing step and reflow) also provides greater flexibility in the assembly line by allowing more time for component placement and inspection before the reflow process. From the figures 8.12 – 8.15, it may be observed that the slumping behaviour was different for horizontal and vertical rows for the identical pad sizes. This implies that the slump behaviour depends on the orientation of the pads on the printed circuit boards (PCB), therefore, must be taken into consideration when designing the PCB. In a previous research work, Durairaj et al (2001) also observed different heights of the paste deposits for pads perpendicular and parallel to the squeegee travel. In some instances where cold slumping behaviour were found increasing with increasing rest time, although an increased bridging due to slump was observed when resting time was increased from 5 minutes to 10 minutes, an unexpected decrease in bridging was observed with a rest time of 15 minutes. This kind of inconsistency in slumping behaviour can be attributed to the changing ambient conditions, as the room temperature and humidity were not controlled. The effect of humidity and temperature on slump has also been emphasized by Lee (2002). With high humidity, the paste can pick up significant amount of moisture which results in low viscosity and increased slump. Viscosity of solder paste generally decreases with increase in temperature and therefore, will yield greater slump. In a study by Riedlin & Ekere (1999), it was estimated that an increase of 1°C results in a decrease in paste viscosity of approximately 20 Pas at a shear rate of 1 s^{-1} between 20° and 30° C. Mindel (1991) in contrast observed a drop of approximately 50 Pas/ $^{\circ}\text{C}$ for the same temperature range.

Table 8.2: Cold slump results, minimum spacing (in mm) where bridging was observed

Rest Time	Pad size: 2.03 × 0.33 mm								Pad size: 2.03 × 0.20 mm							
	P1		P2		P3		P4		P1		P2		P3		P4	
	H	V	H	V	H	V	H	V	H	V	H	V	H	V	H	V
5	0.06	0.06	0.10	0.06	0.10	0.10	0.10	0.10	-	0.075	0.075	0.075	0.075	0.075	0.10	0.10
10	0.15	0.15	0.10	0.10	0.10	0.10	0.10	0.15	0.075	0.075	0.075	0.075	0.10	0.10	0.125	0.125
15	0.10	0.10	0.10	0.10	0.10	0.10	0.10	0.10	0.075	0.075	0.10	0.075	0.10	0.10	0.075	0.10

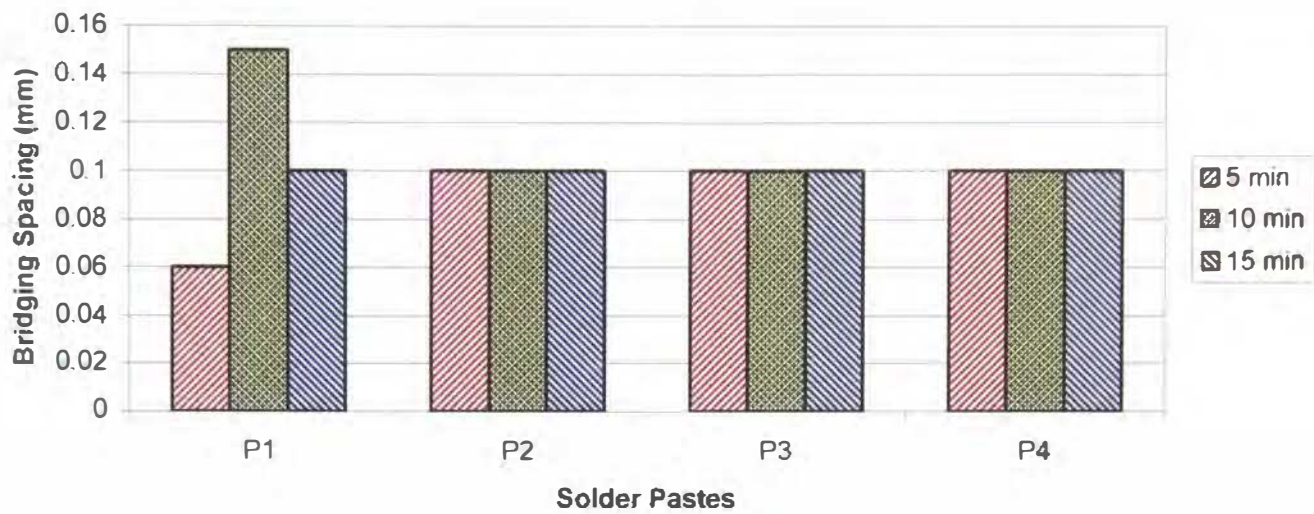


Figure 8.12: Cold slump results for horizontal 2.03 × 0.33 mm pads for different resting time.

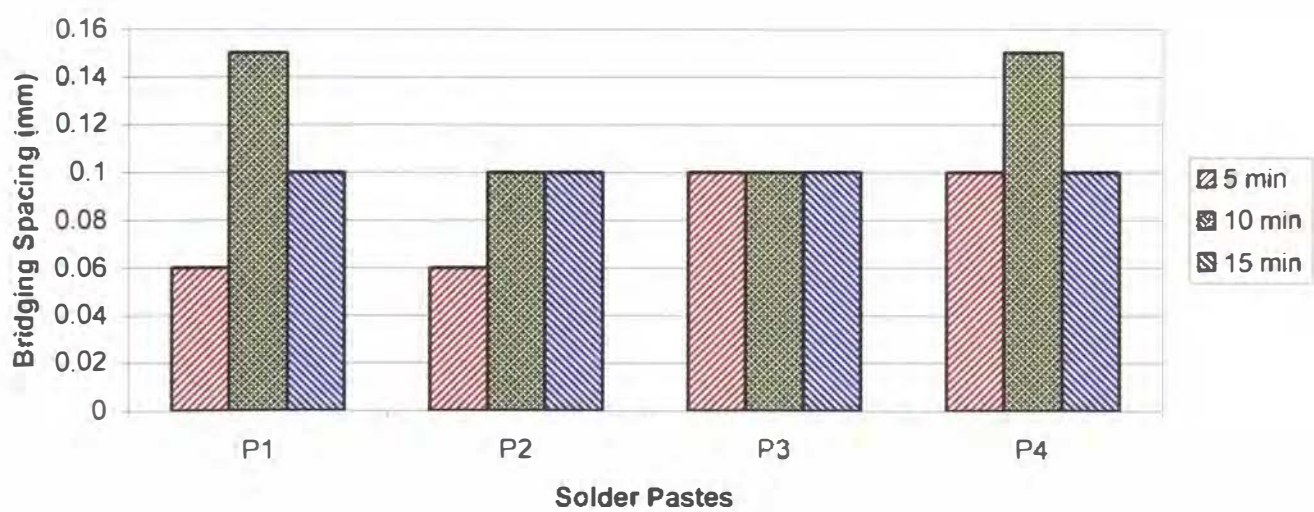


Figure 8.13: Cold slump results for vertical 2.03 × 0.33 mm pads for different resting time.

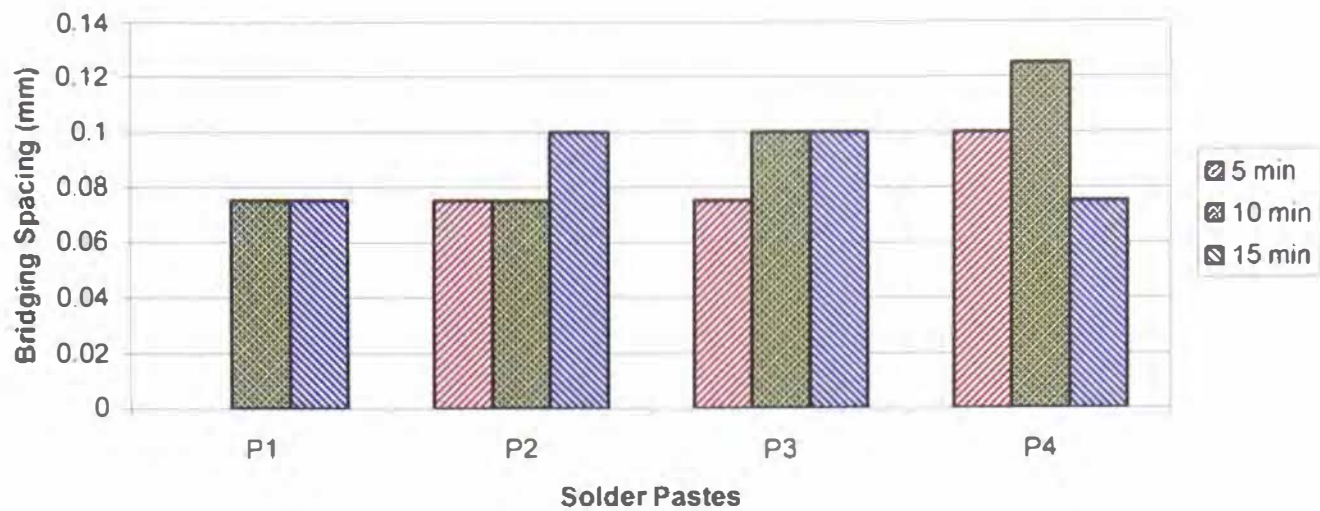


Figure 8.14: Cold slump results for horizontal 2.03 × 0.20 mm pads

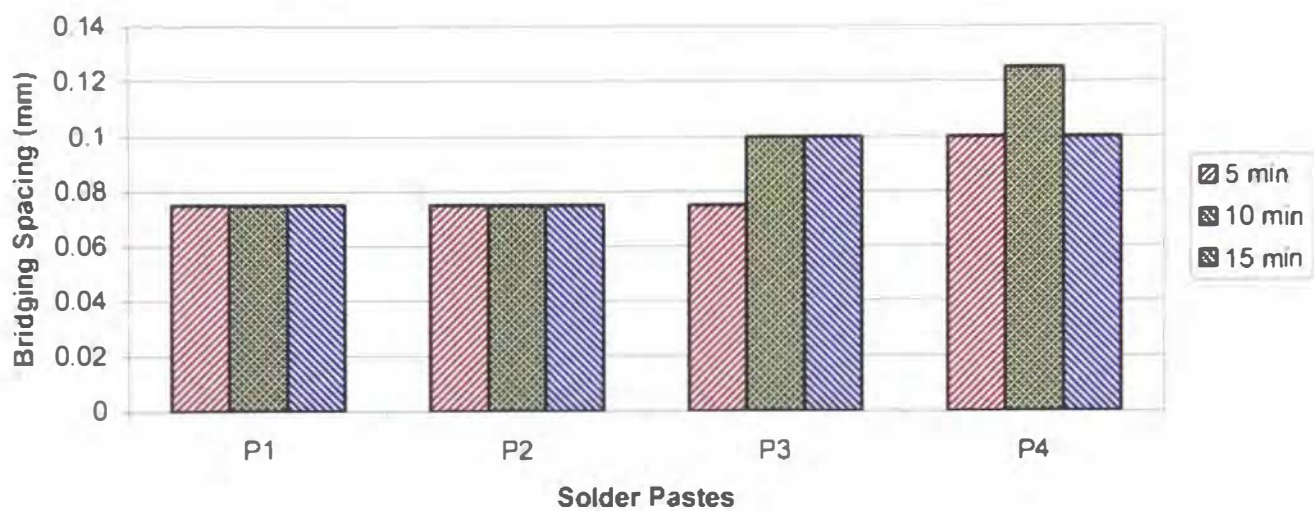


Figure 8.15: Cold slump results for vertical 2.03 × 0.20 mm pads.

b) Hot Slump Results

In contrast with cold slump which occurs at room temperature, hot slump occurs in the preheat section of the reflow profile. Hot slump has the potential to be the most damaging of the two, as excessive slump results in solder bridging (Rowland, 1999). The results from the hot slump tests are presented in Table 8.3 and figures 8.16 to 8.21. As mentioned in the experimental procedure (section 8.2), hot slump tests were carried out by heating the printed board to 150⁰C for 10 minutes. Like cold slump tests, hot slump tests were performed with different resting periods (5, 10 and 15 minutes). The results

were examined at two different locations on the benchmarker-II test stencil/board, as identified by “slump location 1” and “slump location 2” in figure 8.8.

Table 8.3 and figures 8.16 to 8.20 shows the hot slump results observed at slump location 1. At this location hot slump behaviour was examined for three different pad sizes (2.03×0.63 mm, 2.03×0.33 mm and 2.03×0.20 mm) with different spacings both in horizontal and vertical orientation. In table 8.3, the minimum spacing where bridging was observed is recorded for all the solder paste samples (P1 to P4) in horizontal and vertical orientation (denoted by “H” and “V”). During the test no bridging was observed for 2.03×0.63 mm pads, either in the horizontal or in the vertical orientation. The graphical presentation of the hot slump results are shown in figures 8.16 to 8.19. As expected, for all solder paste samples, bridging due hot slump was generally found increasing with increasing resting period. For 2.03×0.33 mm pads, almost identical slumping behaviour was observed for horizontal and vertical orientation. This is in contrast with 2.03×0.20 pads where different slumping behaviour was observed for horizontal and vertical pads. In few instances, solder paste P4 has shown an unexpected decrease in bridging with 15 minutes of rest time. Similar inconsistent slump behaviour was observed in cold slump testing and could be related to variations in room temperature and humidity.

Tables 8.4 and 8.5 show the hot slump results observed at slump location 2. Pads with 0.28 mm and 0.32 mm pitch sizes and 45° orientations were observed. As expected, pads with smaller pitch sizes (0.28 mm) have shown relatively greater hot slump because of the narrower space between the pads. The pictures presented in table 8.4 and 8.5 clearly show that the intensity of bridging due to hot slump was increased with increasing resting time. This increase in slumping can be attributed to the tendency of solder paste to absorb moisture from the atmosphere which ultimately results in reduction in viscosity with time and increase in slump. Another possibility is that the longer the solder paste left idle, the greater the intensity of slump due to gravitational force.

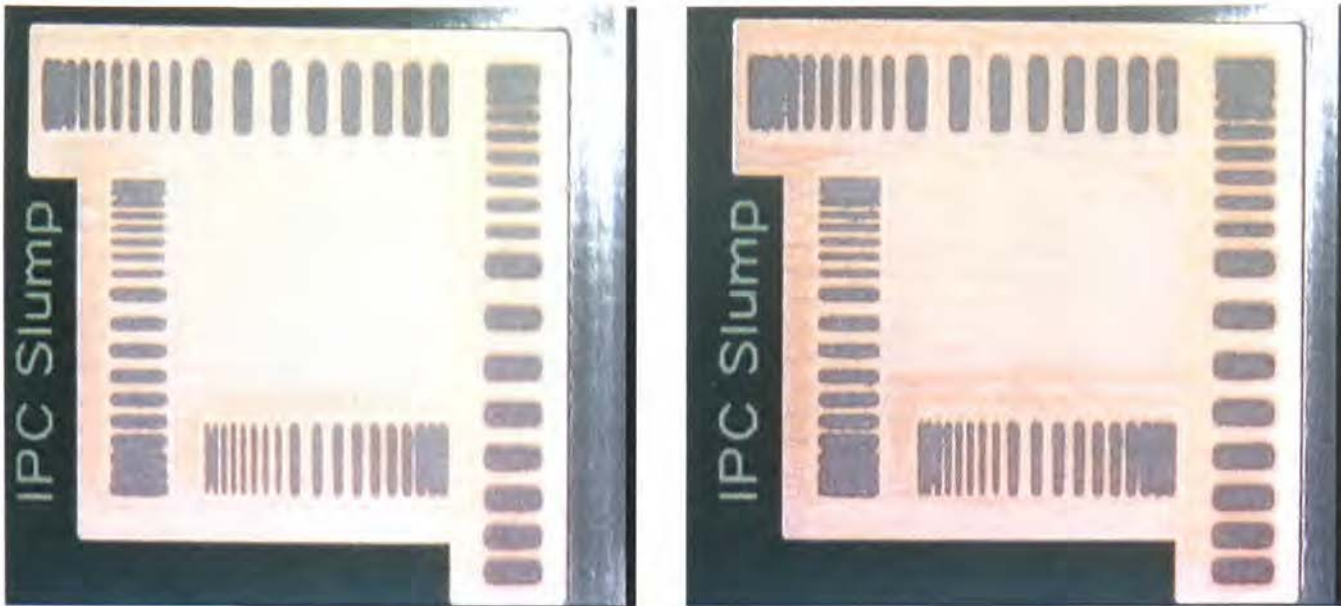


Figure 8.16: Hot slump behaviour of P2 solder paste after 5 minutes (left) and 10 minutes (right) of resting time.

Table 8.3: Hot slump results, minimum spacing values where bridging was observed

Rest Time	Pad size: 2.03 × 0.33 mm								Pad size: 2.03 × 0.20 mm							
	P1		P2		P3		P4		P1		P2		P3		P4	
	H	V	H	V	H	V	H	V	H	V	H	V	H	V	H	V
5	0.15	0.15	0.15	0.15	0.10	0.10	0.20	0.20	0.10	0.10	0.10	0.075	0.10	0.075	0.125	0.15
10	0.20	0.20	0.20	0.15	0.15	0.15	0.25	0.25	0.125	0.125	0.125	0.125	0.125	0.125	0.20	0.15
15	0.20	0.20	0.20	0.20	0.15	0.15	0.20	0.20	0.125	0.15	0.15	0.15	0.125	0.125	0.15	0.15

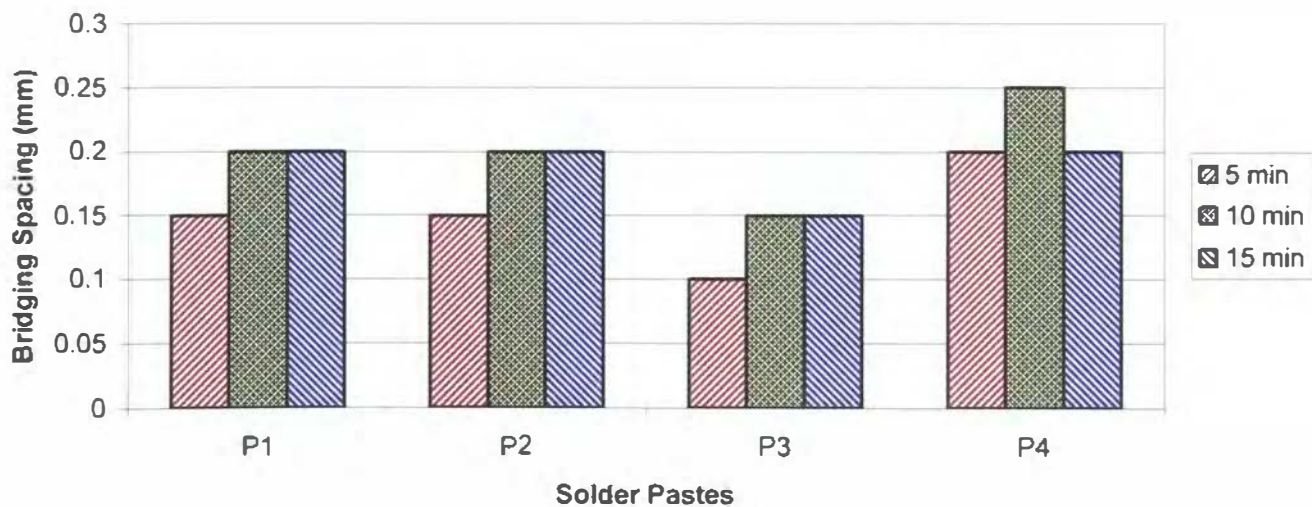


Figure 8.17: Hot slump results for horizontal 2.03 × 0.33 mm pads for different resting periods.

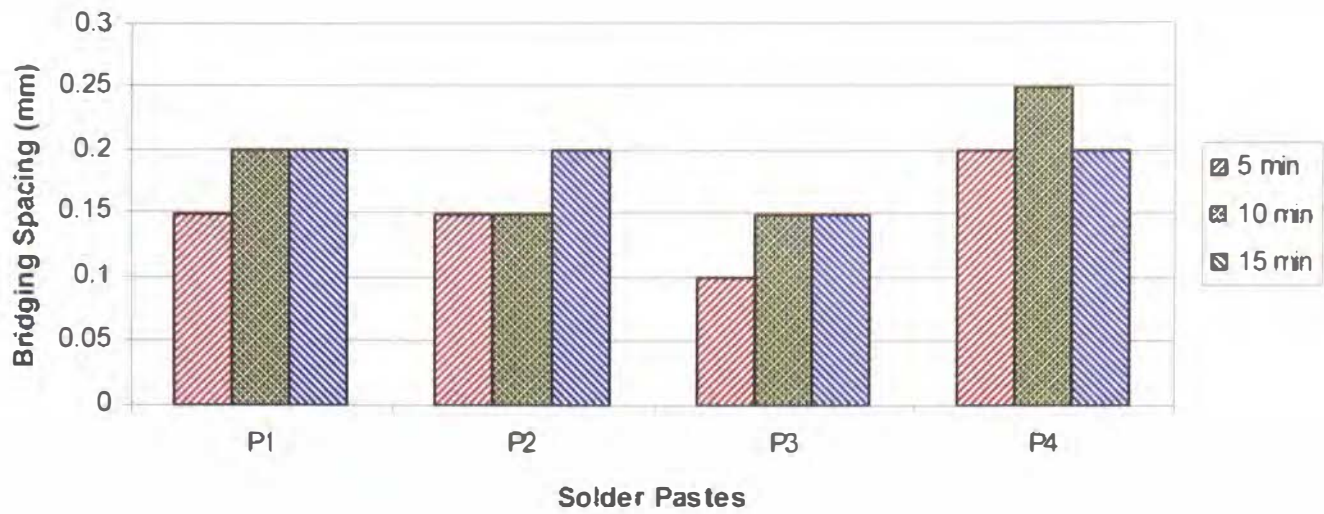


Figure 8.18: Hot slump results for vertical 2.03 x 0.33 mm pads for different resting periods.

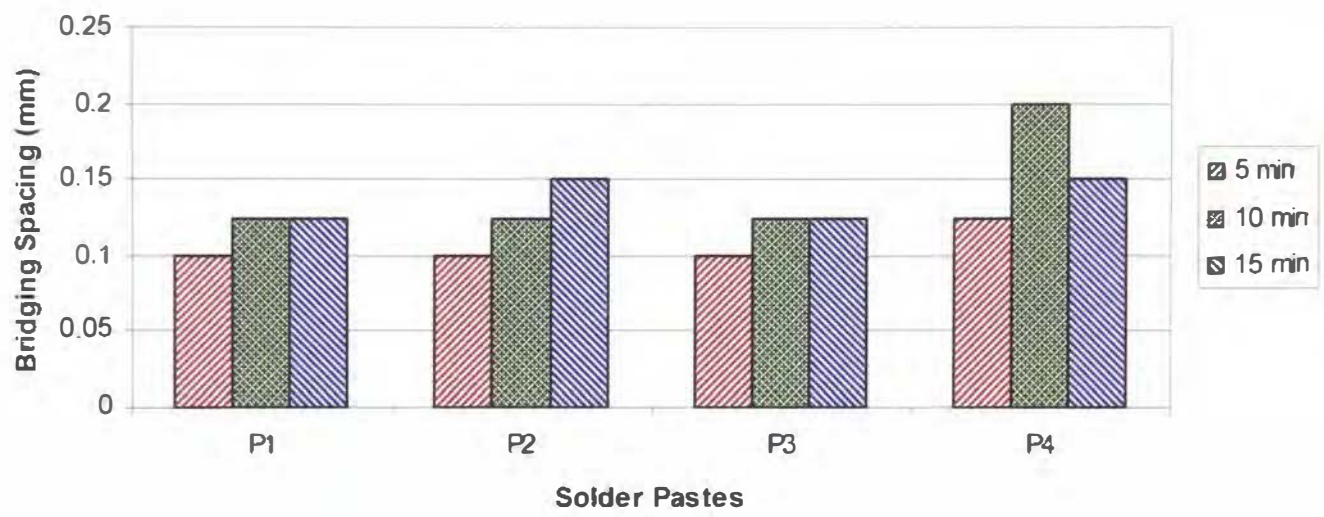


Figure 8.19: Hot slump results for horizontal 2.03 x 0.20 mm pads for different resting periods.

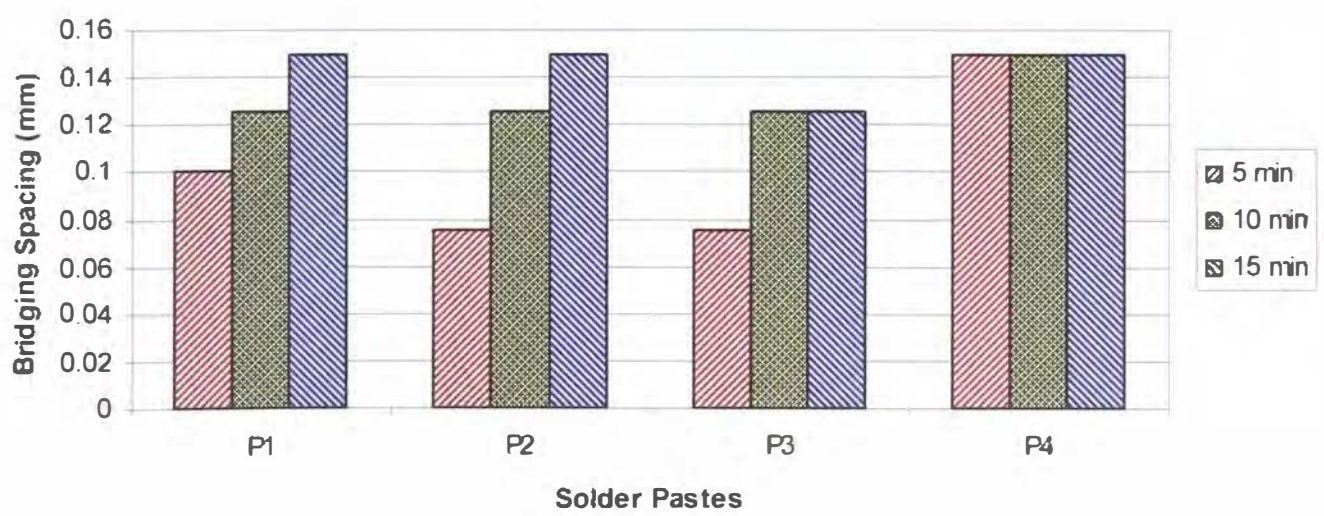


Figure 8.20: Hot slump results for vertical 2.03 x 0.20 mm pads for different resting period.

Table 8.4: Hot Slump results for pads with 45° orientation (0.28 mm pitch)

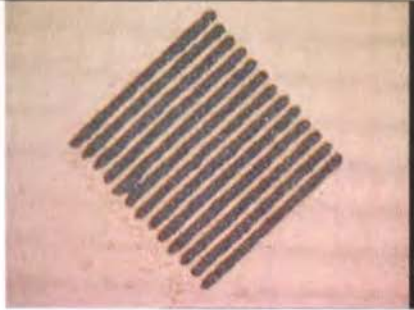
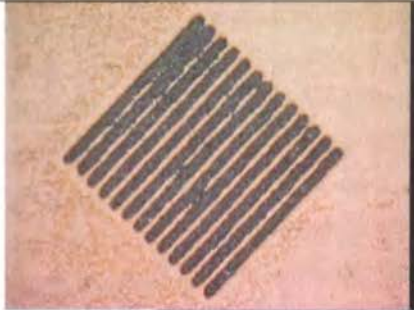
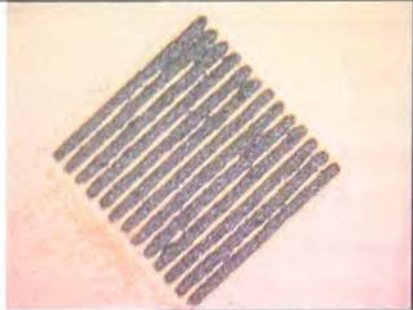
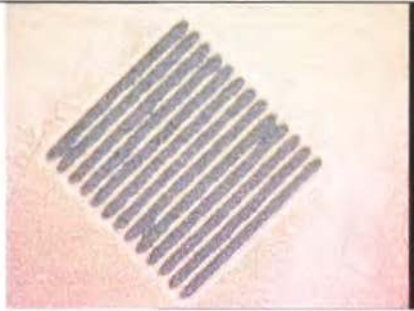
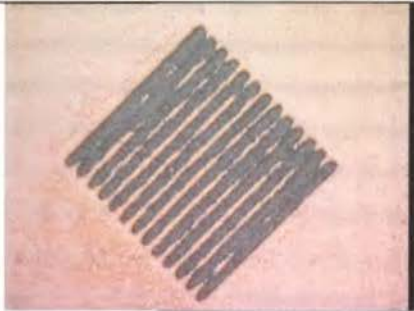
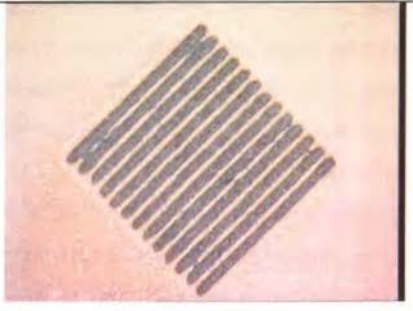
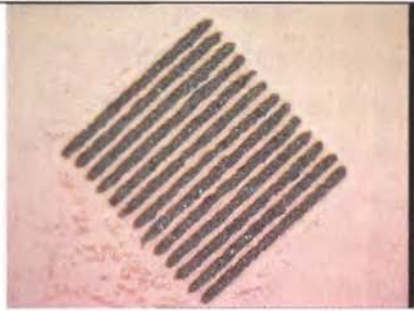
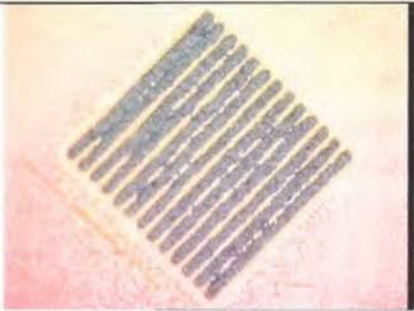
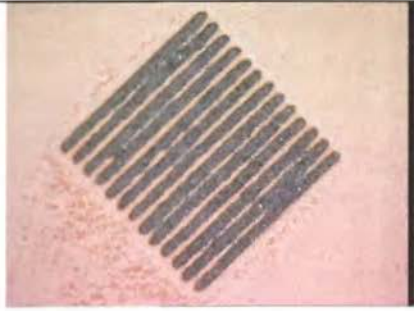
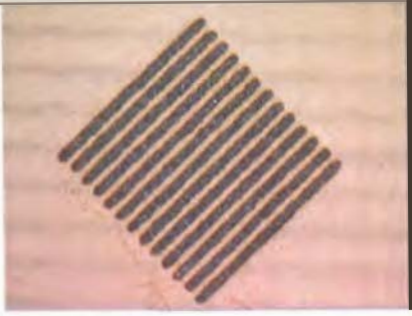
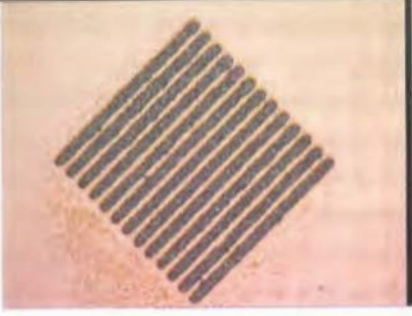
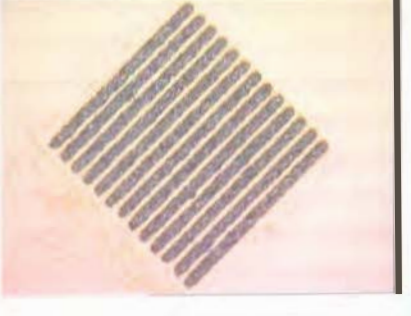
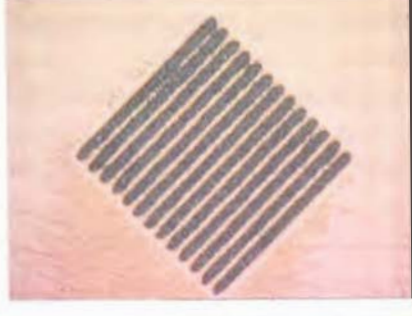
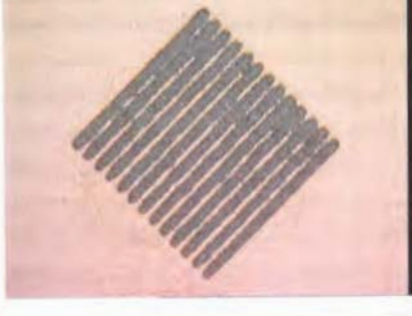
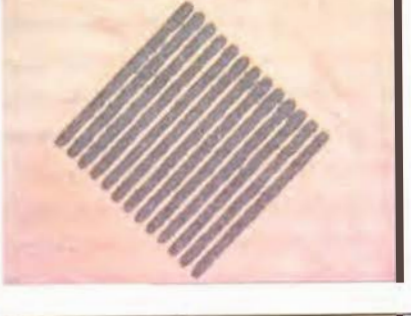
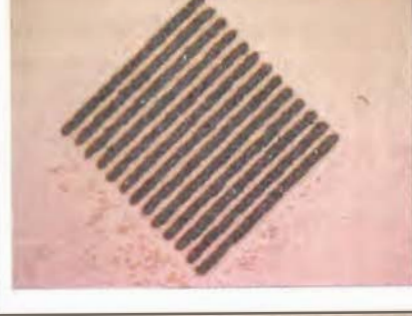
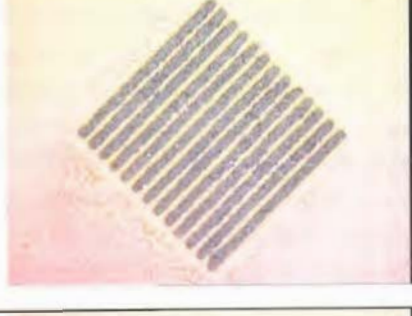
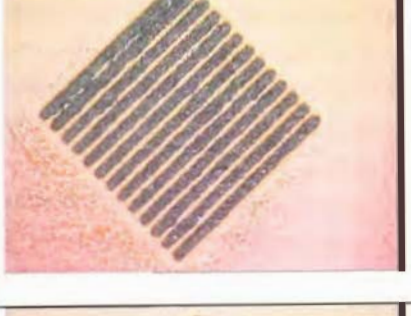
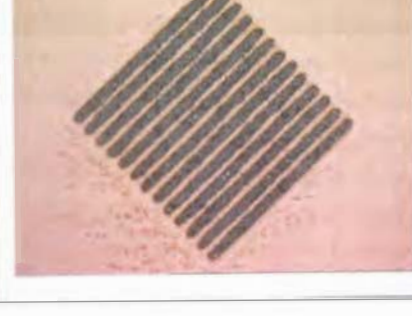
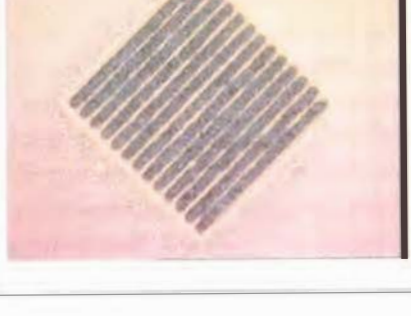
Solder Pastes	Rest Period		
	5 min	10 min	15 min
P1			
P2			
P3			
P4			

Table 8.5: Hot Slump results for pads with 45° orientation (0.32 mm pitch)

Solder Pastes	Rest Period		
	5 min	10 min	15 min
P1			
P2			
P3			
P4			

8.3.2 Spread test Results

The section presents the results of spread tests carried out on the four solder paste samples (P1 to P4). The spread test location (figure 8.21) on the Benchmarker II stencil/board has been utilized for this purpose. The spread test provides a quantitative picture of the slump performance of the solder paste by examining printed deposits before and after being exposed to simulated factory floor conditions (Puttlitz and Stalter, 2004).

The spread test can also be used as a qualitative measure of wettability of solder pastes (the characteristic of spreading out of solder on the substrate). The test therefore, provides a simple and effective way of testing and comparing the solderability of solder pastes with the substrate. In a recent work, Wiese et al (2005) found out that the large PCB pads with narrow spacing manifest spreading behaviour more effectively than fine pitch pads. As shown in figure 8.21, the spread test location consists of relatively wide pads (1.25 mm) in five rows with different gaps between the pads (4 mils to 12 mils).

The spread test carried out in this study measures the increase in soldering defects (in terms of bridging between pads) due to spreading after a pre-determined time period. The effect of three different time periods (5, 10, 15 minutes) on spreading behaviour have been investigated. Spreading behaviour was observed both at room temperature and at elevated temperature (150⁰ C, 10 min). The detail experimental procedure is outlined in section 8.2. The spread test results were examined by inspecting and counting the number of defects that were generated due to spreading. For this test, a defect was identified as any bridge or shorts of the gap between the pads with as little as two particles of solder paste touching each other.

As can be seen in figure 8.22, for spread test results at room temperature, bridging was generally found to increase with the increase in resting time. This behaviour was quite expected as the solder paste tends to spread out if kept idle, due to the gravitational effect. However, the rate of increase in bridging was quite slow, indicating that the solder paste samples possess a good thixotropic behaviour which refrain printed deposits from unnecessary spreading with idle time. From the results presented in figure 8.22, it is also evident that the paste P2 possesses the best spreading behaviour among the four samples, as it produces minimum bridging between pads for all the different resting periods investigated. The rest of the paste samples (P1, P3 and P4) have shown quite similar spreading behaviour with the observed number of defects varying in a short range (from 37 to 41). For P1 and P2 solder pastes, a slight decrease in number of defects was observed when resting/idle time increased from 5 minutes to 10 minutes. This is opposed to the general trend of increasing defects with increasing resting time. One of the reasons

of this inconsistent behaviour might be due to the variations in ambient temperature and humidity, as these were not controlled. The effects of temperature and humidity have also been addressed by Bauer and Lathrop (1998) and Lee (2002) in their work.

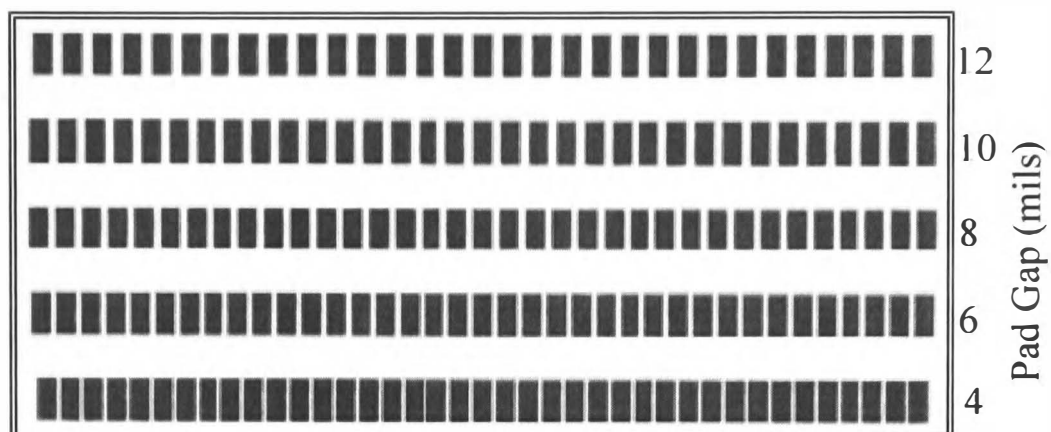


Figure 8.21: Spread Test location

Table 8.6: Spread test results (number of bridges) at room temperature (cold) and at alleviated temperature (hot) for different resting periods.

Resting time	P1		P2		P3		P4	
	Cold	Hot	Cold	Hot	Cold	Hot	Cold	Hot
5	37	122	10	110	39	86	38	145
10	36	141	12	116	38	118	38	147
15	39	142	16	120	41	108	40	160

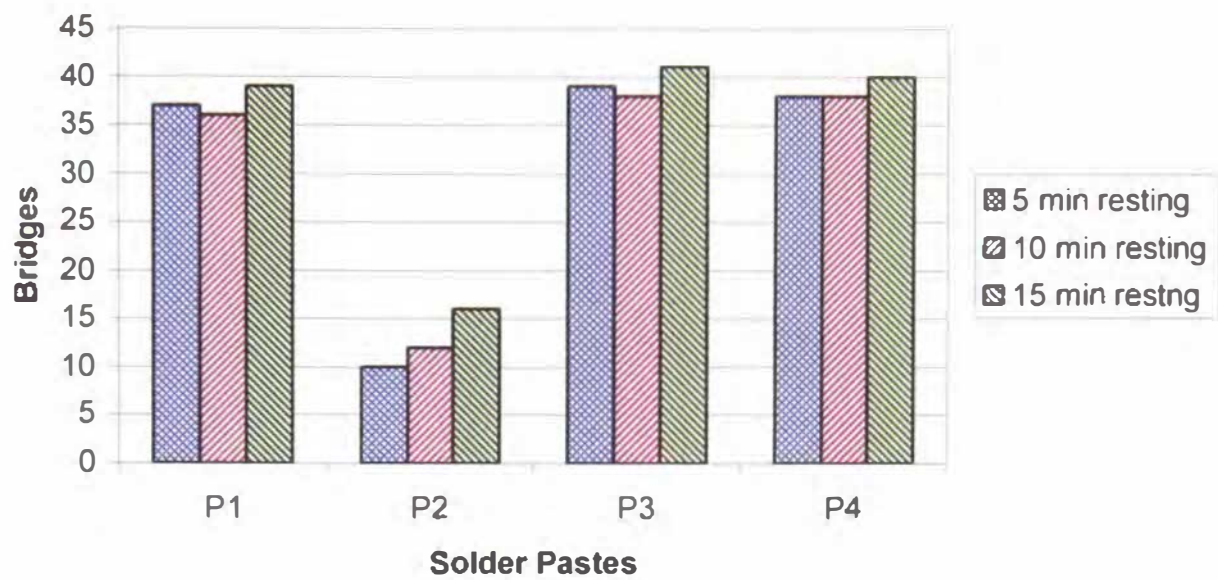


Figure 8.22: Spread test results at room temperature with different resting periods.

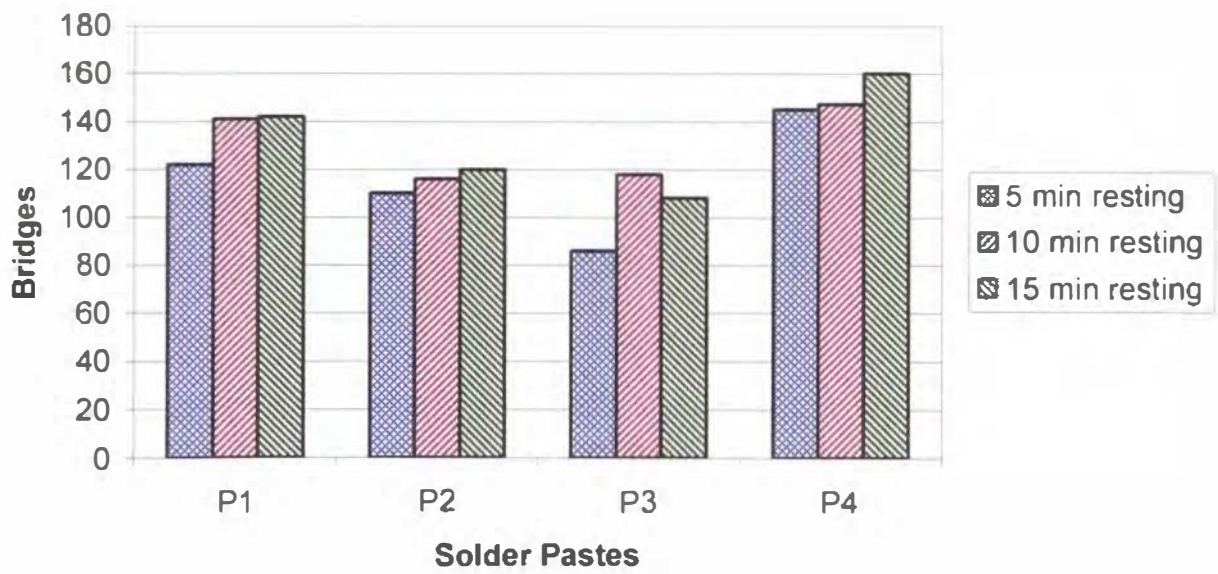


Figure 8.23: Spread test results after temperature conditioning (150⁰ C, 10 minutes) at different resting periods.

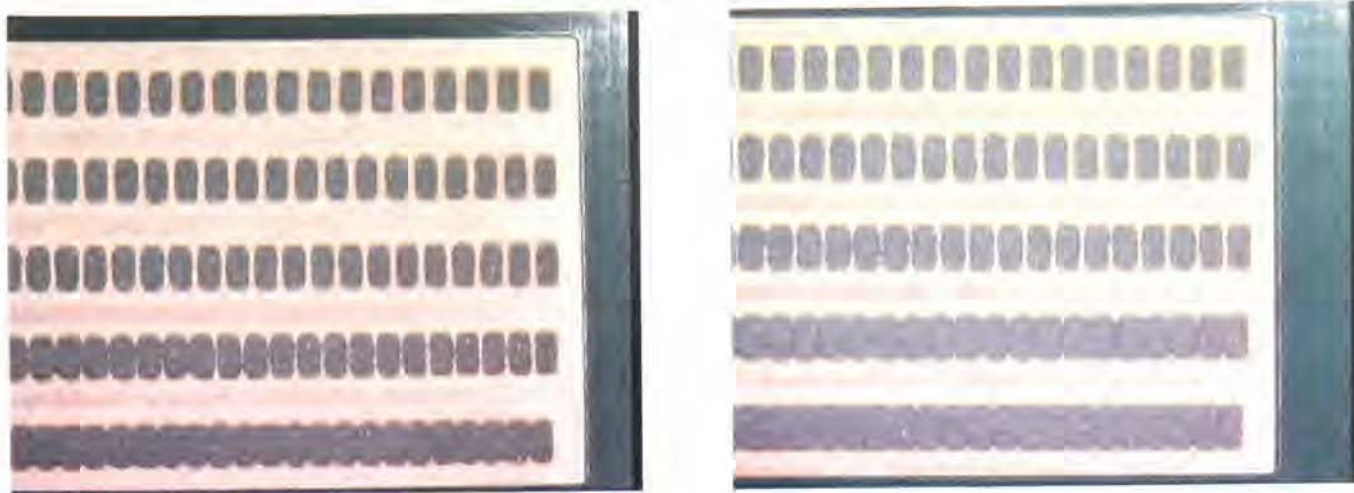


Figure 8.24: High temperature spread test behaviour of P3 solder paste after 5 minutes (left) and 10 minutes (right) of resting time.

Figure 8.23 shows the spread test results for the solder paste samples after temperature conditioning at 150°C for 10 minutes. In order to observe the effect of idle/resting time on spreading behaviour, the printed substrate was left idle or stored for different time periods (5, 10 and 15 minutes) before placing them in the batch oven for temperature conditioning. If compared to the spread test results at room temperature (figure 8.22), figure 8.23 clearly shows that the number of defects has increased greatly at alleviated temperature (up to 11 times increase in bridging for P2 paste was observed). This behaviour indicates that the solder paste samples are more susceptible to spreading at higher temperatures than the normal room temperature. As explained by Tarr (2007), at high temperature the flux vehicle is less viscous and may be less able to hold the heavy solder particles in suspension, so the paste tends to spread due to the effect of gravity. According to Fujii (2004) the spreading of solder paste at alleviated temperature could be either due to excessive flux content in the solder paste or because of low melting point of the thixotropic agent added to the flux. Although paste P2 has showed best spreading behaviour at room temperature, it was paste P3 which performed best at high temperature. This shows that the formulation of solder paste plays an important role in defining its printing behaviour. By controlling the ingredients, a solder paste can be formulated for optimum performance at the required temperature level.

8.4 Correlation of Paste Flow Behaviour to the Printing Results

This section investigates the correlation of the printing results (slump and spread test results) with the flow characterisation and modelling studies carried out in the previous chapters. Several studies (Trease & Dietz, 1972; Ogata, 1991, Lapasin et al, 1994; Anderson et al, 1995; Kolli et al 1997; Bao et al, 1998 and Durairaj, 2006) have been carried out to correlate the flow properties of the solder pastes with the printing performance. The importance of correlating rheological flow behaviours with the paste printing results can be realised from the fact that it helps to validate the rheological test results and therefore, aids in the process optimisation and in predicting paste performance during the printing process. Moreover, it helps to identify the causes of printing defects in the paste printing process. The objective here was to find out if there is any correlation between the time-dependent flow properties and the slump and spreading behaviours of solder paste samples.

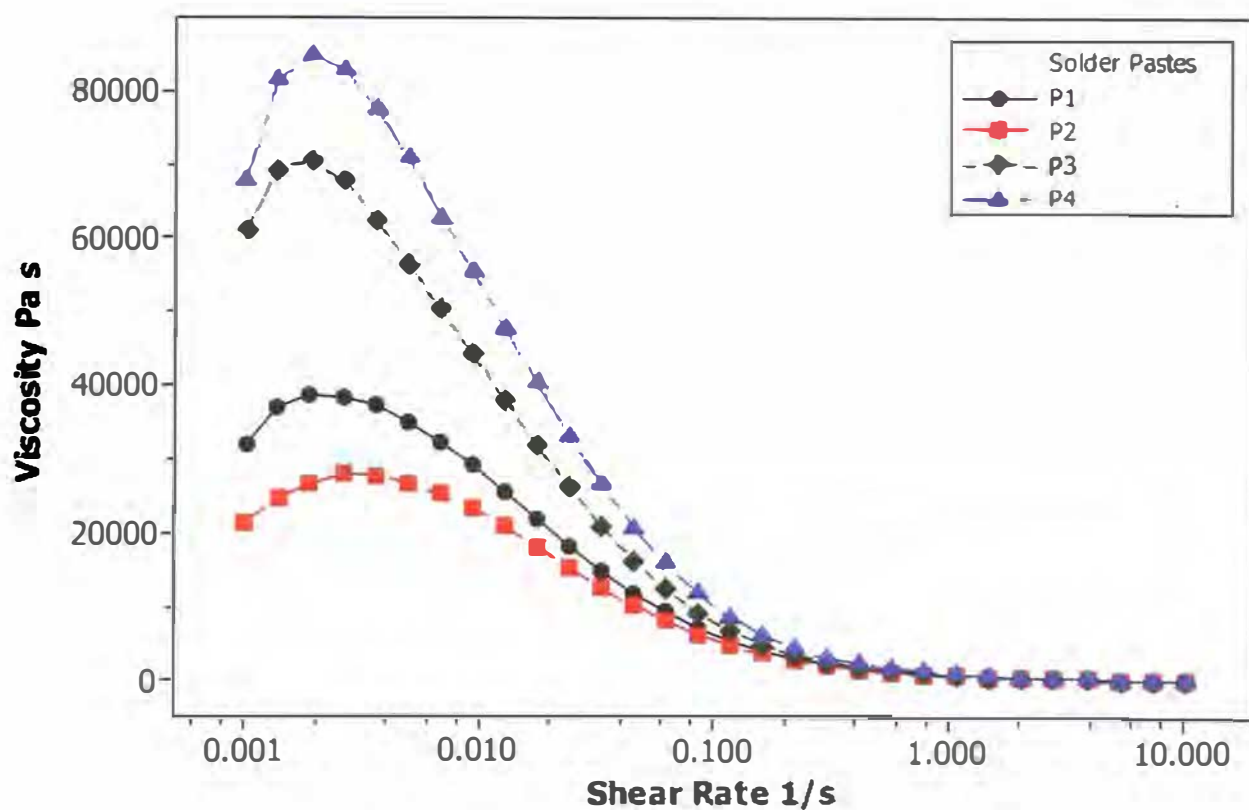


Figure 8.25: Flow curves for the solder paste samples

Table 8.7: Key results from time-dependent flow characterisation and modelling studies.

Solder Paste	Thixotropy coefficient (K_t)	Equilibrium Viscosity (kPa s)	Characteristic Build-up time (sec)
P1	330.7	375.80	286.81
P2	264.9	261.43	368.08
P3	151.6	386.81	231.07
P4	18.8	447.81	244.21

Lee (2002) demonstrated that a solder paste with high yield-stress (high viscosity at zero shear rate) would produce less slump than a solder paste with low yield-stress (i.e. low viscosity at zero shear rate). Figure 8.25 shows the steady state flow curves (samples were pre-sheared at 10 s^{-1} for 30 seconds) for the solder paste samples for a applied shear rate range of 0.001 s^{-1} to 10 s^{-1} . The focus here is not to analyse the flow curves of solder pastes but to rank the solder paste samples according to there viscosity at the low shear rate (0.001 s^{-1}). Based on the descending viscosity values at 0.001 s^{-1} shear rate (figure 8.25), solder paste samples can be ranked as $P4 > P3 > P1 > P2$. Having the highest viscosity value at low shear rate, P4 solder paste is expected to perform best by producing lowest bridging during slump and spread test.

Table 8.7 presents the key results obtained from the studies carried out in the previous chapters. The thixotropic coefficient values in table 8.7 were calculated from hysteresis loop tests, as presented in chapter 5. A high value of thixotropic coefficient usually indicates a high structural breakdown and a poor recovery behaviour. According to the ascending thixotropic coefficient value, the solder paste samples can be arranged as: $P4 > P3 > P2 > P1$. Paste P4 will show highest recovery followed by P3, P2 and P1 pastes. The equilibrium viscosity and the characteristic time values presented in table 8.7 are average values for all the low shear rates investigated in the build-up modelling study carried out in chapter 7. The equilibrium viscosity value represents the viscosity value at the end of short-term build-up periods. Solder pastes with high equilibrium viscosity would be less susceptible to slumping. The characteristic time represents the time the

solder paste would take to recover its structure (quick initial recovery) after printing is completed. A lower value of the characteristic time means a quicker recovery. This also means that the paste will be more susceptible to late slump (with higher resting period). An ideal solder paste will feature a quick recovery of the solder paste structure to the extent that enables proper printing at adequate speed without slumping. Knowing the recover timeline of solder paste is important, as it aids in the paste formulations and also in achieving reproducible measurement (Ineke & Eli, 2007). Based on the equilibrium viscosity and characteristic time, the solder paste samples can be ranked as:

In descending order of equilibrium viscosity: $P4 > P3 > P1 > P2$

In ascending order of characteristic time: $P3 > P4 > P1 > P2$

Although the flow characterisation and model fitting results identified paste P4 as the best to resist slumping, but the actual slump and spread test results did not show any particular trend. From the printing test results, it was found out that different solder paste samples have performed well at different temperature conditions. The aperture sizes and resting periods have also influenced the printing results. It was also noticed that the performances of the solder paste samples varied in a close range which made it quite difficult to rank their performance. Although paste P1 has showed lower viscosity value at low shear rate (figure 8.25), it has outperformed all the other solder paste samples in the cold slump tests (table 8.2, figures 8.12 to 8.15) by producing less bridging on average. Paste P3 was observed to perform best at alleviated temperature for both slump and spread tests (figures 8.16 – 8.20, 8.22 – 8.24). Although paste P2 has produced a lower value of equilibrium viscosity and highest value for the characteristic time (table 8.7), it has showed the best spreading behaviour at the room temperature (figure 8.22).

One of the reasons of the deviation of printing test results from the theoretical predictions could be due to the variations in temperature and humidity in the printing room. Solder paste is known to be very much sensitive to both heat and humidity. The life and printing performance of solder paste could be drastically reduced if exposed to high temperature and humidity. Excessive heat could promote flux separation from the

solder particles, which will alter the rheological properties of the paste, very likely resulting in printing defects (AIM, 2002). Solder paste can pick up moistures if left idle in high humid area and can cause slumping that can lead to bridging (Lee 2002). AIM (2002) recommended that the printing area should be maintained at 40% - 50% relative humidity and 72⁰ – 80⁰ F (22 – 26⁰ C) for optimum printing performance.

Based on the above discussion on the correlation of the test/model parameters and printing performances, some important design principles are proposed to facilitate new paste formulations. These are outlined in the table provided below.

Table 8.8: Design Principles for new solder paste formulation. .

Test/Model Parameters	Level	Expected Outcome
Thixotropy Coefficient	Low	Low structural breakdown, high recovery.
	High	High structural breakdown, poor recovery.
Equilibrium Viscosity	Low	More slumping.
	High	Less slumping.
Characteristic Time	Low	Quicker recovery but susceptible to late slump.
	High	More time for component placement before slumping.

8.5 Summary

The results of a series of extensive printing tests to evaluate the fine-pitch slump and spread behaviour of four commercially available solder paste samples are presented in this chapter. The printing test results were also correlated to the findings from the time-dependent rheological characterisation and modelling studies (reported in previous chapters). Both the slump and spread tests were carried out with different resting periods (5, 10 and 15 minutes), which represent the time between the printing and reflow stage. Cold and hot slump behaviours were examined for three different pad sizes (2.03 × 0.63 mm, 2.03 × 0.33 mm and 2.03 × 0.20 mm) with different spacing both in horizontal and vertical orientation. As expected, for the all the solder paste samples, the intensity of

bridging (for both cold and hot slump) was generally found to increase with increasing resting time. “Moisture absorption” from the atmosphere and the “gravitational effect” are identified as the probable reasons for this increase in slumping behaviour. Slumping behaviour was also found dependent on the orientation of the pads on the printed circuit boards (PCB), and therefore, must be taken into consideration when designing the PCB.

The printing performance (in both slump and spread tests) of all the solder paste samples were observed to vary with the temperature conditions. Although the bridging, as observed from the spread test results at room temperature, was generally found to increase with increasing resting time, the rate of increase in bridging was quite slow. This indicates that the paste samples possess good thixotropic behaviour which refrains printed deposits from unnecessary spreading with idle time.

An attempt was made to correlate slump and spreading behaviour of solder paste samples to the time-dependent flow properties of solder paste (outlined in chapter 5, 6 and 7). From the flow characterisation and modelling results, paste P4 is identified as the most likely to resist slumping among the four solder paste samples. The actual slump and spread test results, however, did not show any particular trend. The printing performance of different solder pastes was different at different temperature conditions. The deviation of printing results from the predictions could be attributed to the uncontrolled printing environment that is, the variation in temperature and humidity in the printing room.

CHAPTER 9

SUMMARY, CONCLUSIONS AND RECOMENDATIONS FOR FUTURE WORK

9.1 Introduction

The work reported in this thesis is concerned with the study of time-dependent rheological characterisation of pastes designed for ultra fine pitch flip chip assembly applications using the stencil printing process. This study on the time-dependent rheological characterisation of solder pastes and flux mediums had four main objectives, as follows:

1. To study the time-dependent flow-behaviour of solder pastes and flux mediums.
2. To model the break-down of the solder paste structure using the Structural Kinetic Model.
3. To model the build-up of the solder paste structure using the Stretched Exponential Model.
4. To correlate the time-dependent rheological behaviour of pastes to the paste printing performance through printing trials.

In order to achieve the first objective, the time-dependent flow behaviours of solder pastes and flux mediums were investigated by using hysteresis loop test and step-shear-rate test methods. The results are outlined in chapter 5 of this thesis. The second and third objectives were met through successfully modelling the structural break-down and build-up of the paste materials. The results of these modelling studies are presented in chapter 6 and 7 of this thesis. In order to achieve the fourth and last objective, an attempt has been made to correlate the time-dependent rheological behaviour of pastes to the paste slumping behaviour through printing trials (presented in chapter 8). However, no

significant correlation was found and therefore, further studies is recommended to carry out the printing trials in a controlled environment.

This chapter is comprised of three sections. First section presents a summary of the key results of the programme of works carried out on the time-dependent flow behaviors of lead-free solder pastes and flux/vehicle mediums; and the results of the printing trials carried out to correlate the time-dependent properties to printing performance. The second section presents the key conclusions that have been drawn from the results of the research programme. The suggestions for future works are provided in the final section.

9.2 Summary

This section summarises the results and findings from this research work and is made up of four sub sections namely; investigation of the time-dependent behaviour of solder pastes and flux mediums, modelling of the break-down of the paste structure using the structural kinetic model, modelling of the build-up of the paste structure using the stretched exponential model and printing test results.

9.2.1 Investigation of the time-dependent behaviour of solder pastes and flux mediums

a) Hysteresis loop test results

The objective of the hysteresis loop test was to qualify and quantify the thixotropic flow behaviour of solder pastes and flux mediums. As expected, all the solder paste samples and flux mediums exhibited shown thixotropic behaviour under the application of shear. The degree of thixotropy was measured by calculating (i) the area between the up and down curve of the hysteresis loop (Durairaj et al, 2004) and (ii) a coefficient of thixotropy (the ratio of the hysteresis loop area and the highest applied shear rate) (Djakovic et al, 1990). The results from the multiple-hysteresis loop test

suggest that the paste rheological behaviour can be strongly affected by the previous shear history and the duration and intensity of the applied shear rate. The changing nature of the solder paste response with increasing hysteresis cycle also suggest that the hysteresis loop can only be used as a qualitative measure of thixotropy as it is highly influenced by the shearing cycle time and the selected shear rates. Mewis (1979) and Barnes (1997) suggested the same in their literature review on thixotropy. Nguyen et al (1998) also made similar comments from the results of hysteresis loop tests carried out on waxy maize starch pastes.

b) Step-shear-rate test results

The objectives here were to characterize the thixotropic behavior by studying the structural breakdown and buildup of paste materials. Step-shear-rate tests were carried out on solder pastes and flux mediums by applying a sequence of step-wise increases and decreases in shear rates. The results from the step-shear-test indicate that the build-up of solder paste structure depends largely on both the previous shear history and the intensity of structural break-down. Lapasin et al (1994) have reported similar behaviour for step-shear-tests carried out on lead-based solder pastes. The results also shows that the flux mediums are more viscous and more shear-thinning compared to solder pastes.

9.2.2 Modelling of the break-down of the paste structure using the structural kinetic model

In this part of the study, the break-down of the paste structure has been modelled using the structural kinetic approach. For all solder paste samples and flux mediums studied, it was found that their apparent viscosity data at constant shear rates can be satisfactorily correlated to the thixotropic behavior with a second-order structural kinetic model (SKM). A good correlation of the model-fitted result and viscosity-time data for all samples was observed. All the samples were sheared for a period of 8 hours at different values of constant shear rates, namely 2, 4, 6, 8 and 10 s⁻¹. The results indicate

that like tooth pastes and honey, the solder paste samples are highly shear thinning in nature. The rate of decay of the apparent viscosity value is quite rapid in the first hour of shearing, but reduces in magnitude as shearing is prolonged to approach the equilibrium state.

Although the rate constant k (one of the model parameter) is expected to increase with increasing shear rate, but the k values from the model-fitting results did not show any definite trend. This could be because of the “close range of shear rates” investigated and the “experimental scattering” of the data. A comparative study of the model fitted results for solder pastes and flux mediums suggest that the rate of structural breakdown (judging from the values of k) for fluxes are greater than the corresponding solder paste samples for the same shear rate. These results imply that the addition of solder particles to the flux medium has made the system more viscous and more resistant to breakdown under the application of shear.

9.2.3 Modelling of the Build-Up of the Paste Structure Using the Stretched Exponential Model

The objective of this part of the study was to investigate the time dependent build-up of solder pastes and flux mediums through experimental and modelling studies. The samples were pre-sheared to break down the paste structure and then allowed to build up at low shear rates.. The experimental results demonstrates that for any applied low shear rate - the rate of structural build-up was quite rapid at first and then slows down as it approaches an equilibrium state. The observed thixotropic build-up behaviour was modelled using the stretched exponential model (SEM). The result showed a good correlation of the model fitted result and the apparent viscosity – time data with the thixotropic buildup behaviour for all the solder paste samples. Both of the SEM parameters - equilibrium viscosity (η_{∞}) and characteristic time (ψ) were found to decrease with increase in shear rates and were satisfactorily fitted by power functions. The time-dependent structural build-up of solder pastes was also investigated using

oscillatory time sweep measurement. The increase in elastic modulus (G') and the subsequent decrease in phase angle (δ) with time have been correlated to the aggregation of solder particles during the resting period. Research carried out on various starch paste suspensions (Ravindra et al 2004, Chang et al 2004) have also shown similar build-up behaviour under the application of oscillatory shear.

9.2.4 Printing test results

a) Slump test results

The slump tests were performed with 5, 10 and 15 minutes of resting time (the resting time here represents the time between the printing step and the reflow). The objective of the investigation was therefore to find out how different resting period affects the cold and hot slump behaviour of solder pastes. Slumping was examined/evaluated by noting the minimum spacing which has bridged for a particular pad size in horizontal and vertical directions. Different solder paste samples exhibited different cold slump behaviours with increasing rest periods. In some cases there was no change/difference observed in cold slump behaviour with the rest periods. However, in most cases cold slumping was found to increase with the increase in rest period. Hot slump tests were carried out by heating the printed board to 150⁰C for 10 minutes. As expected, for all solder paste samples, bridging due hot slump was generally found to increase with increasing resting period. This might be due to the absorption of moisture from the atmosphere which ultimately results in reduction in solder paste viscosity with time and increase in slump. Gravitational effects may also influence slumping behaviour, the longer the solder paste is left idle, the greater the intensity of slump due to gravitational force.

b) Spread test Results

The objective of the spread test was to provide a quantitative measure of the slump performance of the solder paste by examining printed deposits before and after being exposed to simulated factory floor conditions. The effects of three different time periods (5, 10, 15 minutes) on spreading behaviour have been investigated. Spreading behaviour was observed both at room temperature and at elevated temperature (150^o C, 10 min). For spread test results at room temperature, bridging was generally found to increase with the increasing resting time. This behaviour was quite expected as the solder paste tends to spread out if kept idle, due to gravitational effect. However, the rate of increase in bridging was quite slow, indicating that the solder paste samples exhibit a good thixotropic behaviour (i.e. good structural recovery) which restrains the printed deposit from unnecessary spreading with idle time. The results also indicate that the solder paste samples are more susceptible to spreading at higher temperatures than at the normal room temperature.

c) Correlation of Paste Flow Behaviour to the Printing Results

The objective here was to find out if there is any correlation between the time-dependent flow properties (reported in chapter 5, 6 and 7) and solder paste printing performance as measured by the slump and spreading behaviours of solder paste samples. Although the flow characterisation and model fitting results identified paste P4 as the best slump resistant paste, but the actual slump and spread test results did not show any particular trend. It was found that different solder paste samples performed well at different temperature conditions. The results also show that the aperture size and the resting period also directly affect the printing performance. It was also noticed that the performances of the solder paste samples varied in a close range which made it quite difficult to rank their performance. Although paste P1 has showed lower viscosity value at low shear rate, it has outperformed all the other solder paste samples in the cold slump tests by producing less bridging on average. Paste P3 was observed to perform best at

alleviated temperature for both slump and spread tests. The deviation of printing test results from the theoretical predictions could be due to the variations in temperature and humidity in the printing room. Solder paste is known to be very much sensitive to both heat and humidity. The shelf life and printing performance of solder paste could be drastically reduced if exposed to high temperature and humidity.

9.3 Conclusions

The following conclusions can be made from the results of the work presented in this thesis:

1. Hysteresis loop tests can be used as a quick and easy way of qualifying the thixotropic behaviour of solder pastes. The area between the up and down curve of the hysteresis loop and a coefficient of thixotropy can be used as indicators for measuring and comparing the extent of thixotropy between different solder pastes.
2. However, the hysteresis loop test may only be used to qualify the thixotropic nature of solder paste and should not be used to quantify it. This is because the hysteresis loop test results are found to be highly influenced by the previous shear history and the duration and intensity of the applied shear rate.
3. Step-shear-rate test which was chosen to characterize thixotropic behaviour, was found to be quite useful to investigate the time-dependent breakdown and buildup of paste structure. The mechanism of structural change can be clearly understood from the step-shear-rate test results.
4. The Structural Kinetic Model (SKM) which had been used for different dense suspensions (such as red-mud suspension, mayonnaise, starch pastes and yogurt) , was found to be quite useful tool for modelling the time-dependent break-down behaviour of solder paste and flux mediums. The experimental results have shown

a good fit with a second order structural kinetic model for both solder pastes and flux mediums.

5. The constant shear rate experiments conducted in chapter 6 revealed that on average the paste samples took about an hour to reach the equilibrium state (where the apparent viscosity value does not change with time). If correlated to the solder paste printing process, this result would imply that the paste printing performance will not be consistent until the solder paste reaches the equilibrium state after an hour of shearing. This means that the solder paste users should consider pre-shearing the paste for an hour before putting it for printing, to get consistent print deposit.
6. The Stretched Exponential Model (SEM) which was previously used by other researchers to investigate the buildup of newsprint inks, has been successfully used to model the time-dependent structural build-up of solder pastes and flux mediums.
7. An attempt was made to correlate the parameters from the stretched exponential model, such as, equilibrium viscosity (η_{∞}) and characteristic time (ψ) to the shear-thinning and slumping behaviour of solder pastes during the stencil printing process. A higher equilibrium viscosity of solder paste would mean a higher resistance towards slumping. The characteristic time, on the other hand, represents the time frame from the end of stencil printing to the beginning of reflowing process. A higher characteristic time for solder paste would therefore, means more time for component placement by avoiding slumping of the solder paste. The solder paste manufacturers and formulators and the end-users would be able to use these parameters to predict and quantify the slumping behaviour of solder paste.
8. The oscillatory time sweep test method has been successfully used to study the long-term buildup or ageing behaviour of solder paste. The increase of storage

modulus (G') and the decrease of phase angle (δ) with time were correlated to the structure formation within the solder paste during the resting period.

9.4 Recommendations for Future Work

The time-dependent rheological characterisation of pastes designed for ultra fine pitch flip chip assembly and their application to the stencil printing process have been reported in this thesis. Based on the results and findings from the work reported in this thesis, the following areas are recommended for future work:

1. In the thixotropic modelling of the break-down of paste structure (reported in chapter 6), the constant shear rate values applied onto the solder paste samples were quite close to each other. This might be the reason for the inconsistency in the model fitted results. Specially, the values of the parameter k (representing the rate of structural breakdown) did not show any trend or noticeable difference for shear rate values investigated. Therefore, further studies needs to be carried out with a wide range of applied shear rate to study the break-down of paste structure.
2. The effect of temperature has not been considered for the time-dependent break-down and build-up studies reported in chapter 6 and 7. The results however, indicate that this may have an effect on the time-dependent behaviours of solder pastes. The author would have liked to explore this in more detail, but not possible within the work plan. Further work is, therefore, recommended, to study the effect of temperature on the time-dependent flow behaviours of solder pastes.
3. The break-down studies reported in chapter 6 revealed that on average solder paste takes about an hour to reach the equilibrium state (where the structure is completely broken down). However, the preshearing period used in the build-up study (chapter 7) was only 30 seconds. It is suggested that further investigation of build-up behaviour of solder paste should be carried out with 1 hour of preshearing period.

4. The printing trial results were greatly affected by the variation in temperature and humidity of the lab. Therefore, further study is recommended to carry out printing trials in controlled environment with the temperature and humidity being measured and monitored properly. It is also recommended that the printing trials with different idle times (5, 10 and 15 minutes) should be carried out on the same day in order to minimise the effects of temperature and humidity.

Publications

International peer reviewed **JOURNAL** and **CONFERENCE** articles published during this PhD candidature:

1. **Mallik, S.**, Ekere, N. N., Durairaj, R. and Marks, A. E. (2008) “An investigation into the rheological properties of different lead-free solder pastes for surface mount applications”, *Soldering and Surface Mount Technology*, vol. 20, no. 2, pp. 3 -10.
2. Durairaj, R., **Mallik, S.** and Ekere, N. N., (2008) “Solder Paste Characterisation: Towards the Development of Quality Control (QC) Tool”, *Soldering and Surface Mount Technology*, vol.20, no.3, pp. 34-40
3. Durairaj, R., **Mallik, S.**, Seman, A., Marks, A. and Ekere, N. N., (2008), “Rheological characterisation of solder pastes and isotropic conductive adhesives used for flip-chip assembly”, *Journal of Material Processing Technology*. (Article in press)
4. Ekere, N, **Mallik, S.**, (2008) “A Methodology for Characterising New Lead-Free Solder Paste Formulations used for Flip-chip Assembly Applications”, The second international symposium on smart processing technology (SPT 07), Published in *Smart Coating Technology*, vol. 2, pp. 59 – 64.
5. Marks, A. E., Ekere, N. N., **Mallik, S.** and Durairaj, R., (2008) “Effect of Long-Term Ageing on the Rheological Characteristics and Printing Performance of Lead-Free Solder Pastes used for flip-chip assembly”, The second international symposium on smart processing technology (SPT 07), Published in *Smart Coating Technology*, vol. 2, pp.131 – 134.

6. **Mallik, S.**, Ekere, N. N., Durairaj, R., and Marks, A. (2007), “A Study of the Rheological Properties of Lead Free Solder Paste Formulations used for Flip-Chip Interconnection”, 32nd International Electronics Manufacturing Technology Symposium, October 3-5 2007, San Jose/Silicon Valley, California, USA, pp. 165 – 171.
7. Marks, A., **Mallik, S.**, Durairaj, R. and Ekere, N. N. (2007), “Effect of Abandon Time on Print Quality and Rheological Characteristics for Lead-Free Solder Pastes used for Flip-Chip Assembly”, 32nd International Electronics Manufacturing Technology Symposium (IEMT 2007) October 3-5 2007, San Jose/Silicon Valley, California, USA, pp. 14 -18.
8. Durairaj, R., **Mallik, S.**, Marks, A., Winter, M., Bauer, R. and Ekere, N. N. (2006), ‘Rheological Characterisation of New Lead-Free Solder Paste Formulations for Flip-Chip Assembly’, 1st Electronics systemintegration technology conference, Dresden, Germany, pp.995 – 1000.
9. Seman, A., Ekere, N. N., Ashenden, S. J., **Mallik, S.**, Marks, A. E., and Durairaj, R., (2008) “Development of an In-situ, Non-destructive Ultrasonic Monitoring Technique for Solder Pastes”, 2nd Electronics systemintegration technology conference, September 1-4, 2008, London, UK, pp. 209-214.
10. Marks, A. E., **Mallik, S.**, Ekere, N. N. and Seman, A., (2008), “Effect of Temperature on Slumping Behaviour of Lead-Free Solder Paste and its Rheological Simulation”, 2nd Electronics systemintegration technology conference, September 1-4, 2008, London, UK, pp. 829-832.
11. **Mallik, S.**, Schmidt, M., Bauer, R. and Ekere, N. N., (2008), “Influence of Solder Paste Components on Rheological Behaviour”, 2nd Electronics systemintegration technology conference, September 1-4, 2008, London, UK, pp. 1135-1140.

12. **Mallik, S.**, Ekere, N. N., Marks, A. E., Seman, A. and Durairaj, R., (2008), “Modelling of the Time-dependent Flow Behaviour of Lead-Free Solder Pastes used for Flip-Chip Assembly Applications”, 2nd Electronics systemintegration technology conference, September 1-4, 2008, London, UK, pp. 1219-1223
13. Durairaj, R., **Mallik, S.**, Seman, A., Marks, A. E. and Ekere, N. N., (2008) “Viscoelastic properties of solder pastes and isotropic conductive adhesives used for flip-chip”, 33rd International Electronics Manufacturing Technology Symposium (IEMT 2008) 2008, Malaysia
14. Seman, A., Ekere, N. N., Ashenden, S. J., **Mallik, S.**, Marks, A. E. and Durairaj, R., (2008), “In-situ Non-destructive Ultrasonic Rheology Technique for Monitoring Different Lead-free Solder Pastes for Surface Mount Applications”, 10th Electronic Packaging Technology Conference, December 2008, Singapore.
15. Durairaj, R., **Mallik, S.**, Seman, A., Marks, A. and Ekere, N. N., “Investigation of wall-slip effect on paste release characteristic in flip chip stencil printing process”, 10th Electronic Packaging Technology Conference, December 2008, Singapore.

References

- AIM (2002), "AIM Tech-Sheet: Solder Paste Handling Guidelines", Available at: <http://www.aimsolder.com/techarticles/tech%20sheet%20paste%20handling.pdf> (accessed 28 March 2008)
- Abu-Jdayil, B. and Mohameed, H. (2002), "Experimental and modelling studies of the flow properties of concentrated yogurt as affected by storage time", *Journal of Food Engineering*, 52, 359 – 365.
- Abu-Jdayil, B. (2003), 'Modelling the time-dependent rheological behaviour of semisolid foodstuffs', *Journal of Food Engineering*, 57, 97 – 102.
- Ancey, C. (2005), "Notebook: Introduction to Fluid Rheology", Available at: <http://lhe.epfl.ch/cours/cours-DEA.pdf> (accessed 14 April 2008)
- Anderson, R. Maria, F. G. and Kolli, V. G. (1995), "Solder Paste Rheology and Fine Pitch Slump", *Journal of SMT*, pp 12 -18.
- Bao, X., Lee, N., Raj, R. B., Rangan, K. P., Maria, A. (1998), "Engineering solder paste performance through controlled stress rheology analysis", *Soldering & Surface Mount Technology*, Vol. 10 No. 2, pp. 26-35.
- Barnes, H. A., Hutton, J. F., & Walters, K. (1989), "An introduction to rheology", Amsterdam: Elsevier, p. 122.

References

- Barnes, H. A. (1995), "A review of the slip (wall depletion) of polymer solutions, emulsions and particle suspensions in viscometers: its cause, character and cure". *Journal of Non-Newtonian Fluid Mechanics*, 56, pp 221 – 251.
- Barnes, H. A. (1997), "Thixotropy – a review", *Journal of non-newtonian fluid mechanics*, 70, 1 – 33.
- Biocca, P. (2004), "Lead-free SMT Soldering Defects, How to Prevent Them", Available at:http://www.eis-inc.com/Files/pdf/supplier_showcase_page_downloads/kester/HowTo_Prevent_SMT_Defects.pdf (accessed 13 May 2008)
- Bohlin (1994), "Bohlin Instruction Manual: A Basic Introduction to Rheology", Bohlin Instruments, U.K.
- Brian, B. and Lathrop, R. (1998), "An Introduction to Solder Materials", SMT, March 1998.
- Buscall, R., McGowan, J. I. and Morton-Jones, A. J. (1993), "The rheology of concentrated dispersions of weakly attracting colloidal particles with and without wall slip". *Journal of Rheology*, 37, pp 621 – 641.
- Chamberlain, E. K. and Rao, M. A. (1999), "Rheological properties of acid converted waxy maize starches in water and 90% DMSO/10% water", *Carbohydrate Polymers*, Vol. 40, pp. 251-260
- Cheng, D. C. H. and Evans, F. (1965), 'Phenomenological characterization of the rheological behaviour of inelastic reversible thixotropic and antithixotropic fluids.', *British Journal of Applied Physics*, 16, 1599 – 1616.

References

- Cheng, D. C. H. (1984), "Further observations on the rheological behaviour of dense suspensions", *Powder Technology*, 37, 255 – 273.
- Choi, S. J. and Yoo, B., (2005), "Time-dependent Flow Properties of Commercial Kochujang (Hot Pepper-Soybean Paste)", *Food Science and Biotechnology*, Vol. 14, No. 3, pp 413 – 415.
- Clements, D., Desmulliez, M. P. Y. and Abraham, E (2007), "The evolution of paste pressure during stencil printing", *Soldering and Surface Mount Technology*, 19, 3, pp. 9 -14.
- Currie, M. A., (1997), "Characterisation of solder pastes used in reflow soldering of surface mount assembly", PhD Thesis, University of Salford, U.K.
- Djakovic, L., Sovilj, V., Milosevic, S., Sad, N. (1990), "Rheological Behaviour of Thixotropic Starch and Gelatin Gels", *starch/starke*, 42, 10, pp. 380 – 385.
- Durairaj, R, Nguty, T. A. and Ekere, N. N. (2001), "Critical Factors Affecting Paste Flow During Stencil Printing of Solder Paste", *Soldering and Surface Mount Technology*, 13, 2, pp 30 – 34.
- Durairaj, R, Ekere, N. N. and Salam, B. (2004), "Thixotropy flow behaviour of solder and conductive adhesive pastes", *Journal of materials science: materials in electronics*, 15, 677 – 683.
- Durairaj, R (2006), "Rheological Characterisation of Solder Pastes and Isotropic Conductive Adhesives (ICAS) for Microsystems Assembly Technology", Ph.D. Thesis, University of Greenwich.
- Erickson, C. A., (1998), "Wafer Bumping: The Missing Link for DCA", *Electronic Packaging & Production*, July, pp. 43-46.
-

References

- Ferguson, J. and Kemblowski, Z. (1991), "Applied Fluid Rheology", Elsevier Applied Science, London, pp. 47 – 133.
- Fletcher, J. and Hill, A. (2008), "Making the connection - particle size, size distribution and rheology", Available at: <http://www.chemeurope.com/articles/e/61207/> (accessed 29 April 2008)
- Figoni, P. I., & Shoemaker, C. F. (1983), "Characterization of time dependent flow properties of mayonnaise under steady shear". *Journal of Texture Studies*, 14, pp. 431-442.
- Franco, J. M., Gallegos, C. and Barnes, H. A. (1998), "On Slip Effects in Steady-state Flow Measurements of Oil-in-Water Food Emulsions", *Journal of Food Engineering*, 36, pp. 89 – 102.
- Fujiuchi, S. (2004), "Lead-Free Solder Paste and Reflow Soldering", In: *Lead-free Soldring in Electronics – Science, technology and environmental impact*, Marcel Dekker, Inc., New York, pp 243 – 270.
- Fujii, Y (2004), "Capillary Balls: Causes and Countermeasures", *Lead-free electronics*, November 2004.
- Garner et al. (2005), "Finding Solutions to the Challenges in Package Interconnect Reliability", *Intel Technology Journal*, 09, 04, pp. 297 – 307.
- Green, H and Weltmann, R. N. (1943), "Analysis of the thixotropy of pigment vehicle suspensions: Basic principles of the hysteresis loop", *Ind. Eng. Chem. Anal.*, 15, 201 -206.

References

- Geren, N. and Ekere, N. N. (1994), "Solder Paste Dispensing in Robotic SMD Rework". *Soldering and Surface Mount Technology*, vol. 16, pp. 21 – 25.
- Handwerker, C, Kattner, U., Moon, K. (2004), "Materials Science Concepts in Lead-Free Soldering" In: *Lead-free Soldring in Electronics – Science, technology and environmental impact*, Marcel Dekker, Inc., New York, pp 19 – 48.
- Haslehurst, L. and Ekere, N.N. (1996) , "Parameter interactions in stencil printing of solder pastes", *J. of Electronics Manufacturing*, Vol. 6 No. 4, pp. 307-16.
- He, D. and Ekere, N. N. (1996), "The performance of vibrating squeegee in the stencil printing of solder pastes", *Journal of Electronics Manufacturing*, 6/4, pp261 – 270.
- He, D and Ekere, N. N (2001), "Viscosity of concentrated noncolloida bidisperse suspensions", *Rehologica Acta*, 40, 591 – 598.
- Hwang, J. S. (1989), "Solder Paste in Electronics Packaging", Van Nostrand Reinhold, 1989.
- Hwang, J. S. (1994), "Solder/Screen Printing", *SMT/March 1994*, pp 44 – 50.
- Hwang, J. S. (1996), "Modern Solder Technology for Competitive Electronics Manufacturing", McGraw-Hill Professional, p 275.
- Huang, B. and Lee, N. C., (July 2002) "Solder bumping via paste reflow for area array packages", *Proceedings IEMT, SEMICON West 2002, San Jose, CA USA*, pp1-17.
- IPC (1998), "IPC-TM-650 Test Methods Manual", Available at: http://www.ipc.org/4.0_Knowledge/4.1_Standards/test/2.6.13.pdf (accessed 12 March 2008)
-

References

- IPC-SPVC (2005), "Round Robin Testing and Analysis of Lead Free Solder Pastes with Alloys of Tin, Silver and Copper - Final Report", Available at: http://www.ipc.org/3.0_Industry/3.5_Councils_Associations/3.5.1_Industry_Assoc/spvc_bro/SVPC_Final_ExecSumm.pdf (accessed 27 March 2008)
- IPC-SPVC (2006), "Cost of Lead Free Solder Materials", Available at: http://www.dklmetals.co.uk/PDF%20Files/LF_cost_whitePaper_0506.pdf (accessed 13 May 2008)
- Ineke, V. T. A. and Eli, W. (2007), "Thixotropy of Solde Paste Impacts Rheometric Results", Circuits Assembly, Available at: <http://circuitsassembly.com/cms/content/view/5022/95/> (accessed 27 March 2008)
- Jdayil, B. A., Malah, K. L. and Asoud, H (2002) "Rheological characterization of milled sesame (tehineh)". *Food Hydrocolloids*, 16, 55 – 61.
- Jensen, T. and Lasky, R. C. (2006), " Step 3: Solder Materials", SMT, March 2006, Available at: http://smt.pennnet.com/display_article/249822/35/ARTCL/none/none/1/STEP-3:-solder-Materials (accessed 25 March 2008)
- Judd, M. and Brindley, K. (1999), "Soldering in Electronics Assembly", Newnes Publication, pp 95 – 97. Available at: <http://books.google.co.uk/books?id=raOvDxNw2TsC> (accessed 09 April 2008).
- Kardashian, V. S. and Vellanki, S. J. R. (1979), "A Method for the Rheological Characterization of Thick-Film Pastes", *IEEE Transactions on components, hybrids, and manufacturing technology*, vol. CHM-2, No. 2, pp 232 – 239.
- Kasturi, S. (1992), "Fine pitch printing: A manufacturing perspective", *Proceedings of NEPCON West, 1992, Vol 1*, pp 167 – 180.
-

References

- Kolli, V. G., Gadala-Maria, F. and Anderson, R., (1997), "Rheological Characterisation of solder paste for surface mount applications", *IEEE Transactions on Components, Packaging and Manufacturing Technology, Part B*, 20/4, pp 416 – 423.
- Koo, J. M., Kim, Y. N., Yoon, J. W., Ha, S. S., Jung, S. B., (2007), "Reliability of nickel flip-chip bumps with a tin-silver encapsulation on a copper/tin-silver substrate during the bonding process", *Microelectronic Engineering*, 84, 11, pp 2686 – 2690.
- Kozel, B. R. (1983) "Designing solder paste materials to attach surface mounted devices", *Solid State Technology*, p173 – 178.
- Labanda, J, Marco, P and Llorens, J (2004), "Rheological model to predict the thixotropic behaviour of colloidal dispersions". *Colloids and Surfaces A: Physicochemical Engineering Aspects*, 249, 123 – 126.
- Lapasin, R, Dicamp, Sirtori, V. and Casati, D. (1994), "Rheological Characterization of solder pastes", *Journal of Electronic Materials*, 23, 6, 525 – 532.
- Lau, J.H, (1995) "Low Cost Flip Chip Assembly", McGraw-Hill, New York, pp. 30-35.
- Lau, J. H., (2000), "Taguchi Design of Experiment for Wafer Bumping by Stencil Printing", *IEEE Transactions on Electronics Packaging Manufacturing*, Vol. 23, No. 3, pp. 219-225
- Lau, F. K. H. and Yeung, V. W. S., (1997), "A hierarchical evaluation of the solder paste printing process", *Journal of Materials Processing Technology*, Vol. 69 pp. 79-89
- Lee, N. C. (2002), "Reflow Soldering Processes: SMT, BGA, CSP and Flip-Chip Technologies", Newnes Publication, USA, pp. 41 – 44, 101 – 103. Available at: http://books.google.co.uk/books?id=Tv_AuIPrZmEC (accessed 17 March 2008)
-

References

- Macosko, C. W. and Mewis, J. (2004), "Suspension Rheology", In: *Rheology – Principles, Measurements and Applications*, Wiley-VCH, Inc., U.S.A., pp. 425 – 470.
- Maingonnat, J. F., Muller, L. and Leuliet, J. C. (2005), "Modelling the build-up of a thixotropic fluid under viscosimetric and mixing conditions". *Journal of Food Engineering*, 71, 265 – 272.
- Majumdar, A., Beris, A. N. and Metzner, A. B. (2002) "Transient phenomena in thixotropic systems". *Journal of Non-newtonian Fluid Mechanics*, 102, 157 – 178.
- Mannan, S. H., Ekere, N. N., Lo, E. K. and Ismail, I, (1993), "Predicting Scooping and Skipping in Solder Paste Printing for Reflow Soldering of SMT Devices", *Soldering and Surface Mount Technology*, Vol. 15, pp 14 – 17.
- Mannan, S. H., Ekere, N. N., Ismail, I and Lo, E. K., (1994), "Squeegee deformation study in the stencil printing of solder pastes", *IEEE transactions on components packaging, and manufacturing technology – part A*, vol. 17, 3, 470 – 476.
- Mannan, S. H., Ekere, N. N., Ismail, I. and Currie, M. A. (1994a), "Computer simulation of solder paste flow Part 1: Dense suspension theory, *Journal of Electronics Manufacturing*, 4, pp. 141 – 147.
- Mannan, S. H., Ekere, N. N., Ismail, I. and Currie, M. A. (1994b), "Computer simulation of solder paste flow Part II: Flow out of a stencil aperture", 4, 149 – 154.
- Mannan, S. H., Ekere, N. N., Ismail, I. and Currie, M. A. (1995), "Flow processes in solder paste during stencil printing for SMT assembly", *Journal of materials science: materials in electronics*, 6, 1995, 34 – 42.

References

Marks, A., Mallik, S., Durairaj, R. and Ekere, N. N. (2007), 'Effect of Abandon Time on Print Quality and Rheological Characteristics for Lead-Free Solder Pastes used for Flip-Chip Assembly', 32nd International Electronics Manufacturing Technology Symposium (IEMT 2007) October 3-5 2007, San Jose/Silicon Valley, California, USA

Mazzeo, F. A. (2002), "Importance of Oscillatory Time Sweeps in Rheology", Available at:
http://www.tainstruments.co.jp/application/pdf/Rheology_Library/Application_Briefs/RH081a.PDF (accessed 30 April 2008)

Mcketta, J. J. and Cunningham, W. A. (1990), "Encyclopedia of Chemical Processing and Design", Marcel Dekker Ltd., pp. 401 – 404, Available at:
<http://books.google.co.uk/books?id=43QQW5zDB2EC> (accessed 29 April 2008)

Mewis, J (1979), "Thixotropy – A general review", Journal of Non-Newtonian Fluid Mechanics, 6, 1 – 20.

Mindel, M. J., (1991), "Solder Paste Rheology as a Function of Temperature," Proceedings of SMI '91, San Jose, Calif., p. 490-495.

Mitsui-kinzoku, (2002), "Solder powder", Available at: <http://www.mitsui-kinzoku.co.jp/project/kinoufun/en/handa/hzoom2.html> (accessed 30 April 2008)

Monaghan, K., Head, L, Sahay, C. and Constable, (1995), "Analysis of the effects of interior aperture angle on print quality in solder paste stenciling", Material Research Society Symposium Proceedings, Vol 390, pp 213 – 218.

Mooney, M (1931), "Explicit formulas for slip and fluidity", Journal of Rheology, 2, pp. 210 – 222.

References

- Nguyen, Q. D. and Boger, D. V. (1985), 'Thixotropic behaviour of concentrated bauxite residue suspensions', *Rheologica Acta*, 24, 427 – 437.
- Nguyen, Q. D., Jensen, C. T. B., Kristensen, P. G. (1998), 'Experimental and modelling studies of the flow properties of maize and waxy maize starch pastes', *Chemical Engineering Journal*, 70, 165 – 171.
- Nguty, T. A., Ekere, N. N. and Adebayo, A., (1999), "Correlating solder paste composition with stencil printing performance", In: *IEEE/CPMT International Electronics Manufacturing Technology Symposium*, October 18-19, 1999, Austin, Texas, pp. 304 – 309.
- Nguty, T. A. and Ekere, N. N. (2000), "The rheological properties of solder and solar pastes and the effect on stencil printing". *Rheologica Acta*, 39, 607 – 612.
- Nguty, T. A. and Ekere, N. N. (2000a) Modelling the effects of temperature on the rheology of solder pastes and flux systems, *Journal of Materials Science: Materials in Electronics*, 11, pp. 39 – 43.
- Nguty, T. A. and Ekere, N. N. (2000b), Monitoring the effects of storage on the rheological properties of solder paste, *Journal of Materials Science: Materials in Electronics*, 11, pp. 433 – 437.
- Nguty, T. A., Budiman, S., Durairaj, R., Solomon, R., and Ekere, N. N., (Oct 2001), "Understanding the process window for Printing Lead-Free Solder Pastes", *IEEE transaction on Electronic Packaging Manufacturing*, Vol. 24, Issue 4, pp. 249-254
- Nimmo, K (2004), "Alloy Seleacions", In: *Lead-free Soldring in Electronics – Science, technology and environmental impact*, Marcel Dekker, Inc., New York, pp 49 – 90.

References

- Ogata, S. (1991), "Rheology and Printability of Solder Paste", IEICE Transactions, Vol E74, No 8, August 1991, pp 2378 – 2383.
- Orendoff, C. J, Baker, J. M., Rowen, A. M, Yelton, W. G., Arrington, C. L., Gillen, J. R. (2008), "A wet chemistry approach to sub-micron removable flip-chip interconnects.", Nanoengineering: Fabrication, Properties, Optics and Devices V, Edited by Dobisz, E. A, Eldada, L. A., Proceedings of the SPIE, Volume 7039, p 70390R – 70390R-11.
- Owczarek, J. A. and Howland, F. L. (1990a), "A Study of the Off-Contact Screen Printing Process – Part I: Model of the Printing Process and Some Results Derived From Experiments". IEEE Transactions on Components, Hybrids, and Manufacturing Technology, Vol. 13, No. 2, pp. 358 – 367.
- Owczarek, J. A. and Howland, F. L. (1990b), "A Study of the Off-Contact Screen Printing Process – Part II: Analysis of the Model of the Printing Process". IEEE Transactions on Components, Hybrids, and Manufacturing Technology, Vol. 13, No. 2, pp. 368 – 375.
- Paunov, V. N. (2002), "Lecture 3: Non-dlvo interactions in colloids: Are they really an exception from the rule? Available at: <http://www.hull.ac.uk/scg/paunov/paunov06536-3.pdf> (accessed 28 April 2008)
- Pecht, M. (1993), "Soldering Processes and Equipments", John Wiley and Sons, p 22 – 25. Available at: http://books.google.co.uk/books?id=Muo3X_k7p8C (accessed 02 April 2008)
- Perret, D., Locat, J. and Martignoni, P. (1996), "Thixotropic behaviour during shear of a fine-grained mud from Eastern Canada, Engineering Geology", 43(1), pp. 31-44.

References

- Petrellis, N. C. and Flumerfelt, R. W. (1973), 'Rheological Behaviour of Shear Degradable Oils: Kinetic and Equilibrium Properties', *The Canadian Journal of Chemical Engineering*, 51, 291 – 301.
- Poon, G. K. K., & Williams, D. J., (1999), "Characterization of a solder paste printing process and its optimization", *Soldering & Surface Mount Technology*, Vol. 11, No. 3, pp.23-26
- Prasad, R. P. (2000) "Solder Paste Printing", *SMT*, September 2000, Available at: http://smt.pennnet.com/Articles/Article_Display.cfm?Section=Archives&Subsection=Display&ARTICLE_ID=82882&KE (accessed 14 March 2008)
- Pudas, M., Manassis, D., Patzelt, R., Hagberg, J., Leppavuori, S., Vahakangas, J., Ostmann, A. and Reichi, H. (2005), "High-Resolution Electroformed Stencil Manufacturing Method for Ultra Fine Pitch Wafer Bumping Technology", 15th European Microelectronics and Packaging Conference – EMPC 2005, June 12-15, 2005, Brugge, Belgium.
- Puttlitz, K. L. and Stalter, K. A. (2004), "Handbook of Lead-free Solder Technology for Microelectronic Assemblies", Marcel Dekker, New York, p 503, Available at: <http://books.google.co.uk/books?id=H75TywRXUK4C> (accessed 22 March 2008)
- Rahman, M. N. (2003), "Ceramic Processing and Sintering, 2nd Edition", Marcel Dekker Ltd, pp. 230 – 240. Available at: <http://books.google.co.uk/books?id=5yERCU5miKkC> (accessed 28 April 2008)
- Ramaswamy, H. S. and Basak, S., (1992), "Time dependent stress decay rheology of stirred yogurt", *International Dairy Journal*, 2/1, pp. 17 – 31.

References

- Rinne, G. A. (May 1997), "Solder Bumping Methods for Flip Chip Packaging", IEEE Proceedings – 47th Electronic Components and Technology Conference, San Jose, California, pp.240-247
- Riedlin, M. H. A. and Ekere, N. N. (1999), "How Heat Generation in Stencil Printing Affects Solder Joint Quality", SMT, August 1999
- Rizvi, M. J. (2007), "Experimental and Modelling Studies of Electronic Packaging Interconnections Formed with Lead-Free Materials", Ph.D. Thesis, University of Greenwich.
- Roussel, N. (2005), "Steady and transient flow behaviour of fresh cement pastes". Cement and Concrete Research, 35, 1656 – 1664.
- Rowland, R (1999), "Solder Paste", SMT, July 1999, Available at: http://smt.pennnet.com/articles/article_display.cfm?article_id=119864 (accessed 19 March 2008)
- Sci-Tech Encyclopedia (2005), "non-Newtonian fluid." McGraw-Hill Encyclopedia of Science and Technology, The McGraw-Hill Companies, Inc., 2005. Available at: <http://www.answers.com/topic/non-newtonian-fluid> (accessed 24 Apr. 2008).
- Seelig, K, Wertin, J and Suraski, D (2000), "The Quick Pocket Reference for Solder Assembly", AIM, Inc, USA.
- Shea, C., Arora, S. and Brown, S (2007), "Wave Soldering Flux Selection for Pb-Free Assembly", Circuit Assembly March 2007, Available at: <http://circuitsassembly.com/cms/cms/content/view/4511/95/> (accessed 09 April 2008)

References

- Steffe, J. F. (1996), "Rheological Methods in Food Process Engineering", Freeman Press, USA, pp. 1 – 20, 94 – 100.
- Strauss, R. (1998), "SMT Soldering Handbook, 2nd Edition", Newnes, p 163 – 164, Available at: <http://books.google.co.uk/books?id=IN6-cBaeJcsC> (accessed 03 April 2008)
- Suganuma, K (2004), "Introduction to lead-free soldering technology" In: Lead-free Soldering in Electronics – Science, technology and environmental impact, Marcel Dekker, Inc., New York, pp 1 – 18.
- Tarr, M (2007), "Solder Paste Characteristics", Available at: http://www.ami.ac.uk/courses/topics/0246_spc/index.html (accessed 20 March 200)
- Tiu, C. and Boger, D. V. (1974), 'Complete rheological characterization of time-dependent food products.', *Journal of texture studies*, 5, 329 – 338.
- Trease, R. E. and Diets, R. L. (1972), "Rheology of pastes in thick-film printing", *Solid state technology*, January 1972, pp. 39 – 43.
- Usui, H., (1995), "A thixotropy model for coal-water mixtures", *Journal of Non-Newtonian Fluid Mechanics*, 60, pp. 259 -275.
- Verboven, G. J. (2008), " Printing of SMT solder paste", Available at: <http://www.tkb-4u.com/articles/printing/printstmsol/printsmtsol.php> (accessed 16 March 2008)
- Wallevik, J. E. (2005) "Thixotropic investigation on cement paste: Experimental and numerical approach". *Journal of non-Newtonian Fluid Mechanics*, 132, 86 – 99.

References

Wiese, J, Goedecke, A, Audiger, S, Grebner, S, Schmitt, W and Scheikowski, M, (2005), “Development of a Lead Free Solder Paste during the IMECAT Project”, EMPC 2005, June 12-15, Brugge, Belgium, pp 423 – 426.

Yoshimura, A. S. and Prudhomme (1988), “Wall slip corrections for Couette and parallel disk viscometers”, *Journal of Rheology*, 32, pp. 53 – 67.